Unisexual Reproduction in *Cryptococcus*: Evolutionary Implications, Virulence and RNA Silencing

by

Marianna Feretzaki

University Program in Genetics and Genomics
Duke University

Date:_____

Approved:

_____
Joseph Heitman, Supervisor

_____
J. Andrew Alspaugh

_____
Sue Jinks-Robertson

_____
Daniel Lew

_____
Raphael Valdivia

Dissertation submitted in partial fulfillment of
the requirements for the degree of Doctor
of Philosophy, in the University Program in
Genetics and Genomics in the Graduate School
of Duke University

2013

ABSTRACT

Unisexual Reproduction in *Cryptococcus*: Evolutionary Implications,

Virulence and RNA Silencing

by

Marianna Feretzaki

University Program in Genetics and Genomics
Duke University

Date:_____
Approved:

_____
Joseph Heitman, Supervisor

_____
J. Andrew Alspaugh

_____
Sue Jinks-Robertson

_____
Daniel Lew

_____
Raphael Valdivia

An abstract of a dissertation submitted in partial
fulfillment of the requirements for the degree
of Doctor of Philosophy in the University Program in
Genetics and Genomics in the Graduate School of
Duke University

2013

Abstract

Sexual development enables microbial pathogens to purge deleterious mutations from the genome and drives genetic diversity in the population. *Cryptococcus neoformans* is a human fungal pathogen with a defined sexual cycle. Nutrient-limiting conditions and pheromones induce a dimorphic transition from unicellular yeast to multicellular hyphae and the production of infectious spores. *C. neoformans* has a defined **a**-α opposite sexual cycle (bisexual reproduction); however, >99% of clinical and environmental isolates are of the α mating type. Interestingly, α cells can undergo α-α unisexual reproduction, even involving genotypically identical cells. A central question is why would cells mate with themselves given that sex is costly and typically serves to admix pre-existing genetic diversity from genetically divergent parents? Sexual reproduction generates abundant spores that, following inhalation, penetrate deep into the alveoli of the lung, germinate, and establish a pulmonary infection growing as budding yeast. Therefore, sex has been linked with virulence; however, hyphal development has been previously associated with reduced virulence and thus the roles of morphogenesis in virulence have not been extensively analyzed. To further understand the role of unisexual reproduction in *C. neoformans* we investigated the evolutionary implications of α-α mating, explored its role in

pathogenesis, and we dissected the signaling pathway that regulates sexual development.

We isolated α-α unisexual reproduction progeny from the hyperfilamentous strain XL280 and subjected them to a variety of phenotypic and genotypic assays (including whole genome sequencing and comparative genomic hybridization (CGH)). We found that unisexual and bisexual reproduction frequently generates phenotypic and genotypic diversity *de novo*, including aneuploidy. Aneuploidy was responsible for the observed phenotypic changes, as chromosome loss restoring euploidy resulted in a wild-type phenotype. Other genetic changes, including diploidization, chromosome length polymorphisms, single nucleotides polymorphisms (SNPs), and insertion and deletions (indels), were also generated. Our study suggests that the ability to undergo unisexual reproduction may be an evolutionary strategy for eukaryotic microbial pathogens, enabling *de novo* genotypic and phenotypic plasticity and facilitating rapid adaptation to novel environments, such as the mammalian host.

Interestingly aneuploid strains that were fluconazole resistant were as virulent as the WT parental strain XL280. Although XL280 belongs to the serotype D lineage that exhibits limited pathogenicity, we found that it is hypervirulent in the murine model. It can grow inside the lung of the host, establishing a pulmonary infection, and then disseminates to the brain to cause cryptococcal meningoencephalitis. Surprisingly, this hyperfilamentous strain

triggers an immune response polarized towards Th2-type immunity, which is characterized by less protective immunity and is usually observed in the highly virulent sibling species *C. gattii*, responsible for the Pacific Northwest outbreak. These studies: 1) provide a technological advance that will facilitate analysis of virulence genes and attributes in *C. neoformans* var. *neoformans* (serotype D), and 2) reveal the virulence potential of serotype D that is broader and more dynamic than previously appreciated.

Bisexual and unisexual reproduction is governed by shared components of the conserved pheromone-sensing Cpk1 MAPK signal transduction cascade and by Mat2, the major transcriptional regulator of the pathway. However, the downstream targets of the pathway are largely unknown, and homology-based approaches have failed to yield downstream transcriptional regulators or other targets. To address this question we applied insertional mutagenesis via *Agrobacterium tumefaciens* transkingdom DNA delivery to identify mutants with unisexual reproduction defects. In addition to elements known to be involved in sexual development (Crg1, Ste7, Mat2, and Znf2), three key regulators of sexual development were identified by our screen: Znf3, Spo11, and Ubc5. Spo11 and Ubc5 promote sporulation during both bisexual and unisexual reproduction. Genetic and phenotypic analyses provide further evidence implicating both genes in the regulation of meiosis. Phenotypic analysis of sexual development showed that Znf3 is required for hyphal development during unisexual reproduction and

also plays a central role during bisexual reproduction. Znf3 governs cell fusion and pheromone production through a pathway parallel to and independent of the pheromone signaling cascade. Surprisingly, Znf3 participates in transposon silencing during unisexual reproduction and may serve as a link between RNAi silencing and sexual development. In further studies we found that Znf3 is required for sex- and mitotic-induced silencing (SIS and MIS). SIS is less efficient in *znf3*Δ unilateral matings and is abolished in *znf3*Δ x *znf3*Δ bilateral matings, similar to the phenotypes of *rdp1*Δ mutants (the RNA-dependent RNA-polymerase of RNAi pathway). Znf3 is also required for transgene-induced mitotic silencing; *znf3*Δ mutations abrogate silencing of repetitive transgenes during vegetative growth. Znf3 tagged with mCherry is localized in the cytoplasm in bright, distinct foci. Co-localization of Znf3 with the P-body marker Dcp1-GFP further supports the hypothesis that Znf3 is a novel element of the RNAi pathway and operates to defend the genome during sexual development and vegetative growth. In conclusion our studies provide further understanding of unisexual reproduction as a successful strategy for evolution.

Contents

List of Tables

List of Figures

Chapter 1. Introduction[1]

1.1 Sexual reproduction in fungi

Genetic exchange occurs via horizontal gene transfer in bacteria and archea or sexual reproduction in fungal and parasitic eukaryotic microbes. Sexual reproduction is universal, or nearly so, in eukaryotes. Until recently, most eukaryotic pathogens were thought to be clonal and asexual due to the absence of an opposite-mating type partner or the lack of morphological or population genetic evidence for sexual reproduction. However, many of these eukaryotic pathogens have been found recently to have extant cryptic sexual cycles. Fungi have evolved two paradigmatic sexual systems: bisexual and unisexual reproduction. Bisexual reproduction (or heterothallism) requires two compatible partners for mating to occur, while species that engage in unisexual reproduction are self-fertile with a single individual capable of sexual reproduction, even in solo culture. Both modes of sexual reproduction share key features (e.g., ploidy changes, meiosis, production of recombinant progeny) but differ in other characteristics involving aspects of cell or hyphal fusion. Transitions between bisexual and unisexual reproduction are common throughout the fungal kingdom, and both modes can be observed concomitantly in different species of the same

[1] Some of the material in this chapter can be found in Ni, M., M. Feretzaki, S. Sun, et al. (2011). "Sex in fungi." Annu Rev Genet **45**: 405-430. and Feretzaki, M. and J. Heitman (2013). "Unisexual reproduction drives evolution of eukaryotic microbial pathogens." PLoS Pathog **9**(10): e1003674.

genus and sometimes even within the same species (reviewed in Lin and Heitman 2007, Heitman 2010, Ni, Feretzaki et al. 2011).

Sexual reproduction comes with costs. Locating a compatible partner and undergoing mating and meiosis requires time and energy. In addition, sexual reproduction induces genetic diversity, but in so doing rearranges well-adapted genomic configurations. Unisexual reproduction ameliorates the danger of losing a well-adapted phenotype in a particular niche while introducing limited genetic diversity that may enhance the fitness of progeny in response to environmental changes. Mating between cells of the same mating type, via either mother-daughter cell fusion or endoreplication, lowers the barrier to locating a compatible mating partner. Therefore, the transition portrays the balance between outcrossing and inbreeding as responses to specific environmental cues or pressure that favor one or the other breeding strategy.

Recent studies show that unisexual reproduction generates genetic diversity, even in clonal populations of pathogenic fungi (Ni, Feretzaki et al. 2013). From a medical perspective, unisexual reproduction poses a challenge for confronting and controlling the emergence of new strains that have been found to be either hypervirulent or drug resistant to the current standard antifungal course of treatment (Fraser, Giles et al. 2005, Ni, Feretzaki et al. 2013). Similar studies on pathogenic parasites reveal that unisexual reproduction, is not only widespread in other pathogenic microbes, but also can generate “superbugs” that

are resistant to current treatments and are responsible for local outbreaks (Wendte, Miller et al. 2010).

A central conundrum in the field is the studies on *Cryptococcus neoformans* and *Candida albicans*. Both pathogens have extant sexual cycles, however they generate largely clonal populations in nature (Odds, Bougnoux et al. 2007). Recent studies showed that *C. neoformans* and *C. albicans* can undergo unisexual reproduction in nature generating recombinant progeny. These species serve as excellent examples of reproductive plasticity that allows cryptic sexual cycles to enable outcrossing and inbreeding, generating genetic diversity or preserving genetic configurations that confer a fitness advantage in a specific environmental niche.

1.2 Cryptococcus neoformans as a Model Human Fungal Pathogen

Cryptococcus neoformans and its sibling species *Cryptococcus gattii* are basidiomycetes and they are the most common fungal agents of meningoencephalitis in immunocompromised and immunocompetent individuals, respectively. They are encapsulated yeasts with a worldwide distribution found in association with pigeon guano, Eucalyptus and other trees, and soil. *C. neoformans* is divided into three major serotypes: *C. neoformans* var. *neoformans* (serotype D), *C. neoformans* var. *grubii* (serotype A) and a hybrid group between these two (serotype AD). *C. neoformans* species infect patients

with compromised immunity with serotype A strains accounting for more than 95% of cryptococcal infections in immunocompetent individuals worldwide. Serotype D, which is characterized by lower pathogenicity, diverged from serotype A ~18.5 million years ago and is more prevalent in Europe (Xu, Vilgalys et al. 2000). On the other hand, the closely related species *C. gattii* is endemic to tropical regions and causes lethal infections of the central nervous system, often in otherwise healthy individuals. *C. gattii* is the causative agent of the ongoing outbreak of cryptococcosis on Vancouver Island and in the Pacific Northwest region of the US and Canada (Hoang, Maguire et al. 2004).

1.3 Sexual reproduction of C. neoformans

Cryptococcus is typically haploid and grows as a yeast in nature and inside the host. It has a bipolar mating system, α and **a**, and a well-defined sexual cycle (Kwon-Chung 1975, Kwon-Chung 1976). In response to nutrient limitation, such as low glucose and nitrogen, opposite mating type cells secrete pheromones that are sensed by the pheromone receptors, residing on the surface of the cell, and which activate the pheromone-signaling pathway. Pheromone response initiates the formation of conjugation tubes extending towards the pheromone source and triggers a cell-cell fusion event.

Following cell fusion the nuclei remain separate producing a diploid dikaryon that undergoes a dimorphic transition from yeast to hyphal growth (Figure 1). The mating hyphae grow and generate multiple hyphal compartments

wherein the two parental nuclei congress but do not fuse. A special structure called a clamp cell develops on the hyphae and coordinates nuclear division and migration of the two paired parental nuclei. The hyphal compartment cell cycle also generates mitotic daughter cells called blastospores that bear the same DNA content as the hyphae.

At the apex of the hyphae specialized structures are formed wherein nuclear fusion occurs, followed by meiosis. The four post-meiotic nuclei undergo multiple rounds of mitosis and budding to produce four long chains of basidiospores, which are the recombinant haploid meiotic progeny of *Cryptococcus* (reviewed in Idnurm, Bahn et al. 2005, Heitman 2010, Hsueh, Lin et al. 2011). Under laboratory conditions, mating assays are performed on 5% V8 juice agar medium or on MS plant growth medium (Murashige and Skoog agar). Both serotype A and D strains generate robust hyphal development with abundant spores on both mating media (Figure 1). The spores can be isolated either randomly in order to perform linkage analysis or from an individual basidium where the products of a single meiosis event can be analyzed similarly to tetrad analysis (Idnurm 2010).

While the extant sexual cycle occurs under laboratory conditions and the production of hyphae and spores are readily observed, natural populations exhibit an interesting bias towards the α mating type and environmental and clinical isolates are almost exclusively of mating type α (~99%). Therefore, it is

unknown how commonly α-**a** bisexual reproduction occurs in nature. However, a small number of environmental and clinical isolates are diploid hybrids of serotype A and D (**a**ADα or αAD**a** isolates) that harbor both mating types and serve as indirect historic evidence of mating in nature (Lengeler, Cox et al. 2001, Litvintseva, Lin et al. 2007). The first isolate of mating type **a** belonging to the highly pathogenic group of serotype A was isolated from a clinical sample from Tanzania (Lengeler, Wang et al. 2000). In further population genetics studies genotyping of ~3,000 strains showed that 2997 were of mating type α and only three were **a** that exhibited low competence for mating (Lengeler, Wang et al. 2000, Keller, Viviani et al. 2003, Viviani, Nikolova et al. 2003). In addition, a unique population restricted to sub-Saharan Africa is comprised of ~25% mating type **a** individuals (Litvintseva, Marra et al. 2003). *MAT***a** isolates from this population exhibit evidence of recombination and they are robustly fertile under laboratory conditions (Litvintseva, Marra et al. 2003). Thus, the presence of these **a** isolates is geographically restricted and, subsequently, the opportunities for α-**a** bisexual reproduction are limited in nature.

As the vast majority of *Cryptococcus* isolates are mating type α it was thought that the organism was asexual and reproduced largely mitotically. It was hypothesized that the absence of a sexual cycle evolved concomitantly with the emergence of the highly pathogenic isolates. The same notion was hypothesized

for multiple pathogenic fungi, including *C. albicans*, and other eukaryotic parasites (Tibayrenc and Ayala 2012). This theory was fundamentally challenged by evidence of sexual recombination in natural populations exclusively of mating type α (Campbell, Currie et al. 2005). Extensive genotyping and sequencing revealed evidence for both clonal expansion and recombination in serotype A and D isolates from sub-Saharan Africa and the United States (Litvintseva, Marra et al. 2003, Litvintseva, Kestenbaum et al. 2005). Moreover, previous studies showed the formation of hyphae upon solo culture of mating type α isolates on mating media (Wickes, Mayorga et al. 1996). Due to the absence of an opposite mating partner this process was considered to be strictly mitotic and asexual, and was termed monokaryotic or haploid fruiting. Monokaryotic fruiting shares many characteristic features with sexual reproduction, including the production of infectious spores (Wickes, Mayorga et al. 1996).

Lin et al. showed that monokaryotic fruiting is a sexual cycle between cells of one mating type (usually α) generating meiotic recombinant progeny. Nutrient limitation induces a dimorphic transition from yeast to hyphae in cells of the same mating type. During unisexual reproduction either a haploid or a diploid cell initiates hyphal development. Similar to bisexual reproduction, unisexual hyphae grow to form basidia at the tip, where meiosis and multiple rounds of mitosis produce spores. In response to nutrient limitation a haploid cell is able to initiate hyphal development generating haploid hyphae that grow to produce the

basidium where a late endoreplication or nuclear fusion event may occur and produce a transient diploid nucleus that undergoes meiosis and sporulation. Diploidization can also occur early during α-α mating, either through endoreplication of the yeast nucleus or through cell-cell fusion between genetically different or clonal cells (i.e. mother-daughter cell fusion). Unlike bisexual reproduction, in this case the diploid cell is monokaryotic and initiates the formation of hyphae that lead to basidia where meiosis and budding occur to produce the spores (Figure 1). Previous studies have shown that unisexual reproduction generates a mixture of haploid and diploid hyphae, indicating a late or an early diploidization event (Lin, Hull et al. 2005). These findings indicate that unisexual reproduction exhibits more plasticity compared to bisexual reproduction and distinct pathways or molecules may transcriptionally regulate the two processes.

Unisexual reproduction is a novel cryptic sexual cycle that involves ploidy changes (1N→2N→1N) and hyphal development. Lin et al. showed that unisexual reproduction generates high rates of recombination at similar frequency as observed in bisexual reproduction indicating a complete and accurate meiotic cycle (Lin, Hull et al. 2005). Deletion of the highly conserved meiotic factor Dmc1 severely impairs sporulation during unisexual and bisexual reproduction (Lin, Hull et al. 2005). Dmc1 is a “meiosis toolkit” gene and is responsible for the repair of the meiotic double strand breaks by facilitating the

invasion of the DNA strand during the formation of Holiday junctions. The fact that this gene is dispensable for hyphal and basidia development but critical for genetic recombination and sporulation provides further definitive evidence that unisexual reproduction is an extant sexual meiotic cycle.

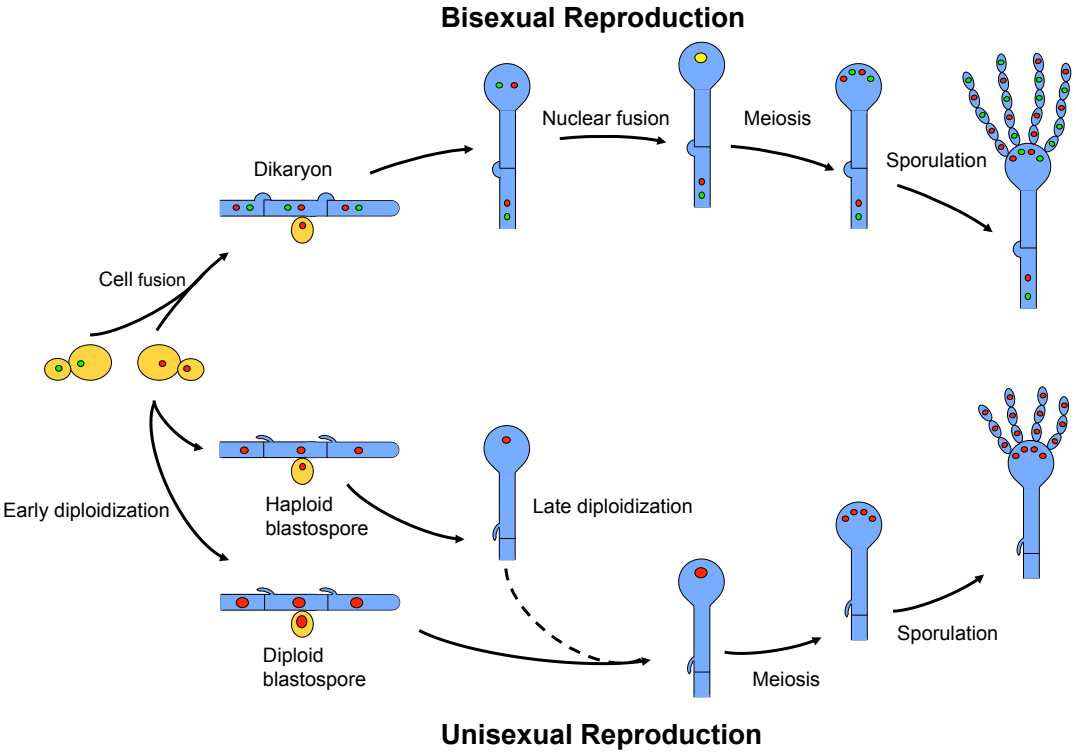

Figure 1. *Cryptococcus neoformans* sexual cycle. During bisexual reproduction opposite mating type cells secrete pheromones under nutrient limiting conditions, initiating the formation of conjugation tubes leading to cell-cell fusion. The two cells form a diploid heterokaryon, which initiates filamentous growth. At the apex of the filaments, specialized structures known as basidia form where nuclear fusion and meiosis occur. Multiple rounds of mitosis and budding produce chains of basidiospores. During unisexual reproduction α cells may undergo an early or late diploidization event to generate a diploid or haploid monokaryotic hyphae, respectively. In both cases meiosis and sporulation produce meiotic progeny with long chains of basidiospores.

1.4 The Pheromone Signaling Cascade

Unisexual reproduction was initially observed only in α mating type cells, thus it was thought the cycle was restricted to α mating type (Wickes, Mayorga et al. 1996). A large-scale analysis revealed that **a** cells also possess the ability to undergo unisexual reproduction (Tscharke, Lazera et al. 2003, Lin, Huang et al. 2006). However, hyphal development is a quantitative trait and analysis of one-quarter of the genome revealed five major QTLs orchestrating hyphal initiation and elongation during unisexual reproduction. The *MAT* locus is the most prominent of these five QTLs and the α allele was found to provide the largest contribution to unisexual reproduction, although in suitable genomic configurations the **a** allele of *MAT* can also suffice for development to occur (Lin, Huang et al. 2006).

The molecular pathway that regulates mating in fungi was initially identified in *S. cerevisiae* three decades ago (Hartwell 1980). These paradigmatic studies on the "sterile genes" identified a transduction pathway activated by binding of pheromones to specialized G-protein-coupled receptors (Burkholder and Hartwell 1985, Whiteway, Hougan et al. 1989). The main downstream targets of the G-coupled receptor are the PAK kinase Ste20 and the scaffold protein Ste5. Activation of Ste5 brings to close proximity Ste20 and the three-tiered phosphorelay system of Ste11 (MAPKKK), Ste7 (MAPKK), and Fus3 (MAPK). Upon pheromone binding and activation of the receptor the signal is

traduced through sequential phosphorylations of the MAPK module to activate the main transcriptional target Ste12, which regulates the expression of several mating-specific genes (reviewed in (Herskowitz 1989, Elion 2000, Dohlman and Thorner 2001). All of these components are required for mating in yeast and it was found that the pathway is conserved among many species in both the ascomycete and basidiomycete phyla. The components of the pheromone pathway are conserved in *C. neoformans* and previous studies showed that the pheromone signaling cascade regulates bisexual reproduction. Thus, it was hypothesized that the pathway also regulates unisexual reproduction.

Previous studies have shown that numerous regulatory molecules of unisexual and bisexual reproduction lie in the mating type locus, among other loci, indicating a shared pathway. Similar to *S. cerevisiae*, the mating pathway is activated by pheromone binding to the G-coupled pheromone receptors that activates the Ste50 scaffold and triggers the three-tier phosphorylation cascade of the major MAP kinases Ste11α/**a** (MAPKKK), Ste7 (MAPKK) and Cpk1 (MAPK) (Alspaugh, Perfect et al. 1997, Wang, Nichols et al. 2002, Davidson, Nichols et al. 2003, Fu, Mares et al. 2011). Interestingly, multiple components of the pathway are encoded by the *MAT* locus, indicating that cells of the two mating types express different alleles of the kinases Ste20 and Ste11 and the transcription factor Ste12.

The pheromone-signaling pathway is structurally and functionally conserved among fungi closely (*Ustilago maydis*) and more distantly (*S. cerevisiae* and *C. albicans*) related to *C. neoformans*, and thus the majority of these components were identified in *Cryptococcus* through homology-based approaches. However, the downstream pathway of the pheromone-signaling cascade exhibits significant rewiring since its divergence from the last common ancestor shared with *S. cerevisiae*. The major transcriptional target of the pheromone signaling cascade in *S. cerevisiae* is Ste12; however, in *Cryptococcus* Ste12, although conserved, is dispensable for hyphal development during unisexual and bisexual reproduction. Recent studies revealed that the major transcription factor responsible for pheromone signaling in *Cryptococcus* is the HMG (high mobility group) protein Mat2 (Lin, Jackson et al. 2010, Kruzel, Giles et al. 2012). Mat2, along with the other components of the pathway, is required for cell-cell fusion indicating an early role during hyphal development. Kruzel et al. showed that Mat2 activates pheromone expression and subsequently triggers the pheromone-signaling cascade by binding directly to a *cis*-regulatory sequence in the promoter region of the pheromone genes known as the pheromone-response element (PRE) (Kruzel, Giles et al. 2012). The transcriptional circuit of the pheromone cascade became more complicated with the identification of Znf2, a novel zinc finger transcription factor. Znf2 is required for hyphal development; however, it is dispensable for cell-cell fusion.

Surprisingly, deletion of the gene increases the efficiency of cell fusion events during bisexual reproduction and stimulates pheromone expression during unisexual reproduction (Lin, Jackson et al. 2010). A major genetic difference between unisexual and bisexual reproduction is the mating-type-specific cell identity determinant molecules Sxi1α and Sxi2**a**. Previous studies showed that the homeodomain proteins Sxi1α and Sxi2**a** are required for bisexual reproduction but are dispensable for unisexual reproduction, indicating that they may have a role further downstream of the pathway (Hull, Davidson et al. 2002, Hull, Boily et al. 2005).

All of these components have been found to be essential for hyphal development during both unisexual and bisexual reproduction (with the exception of Sxi1α). It may be that there are additional components that act downstream of the mating pathway and specifically regulate unisexual but not bisexual reproduction. Further experimentation will allow the identification of these factors and elucidate the pathway.

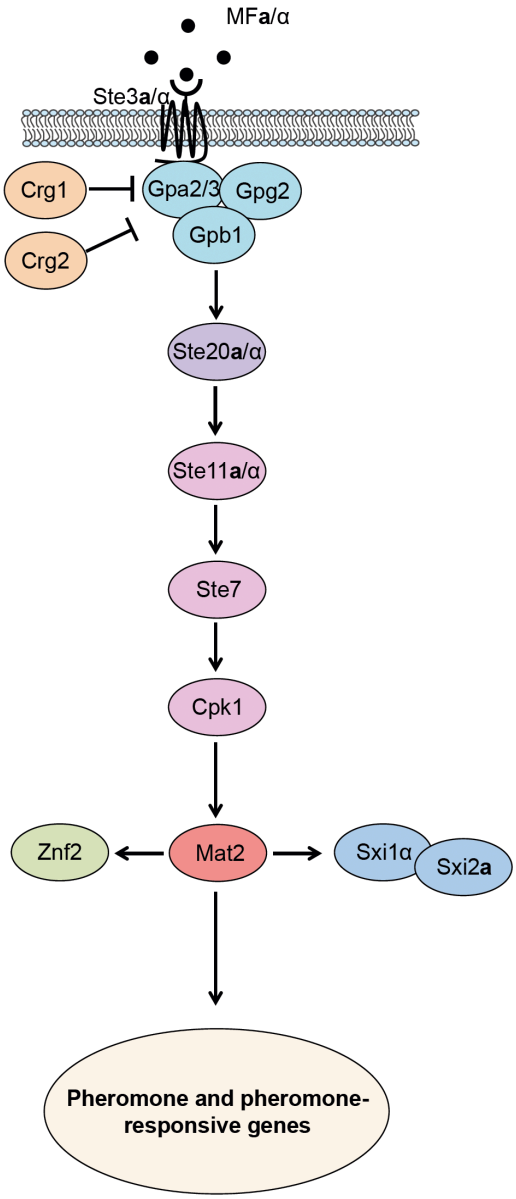

Figure 2. *Cryptococcus neoformans* pheromone response pathway. The pheromone-signaling pathway governs sexual development in *C. neoformans*. Binding of pheromone to the pheromone receptor stimulates the pathway through a G-protein coupled receptor complex that activates the Ste20α/**a** kinase and the three tiered MAPK phosphorelay system. The transcription factor target of the pathway is Mat2, which regulates the expression of sexual- and filamentation-specific genes. Although the signaling-cascade is highly conserved among fungi,

the downstream transcriptional network exhibits extensive rewiring in different species.

1.5 Unisexual reproduction in nature

The components of the mating pathway are highly conserved in the *Cryptococcus* lineages and the sibling species *C. gattii*. However, unisexual reproduction has only been directly observed for the serotype D lineage under laboratory conditions. Recent studies presented evidence that unisexual reproduction also occurs in serotype A and *C. gattii* species. Genotypic analysis of the diploid AD serotype hybrid strains revealed diploid isolates with a homozygous mating type locus produced via α-α mating between α isolates of different serotype αADα (Lin, Litvintseva et al. 2007). Moreover, two independent genetic studies revealed evidence of clonality and recombination in serotype A isolates from trees in India and infected animals in Australia that were exclusively of α mating type (Bui, Lin et al. 2008, Hiremath, Chowdhary et al. 2008). Four identified αAAα diploids were observed to generate hyphae and rare spores when cultured solo on mating media, indicating that unisexual reproduction occurs in this population and these isolates represent an intermediate diploid state of the cycle (Bui, Lin et al. 2008). In an additional study, Lin et al. screened ~500 environmental and clinical isolates and found that ~8% were diploid (Lin,

Patel et al. 2009). Surprisingly, the majority of these were αAAα diploids, among other AD hybrids.

Further studies in the sibling species *C. gattii* yielded similar results. Although *C. gattii* undergoes α-**a** bisexual reproduction under laboratory conditions (Kwon-Chung 1976, Fraser, Subaran et al. 2003), the natural population is predominantly α. Recent genetic studies showed that *C. gattii* isolates from Eucalyptus trees in Australia exhibit evidence of recombination in both mixed and exclusively α mating type populations (Saul, Krockenberger et al. 2008). Moreover, the strains associated with the ongoing outbreak of meningoencephalitis on Vancouver Island and in the Pacific Northwest are mating type α and fertile under laboratory conditions (Kidd, Hagen et al. 2004). Genotypic analysis suggests that the major genotype associated with the outbreak could be the progeny of unisexual reproduction between two parents of α mating type (Fraser, Subaran et al. 2003, Fraser, Giles et al. 2005). In addition, the identification of an α/α diploid intermediate (RB59) and the isolation of particles small enough to be spores present in air samples from Vancouver Island (Fraser, Giles et al. 2005, Kidd, Bach et al. 2007, Kidd, Chow et al. 2007) further strengthens the hypothesis that *C. gattii* undergoes unisexual reproduction in nature. In conclusion, these studies show that unisexual reproduction occurs in nature in several lineages and species of *Cryptococcus*

facilitating the expansion of the pathogen and contributing to the production of infectious spores.

1.6 Environmental and Medical Impact of Unisexual Reproduction

Genotypic analysis of αAAα diploids revealed that the majority of these are homozygous across all of the markers tested, indicating that these isolates are the result of endoreplication or the fusion products of two clonal cells, such as mother-daughter fusion (Lin, Patel et al. 2009). Sexual development typically enables evolution by generating genetic diversity from two genetically distinct parents. Thus, a central question is why undergo unisexual reproduction in a clonal population if there is no pre-existing genetic diversity to admix?

One hypothesis suggests that unisexual reproduction allows cells to generate hyphae and explore their environment. Strains capable of hyphal development invade the growth substratum and forage for nutrients and exhibit a competitive advantage in habitat exploration compared to afilamentous counterparts (Phadke, Feretzaki et al. 2013). We also hypothesize that hyphal development may enhance the ability of the cells to forage for distant compatible mating partners, similar to courtship in *S. cerevisiae*. As mentioned earlier, unisexual reproduction generates a mixture of haploid and diploid hyphae that both generate recombinant progeny. Foraging for mating partners may exert a

selective force on the hyphae to maintain some of the nuclei in a haploid state in case they meet a haploid mating partner to generate a diploid fusion product.

Another model suggests that, in the absence of an opposite mating type partner, unisexual reproduction may serve as practice for sexual development. Sexually active species exhibit enhanced fitness compared to asexual ones, and yet asexual isolates can rapidly emerge in mitotic growth cultures attributable to short term growth advantage. Thus, unisexual reproduction may have evolved to preserve fecundity and confer an evolutionary advantage compared to asexual isolates that may rapidly arise and otherwise overtake vegetative growing populations of cells (Lang, Murray et al. 2009).

However, why an organism would mate with itself when there is no pre-existing genetic diversity to admix remains a mystery. The sexual cycle of *C. albicans* is characterized by the absence of a meiotic cycle. Instead, the **a**/**a**/α/α tetraploid fusion product returns to the diploid state through stochastic chromosome loss that generates a significant level of aneuploidy (2n+1, 2n+2, etc.) (Forche, Alby et al. 2008). During unisexual reproduction between genetically identical cells, this parasexual cycle also generates aneuploid progeny that potentially have a selective advantage compared to their euploid parental strains during infection (Alby, Schaefer et al. 2009). Previous studies have shown that resistance to fluconazole (a major antifungal drug) is attributable to aneuploidy in both *C. albicans* and *C. neoformans* (Selmecki, Forche et al.

2006, Selmecki, Dulmage et al. 2009, Sionov, Lee et al. 2010). Thus, aneuploidy generated via the parasexual cycle during both opposite- and unisexual mating in *C. albicans* may be retained due to selective pressures that favor survival in the mammalian host.

A major disadvantage of bisexual reproduction is the reshuffling of two well-adapted genomes that have already run the gauntlet of adaptive selection. However, unisexual reproduction between genetically identical cells preserves well-adapted genomic configurations and, in the case of both *C. albicans* and *C. neoformans* introduces more limited genetic diversity than outcrossing modes of reproduction. Although this may be a disadvantage in a rapidly changing environment, it has the potential to enhance competitive fitness in response to more subtle changes in the environment, such as the presence of fluconazole during *C. albicans* infection. Therefore, although selfing unisexual reproduction does not admix pre-existing genetic diversity, it is able to generate genetic diversity *de novo* and provide a selective and adaptive benefit during infection.

1.7 Routes of Infection

Sexual reproduction and virulence are tightly linked as sexual cycles can generate and disperse *Cryptococcus* spores in the environment. Infection is thought to be acquired by inhalation of spores or desiccated yeast cells. Early exposure to *Cryptococcus* induces a typically asymptomatic infection that is either cleared by the immune system or develops into a dormant infection as

granulomas that persist for months or even years to decades without causing any overt clinical symptoms (Garcia-Hermoso, Janbon et al. 1999, Goldman, Khine et al. 2001). However, in immunocompromised individuals, such as HIV patients, these dormant fungal cells can reactivate to establish a pulmonary infection (Saag, Graybill et al. 2000). The *Cryptococcus* cells replicate and can then disseminate hematogenously to cause systemic infections of various organs as diverse as skin, liver, the prostate gland, and urinary tract. But most commonly, *C. neoformans* is able to cross the blood-brain barrier and thereby preferentially infect to the brain to cause meningoencephalitis, which is uniformly fatal if untreated.

Interestingly, the sibling species *C. gattii* mainly infects otherwise healthy individuals and is also known to invade both the lungs and the central nervous system (CNS). However, the epidemiology and overall manifestation of the disease is different between the two species. *C. gattii* and *C. neoformans* are equally capable of establishing a pulmonary infection; however, *C neoformans* disseminates to the brain more commonly than *C. gattii*, indicating that the host responds differently to the two pathogens (Kwon-Chung and Bennett 1984, Sirinavin, Intusoma et al. 2004, Shibuya, Hirata et al. 2005).

Both spores and yeast have been found to cause severe infections in the lung and the central nervous system using murine models (Giles, Dagenais et al. 2009, Velagapudi, Hsueh et al. 2009, Springer, Saini et al. 2013). Spores are

readily aerosolized and are of an ideal size to lodge in the alveoli of the lung to cause a pulmonary infection. Moreover, yeast cells are more fragile in the environment, while the spores have a thicker cell wall that confers resistance to desiccation, high temperature, and oxidative stress (Botts, Giles et al. 2009, Velagapudi, Hsueh et al. 2009). Although, spore production has not been directly observed in nature, population genetic studies support the hypothesis that unisexual reproduction and limited bisexual reproduction (wherever an opposite mating type is available) occurs in natural populations, which will allow the production of spores. In addition, recent studies found that a high density of particles small enough to be spores are isolated from air samples from *Cryptococcus* outbreak locations on Vancouver Island (Kidd, Bach et al. 2007, Kidd, Chow et al. 2007). These findings provide further evidence that spores are well suited for air-dispersal and survival, and support the hypothesis that spores are infectious propagules of *Cryptococcus*.

1.8 Unisexual Reproduction, Hyphal Development, and Virulence

Dimorphism is relatively rare in the fungal kingdom, however it is common among pathogenic fungi. One well studied example is the human fungal pathogen *C. albicans*, where transitions between yeast and hyphal growth are required for survival and dissemination during infection (Lo, Kohler et al. 1997). *Candida* typically grows as a yeast and hyphal development is associated with the pathogenic form of the fungus. Following phagocytosis, *C. albicans* produce

hyphae that kill macrophages and allow the fungus to escape and proliferate inside the host (Lorenz, Bender et al. 2004). Surprisingly, fungi that we often encounter in a saprophytic filamentous form in the environment undergo a dimorphic switch to unicellular yeast during infection. *Blastomyces dermatitidis* and *Histoplasma capsulatum* are human pathogens that grow as hyphae in the environment. Inhaled spores reach the lung, where the high temperature of the host induces a dimorphic transition to yeast growth and enables establishment of a pulmonary infection, similar to *Cryptococcus* (Maresca and Kobayashi 2000). The association of yeast growth with the parasitic form of these environmental dimorphic fungi may have evolved due to the selective pressure applied by the mammalian and other heterologous hosts. The morphological differentiation during infection is of great medical importance as it could represent a possible therapeutic target to control fungal systemic infections.

In *C. neoformans* morphological differentiation is closely linked to sexual development. During infection *Cryptococcus* grows as a yeast in various organs. Although rare, hyphae and pseudohyphae have been occasionally observed in human and animal tissues (Freed, Duma et al. 1971, Lurie and Shadomy 1971, Shadomy and Lurie 1971, Anandi, Babu et al. 1991, Williamson, Silverman et al. 1996). The rare observation of *Cryptococcus* hyphae *in vivo* suggests that hyphal development may be associated with lower pathogenicity. A few earlier studies showed that purified hyphae exhibit lower virulence compared to their yeast

counterparts and hyphal fragments *in vivo* were observed only in the lung during the early stages of infection (Shadomy and Utz 1966, Zimmer, Hempel et al. 1983). Previous studies found that high temperature and elevated CO_2 levels inhibit hyphal formation (Sia, Lengeler et al. 2000, Bahn, Cox et al. 2005). Thus, it is possible that hyphal development occurs in the host where the temperature and CO_2 concentration are lower, such as the skin and the upper respiratory tract. Likewise, pseudohyphae are attenuated for virulence in the mammalian host (Williamson, Silverman et al. 1996, Gazzoni, Oliveira Fde et al. 2010); however, pseudohyphal formation is required for survival within *Acanthamoeba* species (Neilson, Ivey et al. 1978). Following exposure to amoeba, surviving *Cryptococcus* strains that exhibited high rates of reversion to yeast growth were restored to pathogenicity in murine animal models (Neilson, Ivey et al. 1978, Magditch, Liu et al. 2012). These results indicate that pseudohyphae and hyphae are less fit for growth inside the mammalian host; however, they may be occasionally induced following phagocytosis by macrophages (or amoeba cells in the environment), which may provide an escape strategy during infection, similar to *C. albicans*.

Hyphal development is triggered during α-**a** bisexual and α-α unisexual reproduction. Thus, the signaling pathway that regulates sexual development has been extensively investigated for its role in virulence. Virulence is specifically linked with the *MAT*α locus, which in part explains the predominance of this

mating type in clinical and environmental isolates (Kwon-Chung, Edman et al. 1992, Nielsen, Cox et al. 2003). The *MAT* locus encodes several components of the pheromone-signaling cascade, including the pheromones, pheromone receptors, kinases (i.e. *STE20*α/**a**), and transcription factors (*SXI1*α/*SXI2***a** and *STE12*α/*STE12***a**). However, the components of the pathway exhibit minimal or no impact on virulence. Nevertheless, it is possible that downstream targets may specifically govern morphogenesis (including cell shape) and play important roles in pathogenesis.

As mentioned earlier unisexual reproduction seems to be a predominant sexual cycle in nature. However, unisexual reproduction has been directly observed under laboratory conditions only in the low pathogenic strains of serotype D. Therefore, possible roles of hyphal development in pathogenesis have not been extensively studied and the link between morphogenesis and virulence remains elusive. Further investigations will elucidate the molecular mechanisms and evolutionary impact of hyphal development on virulence and possibly establish a foundation for future novel therapeutic approaches.

1.9 Cryptococcus Virulence Factors

There are three major virulence attributes that allow *Cryptococcus* to survive and thrive inside the host: melanin, capsule, and the ability to grow at physiological temperature (37^{o}C). Capsule is a polysaccharide structure attached

to the cell wall and it can be analyzed to determine the serotype status of strains. Mutants defective in the synthesis, secretion, or the attachment of capsule are unable to cause disease in animal models (Chang, Wickes et al. 1995, Reese and Doering 2003). Capsule protects cells from dehydration in the environment, and confers resistance to phagocytosis during infection (Kozel and Gotschlich 1982). Melanin is a hydrophobic brown pigment associated with the cell wall that is negatively charged. In the environment it protects the cell from UV irradiation and extreme temperatures (Wang and Casadevall 1994, Rosas and Casadevall 1997). During infection it shields cells from oxidative and nitrosative stress and, together with capsule, it protects the cells from macrophage killing (Wang and Casadevall 1994, Wang, Aisen et al. 1995).

1.10 Cryptococcus and the Immune System

Inhaled spores that reach the lung parenchyma are cleared by a protective immune response. Alveolar macrophages are the front line phagocytes that encounter *Cryptococcus* cells in the lung and are responsible for antigen presentation and cytokine production. Interestingly, spores and yeast cells interact differently with macrophages under laboratory conditions. Yeast cells require opsonization to be phagocytosed by macrophages, while spores are readily engulfed in the absence of an opsonin (Giles, Dagenais et al. 2009, Velagapudi, Hsueh et al. 2009). Spores are able to germinate, grow, and proliferate within macrophages. In immunocompromised individuals the absence

of a T-cell mediated immune response allows intracellular survival and proliferation of yeast cells. There is evidence that fungal cells can cross the blood-brain barrier (BBB) in immunocompromised individuals by a “Trojan Horse” strategy where the replicating cell disseminates by hiding within macrophages that migrate to the brain through blood circulation (Charlier, Nielsen et al. 2009). Remarkably, live *Cryptococcus* cells were found to be expelled by macrophages in a non-destructive expulsion process in which neither the host cell nor the pathogen is killed (Alvarez and Casadevall 2006, Ma, Croudace et al. 2006). This process renders fungal cells “invisible” to the immune system and allows them to evade macrophages without killing them, which would trigger an inflammatory response. Dendritic cells are also thought to be important against pulmonary cryptococcosis and they are responsible for inducing an adaptive immune response by presenting cryptococcocal antigens to naïve T cells (Syme, Spurrell et al. 2002, Levitz and Specht 2006).

Host defenses against *Cryptococcus* and the outcome of disease are orchestrated by T cell-mediated immunity. Exposure to pathogens triggers the production of two groups of cytokines by CD4+ T cells: Th1 and Th2. The balance between Th1 and Th2 cytokines greatly affects the outcome of disease and subsequently survival of the host. The predominance of Th1 cytokines stimulates a protective immune response characterized by high levels of IL-2, IL-12, interferon-gamma (INF-γ), and tumor necrosis factor-alpha (TNF-α). During

C. neoformans infection Th1 and Th2 type cytokines stimulate an influx of neutrophils, dendritic cells, and activated macrophages that deploy a variety of mechanisms to eradicate intracellular Cryptococci, including oxidative and nitrosative stress (Koguchi and Kawakami 2002, Chen, McNamara et al. 2008, Guillot, Carroll et al. 2008, Ma and May 2009). Serotype D isolates of *C. neoformans* predominantly induce an adaptive Th1 protective inflammatory response, while serotype A triggers both Th1 and Th2 immunity that successfully clears the infection in the majority of healthy individuals (Chen, Sorrell et al. 2000, Noverr, Cox et al. 2003, Jain, Zhang et al. 2009, Hardison, Ravi et al. 2010). However, in HIV patients, where T-cell mediated immunity is impaired, the innate immune response is the first and can be the only line of defense against the pathogen and the outcome of the disease is mediated by the interaction between innate immunity and *Cryptococcus* (Shao, Mednick et al. 2005).

On the other hand, *C. gattii* infects immunocompetent individuals and is able to cause severe infections of the central nervous system. *C. gattii* is successful in replicating at higher rates within macrophages, escaping, and preferentially disseminating to the brain, which could contribute to its emergence and expansion beyond Vancouver Island (Byrnes, Bildfell et al. 2009, Byrnes, Li et al. 2009, Ma, Hagen et al. 2009). Surprisingly, a recent study found that the major Vancouver Island strain R265 stimulates the expression of Th2-type cytokines in an animal model (Cheng, Sham et al. 2009). Th2 associated

cytokines, such as IL-4, IL-5, IL-10, and IL-13 induce a non-protective immune response characterized by diffuse inflammation, eosinophil infiltration, alternatively activated macrophages, and immature dendritic cells at the site of the infection. Moreover, during cryptococcal infection high levels of IL-4 and IL-10 suppress the production of INF-γ and IL-12 by macrophages and subsequently inhibit the functions of Th1 cytokines, which attenuates the host immune response and exacerbates disease (Kronstad and Leong 1989). It is possible that the ability of *C. gattii* strains to induce the production of Th2 cytokines in the lungs serves to inhibit neutrophil migration during the initial stages of the infection and thereby blunts the ability to mount a protective Th1 immune response. Therefore, the host is not able to clear the infection, which spreads within the lungs and then later disseminates to the brain.

1.11 Unisexual Reproduction Beyond Cryptococcus Species

Unisexual reproduction is widespread in pathogenic microbes. *C. albicans* is the most common human fungal pathogen and was until recently thought to be strictly asexual. An extant heterothallic parasexual cycle has been defined involving diploid **a**/**a** and α/α cells that undergo cell-cell fusion and nuclear fusion, yielding a tetraploid intermediate (Hull, Raisner et al. 2000, Magee and Magee 2000). Surprisingly, meiosis has not yet been observed in *C. albicans,* and the tetraploid returns to the diploid state through stochastic parasexual chromosome

loss, which generates considerable aneuploidy, as well as infrequent Spo11-dependent recombination (Forche, Alby et al. 2008). Unexpectedly, **a**/**a** cells can express both the **a** and α pheromone genes in response to nutrient limitation (Bennett and Johnson 2006), which led to the discovery of a unisexual cycle in *C. albicans* (Alby, Schaefer et al. 2009). Mutation of Bar1, a protease that cleaves α-factor to regulate autocrine and paracrine signaling, enables an **a**-**a** unisexual cycle (Alby, Schaefer et al. 2009). This homothallic parasexual cycle is also induced in ménage à trois matings in which a third mating type partner in limited abundance donates pheromone to promote **a**-**a** or α-α mating (Alby, Schaefer et al. 2009). Remarkably, pheromones from other species such as *Candida dubliniensis* or *Candida parapsilosis* can induce unisexual reproduction of *C. albicans* (Alby and Bennett 2011).

There are other pathogenic fungi once thought to be asexual that we now appreciate may be cryptically sexual or unisexual. A few examples include species of *Neurospora*, such as *N. africana*, *N. galapagosensis*, *N. dodgei*, and *N. lineolata* that may undergo unisexual reproduction given that their populations appear to harbor only one *MAT* locus idiomorph (Mahoney, Huang et al. 1976, Glass, J. et al. 1988, Arnaise, Zickler et al. 1993, Glass and Smith 1994, Nygren, Strandberg et al. 2011). Furthermore, the obligate intracellular microsporidian fungal pathogen *Encephalitozoon cuniculi* contains two HMG domains similar to the *MAT* locus of zygomycetes, although an extant sexual cycle has not been

observed (Lee, Corradi et al. 2010). Recent studies have revealed low levels of heterozygosity in four *E. cuniculi* strains, indicative of a diploid nuclear state that may reflect a cryptic unisexual cycle in this “asexual” fungus (Selman, Sak et al. 2013).

Until recently the intestinal parasite *Giardia intestinalis* was thought to be asexual; however, population genetic studies revealed evidence of genetic exchange, and the genome harbors a suite of meiotic genes (Ramesh, Malik et al. 2005, Cooper, Adam et al. 2007). This diplomonad parasite is binucleate, and the two diploid nuclei of a single isolate can fuse to exchange genetic information, followed by homologous recombination that is possibly directed by meiotic gene homologs shown to be expressed at appropriate developmental stages (Poxleitner, Carpenter et al. 2008). The cues that trigger cell-cell fusion in the population remain to be explored, however, measures of genetic exchange in the population provide evidence that outcrossing is likely occurring. In the pathogen *Leishmania*, which is highly clonal and was therefore thought to be asexual, recent studies have revealed that an extant sexual cycle occurs in the sand fly vector (Akopyants, Kimblin et al. 2009, Rougeron, Banuls et al. 2011, Inbar, Akopyants et al. 2013). Both outcrossing and selfing have been observed in *Plasmodium* species, in which a single isolate can differentiate and produce fertile male and female gametes that undergo sexual reproduction. In *Trypanosoma,* diploids may fuse to create an intermediate tetraploid that may

undergo random chromosome loss through a parasexual cycle, similar to *C. albicans* (Gaunt, Yeo et al. 2003). In *Toxoplasma gondii*, sexual outcrossing and subsequent self-mating generated highly virulent *T. gondii* clones that were responsible for a toxoplasmosis outbreak in Brazil and other global locales (Wendte, Miller et al. 2010). Unisexual reproduction preserved a well-adapted genomic configuration and generated abundant spores fueling this outbreak.

1.12 Overview of This Work

The theme of this work is centered on unisexual reproduction of *C. neoformans* serotype D strains. We explore the evolution and impact of unisexual reproduction and its links to virulence. We also dissect the genetic elements that orchestrate α-α mating and identify novel regulators involved in diverse mechanisms.

In chapter 2 we report that unisexual reproduction generates phenotypic and genotypic diversity *de novo* in a clonal population, including aneuploidy. We show that the genetically diverse progeny exhibit enhanced competitive fitness and we suggest that unisexual reproduction is an evolutionary strategy to enable rapid adaptation to novel environments, such as the mammalian host. In chapter 3 we explore the link between unisexual reproduction and virulence. We found that a hyperfilamentous strain of the low pathogenic serotype D lineage is hypervirulent in the animal model compared to its avirulent hypofilamentous

parent. Interestingly, we show that this strain elicits a Th2 type immune response that is usually associated with the highly pathogenic strains of *C. gattii* VGII type. In chapter 4 we conducted an *Agrobacterium tumefaciens* insertional mutagenesis screen to identify novel regulators of unisexual reproduction. We found that Spo11 and Ubc5 are required for sporulation and meiosis during unisexual reproduction and we provide evidence to support the hypothesis that the highly conserved regulator Spo11 catalyzes the formation of double strand breaks to initiate meiotic recombination. In addition we found a novel zinc finger protein, Znf3, that is required for hyphal development and pheromone expression during unisexual and bisexual reproduction. To our surprise, a whole genome expression microarray showed that Znf3 inhibits the expression of retrotransposons, indicating that it may be involved in transposable element silencing. In chapter 5 we investigated the roles of Znf3 in mitotic- and sex-induced silencing (MIS and SIS). We demonstrate that Znf3, along with the components of the RNAi machinery (Rdp1, Dcr1/2, and Ago1), is required for MIS and SIS during vegetative growth and sexual development, respectively. (Lin, Hull et al. 2005). We also found that the genome-wide expression profile of *znf3*Δ mutants is very similar to that of *rdp1*Δ mutants, indicating that the two proteins may function in the same pathway during silencing. Localization of Znf3 in P-bodies, the cellular compartments where mRNA decay and RNAi occurs,

further supports the hypothesis that Znf3 is a novel regulator of mRNA silencing that may participate directly or indirectly in RNAi pathways.

Chapter 2. Unisexual and Heterosexual Meiotic Reproduction Generate Aneuploidy and Phenotypic Diversity *de novo* in the Yeast *Cryptococcus neoformans*[1]

2.1 Introduction

Aneuploidy, a condition in which cells have an abnormal number of chromosomes, can cause deleterious effects in organisms throughout the eukaryotic tree of life. Aneuploidy underlies several common human genetic diseases, including trisomy 21 in Down syndrome and trisomy 13 in Patau syndrome (Patau, Smith et al. 1960, Patterson 2009), and is detected in more than 90% of solid tumors (Weaver and Cleveland 2006, Gordon, Resio et al. 2012). The presence of even a single extra chromosome in primary mouse embryonic fibroblasts (MEFs) results in proliferative defects and metabolic aberrations (Williams, Prabhu et al. 2008). In *Caenorhabditis elegans* and *Drosophila melanogaster*, aneuploidy is often lethal (Lindsley, Sandler et al. 1972, Hodgkin 2005), and in budding and fission yeasts, aneuploidy can inhibit cellular proliferation (Torres, Sokolsky et al. 2007, Cetin and Cleveland 2010).

However, aneuploidy can be advantageous in fungi by conferring antifungal drug resistance and enabling rapid adaptive evolution. Aneuploidy

---

[1] Some of the material in this chapter can be found in: Ni, M., M. Feretzaki, W. Li, et al. (2013). "Unisexual and heterosexual meiotic reproduction generate aneuploidy and phenotypic diversity *de novo* in the yeast *Cryptococcus neoformans*." PLoS Biol **11**(9): e1001653.

evokes transcriptomic and proteomic changes in the model yeast *Saccharomyces cerevisiae* (Torres, Sokolsky et al. 2007, Pavelka, Rancati et al. 2010). Mutations in a deubiquitinating enzyme of *S. cerevisiae*, which arose during the evolution of an aneuploid isolate, lead to improved proliferation of many aneuploid strains, likely by promoting degradation of aberrant proteins produced in perturbed stoichiometric ratios (Torres, Dephoure et al. 2010). Rancanti et al. found that aneuploidy facilitated adaptive evolution in yeast cells lacking the conserved motor protein Myo1 involved in cytokinesis (Rancati, Pavelka et al. 2008). Moreover, it has been found that chromosomal duplication may confer a selective advantage to *S. cerevisiae* under stress conditions by promoting genomic instability and mutation, and although it is a transient solution, the short-lived aneuploid intermediate may also serve as a capacitator of evolution (Sheltzer, Blank et al. 2011, Yona, Manor et al. 2012). In the human pathogenic fungi *Candida albicans* and *Cryptococcus neoformans*, aneuploidy can confer resistance to commonly used antifungal drugs such as fluconazole (Selmecki, Forche et al. 2006, Selmecki, Dulmage et al. 2009, Sionov, Lee et al. 2010, Kwon-Chung and Chang 2012). In *C. albicans*, haploids can even arise from concerted chromosome loss from diploid progenitors (Hickman, Zeng et al. 2013). In *C. albicans,* an isochromosome 5 can arise in response to fluconazole treatment and confers drug resistance because the left arm of Chr 5 encodes Erg11 (lanosterol 14α demethylase), the target of fluconazole, and Tac1, a

transcription factor that activates expression of drug export pumps (Selmecki, Forche et al. 2006, Selmecki, Dulmage et al. 2009). Similarly in *C. neoformans*, Chr 1 disomy confers azole resistance because this chromosome harbors *ERG11* and *AFR1* (which encodes the major azole efflux pump) and aneuploidy can also influence the virulence of this pathogen (Hu, Liu et al. 2008, Sionov, Lee et al. 2010, Hu, Wang et al. 2011). Interestingly, a similar drug-resistance phenotype has been observed in the protozoan parasite *Leishmania*, in which resistance to front line antimonial-based drugs similarly emerges via aneuploidy (Ubeda, Legare et al. 2008, Leprohon, Legare et al. 2009).

C. neoformans is a globally distributed human fungal pathogen that causes life-threatening meningoencephalitis (Heitman, Kozel et al. 2011). *Cryptococcus* predominantly infects individuals with compromised immunity, such as HIV/AIDS patients. The United States Centers for Disease Control (CDC) has reported that *C. neoformans* causes more than one million cases of cryptococcosis annually with more than 620,000 attributable mortalities, resulting in approximately one-third of all AIDS-associated deaths (Park, Wannemuehler et al. 2009). This fungal pathogen has now surpassed tuberculosis as a common cause of death in Africa.

C. neoformans is a basidiomycetous fungus that usually grows in the environment as a haploid, budding yeast. This species has a bipolar mating system with two mating types: **a** and α (Hull and Heitman 2002, Lengeler, Fox et

al. 2002, McClelland, Chang et al. 2004). In response to a variety of environmental conditions, **a** and α cells secrete lipid-modified peptide pheromones that induce cell–cell fusion, and the resulting dikaryon undergoes a dimorphic transition to hyphal growth (Kwon-Chung 1976, Hull and Heitman 2002, Nielsen, De Obaldia et al. 2007, Xue, Tada et al. 2007). Ultimately, the hyphal tips form basidia fruiting bodies wherein nuclear fusion and meiosis occur, and multiple rounds of mitosis and budding result in the production of four long chains of infectious spores decorating each basidium. These spores are readily aerosolized and cause infections in humans and animals when inhaled (Giles, Dagenais et al. 2009).

While *C. neoformans* has a defined **a**-α opposite sexual cycle, >99% of natural isolates are of the α mating type (Kwon-Chung and Bennett 1978). *C. neoformans* var. *neoformans* (serotype D) α cells can undergo α-α unisexual reproduction to generate spores under laboratory conditions (Lin, Hull et al. 2005). Recent population genetic studies provide evidence that multiple pathogenic lineages of *C. neoformans* var. *grubii* (serotype A) and the sibling species responsible for the Vancouver outbreak *Cryptococcus gattii* (serotype B and C) undergo α-α sexual reproduction in nature, but this remains to be documented under laboratory culture conditions (Wickes, Mayorga et al. 1996, Lin, Litvintseva et al. 2007, Nielsen, De Obaldia et al. 2007, Bui, Lin et al. 2008,

Hiremath, Chowdhary et al. 2008, Saul, Krockenberger et al. 2008, Lin, Patel et al. 2009, Chowdhary, Hiremath et al. 2011). Under nutrient-limiting conditions α haploid cells form a diploid or a haploid monokaryotic hyphae. The haploid hyphae grow to form basidia where a late diploidization event occurs. In the diploid hyphae diploidization of the nuclear content may be induced early and results in a diploid monokaryon that initiates hyphal growth and the formation of apical basidia. Early diploidization may occur through endoreplication or cell–cell fusion. Cell fusion, followed by nuclear fusion, may be induced in ménage à trois matings where **a** cells serve as pheromone donors to stimulate α-α fusion between genetically different or clonal cells (Lin, Hull et al. 2005). Endoreplication may occur in cells that undergo DNA replication without cell division or they may undergo nuclear division and then fusion. In all cases, the resulting diploid nucleus undergoes meiosis and multiple rounds of mitosis generate the meiotic progeny, the basidiospores. In previous studies, we found that the key meiotic regulators, the endonuclease Spo11 and the meiotic recombinase Dmc1, are required for spore production and germination during unisexual reproduction (Lin, Hull et al. 2005, Feretzaki and Heitman 2013). Deletion of *SPO11* or *DMC1* severely impairs sporulation and the fewer meiotic progeny generated are largely inviable, providing further evidence that unisexual reproduction is a meiotic process (Lin, Hull et al. 2005, Feretzaki and Heitman 2013).

Remarkably, unisexual reproduction has been recently discovered to occur in another common systemic human fungal pathogen, *C. albicans* (Alby, Schaefer et al. 2009). *C. albicans* is known to undergo a parasexual cycle involving heterothallic fusion of α and **a** mating type cells followed by stochastic, concerted loss of chromosomes (Forche, Alby et al. 2008). Similarly, fusion of α-α and **a**-**a** cell unions via homothallic parasexual reproduction occurs when a pheromone-degrading protease (Bar1) is inactivated or in ménage à trois matings, in which a third mating partner serves only as the pheromone donor (Alby, Schaefer et al. 2009).

Sex is costly, and thus the question arises as to why *C. neoformans* or *C. albicans* would undergo inbreeding/selfing unisexual reproduction, which would limit the amount of genetic diversity inherited from the parents, as opposed to **a**-α sexual reproduction, which promotes outcrossing and genetic exchange. We hypothesize that unisexual reproduction is a hypermutagenic process that generates genetic diversity *de novo* and that the resulting progeny can thereby more rapidly adapt to changing environments than cells produced asexually by mitosis.

To test this hypothesis, we isolated progeny generated via selfing α-α unisexual reproduction and subjected them to phenotypic and genotypic analyses. Remarkably, we found that α-α unisexual reproduction generates

frequent phenotypic diversity, including temperature sensitivity, fluconazole resistance or sensitivity, and increased melanin production among other novel traits. Further comparative genomic hybridization (CGH) analysis revealed that the majority of phenotypically diverse progeny are aneuploid. Phenotypic diversity is caused by this aneuploidy, as loss of the aneuploid chromosomes restored both euploidy and the wild-type parental phenotype. Aneuploidy and phenotypic variation was also found to occur at a similar rate following **a**-α bisexual reproduction but not as a result of mitotic asexual vegetative growth. Our findings show that sex can generate phenotypic and genotypic diversity *de novo* in the pathogenic yeast *C. neoformans* with implications for other eukaryotic microbes and pathogens, including other fungi and parasites that are common pathogens of humans.

2.2 Materials and Methods

2.2.1 Ethics Statement

All of the animal studies were conducted in the Division of Laboratory Animal Resources (DLAR) facilities at Duke University Medical Center (DUMC). All of the animal work was performed according to the guidelines of NIH and Duke University Institutional Animal Care and Use Committee (IACUC). The animal experiments were reviewed and approved by the DUMC IACUC under protocol number A266-08-10.

2.2.2 Strains and Media

Strains and plasmids used in this study are listed in Table 1. Yeast cells were grown on YPD media. Mating of *C. neoformans* was conducted on 5% V8 juice agar medium (pH = 7).

Table 1. Strains and plasmids used in Chapter 2

Strain	Genotype	Source/Reference
C. neoformans var. *grubii* (serotype A)		
KN99**a**	*MAT***a**	(Nielsen, Cox et al. 2003)
KN99α	*MAT*α	(Nielsen, Cox et al. 2003)
MN503 to MN596	Mating progeny from KN99**a** × KN99α cross	This study
C. neoformans var. *neoformans* (serotype D)		
XL280	*MAT*α	(Lin, Huang et al. 2006)
JEC20**a**	*MAT***a**	(Kwon-Chung, Edman et al. 1992)
JEC21α	*MAT*α	(Kwon-Chung, Edman et al. 1992)
XL566	*MAT*α *ura5*	(Lin and Heitman, unpublished data)
MN1 to MN90	Progeny from same-sex mating of XL280	This study
MN201 to MN290	Mating progeny from JEC20**a** × JEC20α	This study
MN301 to MN390	XL280 mitotic progeny grown on YPD	This study
MN140.23	*MAT*α *ura5* P_{GPD1}::*SXI2***a**::*URA5*	This study
MN401 to MN501	Progeny from α-α same-sex mating of MN140.23	This study
MN711 to MN806	XL280 mitotic progeny grown on mating V8 media	This study
MF180	MN7 *NEO*	This study
XL561	XL280 *NAT*	(Lin and Heitman, unpublished data)
MF182	Diploid fusion isolate from MN7 *NEO* × XL280 *NAT*	This study
MF183	Diploid fusion isolate from MN7 *NEO* × XL280 *NAT*	This study
MF184	Diploid fusion isolate from MN7 *NEO* × XL280 *NAT*	This study
MF186	MN7 + pMF86	This study
MF187	MN7 + pMF89	This study
Plasmid		
pCH285	P_{GPD1}::*SXI2***a**::*URA5 Amp*^{R}	(Hull, Boily et al. 2005)
pMN7	pCH285 without telomeric sites	This study
pJAF12	*NEO AMP*	(Fraser, Subaran et al. 2003)
pMF86	pJAF12 *HSC20 NEO AMP*	This study
pMF89	pJAF12 *HSC20 NEO AMP*	This study

2.2.3 Sequencing of *C. neoformans*

DNA sequencing was performed on a Genome Analyzer IIx using Illumina Paired Ends technology. The genomic DNA samples were fragmented with a Bioruptor sonicator (Diagenode). Fragmented DNA was used for size selection

by extraction (Qiagen) of 300 to 400 bp DNA fragments from 2% agarose gels after electrophoresis. Size-selected DNA was used for standard Illumina library preparation protocols. Prepared libraries were sequenced using Paired Ends 2×76 cycles. This approach provided the most suitable sequencing data for SNP and small indel detection and deep sequencing coverage.

2.2.4 Genomic Sequence Assembly Protocol

The Illumina-Solexa data were assembled using a combination of *de novo* assembly (Velvet) and reference genome assembly (BWA) to assemble the *Cryptococcus* genomic sequence. We used BWA and SAMtools to determine the depth of sequence coverage and identify polymorphisms, particularly SNPs and indels. In addition to the use of BWA for reference genome assembly, we checked the completeness of the assemblies by extracting all sequence reads that BWA was unable to align to the reference genome and assembled these reads using Velvet. The resulting contigs were compared back to the genome sequence and also used to search GenBank using Blast. This method allows identification of regions with multiple polymorphisms that cannot be identified by BWA due to the inability of the short reads to be aligned to the reference sequence. In addition, these contigs typically originate from highly repetitive sequence, such as the rDNA and telomeres. With this *Cryptococcus* dataset, more than 90% of the unaligned reads were low-quality sequence reads. Overall, the assembly was an iterative process. After polymorphisms were identified in an

initial round of sequence assembly with BWA and Velvet, a new consensus sequence was generated, and the assembly was repeated. In the second and subsequent rounds of assembly, polymorphisms were identified in regions where there were multiple polymorphisms. After several rounds, no additional polymorphisms were identified, and the assembly was considered complete.

2.2.5 Ploidy Determination by FACS

The ploidy of progeny was determined by flow cytometry as described previously (Tanaka, Taguchi et al. 1996). Briefly, cells were collected from overnight YPD liquid medium, washed once in 1X PBS buffer, and fixed in 1 mL of 70% ethanol overnight at 4 °C. Fixed cells were washed once with 1 mL of NS buffer (10 mM Tris-HCl [pH = 7.6]; 250 mM sucrose; 1 mM EDTA [pH = 8]; 1 mM $MgCl_2$; 0.1 mM $CaCl_2$; and 0.1 mM $ZnCl_2$) and then stained with propidium iodide (0.3 mg/mL) in 200 µL of NS buffer containing RNaseA (1 mg/mL) at room temperature for 4 hrs. Then, 50 µL of the stained cell preparation was diluted into 2 mL of 50 mM Tris-HCl (pH = 7.5) and sonicated for 1 min. Flow cytometry was performed on 10,000 cells and analyzed on the FL1 channel of a Becton-Dickinson FACScan.

2.2.6 Complementation of *hsc20-1* TS Mutation in MN7

The strain MN7 was transformed with the dominant selectable drug marker NEO, amplified from plasmid pJAF1 using the universal primers M13F

and M13R. The strain MN7 *NEO* was mixed with strain XL280α *NAT* and incubated on mating media for 48 hrs. The mating culture was scraped off the plate, washed in water, serially diluted, and plated on YPD + NAT + NEO medium. The ploidy of the fusion products was determined by FACS. Multiple diploid isolates were phenotypically analyzed at 30°C and 37°C to determine the recessive nature of the TS mutation in strain MN7.

The wild-type *HSC20* gene with its native promoter (269 bp) and terminator (246 bp) was amplified from XL280α genomic DNA using the primer pair JOHE38840/JOHE38841 and cloned in the pJAF12 plasmid using KpnI restriction enzyme (NEB) (Fraser, Subaran et al. 2003). Two independently derived plasmids, pMF86 and pMF89, were obtained and confirmed by sequencing. The plasmids were introduced into strain MN7 via biolistic transformation, and multiple isolates were obtained and analyzed phenotypically.

2.2.7 Pulsed-Field Gel Electrophoresis (PFGE) of *C. neoformans*

A single colony was inoculated into 5 mL of liquid YPD medium and grown overnight at room temperature (RT) while shaking. Then, 1 mL of the culture was added to 50 mL of yeast nitrogen base minimal medium (YNB) with 1 M NaCl (to suppress capsule formation), which was then grown overnight at RT on a shaking platform incubator. Yeast cells were then washed three times in 0.5 M NaCl/50 mM EDTA (pH = 8.0). Then, 50 mg of cells were mixed with 450 μL of

low-melting point agarose (Bio-Rad 0.5% in 0.1 M EDTA [pH = 8.0]) and 20 μL of cell wall lysing buffer (25 mg/mL Zymolase in 10 mM KPO_4 [pH = 7.5]) and poured into molds. The plugs were solidified for 15 min at RT, transferred into 700 μL of lysing solution (0.5 M EDTA, 10 mM Tris-HCl [pH = 8]), and lysed overnight at 37°C. The next morning, 400 μL of proteinase K solution (5% sarcosyl, 5 mg/ml proteinase K, 0.5 M EDTA [pH = 8.0]) were added, and the plugs were further incubated at 50°C for 5 h. The plugs were then washed three times for 1 h each with wash solution (50 mM EDTA, 10 mM Tris-HCl [pH = 8.0]). Then, 1% gels made with pulse field certified agarose in 0.5X TBE buffer were run with a BioRad CHEF Mapper XA system. Running conditions were according to the CHEF Mapper calculation, with appropriate modifications.

2.2.8 Comperative Genomic Hybridization (CGH) and Band Array

Genomic DNA was ultrasonicated to generate ~500-bp fragments and purified with a DNA Clean and Concentrator kit (Zymo Research, CA). Then, 2.5 μg of DNA was used for Cy3 dUTP or Cy5 dUTP labeling reactions using the Random Primer/Reaction Buffer mix (BioPrime Array CGH Genomic Labeling System, Invitrogen). Labeled DNA was then hybridized to microarray slides of 70-mer oligonucleotides for the *C. neoformans* JEC21 (Kraus, Boily et al. 2004) or the *C. neoformans* JEC21 and H99 genomes (Washington University, St. Louis, MO). After hybridization, arrays were scanned with a GenePix 4000B

scanner (Axon Instruments). Data analysis was performed with Genespring GX v7.3 (Agilent Technologies) and CGH-miner. Band array was performed as described previously (Argueso, Westmoreland et al. 2008). Briefly, chromosomes were separated by PFGE and the bands of interest were excised and treated to extract the DNA. Band DNA was labeled with Cy5 and hybridized to microarrays with Cy3-labeled whole genome DNA.

2.2.9 Multiplex PCR

Genomic DNA was extracted using the CTAB protocol as described previously (Pitkin, Panaccione et al. 1996). We utilized the Qiagen multiplex PCR kit for multiplex PCR. PCR reaction mixtures (25 µL) contained 12.5 µL of Qiagen multiplex PCR master mix, 2 µM equimolar primer mixture (Table 2), and 100 to 300 ng of genomic DNA. Thermal cycling conditions included an initial heat activation of 15 min at 95^{o}C followed by 30 cycles of denaturation for 30 s at 94^{o}C, annealing for 90 s at 58.7^{o}C, and extension for 10 min at 72^{o}C. For bioanalyzer analysis, 1 µL of PCR reaction was examined with the Experion DNA 12K Analysis Kit (Bio-Rad). Multiplex PCR reactions were analyzed by gel electrophoresis using 1.8% agarose gels in 1×TBE buffer (Tris/Borate/EDTA buffer). 2 µL of PCR reaction were loaded in the gels that were run overnight at 30 volts or for 5 hrs at 100 volts. The intensity of the desired bands, which represent the aneuploid chromosomes, was quantified relative to the control

band using the Gel Doc XR+ system of BIO-RAD and Image Lab version 4 software.

Table 2. Multiplex PCR oligonucleotides used in Chapter 2.

Primer	Sequence (5' to 3')	Chr	Positions	Amplicon length (bp)
JOHE21844/MN174	ACGTTTCTTGCCCTACATGG	1	10514	131
JOHE21845/MN175	GTTGTTAGCACGGCCTTTTC	1	10644	
JOHE21846/MN176	GTTGCTGACACCTTGGAACA	2	10778	192
JOHE21847/MN177	ACGTGTATAGGGCCAAGCAG	2	10969	
JOHE21848//MN178	ATCTATCGGAGTGCCTGGTG	3	10027	306
JOHE21849//MN179	TAACCTACGCTTGGCGCTAC	3	10332	
JOHE21850/MN180	GGCGTCAAGTTCTCTTCTGG	4	10335	405
JOHE21851/MN181	GCTGGACCTTTGTGGTTCAT	4	10739	
JOHE21852/MN182	GCTTTCGATGCCCATATTTC	5	20031	491
JOHE21853/MN183	TTAGTTGCTCCGGTGTTTGA	5	20521	
JOHE21854/MN184	AAAGGTCCTCGAGTGTCACG	6	10092	607
JOHE21855/MN185	TCCTTCAACCTCTCCCTTGA	6	10698	
JOHE21856/MN186	CGCCGAAGCGAGATTATTTA	7	10298	701
JOHE21857/MN187	AAGGTGACCAAAGCACCAAC	7	10998	
JOHE21858/MN188	TACAAGCCGAGATTGCACAC	8	80215	794
JOHE21859/MN189	AACTTTGGTAGCGGGTGATG	8	81008	
JOHE21860/MN190	AGGATTCCAAACCGGAGAGT	9	10278	892
JOHE21861/MN191	CGATCCCTTCATGTCACCTT	9	11169	
JOHE21862/MN192	GACGTACGTGGCCTTGAAGT	10	10123	1004
JOHE21863/MN193	CCGATTACCGACATGCCTAT	10	11126	
JOHE21864/MN194	CCACAGTCCCTGGTCATTCT	11	10103	1103
JOHE21865/MN195	TGCCATCCATGACGATAGTG	11	11205	
JOHE21866/MN196	CTCTTTCAAACCGCCAAAAG	12	90284	1196
JOHE21867/MN197	TGCTGAGGAAGCCTTGATTT	12	91479	
JOHE21868/MN198	GCAAGCGTCAATAACCCACT	13	10166	1298
JOHE21869/MN199	GGCGTGTGAGTTCCATTCTT	13	11463	
JOHE21870/MN200	CCTCAGAATGCTGCTGACAA	14	100243	1390
JOHE21871/MN201	ACACGGCGAAAAGGTTACAG	14	101632	

2.2.10 Restriction Fragment Length Polymorphism (RFLP)

RFLP analysis was performed as described previously (Marra, Huang et al. 2004). Based on the SNPs in XL280 and JEC20, we designed two RFLP markers, RFLP3 and RFLP7 (primers are shown in Table 3), and digested with NdeI and XbaI, respectively. Other markers included the *STE20***a** and *STE20*α mating type locus genes to assign the mating type as **a** or α.

Table 3. Oligonucleotides used in Chapter 2.

Primer	Sequence (5' to 3')	Comments
JOHE9028	ATGGGCAGCAACCTTGACATC	*SXI2***a** probe F
JOHE9870	GGATAGATCTTACCCCCTGAGGACTGT	*SXI2***a** probe R
JOHE21313/WL	CACATCTCAGATGCCATTTTACCA	*STE20*_D**a**_F
JOHE21323/WL	TCATCACAATGATCTCATTCACAA	*STE20*_D**a**_R
JOHE21312/WL	AGCACCAGCCTATGGAGTCCGTCT	*STE20*_Dα_F
JOHE21322/WL	TCAAAAGGTTGTCAGACTTGATGT	*STE20*_Dα_R
JOHE24473/MN286	CGAGGATCGTACAGTGCGTA	RFLP-3-NdeI F
JOHE24474/MN287	CGCACTTCTTTCGTCATTCA	RFLP-3-NdeI R
JOHE24481/MN294	TATTCCCTCCTTGCTTGGTG	RFLP-7-XbaI F
JOHE24482/MN295	AACAACCACGTTTCCAGGTC	RFLP-7-XbaI R
JOHE24111/MN264	AAGAGAGGGGGACGAACAAT	Hsc20 SNP_F
JOHE24112/MN265	GCCGAGATTGTGTTGGATTT	Hsc20 SNP_R
JOHE38840/MF281	GGTACCGGATTTATGGTGTAGATGAATG	Hsc20-KpnI_F
JOHE38841/MF282	GGTACCAAGGACATCGGATAGAGATTA	Hsc20-KpnI_R
M13F	GTAAAACGACGGCCAG	
M13R	CAGGAAACAGCTATGAC	

2.2.11 Virulence Studies

Virulence assays were conducted using a murine inhalation model of cryptococcosis. Cohorts of 4- to 8-wk-old female DBA mice were anesthetized through intraperitoneal injection of Nembutal (37.5 mg/kg) and infected intranasally with 5×10^6 cells diluted in sterile PBS. The cells of the inoculum

were diluted and plated onto YPD medium to determine CFU and viability. Mice were monitored twice daily, and moribund individuals were euthanized with CO_2. The survival rates were plotted against time using Kaplan-Meier survival curves, generated with Prism 4.0 (GraphPad software, La Jolla, CA, USA). The *p* values were evaluated by a Log-rank (Mantel-Cox) test. A *p* value of <0.05 was considered significant. The lungs and brains of the euthanized animals were removed, weighed, and homogenized in 2 ml sterile PBS. The samples were serial diluted and plated on YPD media to count CFUs. Twenty random isolates were colony purified and subjected to multiplex PCR to detect aneuploidy.

2.2.12 Competitive Fitness and Growth Curve Assays

XL280, MN55, MN77, MN89 (all NAT sensitive), and XL280 marked with the NAT resistance marker integrated at the *SPO11* genetic locus (XL280 *NAT*) were used to measure the competitive fitness of the aneuploid strains in the presence of fluconazole. Strains were grown overnight in liquid cultures in YPD, washed with sterile water, and diluted to a density of 1×10^7 cells/ml. The following strains were mixed in equal ratios: XL280 with XL280 *NAT*, MN55 with XL280 *NAT*, MN77 with XL280 *NAT*, and MN89 with XL280 *NAT*. The mixtures were spotted on YPD and YPD plus 8 μg/mL fluconazole (FLC) and incubated for 3 d at 30°C. Then, the cells were recovered from the plates, washed with sterile water, and plated on YPD to count CFUs. Following 2 d incubation at 30°C, 300 isolates were replica plated onto NAT selective media and survival rates were

calculated. The experiments were conducted in triplicate. For the growth curve assays, the strains were grown overnight in liquid cultures, washed with sterile water, and diluted into 4×10^4 cells in 200 µL of YPD and YPD plus 2 µg/mL fluconazole (fluconazole concentration was determined experimentally). The cells were incubated at room temperature in 96-well plates, and OD_{600} was measured every 2 hrs for 48 hrs using a Tecan-Sunrise microplate reader. All of the experiments were performed in triplicate.

2.3 Results

2.3.1 Genomic Comparison of Parental Strain JEC21 and Its Hyperunisexual Selfing Progeny XL280

To investigate whether phenotypic and genotypic changes are generated by selfing unisexual reproduction, we analyzed the meiotic progeny produced via this process. To this end, we solo cultured the promiscuous, hypersexual haploid strain XL280 under conditions that support robust α-α unisexual reproduction (V8 media or FA (filament agar) for ~2 weeks) and isolated spores by microdissection. The hyperfilamentous haploid strain XL280 (Lin, Hull et al. 2005, Lin, Huang et al. 2006) generates abundant hyphae, homozygous diploid intermediates, and haploid meiotic spores when grown on mating-inducing media all by itself.

XL280 is a haploid F1 progeny descended from a cross between two exceptionally well-validated haploid sibling parental strains, whose genomes have been both sequenced, B3501α and JEC20**a** (which is isogenic to the sequenced strain JEC21α, with the exception of the mating-type locus) (Figure 3A) (Heitman, Allen et al. 1999, Lin, Hull et al. 2005, Loftus, Fung et al. 2005, Lin, Huang et al. 2006). Thus, while XL280α shares markers with both parents, it only has one copy of each chromosome (it is haploid) and is not heterozygous anywhere in its genome. When it undergoes unisexual reproduction with itself, it forms a transient homozygous diploid (generated through either α-α cell fusion

between mother and daughter cells or via endoreplication) that is identical throughout the diploid, euploid genome, in which each gene is presented in two identical copies.

Hyphae produced by unisexual reproduction grow to form terminal basidia wherein the diploid nucleus undergoes meiosis to generate abundant recombinant progeny. That this is a meiotic process has been established in previous studies (Lin, Hull et al. 2005, Feretzaki and Heitman 2013) that showed both key meiotic genes *SPO11* and *DMC1* are required for spore production and viability. The parental strains B3501α and JEC20**a** share ~50% genetic identity (Loftus, Fung et al. 2005); thus, their F1 progeny (XL280) would be expected to share ~75% genetic identity with both B3501α and JEC21α, whose genomes have been sequenced (Loftus, Fung et al. 2005). Therefore, we used the available JEC21 genomic sequence and genome microarray slides as a foundation to study the genome of XL280 and its α-α unisexual reproduction (Schein, Tangen et al. 2002, Kraus, Boily et al. 2004).

We performed next-generation sequencing (NGS) using high-throughput Illumina sequencing to compare the genomes of XL280α and JEC21α (Bentley 2006). In total, 47,891,302 sequences (paired-end reads) of 75 bp in length were generated, providing 160-fold coverage of the XL280 genomic sequence, which was then analyzed using the known JEC21 genome as the reference for the sequence assembly (Figure S1 and Table S1). All but 4,535,426 sequence reads

(~10%) were used in the genome assembly, and of these remaining reads, the majority were of low quality (90%). We assembled the Illumina reads using a combination of *de novo* assembly (Velvet) (Zerbino and Birney 2008) and reference genome assembly (BWA) (Li and Durbin 2009).

XL280 shares 100% identity with JEC21 over 81% of the overall genome and is 99.88% identical at the sequence level overall (Figure 3C). Among the SNPs and small indels identified, 9,021 were located in exonic regions, 10,254 in intergenic regions, nine in tRNA genes, and 3,849 in intronic regions (31 of which differed in the 5' splice-site and 23 in the 3' splice-site) (Table S2). Among the exonic SNPs and indels, 107 SNPs resulted in the introduction or deletion of stop codons, 68 indels resulted in a frame shift, 14 indels resulted in the loss of amino acids without a frame shift, and 3,943 SNPs resulted in nonsynonymous amino acid substitutions in 960 ORFs (Table S2). Further analysis of the modified ORFs will enable the elucidation of the phenotypic differences between XL280 and JEC21, for example with respect to the hypersexual phenotype (Lin, Huang et al. 2006).

CGH was performed using a 70-mer oligonucleotide microarray covering all predicted ORFs of the JEC21 genome (Kraus, Boily et al. 2004) to detect chromosome copy number alterations. Based on CGH, the genomes of XL280 and JEC21 (Figure 4A) are quite similar and span 14 conserved, linear chromosomes. This enabled use of JEC21-based microarray slides for CGH

analysis of XL280 unisexual progeny. Because this microarray covers only ORFs, no differences could be detected in centromeric or telomeric regions. There is an ~28 kb region absent in XL280; in JEC21 this sequence lies near the right end of Chr 5 and is conserved in many *C. neoformans* strains (Kavanaugh, Fraser et al. 2006). In addition, XL280 is missing one copy of the left end of either Chr 8 or 12, which is a 63-kb duplicated region located on both Chr 8 and 12 of JEC21 (Fraser, Huang et al. 2005). NGS data further confirmed these findings (Figure 4B).

The chromosome content of strain XL280 was compared to JEC21 by clamped homogenous electric field (CHEF) gel electrophoresis to detect any chromosomal translocations. Chr 5 and Chr 8/9 of XL280 are smaller than those of JEC21, while Chr 13 of XL280 is larger (Figure 4C). To ascertain where the sequence similarity of these chromosomes lies, we excised each chromosomal band and performed band array analysis. The configurations of Chr 9 and 12 differed between XL280 and JEC21 (Figure S2). Chr 9 of XL280 hybridized to Chr 8 and Chr 12 of JEC21; Chr 12 of XL280 hybridized to Chr 8 of JEC21. These findings were confirmed by Southern hybridization (Figure 3D). Previous studies reported that this chromosomal translocation and duplication occurred during generation of the JEC21α/JEC20**a** congenic strain pair (Fraser, Huang et al. 2005). During the cross of strains B3501α × B3502**a**, Chr 9 and Chr 12 formed a dicentric chromosome via telomere–telomere fusion and then broke to

form new versions of Chr 12 and Chr 8 in strains JEC21α/JEC20**a** (Fraser, Huang et al. 2005). Our results indicate that Chr 9 and Chr 12 of XL280 are more similar to those of the B3501α parent, whereas other chromosomes are more similar to the JEC20**a** parent (Figure 4E). This comprehensive analysis of the XL280 genome reveals how its genome is derived from two well-validated parental reference strains and allowed detailed molecular analyses of unisexual progeny.

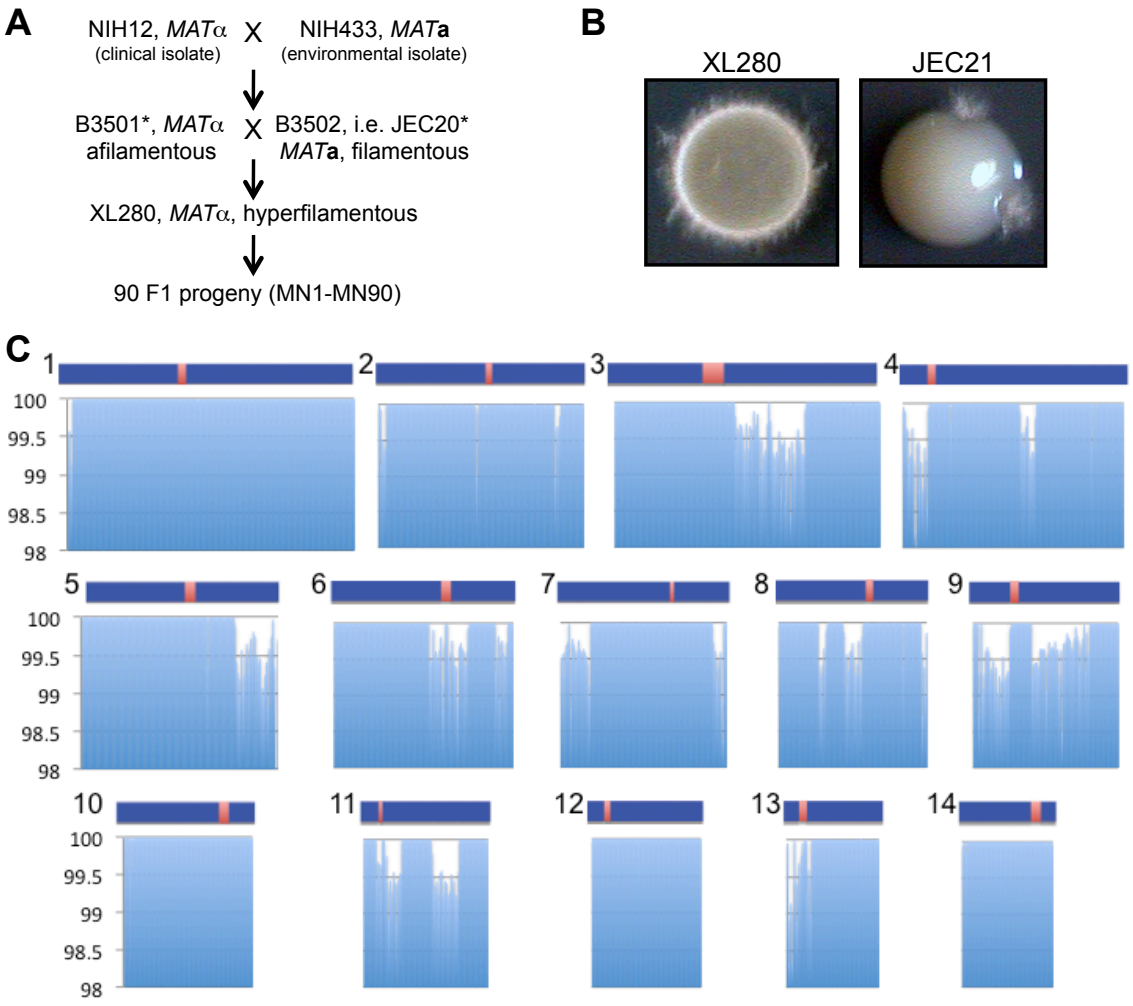

Figure 3. Phenotypic and genomic comparison between XL280 and JEC21. (**A**) The origin of XL280. The parents are NIH12 (*MAT*α), a clinical isolate from the United States, and NIH433 (*MAT***a**), an environmental isolate from Denmark. * indicates that genome sequences are available. (**B**) XL280 is hyperfilamentous. α-α unisexual reproduction generates hyphae, basidia, and meiotic spores along the periphery of yeast colonies incubated on filament agar (FA) at room temperature for 11 d. (**C**) Whole genome comparison between XL280 and JEC21. Distribution of sequence identity (*y*-axis) across the genomes averaged over 10 kb intervals. Blue bars represent the 14 chromosomes of JEC21 (Loftus, Fung et al. 2005), and red regions represent the candidate centromeres (Sun and Xu 2009).

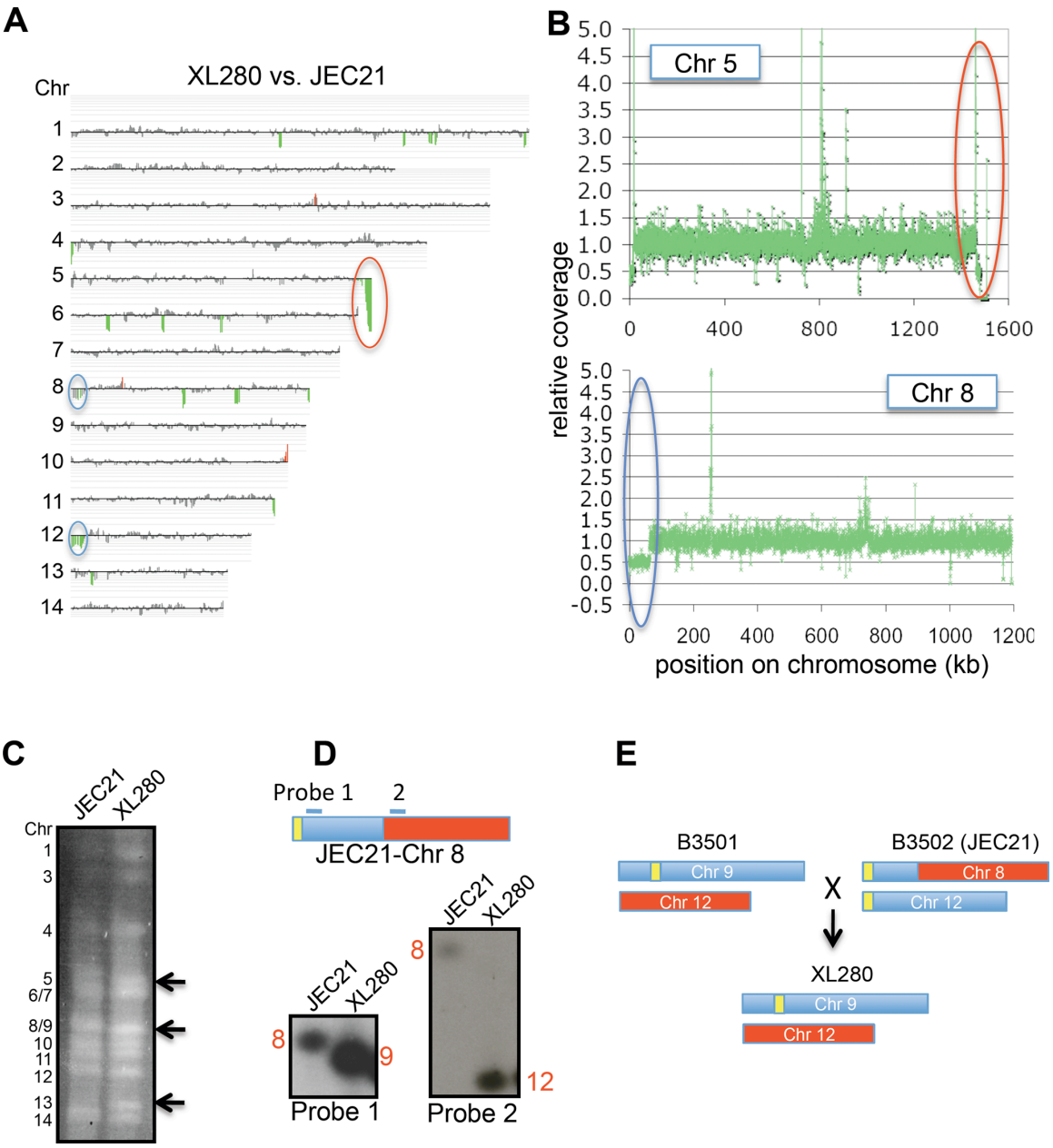

Figure 4. Genome comparison of XL280 and JEC21. (**A**) CGH of XL280 versus JEC21. Coloring indicates gene dosage as follows: gray, no significant change; red, more abundant; green, less abundant. (**B**) Coverage analysis of XL280 Chr 5 and Chr 8 with JEC21 as the reference. The red circle indicates that XL280 lacks ~28 kb near the right end of Chr 5 compared to JEC21. The blue

circle indicates that XL280 has one copy of the 63 kb region that is duplicated in JEC21 and located on the left ends of Chr 8 and Chr 12. (**C**) Chromosome configuration of XL280 versus JEC21. Black arrows indicate the size differences of Chr 5, 8/9, and 13 between the two strains. (**D**) Two probes located before and after the break in Chr 8 of JEC21 hybridized to XL280 Chr 9 and 12, respectively. (**E**) Chr 9 and 12 of XL280 versus JEC21.

2.3.2 Frequent Phenotypic and Genotypic Changes Following *C. neoformans* Unisexual Reproduction

Solo culture of strain XL280 on V8 sexual reproduction-inducing media resulted in robust production of F1 meiotic spore progeny via selfing α-α unisexual reproduction. This process involves ploidy changes (1n $\rightarrow$ 2n $\rightarrow$ 1n) via self cell–cell fusion or endoreplication, meiosis, and sporulation to produce haploid meiotic progeny. In total, 90 α-α unisexual reproduction meiotic progeny were isolated by spore micromanipulation and germination and were examined in a battery of phenotypic analyses (Figure 5). We assessed major virulence factors of *C. neoformans* (growth at 37^{o}C and melanin production on niger seed (NS) or L-DOPA media), sensitivity to the antifungal drugs fluconazole (FLC) or FK506, and unisexual reproduction (self-filamentous growth). In these analyses, six of 90 F1 progeny (~7%) showed a distinct phenotype compared to the haploid parental strain XL280 and the remaining 84 progeny showed no phenotypic differences from the wild-type (Figure 6A). The six isolated variant F1 progeny strains all exhibited temperature-sensitive (TS) growth (Figure 6A). Two progeny (MN77 and MN89) were sensitive to the calcineurin inhibitor FK506 and produced more

melanin, indicating they may have similar genetic changes. MN35 was FLC-sensitive, while the other four progeny (MN27, MN55, MN77, and MN89) were relatively FLC-resistant (Figure 6A). On V8 mating-inducing media (V8 agar), MN27 underwent more robust unisexual development, while MN35, MN55, MN77, and MN89 generated fewer hyphae (Figure 6A). Although the two genomes of cells undergoing α-α unisexual reproduction are identical, phenotypic changes to these and other conditions are clearly evident in even a relatively small sample of progeny produced by this process, which indicates that α-α unisexual reproduction generates phenotypic plasticity *de novo* since there is no preexisting genetic diversity to admix.

We next tested if standard mitotic growth might also lead to phenotypic changes like meiotic unisexual reproduction. A similar set of 96 isolates derived from XL280 by mitotic asexual growth exhibited no phenotypic variation from wild-type in the same battery of phenotypic tests in which phenotypic variation was readily detected in meiotic unisexual reproduction. Thus, we conclude that phenotypic variation occurs following meiotic unisex but not standard mitotic asexual growth.

Phenotypic variation is often attributable to genetic changes. To establish the molecular basis of phenotypic variation of the unisexual progeny, we examined changes in ploidy, whole-chromosome aneuploidy, chromosomal translocations, and single nucleotide polymorphisms (SNPs) by FACS, CGH,

CHEF, and Illumina NGS, respectively. FACS analysis revealed that the hypersexual progeny MN27 was diploid, in accord with previous findings that diploid strains are (1) intermediates or products of unisexual reproduction and (2) hyperfilamentous (Figure 6B) (Lin, Hull et al. 2005). None of the other 90 F1 α-α unisexually produced progeny were diploid (Figure 4B and unpublished data).

Three progeny (MN7, MN55, and MN89) were analyzed by Illumina NGS to examine the presence of SNPs. In total, only three SNPs were identified in the ~20 Mb genomes of the three isolates based on 48,644,802 sequences of 75 bp generated for MN7, 46,089,962 for MN55, and 44,650,780 for MN89 (Figure 6C). One SNP located at position 878,429 on Chr 7 of MN55 resulted in an L318P coding substitution in the hypothetical protein CNJ03170. A second SNP was located at position 491,632 on Chr 8 in both MN7 and MN55, resulting in a cytosine to thymine change in the 5' UTR of the CNH02880 gene. The third SNP was located at position 704,393 on Chr 9 of MN7 and resulted in an H66A amino-acid substitution in the co-chaperone Hsc20 (CNI02610), a heat shock protein that functions in iron–sulfur cluster assembly (Uhrigshardt, Singh et al. 2010). To examine whether this SNP is responsible for the TS phenotype of isolate MN7, we performed a complementation test by introducing the WT allele of *HSC20* into the MN7 TS strain. We first documented that the *hsc20-1* mutant allele is recessive based on analysis of an *hsc20-1*/*HSC20* diploid fusion product of MN7 and XL280α. While the MN7 strain is TS, the MN7 × XL280α diploid fusion

product was temperature resistant, similar to the XL280α parent. The WT allele of *HSC20* was cloned in a plasmid under control of its native promoter and terminator and introduced into strain MN7 by biolistic transformation. In multiple independent transformants, we found that a single copy of the WT *HSC20* allele complemented the TS phenotype of MN7 and restored WT growth similar to the XL280α parent at higher temperature (Figure 6D). Based on these findings we conclude that the TS phenotype of progeny MN7 is attributable to the H66A amino-acid substitution in the co-chaperone Hsc20.

Based on CHEF analysis of the chromosomal karyotype, chromosome site differences were detected in the α-α unisexual F1 progeny MN27, MN55, and MN89 (Figure 7A). For MN27 and MN55, an extra chromosomal band was present and migrated more rapidly than Chr 8/9. For MN89, an extra chromosomal band was observed to migrate more rapidly than Chr 6/7. To further analyze these anomalous chromosomes, we excised the novel chromosomal bands from the CHEF gel and extracted and fluorescently labeled the DNA to generate probes. Band CGH analysis revealed that the excised chromosomal bands covered all ORF regions (the JEC21 expression array covers ORF and not centromeric or telomeric regions) of Chr 9, Chr 9, or Chr 7 in isolates MN27, MN55, or MN89, respectively (Figure 7B) (XL280 Chr 9 hybridizes to Chr 8 and 12 on the JEC21 array). Because all ORFs were recognized despite a shortened chromosomal length, we hypothesized that

centromeric or telomeric regions (not represented on the array) may have suffered significant deletions in the respective strains. To test this hypothesis, we chose MN89 as an example and designed specific probes that hybridize to the centromeric and telomeric regions of Chr 7 (Figure 7C). Restriction enzyme digestion of whole chromosomes and CHEF electrophoresis followed by Southern hybridization revealed that Chr 7 of MN89 has the same telomere lengths as those of XL280, but a shortened centromeric region (Figure 7C). Further whole genome sequencing determined that the size of the deleted centromeric region is 10,257 bp (Figure 7D).

These findings indicate that α-α unisexual reproduction induces phenotypic and genotypic plasticity. However, a common genetic change responsible for the phenotypic changes remained to be identified.

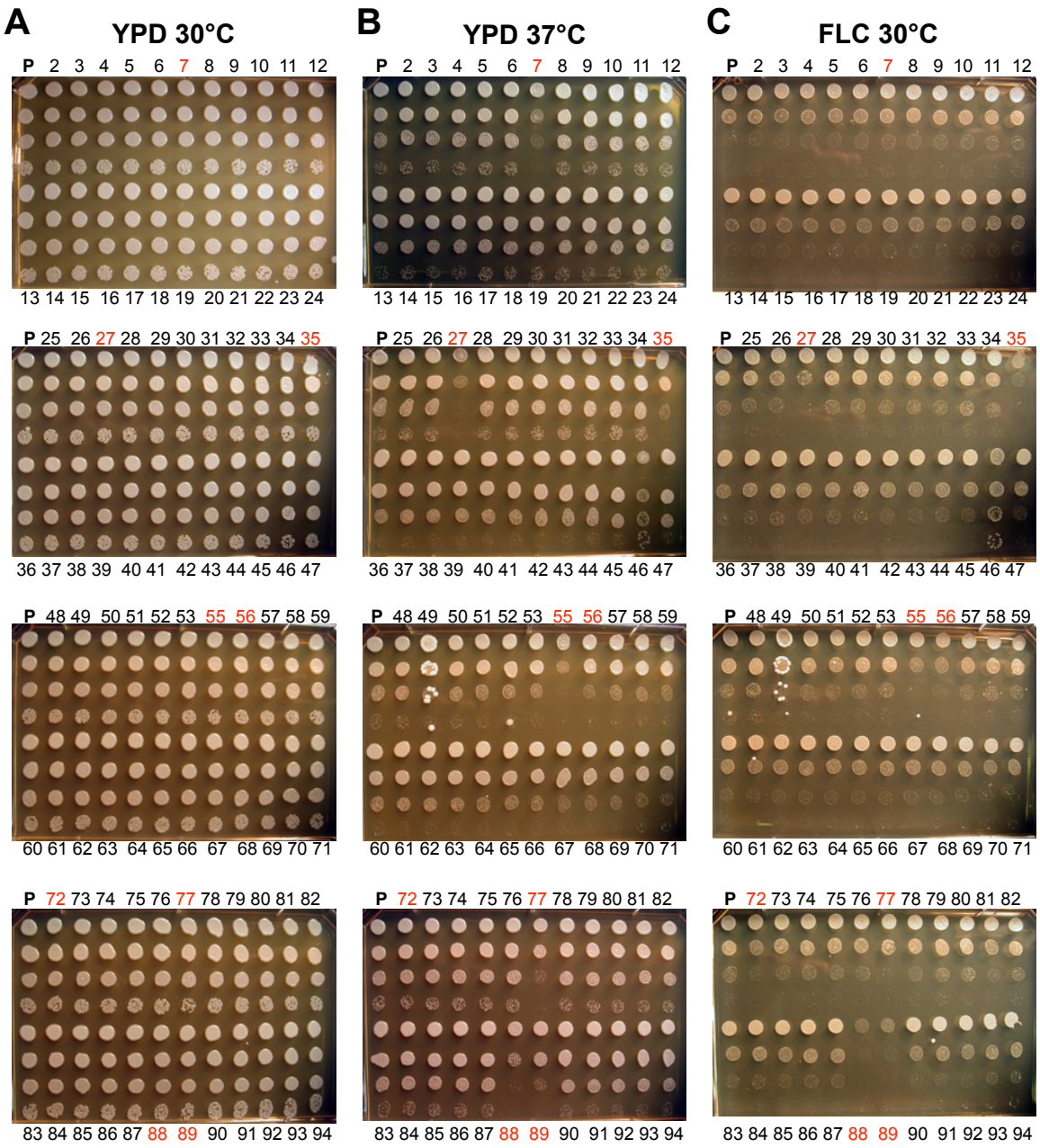

Figure 5. Unisexual reproduction progeny of XL280 exhibit novel phenotypes. Strains were spotted in 10-fold serial dilutions and grown under the following conditions: (A) YPD at 30°C for 2 d, (B) YPD at 37°C for 2 d, and (C) YPD plus 8 μg/mL fluconazole (FLC) at 30°C for 4 d. Red labels indicate the progeny with variant phenotypes compared to the parental strain.

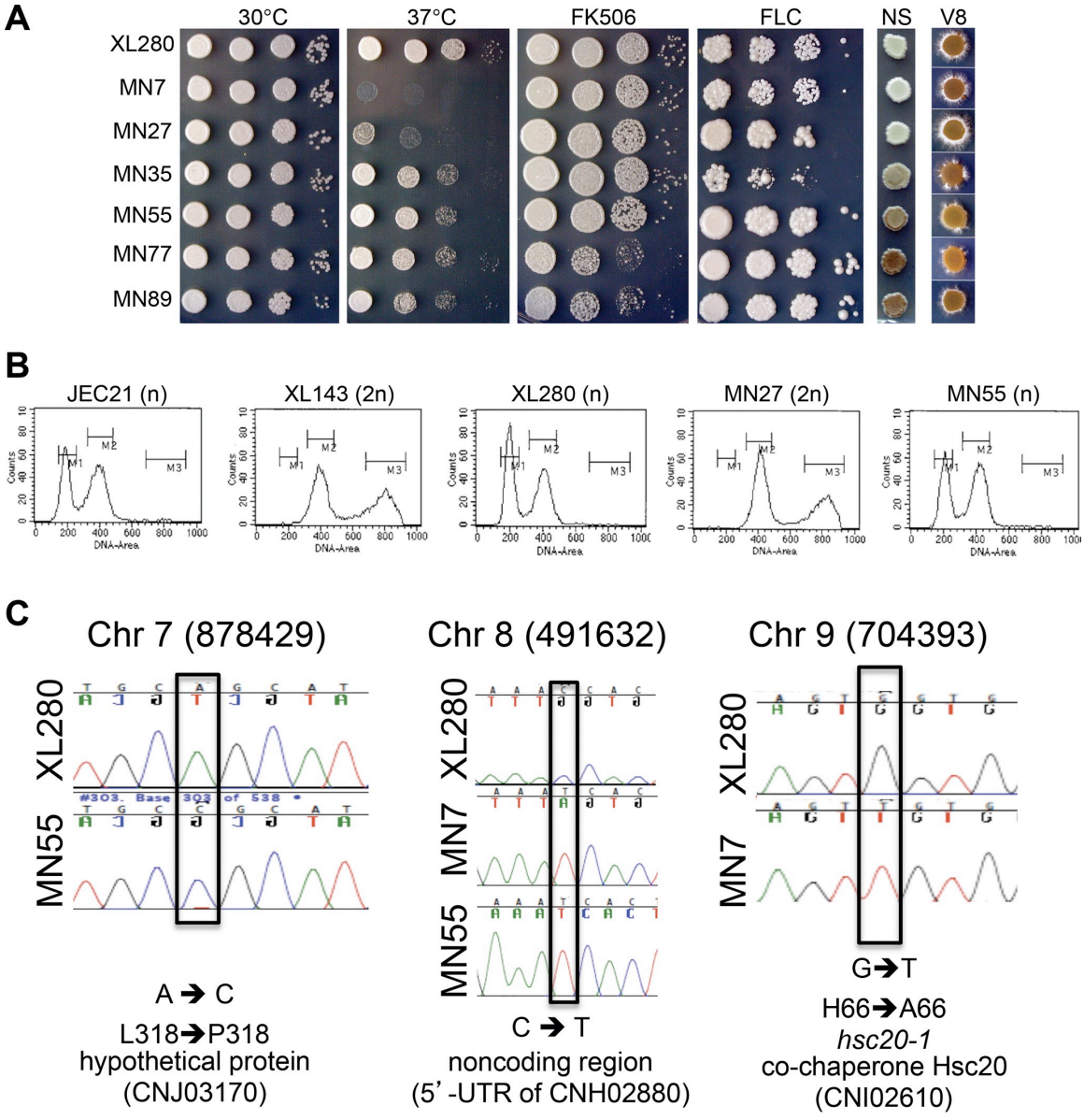
A
30°C
37°C
FK506
FLC
NS
V8
XL280
MN7
MN27
MN35
MN55
MN77
MN89
B
JEC21 (n)
XL143 (2n)
XL280 (n)
MN27 (2n)
MN55 (n)
M1
M2
M3
Counts
DNA-Area
C
Chr 7 (878429)
Chr 8 (491632)
Chr 9 (704393)
XL280
MN55
MN7
A → C
L318→P318
hypothetical protein
(CNJ03170)
C → T
noncoding region
(5' -UTR of CNH02880)
G→T
H66→A66
hsc20-1
co-chaperone Hsc20
(CNI02610)
D
30°C
37°C
WT
hsc20-1
hsc20-1 + HSC20 #1
hsc20-1 + HSC20 #2

Figure 6. Unisexual reproduction generates phenotypic diversity. (**A**) Progeny produced by α-α unisexual reproduction of strain XL280 in solo cultures were grown in 10-fold serial dilution assays and under the following conditions: YPD at 30°C for 2 d; YPD at 37°C for 2 d; YPD plus 1 μg/mL FK506 at 30°C for 2 d; YPD plus 8 μg/mL fluconazole (FLC) at 30°C for 6 d; NS (melanin-inducing media) at 30°C for 3 d; and V8 pH = 7 (mating-inducing media) at room temperature for 11 d. (**B**) Diploid progeny were generated infrequently following unisexual reproduction. Flow cytometry profiles of cells stained with the fluorescent dye propidium iodide. JEC21 (1n, haploid control); XL143 (2n, diploid control); XL280 (1n); MN27 (2n, the only diploid strain identified among the 90 XL280 α-α unisexual reproduction progeny (1.1%). All other XL280 α-α unisexual progeny were haploid (or aneuploid) (e.g., MN55). Nuclear DNA content is indicated by 1n (haploid) and 2n (diploid). The *x*-axis indicates fluorescence intensity reflecting DNA content, and the *y*-axis indicates cell counts. (**C**) Three SNPs identified by NGS from strains MN7 and MN55 and were confirmed by Sanger sequencing. (**D**) The WT allele of *HSC20* was cloned in two independent plasmids, and these were used to transform strain MN7 and independent transformants were analyzed. This complementation test shows that the TS phenotype of MN7 is attributable to the recessive *hsc20-1* mutation.

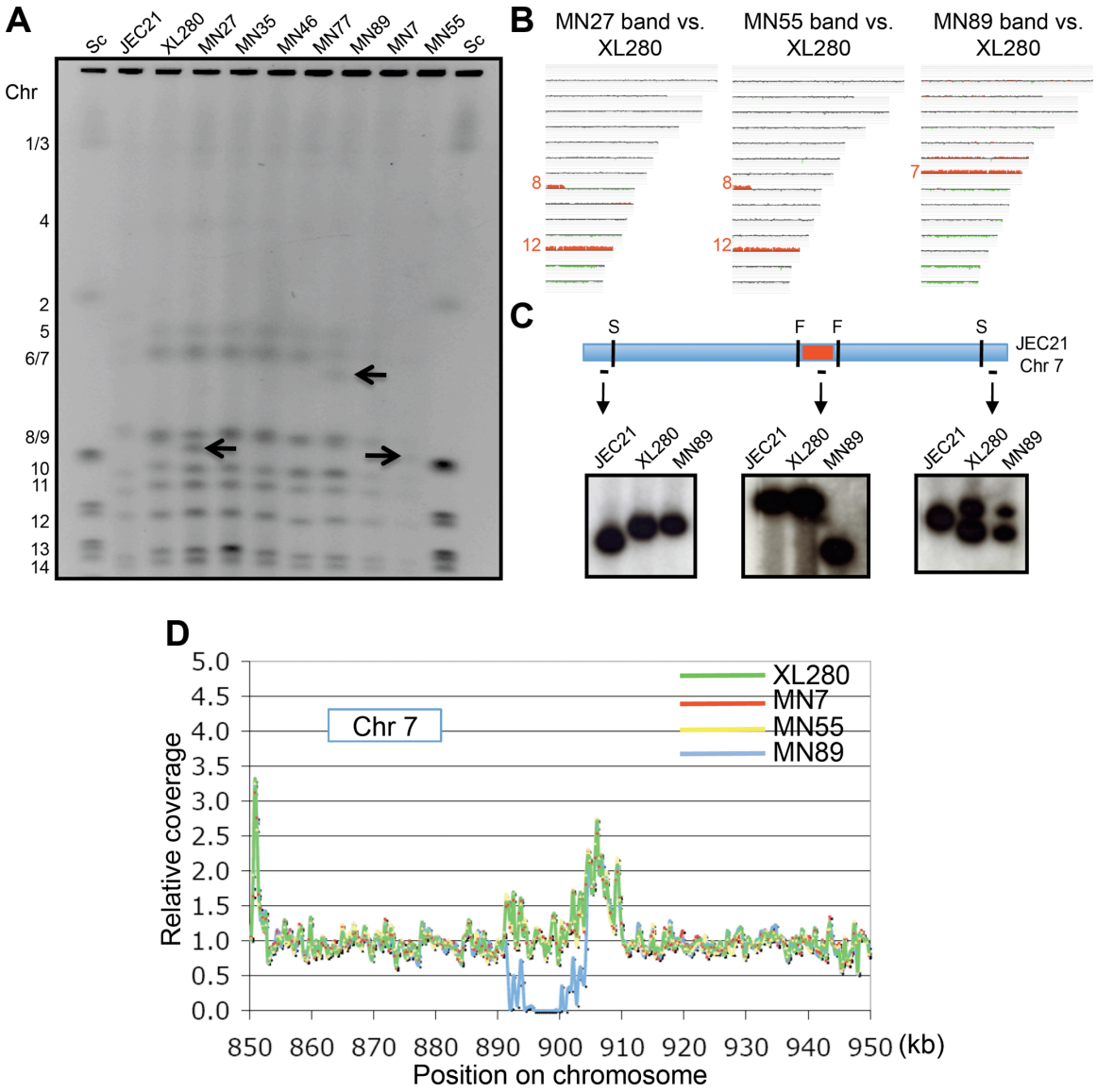

Figure 7. Chromosome deletions arise during unisexual reproduction. (**A**) A PFGE molecular karyotyping of parental strain XL280 and 7 α-α unisexual produced progeny. Chromosome numbers are indicated on the left. Arrows emphasize the chromosomes that differ in size in progeny strains MN27, MN55, and MN89 compared to parental strain XL280. Sc represents the 0.225 to 2.2 Mb *S. cerevisiae* CHEF DNA Size Markers (BioRad 170-3605). (**B**) Band array data for chromosomes indicated with black arrows. DNA of the labeled chromosome band was extracted from the PFGE gel and subjected to CGH. Coloring indicates gene dosage as follows: gray, no significant change;

red, more abundant; green, less abundant. (**C**) A shorter centromere is observed in progeny strain MN89 based on Southern blot analysis. (**D**) The shorter centromere of MN89 was confirmed by genome sequencing. An ~10,257-bp region (blue line) is missing in progeny MN89 compared with parent XL280.

2.3.3 α-α Unisexual Reproduction Frequently Generates Aneuploidy

CGH analysis of the phenotypically variant progeny revealed that four out of six isolates (66.7%) were aneuploid. Isolates MN35, MN55, MN77, and MN89 contained an extra copy of chromosome 13, 9, 10, and 10, respectively, indicating that a high rate (>4%) of aneuploidy is generated as a consequence of α-α unisexual reproduction (Figure 8A). Whole genome sequencing of isolates MN55 and MN89 confirmed the presence of an extra copy of Chr 9 or Chr 10, respectively, in a majority of cells in the population, as ~2-fold higher levels of sequence reads were obtained for these chromosomes compared to other genomic regions (Figure 8B). Interestingly, Sionov et al. previously associated Chr 10 disomy with FLC resistance (Sionov, Lee et al. 2010).

As a complementary approach to CGH, we developed a facile multiplex PCR-based method to detect aneuploidy. In this approach, 14 primer pairs (Table 2) were combined into a single PCR reaction such that each primer pair represents a separate chromosome and amplifies a specific region of different sizes to generate a ladder of 100 to 1400 bp (Figure 8C). PCR products of greater intensity reflect the presence of extra chromosomes (red arrows in Figure 8C). Bioanalyzer analysis further confirmed a ~2-fold increase in PCR product

yield from the additional aneuploid chromosomes present in 1n + 1 isolates. Using multiplex PCR we screened all of the XL280 meiotic (90) and mitotic (96) progeny and we did not detect any additional aneuploid strains from the meiotic progeny and none from the mitotic progeny.

In *S. cerevisiae*, strains aneuploid for different chromosomes all share several common phenotypes, including temperature sensitivity (Torres, Sokolsky et al. 2007). Therefore, we determined whether aneuploid strains of *Cryptococcus* exhibit a similar phenotype. Consistent with the observed consequences of aneuploidy in *S. cerevisiae*, all aneuploid *C. neoformans* strains in our study exhibited a TS phenotype (Figure 6A).

Aneuploidy can compromise growth unless it provides a fitness benefit under stress or other distinct conditions. We found that aneuploid strains exhibit a variety of phenotypes potentially associated with virulence, including antifungal drug resistance. To test if the progeny have a competitive advantage relative to the parental strain, we co-incubated an aneuploid progeny (MN55, MN77, or MN89) with the wild-type parent XL280α (marked with the NAT drug resistance marker) in the presence of fluconazole. As expected, the fluconazole-resistant aneuploid progeny exhibited an increased competitive fitness and outgrew the parental strain in competitive growth assays by a ratio of ~ 4:1 (Figure 9).

Moreover, to investigate the fitness of these aneuploid unisexual progeny, we tested their ability to infect and cause disease in a murine inhalation model.

Mice were infected with the aneuploid strains via intranasal instillation and monitored for signs of pulmonary cryptococcosis or meningoencephalitis. In contrast to the view that aneuploidy is deleterious, the aneuploid unisexually generated isolates MN35 ($n+1^{13}$) and MN55 ($n+1^{9}$) were as virulent as the euploid wild-type parent, despite their modest TS growth at 37^{o}C on YPD rich media *in vitro* (Figure 10). Previous studies have shown that in the clinically important sibling species *C. neoformans* var. *grubii* (serotype A) strains that are disomic for chromosome 13 exhibit a melanin defect and impaired virulence in mice (Hu, Wang et al. 2011). However, we found that disomy 13 in *C. neoformans* var. *neoformans* (serotype D) did not affect melanin production and the MN35 strain was equally virulent as the wild-type. Thus, the specific consequences of aneuploidy may differ between even closely related lineages. Two other aneuploid strains (MN77 and MN89) were both attenuated compared to wild-type and, interestingly, both are aneuploid for chromosome 10 (Figure 10). Cells isolated from lungs of infected animals exhibited relatively stable aneuploid phenotypes and were found to retain their aneuploid chromosome in 70–80% of isolates based on multiplex PCR [20 isolates were analyzed from each strain, 15 were aneuploid for MN35 (75%), 16 for MN55 (80%), 14 for MN77 (70%), and 15 for MN89 (75%)]. Thus, under the stressful gauntlet of the host, several aneuploid progeny appeared as fit as the euploid parent whereas others were attenuated.

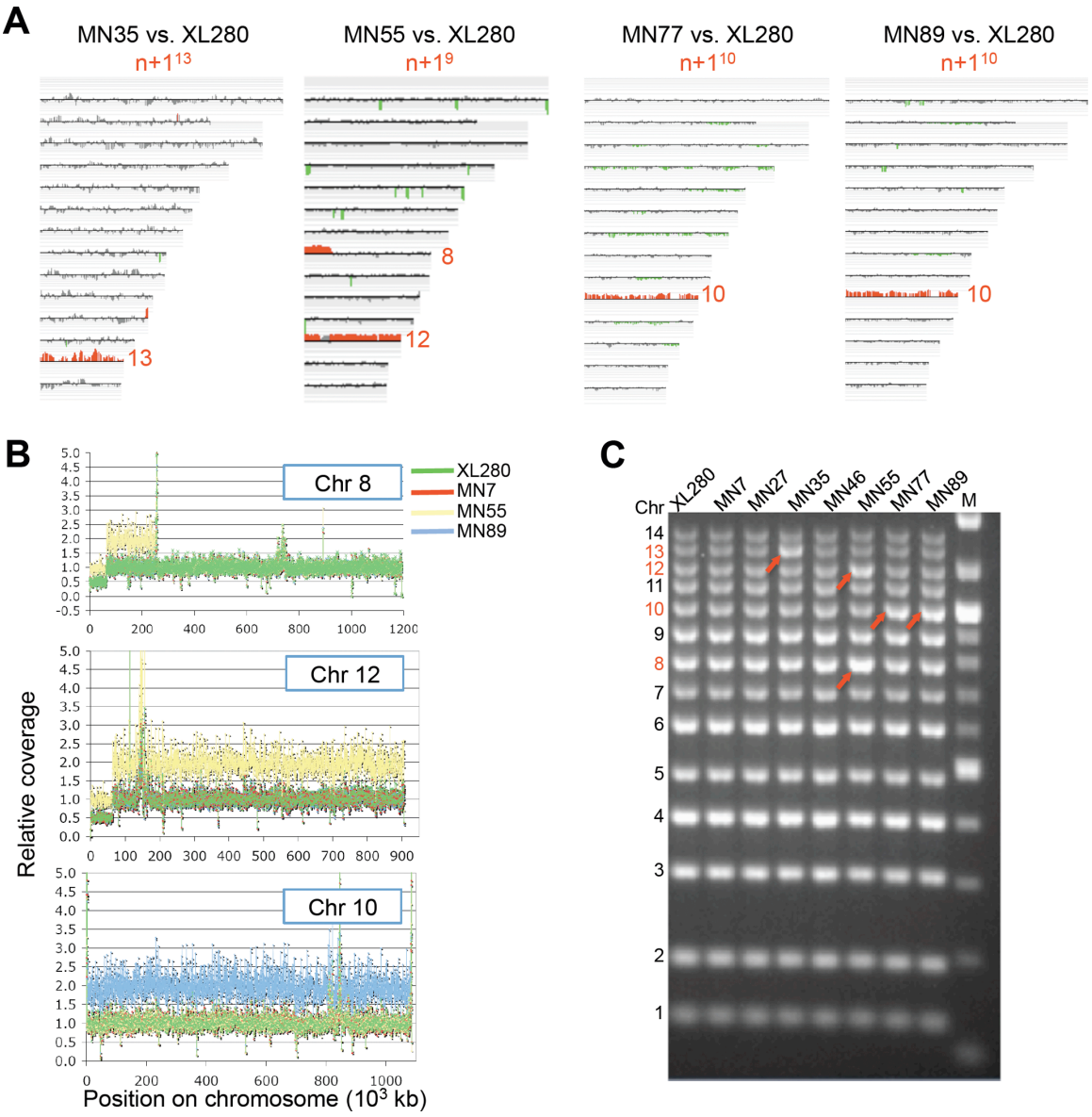

Figure 8. Aneuploidy is generated at a high rate by unisexual reproduction. (**A**) CGH array data for four progeny with novel phenotypes. Progeny strains MN35, MN55, MN77, and MN89 contain an extra copy of Chr 13, Chr 9, Chr 10, and Chr 10, respectively. The colors indicate gene dosage as follows: gray, no significant change; red, amplification; green, deletion. (**B**) NGS is consistent with the CGH data in that 2x coverage was observed for each aneuploid chromosome and no others. MN55 (yellow) has an extra copy of Chr 9, which corresponds to the left arm of Chr 8 and the right arm of Chr 12 of strain

JEC21 (as shown above). MN89 (blue) has an extra copy of Chr 10. (**C**) Multiplex PCR was conducted to detect aneuploidy. Multiplex PCR reactions used the primer sets listed in Table 2. Amplicons (i.e., chromosomes or chromosome regions) that differed in abundance between samples were identified in this assay and quantified by scanning (arrowheads). Chromosome numbers are indicated on the left.

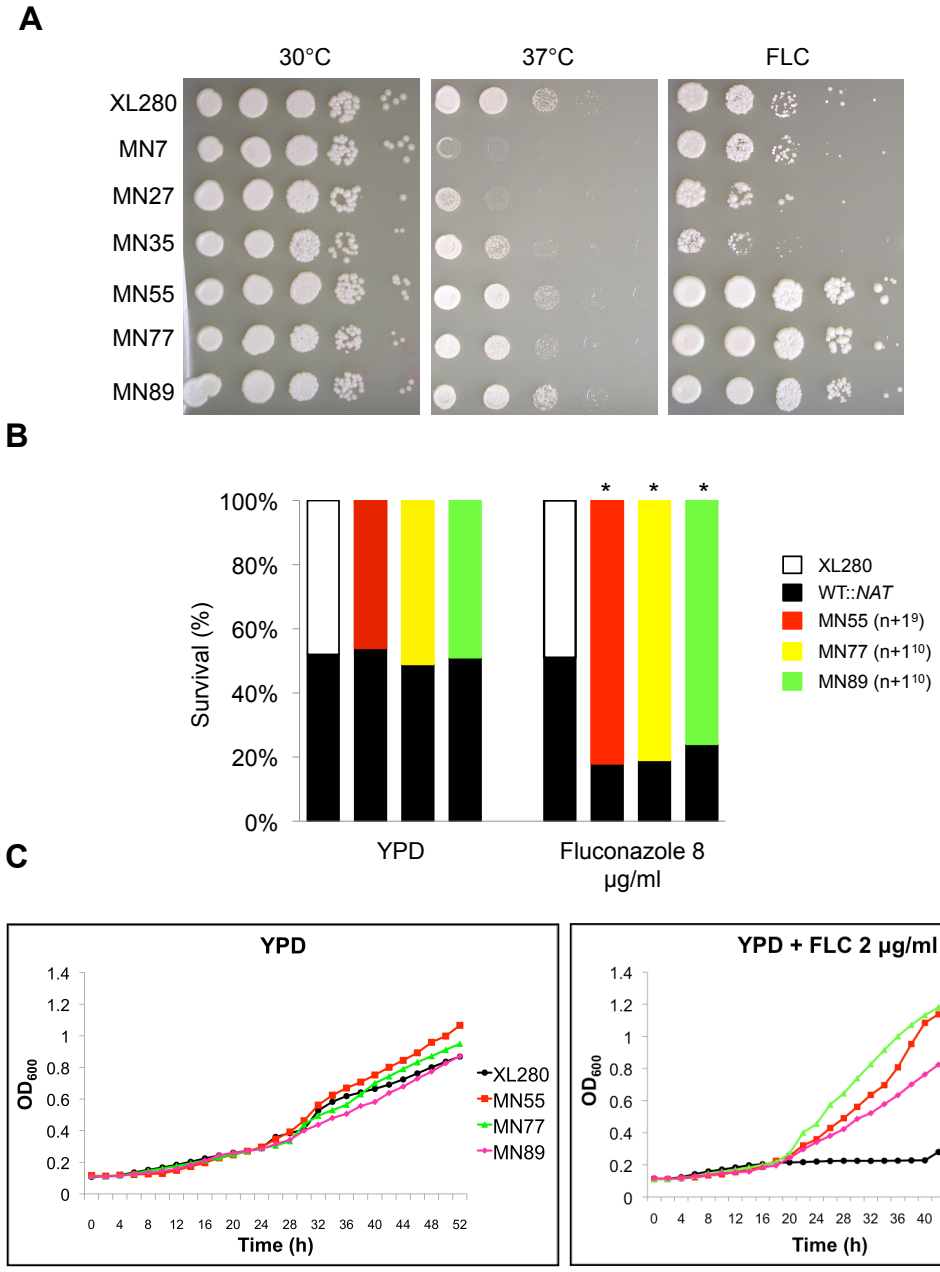

Figure 9. Aneuploid strains are fluconazole resistant. (**A**) XL280 meiotic progeny were grown in YPD, diluted 10-fold in water, spotted, and incubated under the following conditions: YPD at 30°C for 2 d, YPD at 37°C for 2 d, and YPD plus 8 µg/mL fluconazole (FLC) at 30°C for 6 d. (**B**) Three aneuploid strains exhibited increased competitive fitness in competition assays. An XL280 strain marked with a *NAT* resistance marker integrated in the *SPO11* genetic

locus was mixed together at equal abundance with XL280, MN55 (n+1^{9}), MN77 (n+1^{10}), or MN89 (n+1^{10}). The mixtures were incubated on YPD and YPD plus 8 µg/mL fluconazole (FLC) at 30^{o}C for 3 d. The cells were scraped from the plates, serially diluted, and plated on YPD and YPD plus NAT. The ratios of survival of each strain are shown for one representative experiment, and * represents significance at $p < 0.005$ from three independent experiments. We note that the *NAT* marker was neutral in this analysis and served to mark and detect the WT competitor cells. (**C**) The three aneuploid strains exhibited higher growth rates in the presence of fluconazole. Growth curves of the aneuploid strains were similar to the wild-type in rich media. However, in the presence of fluconazole the growth rate of the aneuploid strains was significantly higher than the wild-type.

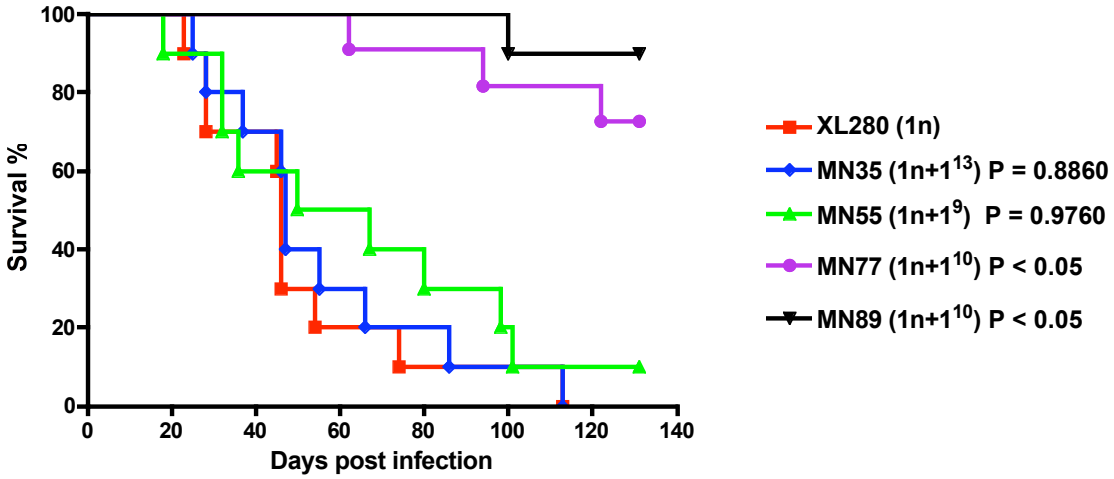

Figure 10. Aneuploid strains are pathogenic in the murine model. Ten female DBA mice per group were infected with 10^{6} cells of aneuploid strains MN35, MN55, MN77, and MN89. The mice were anesthetized by intraperitoneal injection of phenobarbital, and they were infected through intranasal instillation. The animals were monitored daily for clinical sighs of cryptococcal infection and sacrificed at predetermined clinical points that predict imminent mortality.

2.3.4 Aneuploidy Is Responsible for Phenotypic Changes

To examine whether the observed phenotypic changes are a consequence of aneuploidy, we compared the phenotype of aneuploidy strains

and euploid derivatives obtained following loss of the extra chromosome. Aneuploid strains are relatively unstable and frequently lose the 1n + 1 extra chromosomal copy to return to the 1n haploid euploid state. Here, we analyzed isolate MN77, which contains an extra copy of Chr 10 and produces increased amounts of melanin, a readily scorable phenotype. We grew MN77 at 37^{o}C to promote loss of the extra chromosome and isolated 22 randomly selected colonies for phenotypic and genotypic testing (Figure 11). Of these 22 isolates, 14 lost the extra copy of Chr 10 based on multiplex PCR analysis (Figure 11B), and in all cases concomitantly lost the enhanced melanin production phenotype (Figure 11A), therefore suggesting that Chr 10 disomy is responsible for the higher level of melanin produced. The remaining eight isolates that retained the Chr 10 aneuploidy all continued to produce higher levels of melanin (Figure 11A). To test whether Chr 10 disomy is also correlated with other phenotypes, we performed growth dilution assays with fluconazole (at 30^{o}C), FK506 (at 30^{o}C), and for growth at 37 °C. Similar to the melanin phenotype, all isolates that had lost the extra copy of Chr 10 exhibited WT phenotypes similar to the XL280 parent, and all isolates that retained the extra copy of Chr 10 exhibited the variant phenotype (Figure 11C). Similar experiments were performed for isolates MN35 (n+1^{13}) and MN55 (n+1^{9}), and we found that loss of the extra chromosome was linked with loss of the variant phenotypes (fluconazole sensitivity and

fluconazole resistance, respectively). These results indicate that aneuploidy causes the phenotypic changes observed in disomic strains.

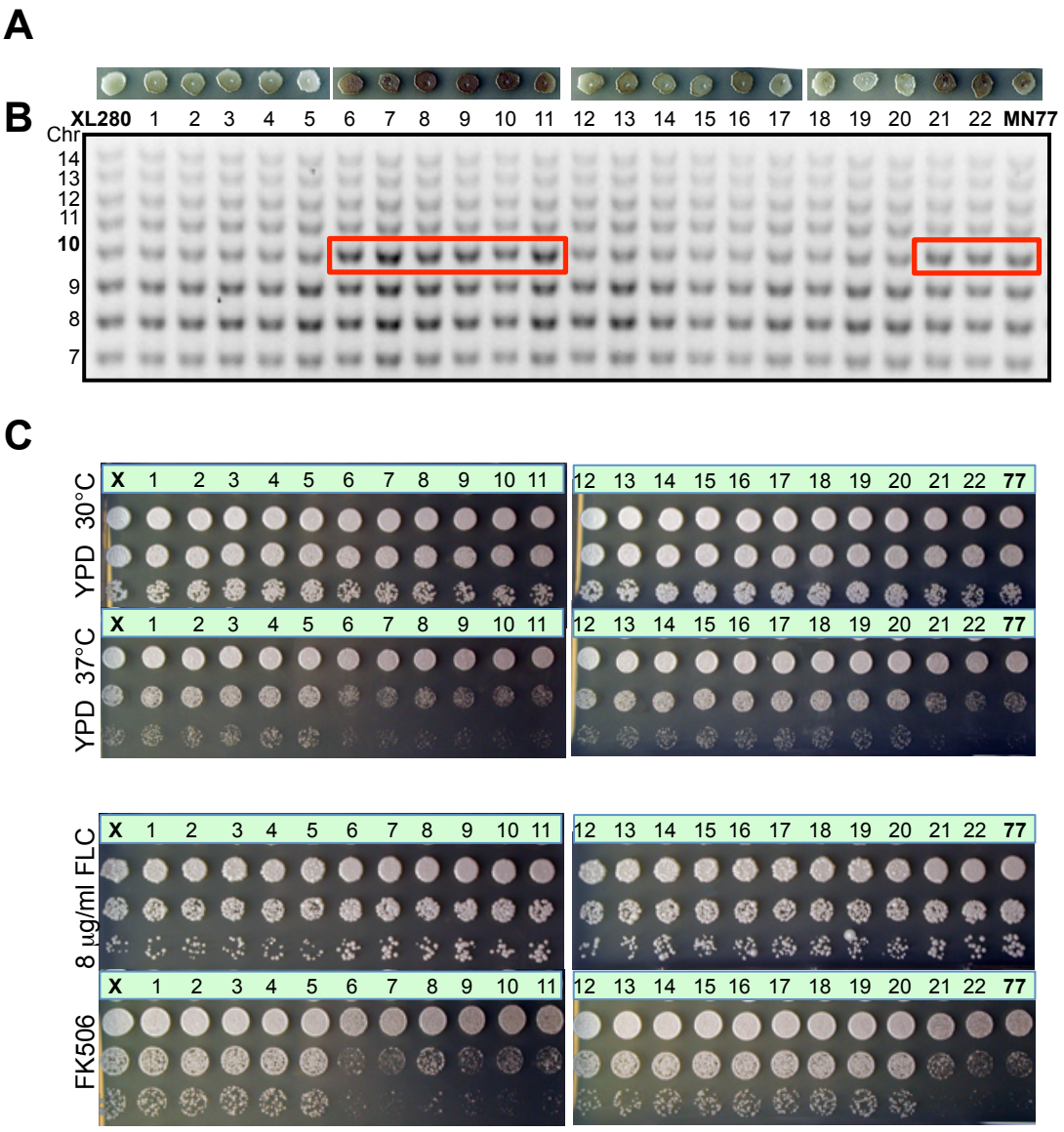

Figure 11. Aneuploidy causes the observed phenotypic changes. Strain MN77, which contains an extra copy of Chr 10 and has increased melanin production, was grown on YPD at 37°C for 3 d to promote aneuploidy loss. The

genotypes and phenotypes of 22 resulting mitotic progeny were analyzed. (**A**) Melanin production of 22 mitotic progeny on NS media at 30^{o}C for 2 d. (**B**) Multiplex PCR of 22 progeny detected an extra Chr 10 in all of the strains with the increased melanin phenotype and loss of the extra copy of Chr 10 in all progeny with a wild-type phenotype. (**C**) Phenotypic analysis of 22 mitotic progeny at high-temperature growth (37^{o}C for 2 d) and with drug treatment (FLC and FK506). XL280 (X) and MN77 (77) are the WT and aneuploid controls, respectively.

2.3.5 Aneuploidy Is Generated During Sexual Reproduction in *C. grubii* and *C. neoformans*

To test whether the generation of aneuploidy is specific to α-α unisexual reproduction, we isolated progeny from asexual mitotic reproduction and a-α opposite-sexual reproduction. We isolated 96 single colonies from yeast extract-peptone-dextrose (YPD) media following asexual mitotic reproduction and from spores produced on V8 agar following a-α sexual reproduction. No phenotypic or genotypic changes were detected among asexual mitotic progeny (0/96).

To test **a**-α sexual reproduction, we first investigated 88 F1 progeny from the cross between strains XL280α and JEC20**a**. To reduce the chance that α-α unisexual progeny from XL280 were mixed with the **a**-α sexual reproduction progeny from the cross, three times more yeast cells from the **a** parent JEC20 were mixed with the XL280α cells in the cross. As these strains are ~81% congenic, but not isogenic, they exhibit different phenotypes under various conditions, and their progeny (88 were examined) showed a range of phenotypes. Among 11 strains that had the most overt phenotypic changes, four

were aneuploid and no other aneuploids were detected in the larger progeny set (Figure 12A). Further PCR and RFLP tests confirmed that these F1 progeny strains were products of meiosis.

In addition, as a previous study showed that the *SXI2***a** homeodomain factor gene is sufficient to drive sexual development of haploid α cells (Hull, Boily et al. 2005), we introduced the *SXI2***a** gene into strain XL280α to mimic **a**-α sexual reproduction, generating strain MN140.23. Among 90 isolates generated from the selfing of this α + *SXI2***a** self-fertile strain, seven strains exhibited phenotypic changes compared to the parental strain. Further CGH analysis showed that two of these strains were aneuploid (Figure 12B). These results provide evidence that aneuploidy is also generated by **a**-α sexual reproduction.

To further examine this hypothesis, we analyzed **a**-α progeny from the cross between the isogenic *C. neoformans* var. *grubii* strains KN99**a** and KN99α. Among 88 progeny, 14 strains exhibited phenotypic changes, and eight were aneuploid (Figure 12C), indicating that **a**-α sexual reproduction between isogenic strains in the serotype A lineage can also generate phenotypic and genotypic diversity frequently involving aneuploid progeny. In summary, aneuploidy is generated during both α-α unisexual and **a**-α congenic sexual reproduction in both *C. neoformans* var. *grubii* (serotype A) and *C. neoformans* var. *neoformans* (serotype D).

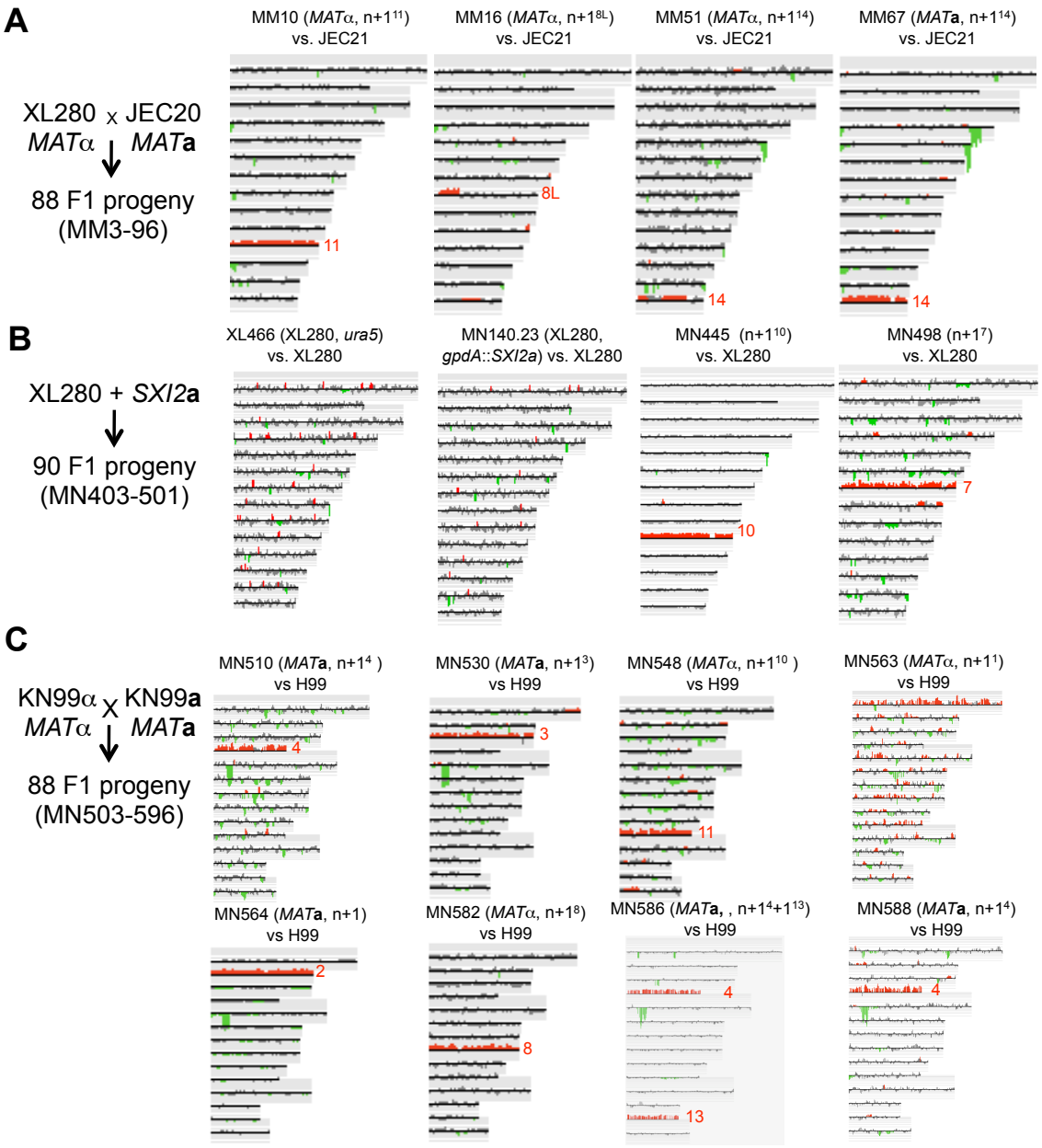

Figure 12. Aneuploidy is generated during a-α sexual reproduction. CGH analysis for representative progeny from (**A**) XL280α crossed with JEC20**a**; (**B**) XL280α "**a**-α" self-sexual reproduction generated via expression of *SXI2***a**;

and (**C**) *C. neoformans* var. *grubii* strain KN99α crossed with congenic strain KN99**a**.

2.4 Discussion

While sexual reproduction serves to admix genetic diversity from two distinct parents to produce progeny with a diverse genetic repertoire, sex also comes with a series of costs. Such costs include: (1) metabolic energy that must be devoted to mating and meiosis; (2) energy and time expended locating a mating partner; (3) that only 50% of parental genes are transmitted to any given progeny or that two individuals are required to produce one progeny (resulting in the so-called 2-fold cost of sex); and (4) the fact that two genomes that have run the gauntlet of adaptive selection are shuffled during the process, breaking apart well-adapted genomic configurations (Otto and Lenormand 2002). A central question then is: Why would an organism engage in unisexual reproduction? In some examples, unisex involves two genetically distinct α mating partners, and this leads to genetic exchange and the production of recombinant progeny, similar to **a**-α sexual reproduction. Also, α-α mating lowers the barrier to finding a rare mate in a predominantly α population, enabling outcrossing even if no **a** partners are available. But in other cases, an α isolate undergoes unisexual reproduction all by itself (via cell–cell fusion or endoreplication), and in these cases *there is no pre-existing genetic diversity to admix*. If there is no heterozygosity of the diploid undergoing meiosis, why undergo sex if the genome is homozygous everywhere?

As shown here, our studies provide direct experimental support for the hypothesis that unisexual reproduction can generate phenotypic and genotypic diversity *de novo*. Why might this be of selective and adaptive benefit? In the context of considering the costs of sexual reproduction, unisexual reproduction is one strategy by which several of the costs normally associated with sex can be lessened or mitigated entirely. First, the cost of finding a mating partner is considerably decreased in the case of mother–daughter cell mating in which the two cells are physically juxtaposed or eliminated entirely, such as in endoreplication, in which a single cell transitions from haploid to diploid as a prelude to meiosis. Second, during selfing unisexual reproduction, ~100% of the parental genes are directly transmitted to the F1 progeny, thus reducing the 2-fold cost of sex. Further, if one considers aneuploidy, >100% of the parental genes are transmitted to progeny. Third, unisexual reproduction eliminates the cost of sex associated with breaking apart well-adapted genomic configurations. Instead, unisexual reproduction preserves well-adapted genotypes by allowing mating between genetically identical cells (i.e., mother and daughter cells) and adding a limited amount of genetic diversity (including aneuploidy, chromosomal size polymorphisms/deletions, and SNPs) to a well-adapted genotype. In essence, unisexual reproduction provides a mechanism by which a well-adapted genotype can be changed much more subtly than standard sexual outcrossing, and in the case of well-adapted genotypes has the capacity to provide a more

parsimonious route to progeny that are enhanced in competitive fitness in response to subtle changes in environmental conditions.

Organisms that reproduce sexually have an advantage over organisms that reproduce asexually, as preexisting genetic diversity will generate novel combinations in the population. Meiosis, through homologous recombination, will generate distinct genetic compositions that may have a selective advantage over the parents in a new hostile environment. Unisexual reproduction is a sexual cycle that can occur between genetically identical cells and, as we observed here, allows the introduction of limited *de novo* genetic diversity through meiosis. As in most species, meiosis in *Cryptococcus* is a highly regulated process. Comparative genomics reveals that *Cryptococcus* species contain the meiotic genes involved in homologous recombination and synaptonemal complex formation (Loftus, Fung et al. 2005, D'Souza, Kronstad et al. 2011). The genes that support the presence of a meiotic pathway (termed the meiotic toolkit genes: *DMC1*, *MND1*, *MSH4*, *MSH5*, *SPO11*, *HOP1*, *HOP2*, and *REC8*) are highly conserved in *Cryptococcus*, and two of these (*SPO11* and *DMC1*) have been found to be critical for sporulation and spore germination during unisexual reproduction (Lin, Hull et al. 2005, Feretzaki and Heitman 2013).

Sex-induced phenotypic and genotypic variation in a clonal population is not restricted to the *Cryptococcus* genus. *Aspergillus nidulans* is a filamentous ascomycete that, along with its well-established sexual cycle, also has a

parasexual cycle wherein haploid mycelia fuse and then their nuclei fuse to form diploid nuclei (Pontecorvo and Kafer 1958). In the parasexual cycle, the diploid mycelium undergoes a transient aneuploid state by repeated loss of whole chromosomes to ultimately regenerate haploid progeny. A recent study has shown that the *A. nidulans* parasexual cycle can drive adaptive evolution. Hoekstra and colleagues generated homozygous diploid strains that were isogenic with their haploid progenitor (Schoustra, Debets et al. 2007). In a laboratory setting, faster growing variants frequently arose from the homozygous diploid strains but not from their haploid parents. Remarkably, all of the faster growing variants derived from a diploid parent were found to be haploids that arose through the parasexual cycle. As few as 3,000 generations were sufficient for the emergence of more rapid growth. Through genetic analysis, this study supported a model wherein the diploid serves as a capacitor for evolution. This enables recessive mutations to arise sequentially in the sheltered state of the diploid where they are complemented, and these mutations do not survive in the haploid because they are individually deleterious and swept from the population before a second mutation can arise (Schoustra, Debets et al. 2007). The parasexual state assorts and releases these mutations into the haploid state, where they exhibit reverse epistasis and only when in combination confer a benefit (i.e., faster growth), whereas individually each recessive mutation was deleterious. If parasexual cycles can function as capacitors to generate, store,

and then release genotypic and phenotypic diversity *de novo*, we propose that sexual cycles, including unisexual reproduction, might also serve such a role in which meiosis rather than parasexual chromosome loss is involved.

A similar unisexual selfing mechanism has been observed in the human fungal pathogen *C. albicans*. Alby et al. found that **a**/**a** cells of *C. albicans* lacking the Bar1 protease that destroys the α-factor mating pheromone undergo **a**/**a**-**a**/**a** unisexual mating, yielding tetraploids that can undergo concerted chromosome loss to complete a parasexual cycle (Alby, Schaefer et al. 2009). In addition, the parasexual cycle is induced between two **a**/**a** mating partners when mixed in ménage à trois matings with a limited number of α/α cells that serve as pheromone donors to trigger unisexual **a**-**a** reproduction (Alby, Schaefer et al. 2009). However, the parasexual progeny of *C. albicans* are characterized by high rates of aneuploidy (Forche, Alby et al. 2008). Although this chromosomal assortment process is imprecise, it may be retained due to a selective pressure that favors aneuploid strains under certain environmental conditions, such as in patients receiving fluconazole, a situation in which an isochromosome 5 derivative that confers drug resistance often arises (Selmecki, Forche et al. 2006). Aneuploidy has been linked to phenotypic changes, including resistance to antifungal drugs in both *C. albicans* and *C. neoformans*, which could provide a selective advantage during infection (Selmecki, Forche et al. 2006, Selmecki, Dulmage et al. 2009, Sionov, Lee et al. 2010).

The positive impact of aneuploidy on evolution and genetic diversification extends beyond the fungal kingdom to other unicellular eukaryotes. The parasitic protozoan *Leishmania* is the etiological agent behind one of the most common neglected diseases, leishmaniasis, a global cause of morbidity and mortality. No vaccine is available, and treatment relies heavily on pentavalent antimonial compounds with diminishing efficacy due to emerging drug resistance (Rojas, Valderrama et al. 2006). Recent studies have shown that aneuploidy is widespread in natural and clinical populations, with variation in the ploidy state (monosomic, disomic, or trisomic) for different chromosomes, even within the same isolate (Mannaert, Downing et al. 2012, Sterkers, Lachaud et al. 2012). Mosaic aneuploidy in *Leishmania* generates dynamic genome plasticity, is well tolerated, and can confer drug resistance (Ubeda, Legare et al. 2008, Sterkers, Lachaud et al. 2012), analogous to fungal azole resistance conferred by aneuploidy.

Given the finding that aneuploidy can underlie and drive adaptive evolution in *S. cerevisiae*, *C. albicans*, *C. neoformans*, and *Leishmania*, it seems likely that beneficial impacts of aneuploidy may be even more ubiquitous and remain to be discovered in other saprobic and pathogenic eukaryotic microbes.

Chapter 3. *Cryptococcus neoformans* Hyperfilamentous Strain is Hypervirulent in a Murine Model of Cryptococcal Meningoencephalitis

3.1 Introduction

Cryptococcus neoformans is an opportunistic fungal pathogen that is distributed worldwide. Pathogenic *Cryptococcus* lineages comprise two main species: *Cryptococcus neoformans* and *Cryptococcus gattii*. *C. neoformans* is classified into two varieties: var. *grubii* (serotype A) and var. *neoformans* (serotype D). The serotype A variety is the most common cause of infection, typically of the central nervous system in immunocompromised individuals, including transplant patients and HIV-infected individuals. Cryptococcal meningitis is the AIDS-defining illness in 30% of HIV infections worldwide and is uniformly fatal if untreated. Even with current antifungal therapies mortality rates remain unacceptably high. Although antiretroviral treatment can be effective in reducing the severity of infection, *Cryptococcus* is still a major cause of mortality in AIDS patients in HIV/AIDS endemic regions, such as Southeast Asia and Sub-Saharan Africa (Imwidthaya and Poungvarin 2000, Litvintseva, Thakur et al. 2006). Amphotericin B in combination with flucytosine has been documented in two clinical trials to be synergistic, but flucytosine is not available in developing nations, including those in Africa and Southeast Asia (van der Horst, Saag et al. 1997, Day, Chau et al. 2013). On the other hand, *C. gattii* infects healthy

individuals and is responsible for the ongoing *Cryptococcus* outbreak on Vancouver Island and in the Pacific Northwest in Canada and the United States (Bartlett, Kidd et al. 2008, Byrnes, Bildfell et al. 2009, Byrnes, Li et al. 2010).

C. neoformans has a defined life cycle and grows in the environment as a haploid budding yeast with α (common) and **a** (rare) mating type cells. Under nutrient limiting conditions it has the ability to mate and undergo a dimorphic transition from vegetative yeast to hyphal growth (Idnurm, Bahn et al. 2005). Hyphal development can occur between cells of the opposite mating type (bisexual reproduction) or cells of one mating type (unisexual reproduction), resulting in production of basidia, where meiosis occurs to generate haploid spores (Lin, Hull et al. 2005). Unisexual reproduction has been directly observed under laboratory conditions for serotype D isolates. Population genetic studies support the hypothesis that unisexual reproduction also occurs in nature in *Cryptococcus neoformans* var. *grubii* and *C. gattii*, and may be responsible for the evolution of highly pathogenic strains (Fraser, Giles et al. 2005, Lin, Litvintseva et al. 2007, Nielsen, De Obaldia et al. 2007, Bui, Lin et al. 2008, Hiremath, Chowdhary et al. 2008, Saul, Krockenberger et al. 2008, Lin, Patel et al. 2009, Chowdhary, Hiremath et al. 2011). Moreover, recent studies demonstrate that unisexual reproduction generates phenotypic and genotypic diversity *de novo* in even clonal populations, generating aneuploid virulent

progeny strains that exhibit significant resistance to antifungal drugs (Ni, Feretzaki et al. 2013).

Cryptococcal infections are thought to be acquired by inhalation of infectious propagules from the environment. Spores are of an ideal size to penetrate and colonize the alveoli of the lung and are proven to be pathogenic (Botts, Giles et al. 2009, Giles, Dagenais et al. 2009, Velagapudi, Hsueh et al. 2009). *C. neoformans* can colonize the host's respiratory tract for years, forming granulomas that persist in an asymptomatic dormant latent state. However, when host immunity is compromised the fungal cells disseminate hematogenously, cross the blood brain barrier, and infect both the meninges and parenchyma of the brain to cause cryptococcal meningoencephalitis, which is the most common clinical manifestation of the disease in immunocompromised individuals. The morphology of the fungus inside the host varies from small round yeast cells to titan cells, which are thought to play roles in survival and evasion of the immune system during infection (Okagaki, Strain et al. 2010, Zaragoza, Garcia-Rodas et al. 2010). However, hyphae or pseudohyphae are rare, as hyphal growth is suppressed by the physiological conditions of the host (high temperature, moisture, and high CO_2 levels) and these morphotypes are associated with low virulence as they can successfully activate protective immunity (Todd and Herrmann 1936, Freed, Duma et al. 1971, Fromtling, Blackstock et al. 1979,

Fromtling, Blackstock et al. 1979, Williamson, Silverman et al. 1996, Wang, Zhai et al. 2012).

Dimorphism is common among other fungi that cause systemic infections (Lin 2009). One example is *Candida albicans*, a fungus that resides as a common commensal in the mammalian gastrointestinal tract. Hyphal formation has been associated with the pathogenic state of *Candida* and the dimorphic transition is required for fungal invasion and dissemination (Lo, Kohler et al. 1997). Similar to *Cryptococcus*, *Histoplasma capsulatum* and *Blastomyces dermatitidis* grow as hyphae in the environment, and in response to high temperature, they undergo a dimorphic transition to their highly virulent yeast form (Nemecek, Wuthrich et al. 2006, Klein and Tebbets 2007, Nguyen and Sil 2008, Webster and Sil 2008).

The mechanism via which infections are acquired is universal for all *Cryptococcus* species; however, the mechanism of immune response in the host can differ significantly between var. *neoformans*, var. *grubii*, and *C. gattii*. In immunocompetent individuals the serotype D spores or yeast propagules that reach the lung are cleared by a protective immune response characterized by elevated expression of Th1-type cytokines (IFN-γ, TNF-α, IL-12, IL-2, etc.) and high concentrations of neutrophils and dendritic cells that successfully clear the infection in the murine model (Koguchi and Kawakami 2002, Chen, McNamara et al. 2008, Guillot, Carroll et al. 2008). In contrast, *C. gattii* infections in mice trigger

a non-protective immune response through high levels of Th-2 associated cytokines (IL-4, IL-5, IL-9, IL-10, and IL-13) (Dong and Murphy 1995, Koguchi and Kawakami 2002, Vecchiarelli, Pietrella et al. 2003, Cheng, Sham et al. 2009). Dong *et al*. hypothesized that *C. gattii* infects healthy individuals because high levels of IL-4 inhibit neutrophil migration to the lung (which is crucial for protective immunity), allowing yeast cells to survive longer inside the host and disseminate successfully to the brain (Dong and Murphy 1995). Interestingly, experimental pulmonary infections with the serotype A strain H99α elicit different types of immunity in different mouse models. In BALB/c mice H99α triggers a Th-2 type immunity that is related to changes in lung function and results in a fatal outcome (Noverr, Cox et al. 2003, Jain, Zhang et al. 2009, Hardison, Ravi et al. 2010), while in the C57BL/6 mouse model serotype A induces a mixed immune response that alternates between Th-1 and Th-2 during the course of the infection that greatly affects the outcome of the disease (Huffnagle, Boyd et al. 1998, Cheng, Sham et al. 2009). Thus, for *Cryptococcus* cells to survive inside the host it may be crucial to induce a less protective immune response.

Population genetics data have shown that unisexual reproduction may occur in nature for serotype A and *C. gattii* species, although the unisexual cycle has not been directly observed under laboratory settings. Thus, although unisexual reproduction plays a crucial role into virulence, through production and dispersal of infectious spores and generation of new virulent strains, possible

roles of morphogenesis in virulence have not been extensively analyzed due to the low pathogenicity characteristic of many serotype D strains. Moreover, many serotype D strains exhibit limited filamentation and produce few spores. Previous studies identified a unique hyperfilamentous serotype D strain that can generate abundant hyphae and spores via unisexual reproduction (Lin, Huang et al. 2006). It was also recently reported that this strain (XL280α) and a congenic partner of opposite mating type (XL280**a**) cause significant mortality in a murine model (Ni, Feretzaki et al. 2013, Zhai, Zhu et al. 2013) compared to previous animal studies on serotype D (Davidson, Nichols et al. 2003, Nielsen, Marra et al. 2005).

In light of these findings, we studied the virulence of the hyperfilamentous strain XL280α in a murine model compared with its well-established parent JEC21α. Although the two serotype D strains are phenotypically similar, we found that XL280 is hypervirulent compared to JEC21. We also found that XL280 causes both pulmonary and central nervous system infections. Although both of these strains grow as budding yeasts inside the host, XL280 cells were significantly larger and oblong, resembling a “football” like shape. Surprisingly, our study revealed high levels of Th2-type cytokines in the lungs of XL280 infected mice, indicative of a less protective immune response, compared to mice infected with JEC21. These findings offer new insights into the roles of unisexual reproduction, morphogenesis, and dimorphism in virulence of *C. neoformans*.

3.2 Materials and Methods

3.2.1 Ethics statement

All of the animal experiments were performed in the Division of Laboratory Animal Resources (DLAR) facilities at Duke University Medical Center (DUMC). All of the mouse experiments were performed according to the guidelines of NIH and Duke University Institutional Animal Care and Use Committee (IACUC). The animal experiments were reviewed and approved by the DUMC IACUC under protocol number A266-08-10.

3.2.2 Strains and Media

The strains used in this study were *Cryptococcus neoformans* serotype A and D. For phenotypic analysis we used the sequenced serotype A laboratory strain H99α and a mutant, *cap59*Δ, defective in capsule production (Chang and Kwon-Chung 1994). XL280α is a serotype D strain and is a sequenced progeny of the two sibling strains B3501α and B3502**a**, and related to the congenic pair JEC21α/JEC20**a** genome reference sequence strains (Kwon-Chung, Edman et al. 1992, Heitman, Allen et al. 1999, Lin, Huang et al. 2006, Ni, Feretzaki et al. 2013, Zhai, Zhu et al. 2013). The *ste7*Δ and *cpk1*Δ pheromone signaling deletion mutants were derived in the XL280 background (Lin, Jackson et al. 2010, Feretzaki and Heitman 2013). The XL280 *crg1* mutant has a T-DNA insertion in the coding region that compromises expression of the gene (Feretzaki and

Heitman 2013). All strains were maintained on yeast extract-peptone-dextrose (YPD) media. Mating cultures were performed on 5% V8 juice agar medium (pH = 5 or 7).

3.2.3 Phenotypic Analysis

To examine the virulent phenotypes of the strains *in vitro*, cells were grown overnight in liquid YPD cultures at 30°C. The next day the cells were washed with sterile water and adjusted to an equal cell density. 10-fold serial dilutions were spotted on YPD at 30°C and 37°C, on YPD + 1 μg/ml FK506 at 30°C and 37°C, and on YPD + 8 μg/ml fluconazole (FLU) at 30°C. To examine melanin production the cells were spotted on niger seed and L-DOPA plates and incubated for 7 days. To visualize the capsule, equal numbers of the cells were diluted into capsule inducing media (Dulbecco's modified Eagle's media with 25 mM $NaHCO_3$), incubated for 7 days at 30°C, and screened by microscopy using India Ink. To estimate shed GXM, cells grown to saturation in capsule inducing media for 7 days were incubated at 70°C for 15 min, centrifuged at 1,600g for 5 minutes, and the supernatant containing shed capsule was filtered with a 0.2 μm filter. Equal volumes from each strain were run on a 0.6% agarose gel at 25 volts for 12 hours and transferred onto a nylon membrane using Southern blot techniques. The membrane was blocked with 5% milk in TBST (1x Tris-buffered saline plus 0.1% Tween) and probed with the monoclonal antibody (MAb)18b7

(1:1,000 dilution) overnight at 4^{o}C (O'Meara, Hay et al. 2010). The membrane was washed with TBST, incubated with a secondary anti-mouse peroxidase-conjugated antibody (1:10,000 dilution), washed again with TBST, and developed with ECL Prime western blotting detection reagent (Amersham).

3.2.4 Murine Infection and Tissue Dissection

Cryptococcus strains were grown overnight in liquid culture of YPD. The next day the cells were washed twice with sterile PBS, counted with a hemocytometer, and diluted to an appropriate cell density (1 x 10^6 cells/ml). To prepare the yeast/hyphae inocula, the cells were spotted on V8 media and incubated for 8 days in the dark at room temperature. The colonies were scraped off the plates, vortexed, washed with PBS, counted with a hemocytometer (yeast cells and spores), and adjusted to a density of 1 x 10^6 cells/ml. The intranasal instillation method was performed as previously described (Lin, Nielsen et al. 2008). Briefly, groups of 10 mice female DBA mice (6- to 8-weeks old) were anesthetized by intraperitoneal injection of Phenobarbital (Nembutal) (37 mg/kg), and infected intranasally with 1 x 10^6 cells/ml in 50 μl PBS. The cell density of the inocula was confirmed by plating serial dilutions and counting CFUs following infection. The animals were monitored twice daily through the course of the experiments. The animals showing signs of morbidity (weight loss, extension of the cerebral portion of the cranium, imbalance, gait changes, paralysis, seizures, convulsions, or coma) were sacrificed by CO_2 inhalation. The survival rates were

plotted against time using Kaplan-Meier survival curves, generated with Prism 4.0 (GraphPad software, La Jolla, CA, USA). The P values were calculated with the Log-rank (Mantel-Cox) test and a P value of <0.05 was considered significant. To determine the fungal burden in the infected tissues, the lungs and brains of the euthanized animals were removed, weighed, and homogenized in 2 ml sterile PBS. Serial dilutions of the samples were plated on YPD media containing 100 μg/ml chloramphenicol to enumerate CFUs.

3.2.5 Cytokine Analysis

Mice were infected with strain XL280 or JEC21 via intranasal instillation. At 3, 7, and 10 days post infection lung tissues were excised, homogenized in 1 ml PBS, and 50 μL were diluted and plated on YPD to determine fungal burden at designated time points. 1 ml of 2x protease inhibitor buffer (containing PBS, Complete Protease tablets (Roche) and 0.05% Triton X100) was added and the homogenate was centrifuge at 3,500 RPM for 15 min at 4^{o}C. Cytokine production in the pulmonary tissues was measured using the Bio-Plex Protein Array System (Luminex-based technology) (Bio-Rad Laboratories, Hercules, CA). The supernatants of the homogenized lungs were assayed for the presence of interferon (IFN)-γ, interleukin (IL)-1α, IL-1β, IL-2, IL-4, IL-5, IL-10, IL-12 p70, IL-17, tumor necrosis factor (TNF)-α, and granulocyte-colony stimulating factor [G-CSF] levels as well as chemokines (macrophage inflammatory protein [MIP]-1α

(CCL3), MIP-1β (CCL4), macrophage chemoattractant protein [MCP]-1 (CCL2), and keratinocyte-derived chemokine (KC) (CXCL1)). Cytokine and chemokine data was derived from four independent experiments and analyzed using Prism 4.0 (GraphPad software, La Jolla, CA, USA). P values were calculated using two-way ANOVA statistical analysis and a P value of <0.05 was considered significant.

3.2.6 Histopathology

Lungs of infected DBA mice were inflated and harvested in 10% neutral buffered formalin at 3, 7, and 10 days post infection. The fixed tissues were embedded in paraffin, cut into 5 μm sections and stained with hematoxylin and eosin (H&E), mucicarmine, or Periodic acid–Schiff (PAS stain) at the Research Histology Laboratory, Department of Pathology, Duke University Medical Center. The slides were visualized by light microscopy and the images were processed using MetaMorph Premier at the Duke University light microscopy core facility.

3.3 Results

3.3.1 Phenotypic Characterization of XL280

To investigate the impact of hyphal development during unisexual reproduction we utilized the serotype D hyperfilamentous strain XL280α. XL280α is a haploid progeny of two well-validated and sequenced sibling strains, a hypo-filamentous isolate B3501α and a self-filamentous isolate of strain B3502**a** (which is congenic with the congenic pair JEC21α/JEC20**a**) (Heitman, Allen et al. 1999, Loftus, Fung et al. 2005, Lin, Huang et al. 2006). B3501α/B3502**a** are F1 progeny descended from a cross between a clinical (NIH12α) and an environmental isolate (NIH433**a**) (Heitman, Allen et al. 1999), and XL280 is an F1 progeny from a B3501α x B3502**a** cross (Lin, Huang et al. 2006). In recent studies, the genomes of XL280 and strain JEC21 (JEC21α/JEC20**a** are congenic with the XL280 parental strain B3502**a**) were compared by next-generation sequencing (NGS) revealing that the two strains are genetically identical across 81% of the genome, the remaining 19% differs by 0.5%, and overall they are 99.88% identical at the sequence level (Ni, Feretzaki et al. 2013). Extensive genetic, molecular, and genomic analysis showed that XL280 is a euploid, haploid strain that undergoes robust hyphal development during unisexual reproduction characterized by a mixture of haploid or diploid hyphae that

generate abundant haploid recombinant spore progeny produced by meiosis (Feretzaki and Heitman 2013).

Serotype D clinical isolates are rare compared with the highly virulent serotype A clinical strains that usually infect immunocompromised individuals. Moreover, previous studies showed that serotype D strains (including JEC21) exhibit low virulence *in vivo* and usually require high inocula for intranasal instillation or tail vain injection in a murine infection model (Heitman, Allen et al. 1999). However, in previous studies Zhai *et al*. and we showed that a lower inocula of XL280 could successfully infect and cause disease in mice (Ni, Feretzaki et al. 2013, Zhai, Zhu et al. 2013), similar to what we have observed for highly virulent serotype A strains (Nielsen, Cox et al. 2003).

Cryptococcus must evade and escape the immune system to successfully colonize the respiratory tract of the host and disseminate to the CNS. Thus we assessed major virulence attributes (growth at 37^{o}C, melanin production on niger seed or L-DOPA media, and capsule production), antifungal drug sensitivity (fluconazole and FK506), and unisexual reproduction. The strains both grew well at higher temperature but exhibited growth differences in the presence of fluconazole or FK506 (Figure 13A). Melanin is a dark cell wall-associated pigment that is negatively charged and protects *Cryptococcus* from macrophage killing and oxidative, and possibly also nitrosative, stress challenge (Wang, Aisen

et al. 1995, Gomez and Nosanchuk 2003). Melanin production was similar on L-DOPA, whereas JEC21 exhibited higher levels of melanin on niger seed medium.

Capsule is a polysaccharide structure that can inhibit phagocytosis of *Cryptococcus* and also enhances intracellular replication of yeast cells that have been phagocytosed by macrophages (Kozel 1995, Tucker and Casadevall 2002). Capsule secretion and attachment to the cell wall are essential for virulence and acapsular mutants (i.e. *cap59*Δ) are severely attenuated/avirulent in disease progression models (Chang and Kwon-Chung 1994, Moyrand, Chang et al. 2004). XL280 and JEC21 were equally capable of secreting and attaching the capsule on their cell wall under capsule-inducing media and under physiological conditions (DMEM at 37^{o}C under 5% CO_2) (Figure 13C and 11D).

A major difference was observed in hyphal development during α-α unisexual reproduction. As previously reported, JEC21α generates only a limited amount of hyphae after prolonged incubation (~2 weeks) on mating media, manifested as only one or a few tufts of hyphae along the growth periphery (Wickes, Mayorga et al. 1996, Lin, Hull et al. 2005). In contrast, XL280α is hyperfilamentous with abundant hyphae emerging as soon as 24 hrs after plating on mating media that develop along the entire circumference of the growth periphery (Figure 13B). Thus, apart from hyphal development, the phenotypic analysis revealed that the major virulence factors of XL280 and JEC21 *in vitro*

are similar and a possible impact on virulence may be attributable to the differences in hyphal development or other attributes not analyzed here.

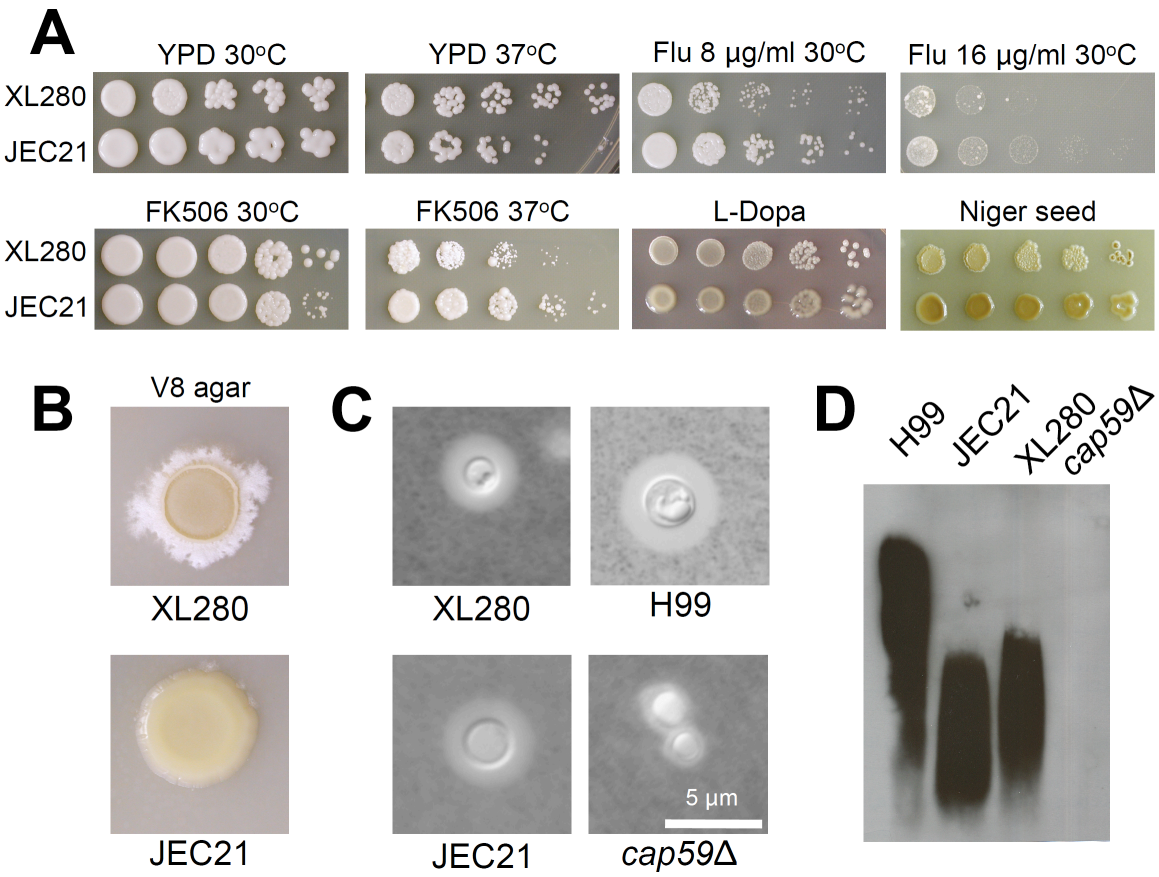

Figure 13. Phenotypes of virulence factors. In vitro phenotypic assays of virulence associated attributes of XL280 and JEC21. (**A**) The strains were grown in liquid YPD, washed with water, and spotted in 10-fold serial dilutions on the following media and conditions: YPD at 30°C and 37°C for 2 days, YPD plus 8 and 16 µg/ml of fluconazole at 30°C for 6 days, YPD plus 1 µg/ml of FK506 at 30°C and 37°C for 3 days, L-Dopa at 30°C for 3 days, and niger seed at 30°C for 6 days. (**B**) Unisexual reproduction cultures were incubated on V8 agar (pH=7), for 2 - 3 weeks in the dark at room temperature. (**C**) For capsule evaluation, cells were grown in DMEM for 6 days and visualized by light microscopy using India ink and (**D**) supernatants of the cells containing secreted capsule was isolated,

subjected to gel electrophoresis, and then immunoblotted with an anti-GXM antibody.

3.3.2 XL280 is a Hypervirulent Serotype D Strain

Previous studies showed that even a low inocula of XL280α yeast cells (5 x 10^5 cells/ml) displayed high levels of virulence in the murine model (Ni, Feretzaki et al. 2013, Zhai, Zhu et al. 2013). Virulence assays were performed using the inhalation instillation infection model to compare the relative pathogenicity of XL280 with JEC21. The mice were infected with one dose (1 x 10^6 CFU/animal) using either yeast cells or a yeast/spore mixture produced by a mating culture incubated on V8 media to stimulate sexual reproduction. Survival was monitored for 125 days after infection. We found that XL280 was significantly more virulent than JEC21 (Figure 14A). Mice infected with an XL280 yeast inoculum succumbed to the disease by 35 days post infection, while in the yeast/spore mixed infection the animals progressed to lethal infection by 80 days (Figure 14A). The lower pathogenicity of the yeast/spore mixture may be attributable to the presence of hyphae generated during mating, which have been associated with low virulence in previous studies (Wang, Zhai et al. 2012, Zhai, Zhu et al. 2013). On the other hand JEC21 was severely attenuated for virulence in both cases. The first signs of pulmonary cryptococcosis (tachypnia, weight loss) were observed as early as 6 days post infection in mice infected with XL280. We also noticed that moribund XL280 infected mice exhibited severe

neurological symptoms often associated with cryptococcal meningitis (disorientation, balance disorder, and hydrocephalus due to accumulation of cerebrospinal fluid (CSF), and these were not observed in any of the JEC21 infected animal cohorts). These findings indicate that XL280 is highly pathogenic in the murine model, compared to the hypo/avirulent strain JEC21.

Previous studies have shown that there is a genetic link between virulence and the signaling pathways that regulate morphogenesis. It has been shown that virulence and hyphal development are quantitative traits and some components of the pheromone signaling cascade are involved in pathogenesis. However, the majority of hyphal development genes tested were found to be dispensable for virulence in the low virulence serotype D strains (Chang, Penoyer et al. 2001, Clarke, Woodlee et al. 2001, Davidson, Nichols et al. 2003, Wang, Cutler et al. 2004, Lin, Huang et al. 2006, Ren, Springer et al. 2006, Wang, Zhai et al. 2012). We therefore tested several well characterized genes known to be involved in hyphal development. Crg1 is an RGS protein and a negative regulator of the pheromone-signaling cascade; mutation of the gene enhances hyphal development (Wang, Cutler et al. 2004). In previous studies we isolated an insertional mutant of *CRG1* in the XL280 background, which is more hyperfilamentous than the WT during unisexual reproduction (Feretzaki and Heitman 2013). On the other hand, Cpk1 and Ste7 are a highly conserved MAP kinase and MAP kinase kinase that play central roles in the pheromone response

pathway and both are required for filamentation during unisexual and bisexual reproduction (Davidson, Nichols et al. 2003, Lin, Jackson et al. 2010, Feretzaki and Heitman 2013). Mice were infected intranasally with XL280 WT and *crg1*, *ste7*Δ, and *cpk1*Δ mutant strains. Virulence of the *ste7*Δ and *cpk1*Δ mutant strains was comparable to the WT, while the *crg1* insertion mutant was more virulent than the WT (Figure 14B). These phenotypes are consistent with previous observations in both the hypovirulent serotype D and the highly virulent serotype A strain backgrounds (Davidson, Nichols et al. 2003, Shen, Wang et al. 2008, Lin, Jackson et al. 2010).

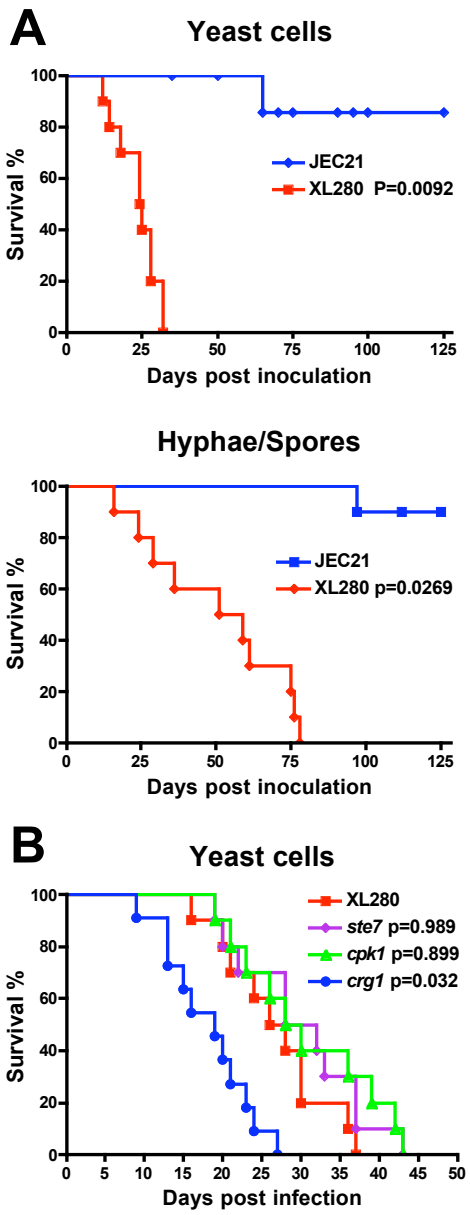

Figure 14. XL280 is hypervirulent compared with JEC21. 10 DBA mice were infected intranasally with 1 x 10^6 yeast cells or a mixture of yeast and spores isolated from a unisexual reproduction culture from each strain. Animal survival was monitored for 125 days post infection. (**A**) The XL280 strain was significantly more virulent than JEC21 in both cases (p=0.0092 and p=0.0269). (**B**) The components of the pheromone signaling cascade are dispensable for

virulence in the XL280 background (*ste7* p=0.989 and *cpk1* p=0.899). However, the *crg1* mutant was significantly more virulent than WT (p=0.032). Statistical analysis was performed using the Log-rank (Mantel-Cox) test.

3.3.3 Progression of XL280 Infection

Although strain JEC21 is attenuated for virulence, during the course of the experiment a few mice exhibited signs of temporary distress that are typically associated with pulmonary infections. Thus, we hypothesized that the two strains might cause disease in different ways. To investigate the progression of disease during XL280 and JEC21 infections, growth and dissemination of the fungal cells to various organs were examined. 10 mice for each group were infected through intranasal instillation using a 2-fold lower inocula of yeast cells (5×10^5 CFU/animal). This dose served to delay the pathogenicity of XL280 and allowed monitoring of the progression of the infection over the course of a month. Therefore, we measured the prevalence of the cells at an early time point in the infection course (2 weeks) and a later one (4 weeks). Higher numbers of CFUs in the lungs are indicative of a predominant pulmonary infection while presence of CFUs in the brain reflects dissemination to the central nervous system. We found that both strains were able to survive inside the host, and their levels in the lung were similar at two weeks, although by four weeks JEC21 was considerably less prevalent (Figure 15A). Interestingly, XL280 was at a significantly higher abundance in the brain at both time points, while JEC21 infection was cleared from the CNS by four weeks post infection (Figure 15A). These results indicate

that XL280 and JEC21 are both capable of surviving and replicating inside the host; however, XL280 more successfully establishes an infection in the lung and then disseminates to the central nervous system to cause meningoencephalitis.

XL280 and JEC21 both grow as a yeast on solid and in liquid media under laboratory conditions. However, XL280 produces abundant hyphae during solo incubation on mating inducing media leading to unisexual reproduction. Although physiological conditions inhibit hyphal development inside the host, there are rare cases where hyphae have been observed to develop during infection (Todd and Herrmann 1936, Freed, Duma et al. 1971, Williamson, Silverman et al. 1996, Wang, Zhai et al. 2012). To examine the fungal morphology of XL280 and JEC21, mice were infected intranasally, and histological examination of the lungs and brains was conducted at two and four weeks post infection. As expected hyphae or pseudohyphae were absent from the samples and only yeast cells were observed with both strains (Figure 15B). However, in the lung tissues of *Cryptococcus* infected mice the morphology of the XL280 cells differed from the typically round yeast cells observed *in vitro*. The cells were more elongated, oblong, and resembled “football” like structures (Figure 15B). We excluded the possibility that this cell morphology was an artifact caused by the fixation or staining process, as tissues from both XL280 and JEC21 infected mice were processed by the same technical procedure. Moreover, this phenotype was observed in multiple independent experiments and at different time points.

However, we were not able to observe this morphology under laboratory conditions outside the host. These “football” shaped cells seemed larger than their counterpart round yeast cells, which could contribute to the virulence of this strain. Previous studies have shown that morphological changes that result in giant/titan cells affect the virulence of *Cryptococcus* and increase pathogenicity (Okagaki, Strain et al. 2010, Zaragoza, Garcia-Rodas et al. 2010, Crabtree, Okagaki et al. 2012). The heightened virulence of the XL280 strain might be attributed to higher levels of capsule produced by these larger cells, which may negatively impact the immune system of the host. Moreover, this unique morphology and the larger size of the cells may confer protection against phagocytosis by alveolar macrophages and allow more rapid dissemination to the CNS.

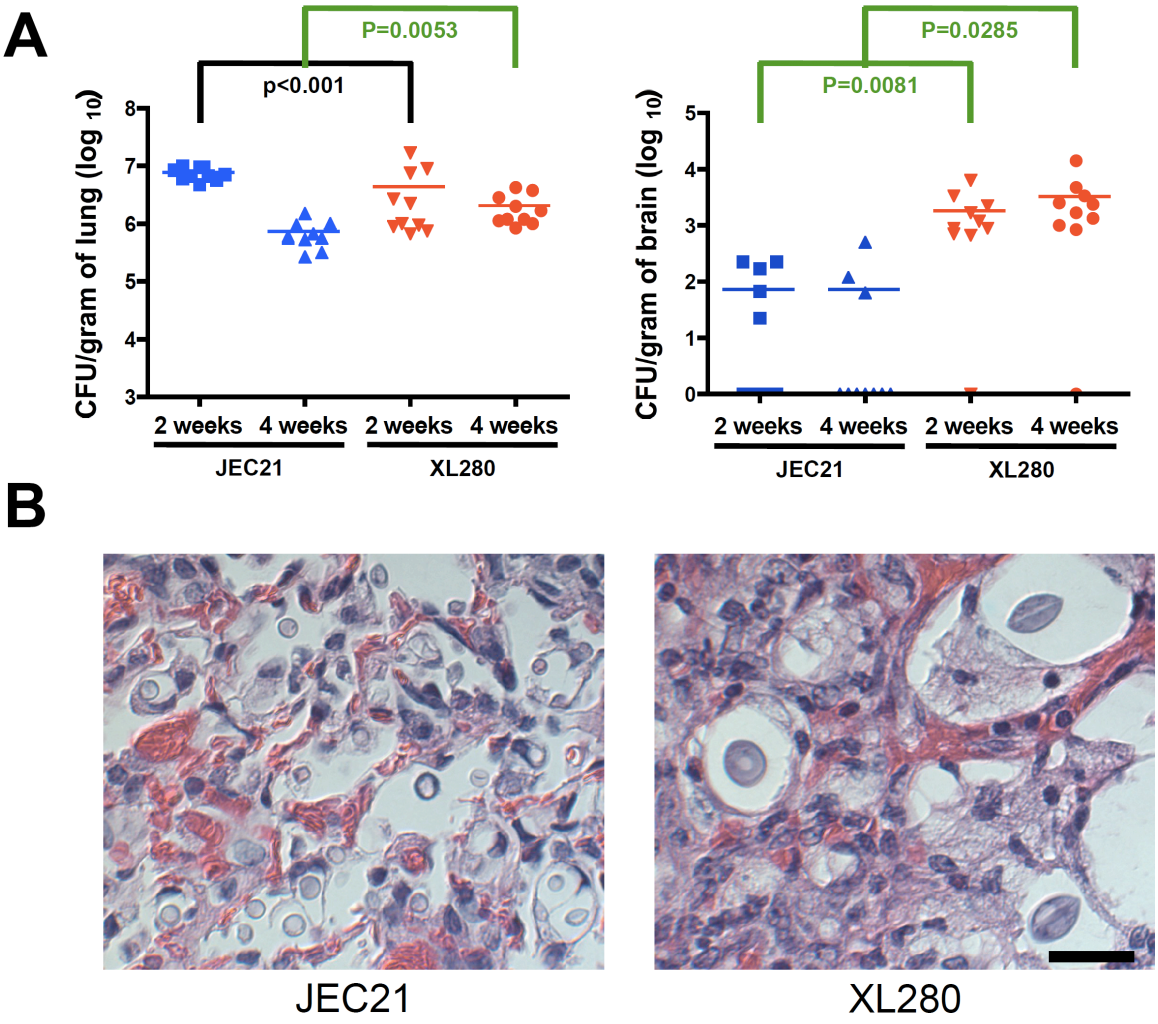

Figure 15. XL280 disseminates to the brain. (**A**) Mice were infected intranasally with 5 x 10^5 yeast cells. At two and four weeks post infection the lungs and brains were isolated from 10 animals infected with each strain. The tissues were homogenized and serial dilutions were plated to recover CFUs and calculate the fungal tissue burden. XL280 fungal burden was significantly higher in both the lung and brain at four weeks post infection (p=0.0053 and p=0.0285). (**B**) Based on histopathological analysis of pulmonary tissues, XL280 yeast cells were morphologically different from JEC21. They were significantly larger and exhibited a "football" like structure. Scale bar = 20 μm.

3.3.4 XL280 Infected Animals Exhibit a Th2-Biased Cytokine Profile

Previous studies have shown that the cytokine profile of *Cryptococcus* infection differs significantly between the different lineages and is usually indicative of the immune response and the outcome of the disease. A recent study showed that cytokine expression during *C. gattii* infection in mice induces a Th2-type immune response associated with less protective immunity (Cheng, Sham et al. 2009). Thus, it has been hypothesized that *C. gattii* lung infections are not efficiently cleared by the immune system of immunocompetent individuals, and this is because they fail to induce protective Th1-type immunity usually observed in response to var. *neoformans* infections (Wright, Bubb et al. 2002, Cheng, Sham et al. 2009). On the other hand, experimental and clinical studies conclude that *C. neoformans* var. *grubii* isolates elicit both Th-1 and Th-2 immune response in healthy individuals, which are resistant to serotype A infections. The balance of the associated cytokines triggers a synergistic effect between Th-1 and Th-2 immunity that clears the infection and promotes the development of a protective immune response (Huffnagle and Lipscomb 1998, Beenhouwer, Shapiro et al. 2001, Williams, Wormley et al. 2011). These findings are in accord with *C. gattii* infections occurring commonly in immunocompetent hosts, while *C. neoformans* is most frequently associated with infections in immunocompromised individuals.

To determine the cytokine profile during infection by XL280 or JEC21, mice were infected with yeast cells from each strain and lungs were collected at three time points early in the course of infection (3, 7, and 10 days post infection) (Figure 16A). No significant differences were apparent for the majority of cytokines expressed in XL280 and JEC21 infected mice (Figure 16B). However, IL-4, IL-5, and IL-10 ($p<0.05$) levels were was significantly higher in XL280 infected mice compared with JEC21 (Figure 16C). All three cytokines have been associated with Th2 immunity; IL-4 is a major determinant of the differentiation of T cells into Th2 cells, while IL-10 can downregulate Th1 responses. The balance between Th1 and Th2 cytokines defines the progression and the outcome of the disease. To assess the overall Th1/Th2 cytokine balance the ratio of the IL-4 Th2 cytokine to IFN-γ, a Th1 associated cytokine critical for innate and adaptive immunity, was calculated. At 7 and 10 days post infection cytokine production was significantly polarized towards Th2 immunity in XL280 infected mice (Figure 16D). These findings are in accord with our observation that XL280, a serotype D strain associated with high mortality, is able to evade the immune system and successfully disseminate to the CNS. Thus, we hypothesize that XL280 induces an immune response that is polarized towards Th2 immunity and higher levels of IL-4 may downregulate cell-mediated immunity and host protection and as a consequence exacerbate the course of disease progression.

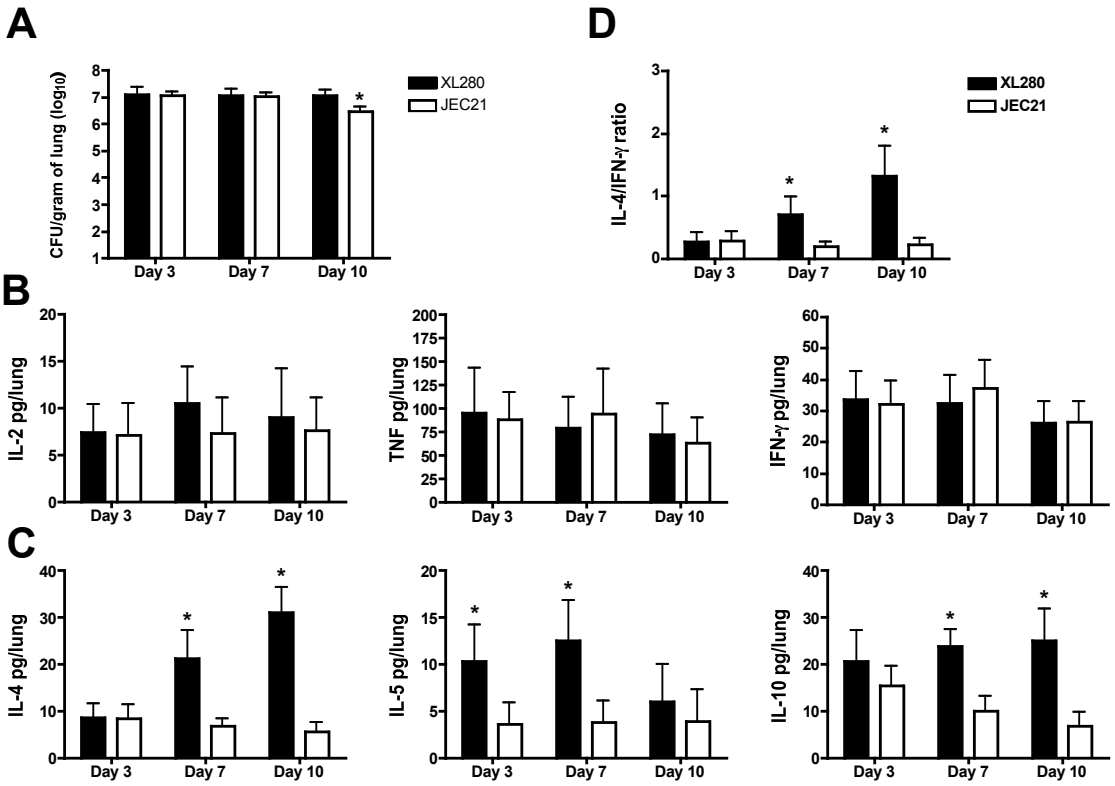

Figure 16. Immune response to XL280 is polarized towards Th2-type immunity. Mice were infected intranasally with 1 x 10^6 yeast cells and cytokine production was assayed at 3, 7, and 10 days post infection. (**A**) The lungs were isolated, homogenized, serially diluted, and plated for CFUs. (**B**) The Th1 cytokines IL-2, TNF, and IFN-γ were similar between XL280 and JEC21 infected mice. (**C**) In contrast the Th2-type associated cytokines IL-4, IL-5, and IL-10 were significantly higher in XL280 infected mice. (**D**) The ratio of IL-4/IFN-γ is significantly higher in XL280 at 7 and 10 days post infection. The data represents four independent experiments. The asterisk (*) signifies a $p<0.05$, derived from two-way ANOVA statistical analysis.

3.3.5 Histological Analysis of XL280 and JEC21 Pulmonary Infections

Our cytokine analysis revealed a Th2 biased production during XL280 infection. To determine whether XL280 challenged mice developed lung lesions

indicative of an allergic Th2 bronchopulmonary response, we isolated lung tissues from JEC21 and XL280 infected animals 10 days post infection. Histological sections were stained with hematoxylin/eosin and mucicarmine and analyzed by light microscopy. The overall pathology was significantly different between the two strains. In the lungs of mice infected with JEC21 the cellular infiltrate surrounding the airways appeared to be densely packed with leukocytes, mostly neutrophils and macrophages, forming tight inflammatory foci (Figure 17A). Although cryptococcal growth was observed to be widespread, it appeared to be contained in these inflammatory foci of the infected lung. Interestingly, a majority of the JEC21 cells appeared to be within macrophages with some of them harboring more than one *Cryptococcus* cell (Figure 17C and 15E). In contrast, the cellular infiltrate appeared more diffuse in the lungs of XL280 infected animals (Figure 17B), with scattered dense areas of leukocytes characterized by the presence of numerous eosinophils (Figure 17D). Growth of XL280 cells was widespread around the bronchiolar and alveolar airspaces, within and outside of inflammatory foci. Surprisingly, XL280 cells appeared to be resistant to phagocytosis, as we were not able to observe any macrophages containing yeast cells (although macrophages were widespread in the lung tissues). In addition, we observed changes in the airway morphology of the lung. XL280 infected mice displayed goblet cell metaplasia surrounding small blood vessels and airways, stimulating extensive mucin secretion (confirmed by PAS

staining) (Figure 17F). Diminished leukocyte infiltration, goblet cell metaplasia, and recruitment of eosinophils at the site of infection are all indicative of a non-protective Th2 immune response to XL280 but not JEC21.

Based on cytokine analysis and lung pathology we conclude that XL280 induces a less protective Th2 polarized immune response which exacerbates cryptococcal infection. Moreover, the significantly larger size and the unique morphology of XL280 cells may impair phagocytosis by macrophages, and thereby allow the cells to grow and proliferate inside the host and successfully disseminate to the brain.

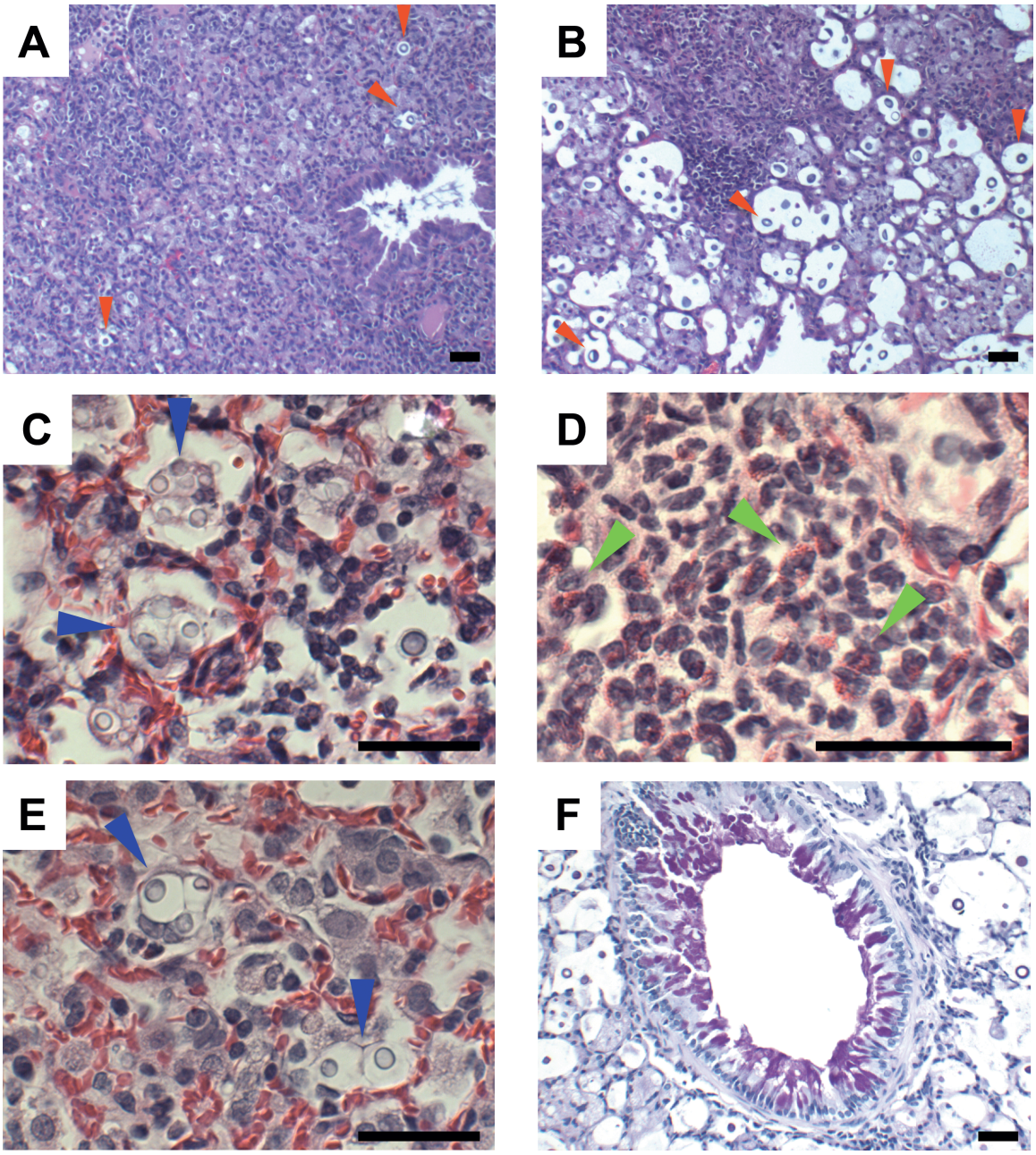

Figure 17. XL280 infection results in eosinophil infiltration and goblet cell metaplasia. Lungs of mice challenged with JEC21 and XL280 were isolated 10 days post infection, fixed in formalin, and processed for histological analysis. Tissue sections were either stained with H&E and photographed with a 10x (A and B), 40x (D), or 60x objective (C, E), or stained with PAS stain and

photographed at 20x (F). JEC21 caused marked inflammation in the lung (**A**) with widespread growth of *Cryptococcus* and enlarged macrophages with proliferating intracellular cryptococci (red arrows) (**C** and **E**). In contrast, XL280 yeast cells (red arrows) stimulated a diffuse inflammatory response (**B**) with pulmonary eosinophilia (green arrows) (**D**) and PAS-positive goblet cells (**F**). Internalized yeast cells were not detected in XL280 infected pulmonary tissues. Scale bar = 50 μm.

3.4 Discussion

Cryptococcus neoformans causes lethal infections of the central nervous system in immunocompromised individuals. The A and D serotypes contribute differentially to the magnitude of infection by this organism. The vast majority of these infections worldwide (~95%) are caused by highly virulent strains of serotype A (Lin, Nielsen et al. 2008, Heitman, Kozel et al. 2011). A direct comparison of two widely used serotype A and D laboratory strains, H99 and JEC21, showed that H99 responds differently to stress, produces more melanin, exhibits higher rates of proliferation inside the host, and is significantly more virulent than JEC21 (Barchiesi, Cogliati et al. 2005, Lin, Litvintseva et al. 2007, Lin, Nielsen et al. 2008). In healthy individuals serotype A and D isolates induce a strong inflammatory immune response that clears the infection and prevents the fungus from disseminating to the brain and causing meningoencephalitis. In this study we report a serotype D strain, XL280, which is significantly more virulent than its parental strain JEC21. Moreover, we found that the pathogenicity of XL280 is comparable to the highly virulent strain H99 based on previous studies. Surprisingly, XL280 induces a less protective immune response during pulmonary infection, which is characterized by high levels of Th2 type associated cytokines in the lung. Furthermore, lung pathology confirmed a polarization towards Th2 immune response based on the presence of eosinophils and goblet cell metaplasia in XL280 infected mice.

XL280 is a serotype D strain derived by the cross of two sibling strains, one of which is congenic with the widely used sequenced strain JEC21 (Heitman, Allen et al. 1999, Lin, Huang et al. 2006). In previous studies, we sequenced the XL280 genome and found that it shares 81% genetic identity with the JEC21 (Ni, Feretzaki et al. 2013). Therefore, it was expected that the two strains would behave similarly in a variety of phenotypic assays, including virulence associated phenotypes. However, a major difference is that XL280 is hyperfilamentous compared to JEC21. During unisexual reproduction, XL280 generates abundant hyphae around the circumference of the colony, while JEC21 hyphae are scarce and limited. The hyperfilamentous phenotype of XL280 results in the production of massive numbers of spores that are considered to be the infectious propagules of *Cryptococcus* (Giles, Dagenais et al. 2009, Feretzaki and Heitman 2013, Ni, Feretzaki et al. 2013). Interestingly, it has been proposed that the unique ability of α strains to generate hyphae and spores during unisexual reproduction has contributed to the predominance of this mating type in clinical isolates (Lin, Patel et al. 2009). However, unisexual reproduction has been directly observed under laboratory conditions only for the low pathogenic strains of serotype D. Surprisingly, we found that the hyperfilamentous XL280 is hypervirulent in the murine model compared with JEC21. The pathogenicity of XL280 has been previously reported; however, there was no direct comparison to other serotype D strains (Ni, Feretzaki et al. 2013, Zhai, Zhu et al. 2013). In this

study we show that XL280 is highly pathogenic and the spores produced during unisexual reproduction can spread, germinate, and potentially infect and kill a host.

Hyphal development in *C. albicans* is essential to survive inside the host; nonfilamentous mutants are attenuated for virulence in the murine model (Lo, Kohler et al. 1997). During infection *C. albicans* hyphae invade epithelial and endothelial cells causing severe tissue damage and gaining access to the bloodstream resulting in dissemination of the fungus to various organs (Dalle, Wachtler et al. 2010, Zhu and Filler 2010, Sudbery 2011). More importantly, yeast cells engulfed by macrophages switch to hyphae that perforate the mammalian cells and enable the fungus to escape and survive inside the host (Lorenz, Bender et al. 2004). Although *C. neoformans* hyphae are rare *in vivo* and are associated with low virulence, pseudohyphae have been observed in histological samples and they were found to confer resistance to *Acanthamoeba* spp. phagocytosis (Neilson, Ivey et al. 1978, Williamson, Silverman et al. 1996, Gazzoni, Oliveira Fde et al. 2010, Magditch, Liu et al. 2012). Although pseudohyphae are dispensable for virulence (Lee, Phadke et al. 2012), stochastic transitions from yeast to pseudohyphae may serve as an escape strategy and confer resistance to phagocytosis by mammalian macrophages similar to giant/titan cells.

Interestingly, the progression of the disease was quite different between the two strains. Fungal proliferation was observed in the lung and the brain for both XL280 and JEC21 early in the infection (two weeks), however, the fungal burden for XL280 was significantly higher in both organs at a later time point (4 weeks). In addition, moribund mice infected with XL280 exhibited severe neurological defects associated with central nervous system disorders. This type of phenotype is often associated with *C. neoformans* infections that primarily cause severe cryptococcal meningitis, while pulmonary infections are more common in *C. gattii* infected individuals (Chen, Sorrell et al. 2000, Galanis, Macdougall et al. 2010). A recent study found that *C. neoformans* preferentially disseminated to the brain during infection, while *C. gattii*, which fostered a fatal lung infection, failed to cause lethal meningoencephalitis in two animal models (Ngamskulrungroj, Chang et al. 2012). These results confirm clinical observations where 70% of *C. gattii* cases suffer from pulmonary infections and only 7.8% of patients presented with CNS infections (Galanis, Macdougall et al. 2010). *C. neoformans* is known to elicit massive inflammation in the lung, which could inhibit proliferation in pulmonary tissues and facilitate migration to the CNS. On the other hand, the immunosuppressive nature of *C. gattii* may allow it to evade the immune system and preferentially establish an infection in the lung. Our results suggest that the serotype D strain XL280 fosters an infection in both organs that possibly contributes to its pathogenicity.

We also found that XL280 cells were significantly larger than JEC21 inside the host, and adopted a “football” like morphology that was widely observed in multiple independent samples and at different time points. Based on lung pathology, we also observed that XL280 cells were resistant to phagocytosis by macrophages. Previous studies have shown that giant/titan cells observed during cryptococcal infections are resistant to phagocytosis and can contribute to pathogenesis (Zaragoza, Garcia-Rodas et al. 2010, Crabtree, Okagaki et al. 2012). Possibly, the larger size and morphology of the cells obstructed macrophages from phagocytosing XL280, which proliferated unchecked in the lung and then disseminated to the brain. Although capsule production was similar between JEC21 and XL280 *in vitro*, the large size of XL280 *in vivo* may result in significantly higher levels of capsule volume, which is known to protect against oxidative stress and may have contributed to the survival of the strain. Previously, it has been reported that rapid changes in cell size and capsule structure, occurring in pulmonary tissues, are associated with tissue invasion and may favor crossing of the blood-brain barrier (Garcia-Hermoso, Dromer et al. 2004, Charlier, Chretien et al. 2005). These alterations in cell surface composition may enhance organ invasion and cause higher affinity of *Cryptococcus* cells to the brain.

Our findings suggest a different pattern of infection between XL280 and JEC21. The immunological response elicited by pathogens can greatly affect the

outcome of the disease. Host defense against *Cryptococcus* is mediated by T cell mediated immunity. Previous studies have shown that the different species of *Cryptococcus* induce distinct immune responses inside the host (Chen, McNamara et al. 2008, Cheng, Sham et al. 2009, Hardison, Ravi et al. 2010, Williams, Wormley et al. 2011). In this study we found that the cytokine profile of XL280 infected mice is shifted towards Th2 type immunity. The major Th2 associated cytokines, IL-4 and IL-5, were elevated in lungs of mice infected with XL280 and the ratio of IL-4/TNF-α was significantly higher than for JEC21. In addition, histopathological analysis confirmed the presence of numerous eosinophils and goblet cell metaplasia around the airways in XL280 infected lungs, indicative of Th2 immunity. Interestingly, bronchovascular infiltration was diffuse reflecting less inflammation in mice infected with XL280. On the other hand, JEC21 caused a strong inflammatory response, with massive infiltration of neutrophils and macrophages. At day 10 post infection the majority of JEC21 cells were within macrophages in these inflammatory foci. These findings suggest that XL280 thrives inside the host possibly because it fails to induce protective inflammation during infection. Surprisingly, this phenotype is similar to *C. gattii* infections that skew the immune response towards Th2 immunity, which allows them to evade the immune system, proliferate in pulmonary tissues and establish a fatal infection, if untreated, in healthy individuals (Cheng, Sham et al. 2009). We therefore consider the possibility that XL280 similarly evades the

immune system, by inducing a Th2 polarized immune response, and resisting phagocytosis by macrophages. These conditions allow the cells to survive and proliferate in the lung before disseminating to the brain. It is also possible that XL280 failed to provoke migration of neutrophils to the lung, which are essential for protective immunity and were observed with JEC21. We note that our observations are different from those usually reported for *C. neoformans* infections. The virulent strains of serotype A are known to induce Th1 and Th2 protective immunity in healthy individuals, while serotype D induced immune response is not considered of high medical importance due to the low pathogenicity of this group (Koguchi and Kawakami 2002, Lin and Heitman 2006, Chen, McNamara et al. 2008, Guillot, Carroll et al. 2008, Cheng, Sham et al. 2009, Bartlett, Cheng et al. 2012). However here we report a serotype D strain that is highly virulent and able to skew the immune response towards a less protective Th2 immunity inside the host. XL280 is an F2 progeny derived from NIH12 (clinical isolate) and NIH433 (environmental isolate). The differences we observe in this hyperfilamentous strain in terms of morphogenesis and virulence are due to meiotic recombination between the genomes and novel genetic diversity introduced during bisexual reproduction (as has been previously reported) (Ni, Feretzaki et al. 2013).

Taken together our results provide novel insights into pathogenicity of *C. neoformans* and the role of hyphal development during unisexual reproduction.

This the first report of a hypervirulent strain of the serotype D lineages that induces less protective immunity during infection, similar to *C. gattii* in healthy individuals, and our findings suggest that other clinical serotype D isolates may share similar virulence attributes that may underlie and explain their more frequent occurrence in certain geographical regions, such as Europe.

Chapter 4. Genetic Circuits that Govern Bisexual and Unisexual Reproduction in *Cryptococcus neoformans*[1]

4.1 Introduction

Sexual reproduction in eukaryotes facilities genetic diversity and eliminates deleterious mutations leading to better fit progeny. In fungi, sex often involves two cells of opposite mating type (heterothallism) that secrete pheromones in order to induce cell fusion. Subsequently, nuclear fusion and meiosis generate recombinant progeny. However, in other fungi, solo incubation of an individual isolate can result in sexual reproduction, and this selfing process is referred to as homothallism. Homothallism can involve 1) mating type switching, 2) the presence of both mating type alleles (fused or unlinked), or 3) unisexual reproduction of just one mating type (Lin and Heitman 2007). Paradigmatic examples of fungi with both modes of sexual reproduction are *Saccharomyces cerevisiae* and *Cryptococcus neoformans*.

S. cerevisiae has served as a model for the exploration and elucidation of molecular mechanisms of the dimorphic switch and therefore serves as a framework for morphogenesis in other dimorphic fungi (Madhani and Fink 1998). Pheromones produced by the opposite-mating type partner activate the mitogen-activated protein kinase (MAPK) signaling cascade (which is also called the

---

[1] Some material in this chapter can be found in: Feretzaki, M. and J. Heitman (2013). "Genetic circuits that govern bisexual and unisexual reproduction in *Cryptococcus neoformans*." PLoS Genet **9**(8): e1003688.

pheromone response pathway) to induce mating, pseudohyphae, and invasive growth (Liu, Styles et al. 1993, Roberts and Fink 1994). Additional environmental cues are known to regulate pseudohyphae formation. Nutrients activate cellular receptors and the cAMP-dependent pathway to govern the expression of genes evoking the dimorphic transition (Rupp, Summers et al. 1999). Core components of these pathways are highly conserved throughout the fungal kingdom; however, the downstream targets are often species-specific.

Cryptococcus neoformans is a human fungal pathogen that grows as a yeast in the environment and inside the host. It causes severe central nervous system infections in HIV-infected patients and less frequently in immunocompetent individuals. Cryptococcal meningitis is an AIDS-defining illness in 30% of HIV infections worldwide and is uniformly fatal if untreated (Heitman, Kozel et al. 2011).

C. neoformans yeast cells undergo a dimorphic switch into hyphae during sexual development. The organism has a defined life cycle with α (common) and **a** (rare) mating type cells. Under nutrient-limiting conditions or in response to inositol, cells of the opposite mating type secrete pheromones leading to cell-cell fusion (Kwon-Chung 1975, Kwon-Chung 1976, Heitman, Allen et al. 1999, Hull and Heitman 2002). The two cells fuse to form a stable heterokaryon, which undergoes the dimorphic switch to filamentous growth. The two haploid nuclei remain separate in the growing hyphae and migrate from one hyphal cell to the

adjacent one through clamp cells that fuse to connect the neighboring hyphal cells. At the apex of the aerial filaments, specialized, swollen structures known as basidia form where nuclear fusion and meiosis occur (Kwon-Chung 1976). Multiple rounds of mitosis and budding produce four chains of spores, which are dispersed by air and germinate to re-enter the life cycle (Idnurm, Bahn et al. 2005). The dimorphic switch during bisexual reproduction occurs in both the A and D serotypes of *C. neoformans*, as well as in the sibling species *C. gattii* (Kwon-Chung 1976, Kwon-Chung 1976, Fraser, Subaran et al. 2003, Nielsen, Cox et al. 2003). Meiosis and sporulation are integral to the *C. neoformans* life cycle and play important roles in virulence. Cryptococcal infections are acquired by the inhalation of infectious particles, spores or desiccated yeast cells, from the environment. Spores are of an ideal size to penetrate and colonize the alveoli of the lung and are pathogenic (Giles, Dagenais et al. 2009, Velagapudi, Hsueh et al. 2009).

The predominance of the α mating type in all varieties of *Cryptococcus* and the presence of highly clonal populations led to the hypothesis that this pathogen might have a predominantly asexual life cycle. However, previous studies have shown that the dimorphic switch can occur during unisexual reproduction involving cells of only one mating type (Wickes, Mayorga et al. 1996, Lin, Hull et al. 2005). Unisexual reproduction has been directly observed under laboratory conditions mainly in the serotype D lineage. In response to

nutrient limitation, α cells of a single haploid isolate grown in solo culture can form a haploid or a diploid monokaryotic hyphae. Like bisexual reproduction (which can produce either a dikaryotic mycelium with paired haploid nuclei or a diploid monokaryotic mycelium (Sia, Lengeler et al. 2000)), during unisexual reproduction the haploid nuclei can either diploidize early or later in the basidium just prior to meiosis (Figure S1). Diploidization can result from either cell-cell and then nuclear fusion, or via endoreplication. The resulting hyphae grow to form basidia where meiosis and repeated rounds of mitosis and budding occur to produce haploid meiotic progeny as long chains of spores (Lin, Hull et al. 2005). That the meiotic recombinase Dmc1 is required for spore production and germination shows definitively that unisexual reproduction is a meiotic process (Lin, Hull et al. 2005). *Candida albicans* also has been found to undergo unisexual reproduction in the absence of the Bar1 protease, or in ménage à trois matings (Alby, Schaefer et al. 2009), similar to α-α cell fusion stimulated by **a** cells in *Cryptococcus* (Lin, Hull et al. 2005). Unisex may serve to introduce genetic diversity and confer adaptive benefits.

The MAPK pheromone response signaling cascade governs dimorphism during bisexual and unisexual reproduction in *C. neoformans*. This signaling circuit is structurally and functionally conserved among both closely (i.e. *Ustilago maydis*) and distantly related fungi (i.e. *S. cerevisiae*). The pathway is activated by pheromones and orchestrates signal transduction through sequential

phosphorylations evoked by the Ste20α/**a** (p21-activated kinase, PAK), Ste11α/**a** (MAPK kinase kinase), Ste7 (MAPK kinase), and Cpk1 (MAPK) kinases (Davidson, Nichols et al. 2003, Nichols, Fraser et al. 2004). Deletion of the corresponding genes severely impairs hyphal development during sexual development (Wang, Nichols et al. 2002, Davidson, Nichols et al. 2003). In *S. cerevisiae*, the main transcriptional target of the pathway is Ste12, and a conserved *STE12*α/**a** homolog is present in the mating-type locus of *C. neoformans* (Wickes, Edman et al. 1997, Chang, Wickes et al. 2000). Recent studies have shown that the MAPK pathway target is Mat2, an HMG protein essential for bisexual and unisexual reproduction (Lin, Jackson et al. 2010), that binds Pheromone Response Elements (PRE) in the promoters of the pheromone genes and 11 other pheromone induced genes (Kruzel, Giles et al. 2012). A conserved cAMP pathway and a MAPK signaling cascade govern mating, morphogenesis, and pathogenicity in the closely related basidiomycete *Ustilago maydis*. However, the downstream transcription factor is a distinct HMG protein, Prf1, which regulates virulence and is pheromone-induced (Klosterman, Perlin et al. 2007). Thus the molecular pathway governing sexual development has been rewired since the divergence of both *U. maydis* and *C. neoformans* from their last common ancestor shared with *S. cerevisiae*.

While **a**-α bisexual reproduction and α-α unisexual reproduction are related sexual cycles, there are distinguishing characteristics. Notably, the cell

identity homeodomain Sxi1α/Sxi2**a** protein complex is specifically required for bisexual mating but dispensable for unisexual reproduction (Lin, Hull et al. 2005). Other distinct elements that may specifically regulate the two sexual cycles, and which remained to be identified are involved in hyphal elongation, basidia formation, meiosis, and sporulation.

The aim of this study was to identify and characterize unique regulators of unisexual reproduction. We employed a high-throughput genetic screen using an *Agrobacterium*-transkingdom DNA delivery approach to isolate random insertional mutants (Idnurm, Reedy et al. 2004, Idnurm and Heitman 2005, Chun and Madhani 2010, Lin, Jackson et al. 2010) in a genome-sequenced self-fertile haploid strain and isolates with filamentation defects were identified by microscopy. We also disrupted genes encoding three regulators of unisexual development: Spo11, Ubc5, and Znf3. Spo11 is the homolog of *S. cerevisiae* Spo11, which induces DNA double-strand breaks (DSBs) that promote meiotic recombination (Keeney, Giroux et al. 1997). *UBC5* encodes a ubiquitin-conjugating enzyme that degrades short-lived or abnormal proteins in *S. cerevisiae* and also has a role in sporulation (Seufert and Jentsch 1990). Deletion of either the *SPO11* or the *UBC5* gene significantly reduced spore number and germination providing additional definitive evidence, beyond the established role of Dmc1, that *Cryptococcus* unisexual reproduction is a meiotic process. Znf3 is a novel zinc finger protein. Phenotypic analysis of Znf3 insertion

and deletion mutants showed that this component regulates hyphal development during both bisexual and unisexual reproduction. *znf3* mutations impaired cell-cell fusion and blocked hyphal development, indicating a role in the early steps of sexual reproduction. Based on epistasis analysis, Znf3 is not a transcriptional target of the pheromone signaling cascade, but rather contributes to modulate Mat2 expression and is required for pheromone expression. Surprisingly, deletion of *ZNF3* increased expression of transposons and transposon-related genes during unisexual reproduction. These results support the conclusion that Znf3 regulates sexual development through a different circuit parallel to the pheromone response pathway and governs pheromone gene expression and silences transposons, either directly or indirectly. Taken together these results proffer new insights into the control of hyphal development during bisexual and unisexual reproduction.

4.2 Materials and Methods

4.2.1 Strains, Media, and Growth Conditions

C. neoformans strains and plasmids used in this study are summarized in Table 4. *Cryptococcus* strains were maintained in -80^{o}C glycerol stocks and grown at 30^{o}C on rich YPD media (Yeast extract Peptone Dextrose). Strains harboring dominant selectable markers were grown on YPD containing nourseothricin (NAT) or G418 (NEO). Mating assays were performed on 5% V8 juice agar medium (pH=7) in the dark at room temperature for the designated incubation period. To visualize spores and spore chains, mating assays were conducted on either V8 solid agar or on MS (Murashige and Skoog) medium minus sucrose (Sigma-Aldrich).

Table 4. Strains and plasmids used in Chapter 4.

Strain Name	Background Genotype	Sources and comments
XL280α	*MAT*α	~81% genome identity with JEC21α (Ni, Feretzaki et al. 2013)
JEC21α	*MAT*α	
JEC20**a**	*MAT***a**	congenic with JEC21
MF01	XL280α *znf3*Δ::*NAT*	This study
MF38	XL280α *znf3*Δ::*NAT*	This study
MF39	JEC21α *znf3*Δ::*NAT*	This study
MF40	JEC20**a** *znf3*Δ::*NEO*	This study
MF41	JEC20**a** *znf3*Δ::*NEO*	This study
MF29	XL280α *ste7*Δ::*NAT* P_{GPD1}-*ZNF3*	XL946 transformed with pMF1
MF34	XL280α P_{GPD1}-*ZNF3*	This study
MF35	XL280α *mat2*Δ::*NAT* P_{GPD1}-*ZNF3*	XL942 transformed with pMF1
MF54	XL280α *znf3*Δ::*NAT* P_{GPD1}- *MAT2*	MF01 transformed with pDX64 (Lin and Heitman, unpublished data)
XL143	JEC21α *MAT*α/ *MAT*α	(Lin, Hull et al. 2005)
XL561	XL280α *NAT*	(Lin and Heitman, unpublished data)
XL491	JEC20**a** *NEO*	(Lin and Heitman, unpublished data)
XL574	XL280α *znf2*Δ::*NAT*	(Lin, Jackson et al. 2010)
XL867	JEC20**a** *znf2*Δ::*NAT*	(Lin, Jackson et al. 2010)
XL942	XL280α *mat2*Δ::*NAT*	(Lin, Jackson et al. 2010)
XL961	JEC20**a** *mat2*Δ::*NEO*	(Lin, Jackson et al. 2010)
XL946	XL280α *ste7*Δ::*NAT*	(Lin, Jackson et al. 2010)
RDC25-2	JEC20**a** *ste7*Δ::*ADE2 ade2*	(Davidson, Nichols et al. 2003)
XL1108	XL280α *sxi1*αΔ::*NAT*	(Lin and Heitman, unpublished data)
CHY766	JEC20**a** *sxi2***a**Δ::*URA5 ura5*	(Hull, Boily et al. 2005)
MF42	XL280α *spo11*Δ::*NAT*	This study
MF43	XL280α *spo11*Δ::*NAT*	This study
MF44	JEC21α *spo11*Δ::*NAT*	This study
MF45	JEC21α *spo11*Δ::*NAT*	This study
MF46	JEC20**a** *spo11*Δ::*NEO*	This study
MF47	JEC20**a** *spo11*Δ::*NEO*	This study
MF56	XL280α *spo11*Δ::*NAT SPO11-NEO*	Complementation of MF42
MF57	JEC21α *spo11*Δ::*NAT SPO11-NEO*	Complementation of MF44

MF58	JEC20**a** *spo11*Δ::*NEO SPO11-NAT*	Complementation of MF46
MF48	XL280α *ubc5*Δ::*NEO*	This study
MF49	XL280α *ubc5*Δ::*NEO*	This study
MF50	JEC21α *ubc5*Δ::*NAT*	This study
MF51	JEC21α *ubc5*Δ::*NAT*	This study
MF52	JEC20**a** *ubc5*Δ::*NEO*	This study
MF53	JEC20**a** *ubc5*Δ::*NEO*	This study
MF59	XL280α *ubc5*Δ::*NEO UBC5-NAT*	Complementation of MF48
MF60	JEC21α *ubc5*Δ::*NAT UBC5-NEO*	Complementation of MF50
MF61	JEC20**a** *ubc5*Δ::*NEO UBC5-NAT*	Complementation of MF53
MF121	XL280α *znf3*Δ::*NEO ura5*	This study
MF165	XL280α *znf3*Δ::*NAT* P_{GPD1}*-ZNF3*	MF01 transformed with pMF1
MF166	XL280α *znf3*Δ::*NAT* P_{GPD1}*-ZNF3*	MF38 transformed with pMF1
Plasmids		
pXL1	P_{GPD1} *NEO AMP*	(Lin and Heitman, unpublished data)
pJAF12	*NEO AMP*	(Fraser, Subaran et al. 2003)
pJAF13	*NAT AMP*	(Fraser, Subaran et al. 2003)
pDX64	pXL1 P_{GPD1}*-MAT2 NEO AMP*	(Lin and Heitman, unpublished data)
pMF1	pXL1 P_{GPD1}*-ZNF3 NEO AMP*	This study
pMF44	pJAF12 *UBC5 NEO AMP*	This study
pMF46	pJAF13 *UBC5 NAT AMP*	This study
pMF52	pJAF12 *SPO11 NEO AMP*	This study
pMF54	pJAF13 *SPO11 NAT AMP*	This study

4.2.2 Insertional Mutagenesis and Phenotypic Analysis of the Mutants

Agrobacterium tumefaciens-mediated transformation was performed as previously described (Idnurm, Reedy et al. 2004). *A. tumefaciens* strain EHA105 transformed with the pPZP-NAT1cc plasmid was grown on Luria-Bertani (LB) medium containing kanamycin for 48 h at 25°C with shaking. The cells were washed briefly with sterile ddH_2O and diluted in induction medium containing 100 μM acetosyringone to obtain an optical density of 0.15 at 660 nm. The cells were then incubated for 6 h while shaking at room temperature. The *C. neoformans*

serotype D strain XL280α was grown overnight in YPD, washed with induction medium, and resuspended to a final density of 10^7 cells/ml. Equal aliquots of *C. neoformans* and *A. tumefaciens* (200 μl) were mixed and plated on induction medium agar containing acetosyringone. The cells were co-cultured for three days, scraped from the plates, and transferred to selective medium (YPD + NAT + 100 μg/ml cefotaxime). The colonies were transferred into 96-well plates and grown in YPD + NAT + 100 μg/ml cefotaxime as shaking cultures. A total of 6,100 transformants were spotted on V8 solid medium, incubated for 14 days in the dark at room temperature, and examined for hyphal development using light microscopy. Mutants with a stable filamentation defect were selected and clustered into groups based on similar phenotypes. Linkage between NAT resistance and the phenotype was assessed by crossing the insertional mutants with the JEC20**a** mating partner. Individual spores were isolated using a microdissection microscope, and the progeny were screened for the mutant phenotypes and NAT resistance. To identify the insertion sites, genomic DNA was digested with multiple restriction enzymes, purified, self-ligated, and subjected to inverse PCR using the pre-selected primers AI076/AI077. The PCR products were sequenced and the flanking regions were used in BLAST searches against the *Cryptococcus* genome to identify the mutated genetic loci (McCullagh, Seshan et al. 2010).

4.2.3 Genomic DNA Preparation

Cells were grown overnight in 50 ml YPD at 30^{o}C in shaking cultures. The cells were harvested, washed three times with ddH_2O, and frozen at -80^{o}C overnight. The next day, they were lyophilized overnight and either stored at -20^{o}C or genomic DNA was isolated using the CTAB protocol as previously described (Pitkin, Panaccione et al. 1996).

4.2.4 Gene Disruption, Complementation, and Overexpression

Genes of interest were disrupted using an overlap PCR approach (Davidson, Blankenship et al. 2002, Fraser, Subaran et al. 2003). The 5' and 3' flanking sequences of *ZNF3*, *SPO11*, and *UBC5* were amplified from either XL280α or JEC21α genomic DNA. The dominant selectable markers *NAT* and *NEO* were amplified from plasmids pAI3 and pJAF1 respectively, with the universal primers M13F and M13R. The flanking sequences and the selectable markers were used to generate full-length deletion cassettes in an overlap PCR reaction. The construct was purified, precipitated onto gold microcarrier beads (0.6 mm, Bio-Rad), and introduced into strains XL280α or JEC20**a** via biolistic transformation as previously described (Davidson, Cruz et al. 2000). Genes were replaced via homologous recombination and confirmed with PCR and Southern hybridization. Primers used to generate mutations are listed in Table 5. For complementation, the wild type *SPO11* and *UBC5* genes, along with their

endogenous promoters and terminators, were amplified from XL280α genomic DNA with primer pairs JOHE37665/JOHE37666 and JOEH37667/JOHE37668, respectively, and cloned into the pJAF12 and pJAF13 vectors (Fraser, Subaran et al. 2003). The plasmids were confirmed by sequenced, and *spo11*Δ and *ubc5*Δ mutants were biolistically transformed. The transformants were screened for spore production during mating by light microscopy. The wild type *ZNF3* gene is exceptionally large (~7,000 bp including promoter and terminator) and the construction of a complementation allele was challenging. To show that the hyphal defect was attributable to disruption of the gene, we screened and found a consistent afilamentous phenotype in several insertional mutants with independent insertions in *ZNF3* and also in two independently derived *znf3*Δ mutants. To generate the *ZNF3* overexpression plasmid pMF3, the wild type *ZNF3* allele was amplified from XL280α genomic DNA using primer pair JOHE21470/JOHE21471. The gene was cloned into the pXL1 vector under the control of the constitutively expressed *GPD1* promoter (Xue, Bahn et al. 2006). *Cryptococcus* strains were transformed with the circular plasmid via biolistic transformation. Independent transformants were selected for RNA extraction and screened to determine the expression levels of *ZNF3* by RT-PCR.

Table 5. Oligonucleotides used in Chapter 4

Primer name	Sequence (5' to 3')	Description
M13F	GTAAAACGACGGCCAG	
M13R	CAGGAAACAGCTATGAC	
AI076	AACAGTTGCGCAGCCTGAATG	Primer for inverse PCR
AI077	AGAGGCGGTTTGCGTATTGG	Primer for inverse PCR
JOHE8744	AGCAAAGCGAAAAGCT	*BWC1* screening
JOHE8745	ATACGCCTACCTACGTGCTAGC	*BWC1* screening
JOHE17111	GGAGGGAAAAGGAACCTTG	*BWC2* screening
JOHE17111	CTAACTGGGCTGTTTCAATC	*BWC2* screening
JOHE13684	CGCAGGGCGAAACTTTGTG	*ZNF2* screening
JOHE13683	CCTCATCTCTCGCTCAGCCTC	*ZNF2* screening
JOHE14082	CATCCCTTATCCTCACTGCC	*MAT2* screening
JOHE14088	GCTTTCCCTCCGCTTCCTG	*MAT2* screening
JOHE14068	GCGCTGGGCAAGATGCAAG	*STE7* screening
JOHE14074	GGCCGACCATGGATTGAGC	*STE7* screening
JOHE20489	AAAGCTTTTTAATCGTCAGTCT	*CPK1* screening
JOHE20494	TACATCCACCACCCGATCCTTA	*CPK1* screening
JOHE20806	GTCACTATGTGTTACAGAGCTG	*CRG1* screening
JOHE20809	ACGAACTCTTGACATTGTCGTCAAC	*CRG1* screening
JOHE15244	GCCTTCTTGCCACTGTCG	*SPO11* disruption
JOHE15245	CTGGCCGTCGTTTTACCAACCCAGAAGGACAACCG	*SPO11* disruption
JOHE15246	GTCATAGCTGTTTCCTGCACATCTATGGCTAGCGATAGTG	*SPO11* disruption
JOHE15247	GCCCACAAAGTCTTTCGAC	*SPO11* disruption
JOHE15248	ATGCTTCGTACAATGCCTTC	*spo11* screening
JOHE15250	CGTCAGGAAGAGGCTGCC	*spo11* screening
JOHE20738	CTGATTTCGCCTTCTTCCTTGT	*ZNF3* disruption
JOHE20745	AGCATCTAGGACTAAAAGTCAGC	*ZNF3* disruption
JOHE20800	CTGGCCGTCGTTTTACGGGGTTAGTAGCTGGCTGTTT	*ZNF3* disruption
JOHE20801	GTCATAGCTGTTTCCTGGTGGGGACAGCAATTCATATAAG	*ZNF3* disruption
JOHE20739	AGCTGCATTTGATGGATGGAAC	*znf3* screening
JOHE20740	TGAGCTTCCTATCTTACGTCTC	*znf3* screening
JOHE20741	TTGCTAGAAGTCAAGTCGTCCT	*znf3* screening
JOHE20742	AAGACGTCGACTTTGAGCTTCCT	*znf3* screening
JOHE20743	CTCACTGCTGAAGGGTAGATCTTA	*znf3* screening
JOHE20744	AGGAGTTCAAGCTTCAATGGTG	*znf3* screening
JOHE21470	TTATGGCCGGCCATGCTCACAGCCTTCTTCGGCTACGTTA	*ZNF3* overexpression
JOHE21471	ACACGCCTTAATTAATCACCAGCCACCAGTGTCTCCGTCT	*ZNF3* overexpression
JOHE24424	TGAAAACAACTACGACGGTCGGTACATTGAGCC	*ZNF3* RT-PCR
JOHE24425	ATCCATCCTGTTGGAGAGCAGCTG	*ZNF3* RT-PCR
JOHE24426	AGGAAGCTCGAGCATCGAAAGCTGTAT	*MAT2* RT-PCR
JOHE24427	TGAGCTGCAGTAGCTCGTAAATCTGAC	*MAT2* RT-PCR
JOHE24428	ACCCTTTCCAACCCCTTGTCAACG	*ZNF2* RT-PCR
JOHE24429	AAGGACGTTTCCCAGTGTGAATACGCC	*ZNF2* RT-PCR
JOHE24430	GTCACTTTTGCTAGATGAAGGGCAAAGTCG	*SXI1*α RT-PCR
JOHE24431	GATCACCACCACACCACACGTTCA	*SXI1*α RT-PCR

JOHE24434	CTACCGACCAGCAACCAACCATCGCTAC	*MFα1* RT-PCR
JOHE24435	GTCAATACCATCTAAACAAGTCCCATACGCTTC	*MFα1* RT-PCR
JOHE24436	CAGGTTCAACGTCGGCAACAACTA	*CPK1* RT-PCR
JOHE24437	TCAAGTCGCGATGGATGATTTCAGCAG	*CPK1* RT-PCR
JOHE26873	GCCGCCGTTAATTGGATGTTGGAT	*CRG1* RT-PCR
JOHE26874	AGTGATGTACGGCGTTGTACGGAA	*CRG1* RT-PCR
JOHE26875	TGCGAGCTAAAGCCTTTGCCAATC	*CRG2* RT-PCR
JOHE26876	AAAGTACCGACGCTCCGACAATGA	*CRG2* RT-PCR
JOHE37497	TGCCGCAATTACGACCACGT	*UBC5* disruption
JOHE37498	CTGGCCGTCGTTTTACCAGGCGTTGAATTAAACGGT	*UBC5* disruption
JOHE37499	GTCATAGCTGTTTCCTGAAGTCCTTGTAACAATATCTT	*UBC5* disruption
JOHE37500	TATCGACTCTCTCGGAGAGGAGTT	*UBC5* disruption
JOHE37501	ACCAATAGGCACTCCAAAGAGCG	*ubc5* screening
JOHE37502	TTCCGCCTGCATCATTCTAACGT	*ubc5* screening
JOHE37665	ATTACTCGAGCTTCTTGAAGGCTTTCGTAG A	*SPO11* complementation
JOHE37666	ATTACTCGAGCCAAGGCCAAACAAAGTGTTT	*SPO11* complementation
JOHE37667	TATGTTCTAGAGAACGCACGACTTTCAGATGT	*UBC5* complementation
JOHE37668	TATGTTCTAGACATGAGAACTCCAGGGCATAA	*UBC5* complementation

4.2.5 RNA Extraction and RT-PCR

RNA from cells undergoing bisexual reproduction was isolated by mixing equal amounts of **a** and α cells in an eppendorf tube. Then, 5 ml of cells were spotted on V8 medium and incubated for 24 hours at room temperature in the dark. RNA was isolated from unisexual reproduction cultures by spotting 5 ml of α cells on V8 for 48 hours at room temperature in the dark. Mating cultures were harvested, washed with ddH_2O, and lyophilized overnight. RNA was extracted using TRIzol Reagent following the manufacturer's instructions (Invitrogen). Then, 5 μg of total RNA were subjected to DNAse treatment using Turbo DNAse (Ambion), and single-stranded cDNA was synthesized by AffinityScript RT-RNAse (Stratagene). Quantitative Real-Time PCR (RT-PCR) was performed on

an Applied Biosystems 7500 Real-Time PCR System using Brilliant SYBR Green qRT-PCR master mix (Stratagene). For each target, a “no template control” was included and melting curves were analyzed to exclude primer artifacts and a single PCR product. All assays were conducted in triplicate. Data was normalized relative to the reference gene *GPD1*, and expression was determined using the $2^{-\Delta\Delta CT}$ approach. The primers used for RT-PCR are summarized in Table 5. The Student’s t-test was employed to determine if the relative expression of the mutants was significantly different compared with the wild type (significance $p<0.05$).

4.2.6 Mating Assays and Microscopy

Each **a** and α mating partner was grown on YPD solid agar overnight at 30^{o}C. The cells of each mating type were either mixed for bisexual reproduction or spotted individually for unisexual reproduction on V8 solid medium (pH=7) for 7 or 14 days at room temperature in the dark. Hyphal structures and spores were visualized with an Eclipse E400 microscope (Nikon) equipped with a DXM1200F digital camera (Nikon) and interfaced with ACT-1 software (Nikon). Individual spores were isolated using a microdissection microscope equipped with a 25-μm microneedle (Cora Styles Needles ‘N Blocks, Dissection Needle Kit) as previously described (Hsueh, Idnurm et al. 2006).

To visualize nuclear position and fusion in basidia and the hyphae, mating assays were fixed in 4% paraformaldehyde for 20 minutes and then washed three times with sterile PBS. The cells were stained with 1 mg/ml Hoechst dye, incubated for 20 min, and washed with sterile PBS. The mating structures were mounted and captured by brightfield, differential interference (DIC), and fluorescence microscopy (DAPI channel) using a Zeiss Axioskop 2 PLUS equipped with an AxioCam MRm camera (Carl Zeiss Inc., Thornwood, NY).

For scanning electron microscopy, the mating samples were processed at the North Carolina State University Center for Electron Microscopy, Raleigh, NC, USA. Briefly, 1 mm^3 blocks of matings performed on MS medium were excised from the agar and fixed with 0.1 M Na cacodylate buffer (pH=6.8) containing 3% glutaraldehyde for several weeks at 4°C. The block was then rinsed with cold 0.1 M Na cacodylate buffer (pH=6.8) three times and post-fixed in 2% osmium tetroxide in cold 0.1 M Na cacodylate buffer (pH=6.8) for 2.5 hours at 4^oC. Before viewing, the samples were critical-point dried with liquid CO_2 and sputter coated with 50 Å of gold/palladium using a Hummer 6.2 sputter coater (Anatech). The samples were viewed at 15 kV with a JSM 5900LV scanning electron microscope (JEOL) and captured with a Digital Scan Generator (JEOL) image acquisition system. All of the microscopic images were processed with PhotoShop (Adobe).

4.2.7 Cell-Cell Fusion Assay

To determine the cell-cell fusion frequency of wild type and mutant cells during bisexual reproduction, wild type strains XL561 (XL280α *NAT*) and XL491 (JEC20**a** *NEO*) and *znf3*Δ mutants MF38 (XL280α *znf3*Δ::*NAT*) and MF40 (JEC20**a** *znf3*Δ::*NEO*) were grown overnight in YPD liquid medium at 30°C. The cells were washed twice with ddH_2O and diluted to a final density of 10^7 cells/ml. Both unilateral and bilateral mutant matings were assessed using XL926α (XL280α *mat2*Δ::*NAT*) and XL961**a** (JEC20**a** *mat2*Δ::*NEO*) mutants as negative controls. Equal amounts of cells were mixed (500 μl) and spotted on V8 medium (pH=7) and incubated for 15 and 24 hours in the dark at room temperature. The cells were then removed, washed with ddH_2O, and plated in serial dilution on YPD+NEO+NAT media to select for cell-cell fusion products. The cells were incubated for five days at room temperature. Cell-cell fusion efficiency was measured by counting the average number of double drug resistance CFU/total CFU in the wild type and mutant crosses.

4.2.8 Microarray and Data Analysis

To obtain RNA for microarray analysis, XL280α and the congenic *znf3*Δ mutant were grown in liquid cultures, washed in water, and spotted on V8 medium for 24 hrs. The unisexual reproduction cultures were harvested, washed in water, and lyophilized overnight. Three independent cultures were isolated for

each strain and prepared for RNA isolation as biological replicates. The RNA was isolated using the RiboPure™-Yeast Kit (Ambion) according to the manufacturer's instructions (Life Technologies #AM1926). cDNA was synthesized using AffinityScript reverse transcriptase (Stratagene). cDNA was Cy3/Cy5-labeled and hybridized to a *C. neoformans* 70-mer microarray slide developed by the *Cryptococcus* Community Microarray Consortium (Washington University, St. Louis, MO). The arrays were washed and scanned with a GenePix 4000B scanner (Axon Instruments at Duke University DNA Microarray Core Facility) (Ko, Yu et al. 2009). Three independent DNA microarrays were performed with three independent biological replicates. For statistical analysis, data was analyzed using GeneSpring software (Agilent) by employing Lowess normalization, reliable gene filtering, ANOVA analysis (significance $p<0.05$), and Microsoft Excel Software.

For the hierarchical clustering analysis the microarray expression data was carried out using the Limma Bioconductor package of the R statistical programming language (Gentleman, Carey et al. 2004, Smyth 2005). Briefly, normal exponential background subtraction was applied to the data followed by Lowess normalization. Significance of differential expression for the comparisons of the wild type versus mutant strains was then carried out using an empirical Bayes' moderated t-test. The False Discovery Rate method was applied to correct for multiple hypothesis testing (Benjamini and Hockberg 1995).

Hierarchical clustering (complete-linkage, correlation distance) was accomplished using the R statistical programming language.

4.2.9 Fluorescence Activated Cell Sorting (FACS) analysis

Strains were processed for flow cytometry using XL280α as a haploid control and XL143 as a diploid control, as previously described (Sia, Lengeler et al. 2000). Cells were grown overnight in YPD liquid media at 30°C, harvested, and washed with PBS buffer. They were fixed with 70% ethanol and incubated at 4°C overnight. The strains were washed with 1 ml of NS buffer [(10 mM Tris-HCl (pH=7.2), 250 mM sucrose, 1 mM EDTA (pH=8.0), 1 mM $MgCl_2$, 0.1 mM $CaCl_2$, and 0.1 mM $ZnCl_2$], treated with 1 mg/ml RNase, and stained with 10 mg/ml propidium iodide in a final volume of 200 μl at 4°C overnight. Then, 50 μl of stained cells were diluted in 2 ml of 50 mM Tris-HCl (pH=8.0) and sonicated for 1 min. Flow cytometry was performed on 10,000 cells and analyzed on the FL1 channel with a Becton-Dickinson FACScan at the Duke Cancer Institute Flow Cytometry Shared Resource.

4.2.10 X-Irradiation Procedures

Strains were grown overnight in liquid cultures, washed with water, and spotted on V8 medium pH=7. It is crucial to impose irradiation treatment soon after karyogamy is completed and after the initiation of premeiotic DNA synthesis; however, the timing of these two processes are unknown in

Cryptococcus. Therefore, we X-irradiated cultured crosses undergoing sexual reproduction at different time points (3, 4, 5, 6, 7, and 8 days incubation on V8 media) at a dose rate of 420 rad/min in an X-RAD 320 X-ray irradiator set at 320 kilovolts and 10 milliamps. Unirradiated cultures were plated in the same fashion and transferred to the X-ray machine to avoid inadvertent effects of these manipulations. Vegetative asexual cultures were plated in serial dilutions on solid YPD media and irradiated together with the sexual cultures to determine the vegetative survival rate and the presence of growth defects in response to radiation. After X-irradiation, crossing cultures undergoing sexual reproduction were incubated at room temperature in the dark for two additional days and assessed for sporulation efficiency with light microscopy. Germination rate was determined by isolating individual spores micro-manipulation from each culture and incubating these on YPD media to determine the number that formed a colony.

4.3 Results

4.3.1 Mutants Altered for Self-Filamentous Unisexual Reproduction

To identify genes encoding novel components governing unisexual reproduction we utilized the ability of *A. tumefaciens* to transfer and mutagenize its target by randomly introducing a known DNA sequence into the genome. *A. tumefaciens*-mediated transkingdom DNA delivery has been successfully applied in *C. neoformans* to identify and characterize novel virulence factors and components of other sensing pathways (Idnurm and Heitman 2005, Walton, Idnurm et al. 2005, Chun and Madhani 2010, Lin, Jackson et al. 2010). Similar *Agrobacterium*-mutagenesis studies by Lin *et al*. investigated the transition from yeast to hyphae with a limited number of mutants and identified Mat2, the major transcriptional regulator of the pheromone response signaling cascade (Lin, Jackson et al. 2010) whereas Fu *et al*. identified the scaffold protein Ste50 (Fu, Mares et al. 2011).

Here, we sought to dissect each of the sequential steps of unisexual reproduction. A large library of insertion mutants was screened to identify and characterize genes required for hyphal initiation, hyphal elongation, basidia formation, and spore production. We utilized the haploid serotype D strain XL280α that, when solo cultured on appropriate media (V8, MS, FA, SLAD), undergoes robust hyphal development via unisexual reproduction (Lin, Huang et al. 2006). The nuclear content of the vegetative yeast cells budded from the

hyphae (blastospores) reflect the ploidy of the hyphae. XL280 generates a mixture of diploid and haploid hyphae during unisexual reproduction based on FACS (Fluorescent-Activated Cell Sorting) analysis in two independent experiments. Diploid blastospores [5/19 (26%) and 9/24 (37.5%) hyphae examined] are produced by budding from a diploid monokaryotic hyphae that is generated by early nuclear diploidization. In the haploid monokaryotic hyphae [14/19 (74%) and 15/24 (62.5%) hyphae examined] late diploidization occurs in the basidium to generate a diploid nucleus (Lee and Heitman 2012). In both cases the homozygous diploid nucleus undergoes meiosis and sporulation to produce the basidiospores that form four chains of spores on the surface of the basidium. Ploidy was congruent in all cases with hyphal behavior: diploids were hyperfilamentous compared to haploids.

XL280α is a laboratory strain derived from a cross of two sibling strains, JEC20**a** (congenic with JEC21α) and B3501α, which share ~50% genome identity. Both of the parental strains have been sequenced (Loftus, Fung et al. 2005). Whole genome sequence analysis of XL280α reveals that it shares ~81% genome identity with the congenic strains JEC20**a** and JEC21α (Ni, Feretzaki et al. 2013).

A. tumefaciens mediated insertional mutagenesis generated approximately 6,100 mutants yielding ~1x genomic coverage. The mutants were transferred onto unisex-inducing V8 medium and incubated at room temperature

in the dark for 14 days. The mutant library was then screened microscopically for enhanced or diminished hyphal development during unisexual reproduction. The library was also incubated on V8 medium for 14 days under constant light conditions. Light inhibits sexual development in *Cryptococcus* and this process is genetically regulated by the two light sensing genes *BWC1* and *BWC2* (Idnurm and Heitman 2005, Lu, Sun et al. 2005). To identify candidate genes for light sensing, we also screened the library for mutants that filamented equally well in the dark and the light.

We identified 225 mutants that exhibited a stable filamentation difference resulting in no hyphal growth (16), short hyphae (131), abnormal hyphae (21), more abundant hyphae (46), sporulation defects (2), increased chlamydospore production (6), or altered light response (3) (Figure 18). Mutants with sporulation defects and no hyphal growth or a hyperfilamentous phenotype were subjected to PCR to identify insertions in known candidate genes. Our screen was successful in isolating mutations in the previously identified genes *CRG1*, *STE7*, *MAT2* (two independent mutants), and *ZNF2*, whose products are key components of the pheromone signaling cascade and in *BWC2*, which encodes a major regulator of light sensing (Davidson, Nichols et al. 2003, Nielsen, Cox et al. 2003, Idnurm and Heitman 2005, Lin, Jackson et al. 2010). Isolates with increased ploidy (2N diploid or 3N triploid) are known to exhibit more robust filamentation during unisexual reproduction compared to congenic haploid strains

(Lin, Hull et al. 2005). All of the hyperfilamentous mutants were subjected to FACS analysis to determine their ploidy state, and four hyperfilamentous mutants were found to be diploid (2N). Using a microdissection microscope, 20 basidiospores were isolated from each diploid isolate; hyphal development of all of these progeny was similar to the wild type XL280α parental strain. FACS analysis of 15 progeny from each diploid showed that they were all haploid, indicating that their hyperfilamentous phenotype was due to an increase in ploidy (2N) and not to a mutation enhancing diploidization. These findings further confirm that 1) α/α diploid isolates undergo unisexual reproduction to produce haploid progeny and 2) diploid spore isolates can be recovered from the sexual cycle (see also Sia, Lengeler et al. 2000).

To identify insertions in unknown genes, the mutants were subjected to linkage analysis, inverse PCR, and sequence analysis. Linkage analysis of the mutants identified 12 in which the insertion was not linked with the mutant phenotype and these were excluded from further characterization. Of the remaining mutants 31 yielded an inverse PCR product. The sequences obtained were used in BLAST searches against the *C. neoformans* JEC21 genome database to identify the disrupted genes. Table 6 summarizes the insertion sites for 31 mutants. One of the newly identified genes from mutants that were afilamentous, CNK01880, encodes a protein with three zinc finger domains. Zinc finger proteins are often involved in binding to nucleic acids (DNA and RNA), and

the C2H2 motif is often a feature of transcription factors. The presence of three C2H2 zinc finger domains prompted us to name this protein Znf3 to distinguish it from two other genes encoding zinc finger transcription factors (Znf1 and Znf2) (Lengeler, Fox et al. 2002, Lin, Jackson et al. 2010). Two sporulation defective mutants had insertions in two highly conserved genes. The first gene, CNH01330, encodes a topoisomerase homolog and the second, CND02770, encodes a ubiquitin-conjugating enzyme. Because these genes are the orthologs of the *S. cerevisiae* meiosis-specific endonuclease Spo11 and the ubiquitin-conjugating enzyme Ubc5, we named the *Cryptococcus* genes *SPO11* and *UBC5*, respectively.

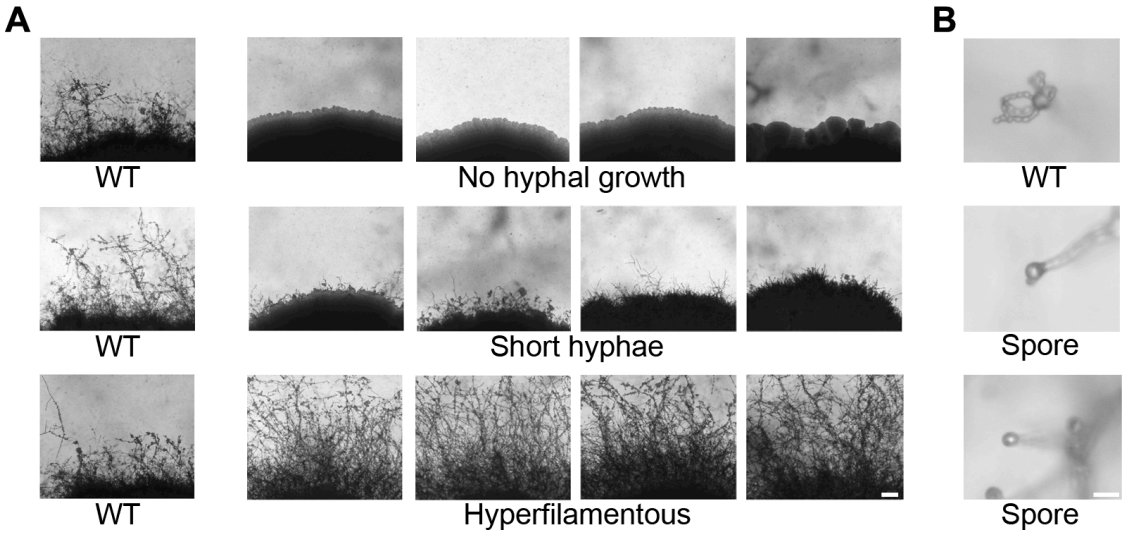

Figure 18. Phenotypic analysis of insertion mutants altered in unisexual reproduction. Nourseothricin (NAT)-resistant *Agrobacterium* transconjugant mutants of XL280α were grown on V8 solid agar for 14 days in the dark at room temperature to examine hyphal development during sexual reproduction by light microscopy. (**A**) The wild type strain XL280α undergoes robust hyphal growth during unisexual reproduction. The most extreme mutant

phenotypes include no hyphal development, short hyphae, or hyperfilamentous strains. The scale bar represents 100 μm. (**B**) The progeny of wild type strain XL280α are organized in four long chains of spores that emerge from the surface of the basidium. Sporulation was severely impaired in several insertion mutants. The scale bar represents 10 μm.

Table 6. Gene governing unisexual reproduction.

Genbank Accesion	Protein class/ Identifiable motifs[c]	Gene disrupted	Close homolog/ Known role
	No hyphal growth		
CNM02020	HMG domain at N-terminus	*MAT2*[a,b]	Sexual development transcription factor
CNE04290	Rab-GTPase activation domain at N-terminus		**Gyp5**, polarized growth in *S. cerevisiae*
CNF02400	Cell wall and biogenesis related protein	*SLA2*[b]	**Sla2**, cytoskeleton factor in *S. cerevisiae*
CNK01880	Two C2H2-type zinc finger domains	*ZNF3* [a.b]	
CNC02350	Mitogen activating protein kinase kinase	*STE7*[a]	MAP kinase kinase mating factor
CNF04390	Velvet-like factor	*VEA2*[a]	Velvet factor **VeA** in *Aspergillus*
CNG02160	Two C2H2-type zinc finger domains	*ZNF2*[a]	Mammalian **Znf2.2** factor
	Hyperfilamentous growth		
CNC02080	Rta1-like protein		Lipid-translocating exporter in *S. cerevisiae*
CNG01130	NAD epimerase		Highly conserved eukaryotic protein
CNB02170	Transmembrane efflux protein		**EncT** ergosterol transport in *C. neoformans*
CNI00820	Histidine phosphatase domain of mutases		Highly conserved eukaryotic protein
CNJ01220	Hypothetical protein		Conserved in Tremellaceae protein
CNA03100	single-stranded DNA endodeoxyribonuclease		Highly conserved eukaryotic protein **Rad2**
CNC01470	GTP-binding protein		Highly conserved GTPase protein
CNC03490	Leucine rich repeats		Septation initiation scaffold **Cdc11** *S. pombe*
CNA02470	Fungal gamma tubulin protein		**Spc97** microtubule complex in *S. cerevisiae*
CNC02700	Mitochondrion organization-related protein		Homolog of human **Letm1**
CNG04300	3-hydroxyacyl-CoA dehydrogenase		Highly conserved eukaryotic protein
CNF04140	Rho small monomeric GTPase		**Rho2,** involved in cell polarity in *S. cerevisiae*
CNG03390	Yippee-like putative protein		Highly conserved eukaryotic protein
CNH01390	Fungal specific transcription factor		Highly conserved fungal protein
CNH02070	Serine/threonine protein kinase		**Kin4,** inhibits mitotic exit network in yeast
CNC02950	Hypothetical protein		Conserved in Tremellales
CNA01150	Regulator of G protein signaling domain	*CRG1*[a]	Crg1 negative regulator of mating in *C. neoformans*
CNK02180	GMP synthase		**Gua1**, negatively regulated by nutrient starvation in *S. cerevisiae*
CNG04410	Hypothetical protein		Basidiomycota conserved protein
CNL03660	Hypothetical protein		Sga1, glycogen starvation in *S. cerevisiae*
	Sporulation defect		
CND02770	Ubiquitin-conjugating enzyme E2-domain	*UBC5*[a]	**Ubc5**, Ubiquitin-conjugating enzyme in *S. cerevisiae*
CNH01330	Type IIB DNA topoisomerase VI	*SPO11*[a]	**Spo11**, catalyzes DSB in *S. cerevisiae*
	Light sensing defect		
CNE01220	ZnF-GATA and PAS domains	*BWC2*[a]	**Wc1**, role in light sensing and circadian rhythm in *N. crassa*
CNJ01160	Arylsulfotransferase	*BWC3*[a,b]	Highly conserved eukaryotic protein

Linkage analysis showed that the insertions in these mutants are linked to the phenotype.
[a]: *De novo* gene disruption confirmed the mutant phenotype.
[b]: Multiple independent insertion mutants were isolated.
[c]: Conserved domains were identified using the InterProScan Sequence Search tool of EMBL-EBI (http://www.ebi.ac.uk/Tools/pfa/iprscan/).

4.3.2 Znf3 is Essential for Unisexual Reproduction

The genetic screen revealed five different mutants with a similar filamentation defect, each with an insertion into a different site in the *ZNF3* gene. One insertion was in the coding region of the gene, and four other insertions were in different positions of the promoter region. Insertion in promoters or terminators of a gene is a common feature of T-DNA insertions, which exhibit a bias towards promoters and 5' and 3' UTRs (Alonso, Stepanova et al. 2003). To elucidate the role of Znf3 in unisexual reproduction, we deleted the complete gene, from start to stop codon, in XL280α via biolistic transformation and homologous recombination. Two independent *znf3*Δ deletion mutants were generated, and the deletions were verified by Southern blot and PCR analyses. We assessed the ability of the insertion and deletion mutants to undergo unisexual reproduction by incubating the strains in the dark for two weeks on different filamentation-inducing media and examining them by light microscopy. The wild type XL280α strain formed hyphae along the entire periphery of the colony, while two *znf3* insertion mutants were defective in hyphal production (Figure 19A). The *znf3*Δ mutation blocked hyphal development in both independent mutants (Figure 19A). Prolonged incubation on filamentation inducing media (≥3 weeks) did not result in the production of any hyphae, indicating that Znf3 is critical for the dimorphic transition during unisexual reproduction.

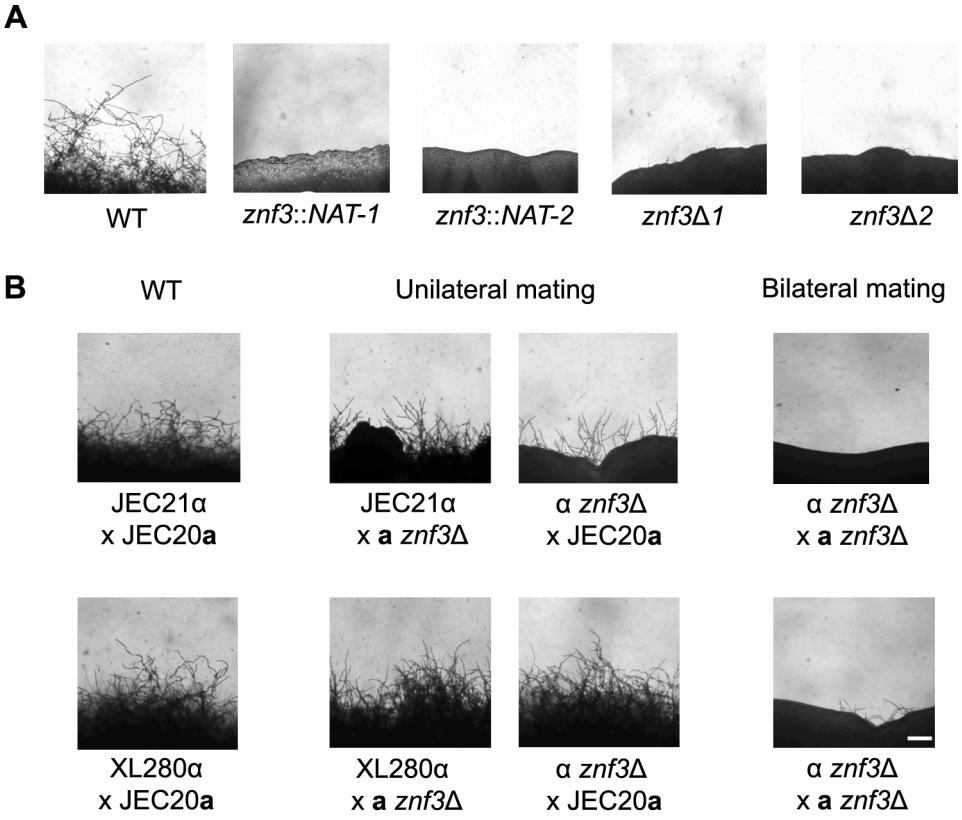

Figure 19. Deletion of *ZNF3* impairs hyphal development during bisexual and unisexual reproduction. (**A**) XL280α, two mutants with independent insertions in *ZNF3* (II-12, II-147), and two independent *znf3*Δ deletion mutants (MF01, MF38) were incubated on V8 medium in the dark at room temperature for 10 days and hyphal formation during unisexual reproduction was assessed by microscopy. (**B**) Bisexual wild type crosses (JEC21α x JEC20**a** and XL280α x JEC20**a**), unilateral mutant crosses (α *znf3*Δ x WT**a** and WTα x **a** *znf3*Δ), and bilateral mutant crosses (α *znf3*Δ x **a** *znf3*Δ) were conducted on V8 medium in the dark at room temperature for 7 days and photographed. The scale bar represents 100 μm.

4.3.3 Znf3 Plays a Role in Hyphal Development During Bisexual Reproduction

Because the pheromone signaling cascade components are known to regulate both bisexual and unisexual reproduction (Davidson, Nichols et al. 2003), we hypothesized that Znf3 might also play a role in the dimorphic transition during bisexual reproduction. As mentioned earlier, the **a**-α sexual cycle is induced by the fusion of opposite-mating type cells to form a dikaryon, which initiates the development of dikaryotic hyphae and leads to the formation of basidia, where nuclear fusion and meiosis occur to produce chains of spores. To determine the role of Znf3 in bisexual reproduction, we deleted the gene in both strains of the serotype D congenic mating pair JEC21α and JEC20**a** via biolistic transformation. Because two different mating type partners are involved we used unilateral (one mating partner is mutant) and bilateral (both mating partners are mutant) mating assays to examine the role of Znf3. In the wild type JEC21α x JEC20**a** cross, filamentation was robust, with basidia and spores forming after 7 days of incubation on V8 medium. However, unilateral crosses of *znf3*Δ (α *znf3*Δ x WT or WT x **a** *znf3*Δ) produced significantly fewer hyphae, while in bilateral crosses (α *znf3*Δ x **a** *znf3*Δ), hyphal development was severely impaired (Figure 19B). Unilateral mutant crosses were able to complete the sexual cycle and form spores following prolonged incubation on V8 (~2 weeks), while bilateral mutant crosses produced only sporadic hyphae. In contrast, the

*znf3*Δ mutant phenotype was less severe in the hyperfilamentous XL280α background. Unilateral matings exhibited hyphae with basidia and spores at approximately wild type levels (Figure 19B). However, hyphal development was impaired in bilateral matings with sporadic short hyphae that eventually grew long enough to produce basidia and spores (~3 weeks). Based on these findings, we conclude that Znf3 plays an important role during **a**-α mating.

Defects in hyphal development could be due to defects in fusion of α and **a** mating partners. Because the *znf3*Δ mutation blocked the dimorphic transition during bisexual reproduction, Znf3 could be involved in the initial step of mating. Cell-cell fusion assays were employed to determine the role of *ZNF3* in cell-cell fusion. Wild type α and **a** strains and α *znf3Δ* and **a** *znf3Δ* mutant strains genetically marked with different drug resistance markers were mated on V8 medium for 15 or 24 hours in the dark. The cells were collected and plated in serial dilutions on media that select for doubly drug-resistant fusion products (to measure cell-cell fusion) or allow all cells to grow (to determine total CFU). In *znf3*Δ x WT unilateral matings, the relative fusion efficiency was ~ 50% at 15 hours of co-incubation and ~70% at 24 hours compared to wild type. Interestingly, in *znf3*Δ x *znf3*Δ bilateral matings, the fusion efficiency was reduced to ~15% after 15 hours of co-incubation and ~50% after 24 hours of co-incubation. In contrast, disruption of the *CPK1* MAPK and *MAT2* transcription

factor genes essentially abolished cell-cell fusion in both unilateral and bilateral mating assays, indicating an essential role in the first steps of sexual reproduction (Davidson, Nichols et al. 2003, Lin, Jackson et al. 2010). These observations support the hypothesis that Znf3 plays a modest role in cell-cell fusion events early in mating. However, with prolonged incubation times, *znf3Δ* mutant cells do undergo efficient cell-cell fusion. A possible explanation could be that Znf3 acts in parallel with the pheromone signaling cascade and that it is required to enhance the intracellular signal for the dimorphic transition during bisexual reproduction.

4.3.4 Znf3 Regulates Pheromone Production

The dimorphic transition during bisexual and unisexual reproduction is in part induced by the production of peptide pheromones. The Cpk1 MAPK signaling cascade mediates sensing and pheromone production during sexual development (Davidson, Nichols et al. 2003, Lin, Jackson et al. 2010). To determine whether Znf3 plays a role in the pheromone-sensing pathway, we generated expression profiles for the *ZNF3*, *MAT2*, *SXI1α*, and *MFα1* genes in wild type, *ste7Δ, mat2Δ, znf2Δ, sxi1αΔ*, and *znf3Δ* mutant backgrounds. Gene expression was monitored during bisexual and unisexual reproduction by RT-PCR. We determined that expression of these genes in wild type bisexual reproduction reached the highest levels after 24 hours of incubation on

filamentation-inducing V8 medium (Figure 20). *MFα1* expression, which increased ~2,500-fold, served as a positive control. During unisexual reproduction, expression of the genes in XL280α reached the highest level after 48 hours of incubation on V8. These time points were chosen to determine the expression of the genes in the different mutant backgrounds.

Both bilateral bisexual and unisexual reproduction were performed on V8 media and the cells were harvested at the designated times. RNA was isolated, and RT-PCR was employed to determine the transcript levels in each mutant. *ZNF3* expression remained the same and similar to wild type, even when components of the MAPK signaling cascade were absent during crosses (Figure 21A). This indicates that Znf3 is not a transcriptional target of the pheromone-signaling cascade and that expression does not depend on the MAPK pathway. However, during bisexual reproduction, *MAT2* expression was decreased in the *znf3*Δ mutant in an expression pattern similar to that of *ste7*Δ mutants previously observed (Figure 21B) (Lin, Jackson et al. 2010). The *ste7*Δ phenotype is in accord with the hypothesis that Mat2 is the direct target of the MAPK signaling cascade; however, Znf3 may moderately co-regulate the expression levels of Mat2 during hyphal development, and in fact *MAT2* expression was also decreased in the *znf3*Δ mutant during unisexual reproduction. A similar phenotype was observed for Sxi1α. Previous studies have shown that Mat2

governs *SXI1*α through the Cpk1 MAPK cascade in bisexual reproduction (Lin, Jackson et al. 2010). *SXI1*α expression was abolished in *ste7*Δ and *mat2*Δ mutant backgrounds. Deletion of *ZNF3* significantly decreased the transcript levels of *SXI1*α compared to wild type; however, the level of inhibition was less severe than in the *ste7*Δ and *mat2*Δ mutant backgrounds (Figure 21C). In unisexual reproduction, the *znf3*Δ mutant decreased *SXI1*α expression similar to *ste7*Δ and *mat2*Δ mutants (Figure 21C). Interestingly, the inhibition profile of *SXI1*α during bisexual reproduction was similar to unisexual reproduction, even though *SXI1*α does not participate in hyphal development during unisex.

In further experiments, we determined the expression levels of other components of the MAPK signaling cascade. During bisexual reproduction the transcriptional profile of *CPK1* was similar to *MAT2* with modestly reduced levels in *znf3*Δ bilateral crossing cultures (Figure 22). We also assessed the expression levels of two negative regulators of the pheromone pathway, *CRG1* and *CRG2*, in the absence of components of the MAPK signaling cascade during unisexual reproduction (Figure 22). *CRG2* expression levels were slightly reduced in the deletion mutants. *CRG1* transcription significantly increased in the *znf2*Δ mutant, which may contribute to the inhibition of hyphal development. However, expression of these negative regulators was not significantly altered in the *znf3*Δ mutant.

Pheromones are key activators of sexual development, as well as important targets. During vegetative growth the pheromones are expressed at basal levels and in a nutrient-limited environment the pathway is activated by a massive increase in pheromone production enforced by a positive feedback loop. Deletion of components of the Cpk1 MAPK cascade blocks expression of the pheromones and inhibits responses (Davidson, Nichols et al. 2003, Lin, Jackson et al. 2010). By measuring the transcript levels of *MFα1* in bilateral bisexual and unisexual reproduction in *ste7*Δ and *mat2*Δ mutant backgrounds, we found that the inducible expression level was completely blocked compared to the wild type (Figure 21D). In contrast, Znf2 functions further downstream and regulates hyphal formation without participating in the initiation of the pheromone signal (Lin, Jackson et al. 2010). *MFα1* expression in the *znf2*Δ mutants was significantly increased in both sexual cycles, as previously observed (Figure 21D) (Lin, Jackson et al. 2010). On the other hand, the *sxi1*αΔ mutation modestly increased pheromone expression during bisexual reproduction as previously observed (Hull, Davidson et al. 2002). However, *MFα1* production was significantly reduced in the *znf3*Δ mutant. During both bisexual and unisexual reproduction of *znf3*Δ mutants the expression of the pheromone gene was severely impaired (Figure 21D). This indicates that Znf3 is important for pheromone production, and the hyphal defect of *znf3*Δ mutants may result in part

from impaired *MFα1* expression. Nevertheless, the expression of the pheromone was not completely blocked and the expression profile pattern was similar to *MAT2* and *SXI1α* expression in the *znf3Δ* mutant. Taking these results together, we can conclude that Znf3 is not regulated by the pheromone-signaling cascade; however, it may act in a parallel pathway that regulates the expression of the pheromone or Mat2 and consequently its targets, including Sxi1α.

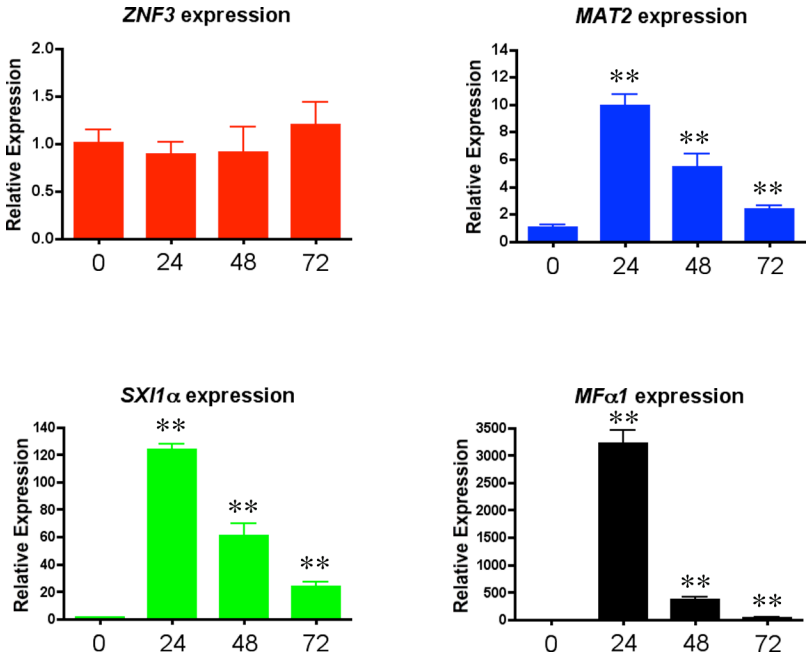

Figure 20. Expression profiles of *ZNF3*, *MAT2*, *SXI1α*, and *MFα1* during bisexual reproduction. WT α and **a** cells were mixed in equal numbers, co-cultured on V8 medium, and incubated in the dark for 0 (vegetative growth), 24, 48, or 72 hrs. The cells were harvested and RNA was isolated from both yeast cells and hyphae. RT-PCR showed that *ZNF3* expression during bisexual reproduction remained similar to vegetative growth. *MAT2*, *SXI1α*, and *MFα1* expression increased significantly at 24 hrs. The error bars represent the standard deviations from the mean for the three biological replicates.

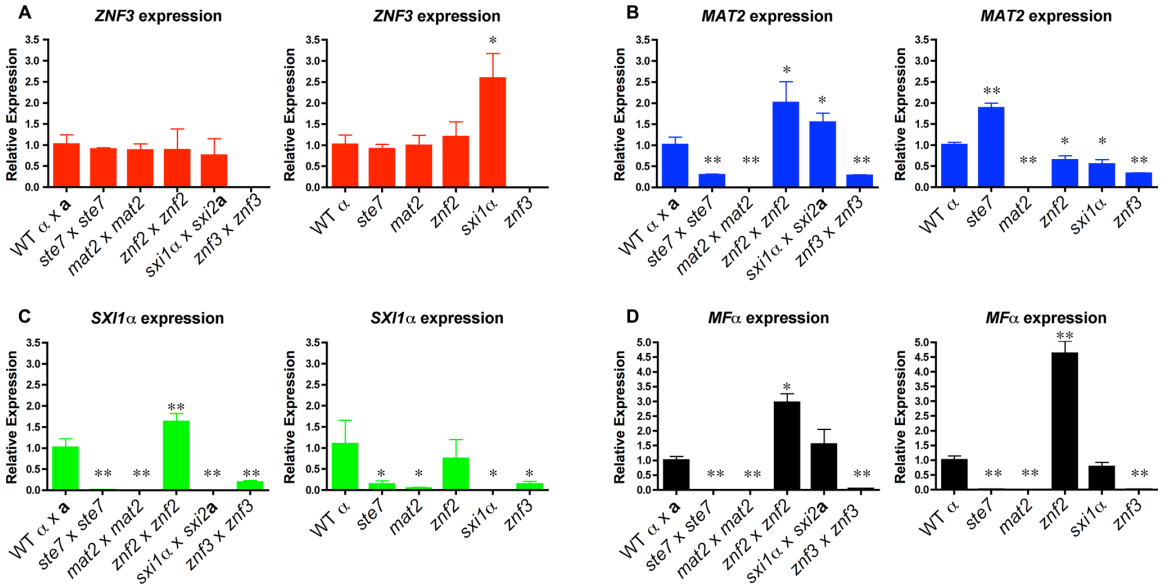

Figure 21. Znf3 regulates the expression of Mat2 and promotes pheromone production. Cells were incubated for 24 hours on V8 medium for bisexual and 48 hours for unisexual reproduction. Yeast and hyphal cells were harvested and RNA was isolated. The expression of the (**A**) *ZNF3*, (**B**) *MAT2*, (**C**) *SXI1*α, and (**D**) *MF*α*1* genes was measured by RT-PCR in wild type, *ste7*Δ, *mat2*Δ, *znf2*Δ, *sxi1*αΔ, and *znf3*Δ mutants (* indicates P < 0.05 and ** indicates P < 0.005 compared to the WT). The error bars represent the standard deviations from the mean for the three biological replicates.

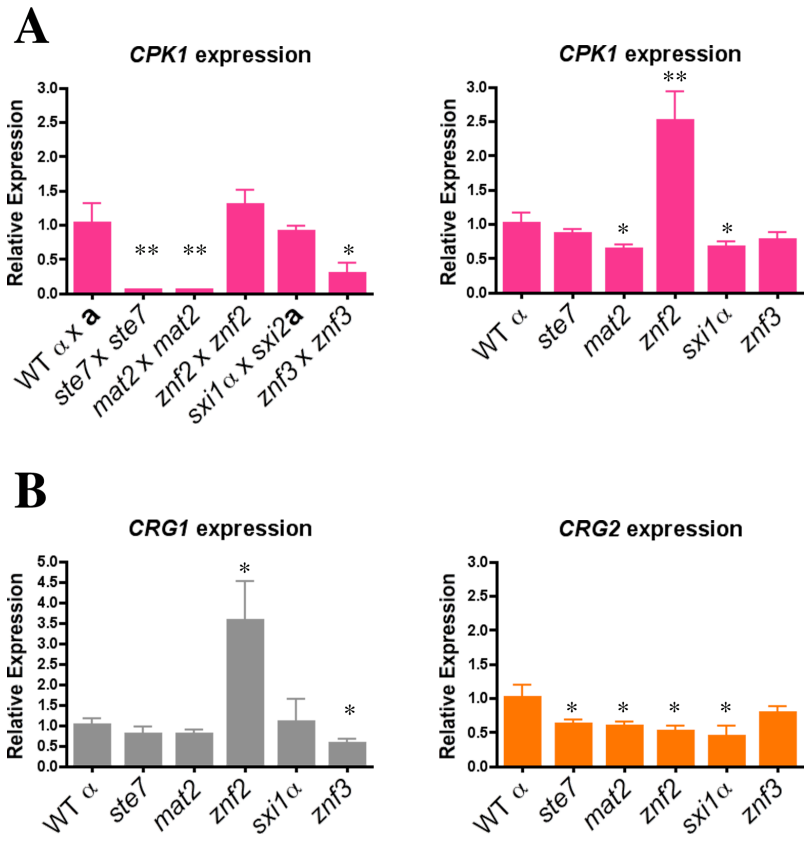

Figure 22. Expression profile of genes encoding Cpk1, Crg1, and Crg2. Cells were incubated for 24 hours on V8 medium for bisexual and 48 hours for unisexual reproduction. Yeast and hyphal cells were harvested and RNA was isolated. Expression was measured by RT-PCR in wild type, *ste7*Δ, *mat2*Δ, *znf2*Δ, *sxi1*αΔ, and *znf3*Δ mutants. (**A**) The MAP kinase *CPK1* transcriptional profile is similar to *MAT2*, and its expression is possibly regulated by the pheromone signaling cascade. (**B**) Expression of the negative regulator *CRG1* was significantly increased in the *znf2*Δ mutant. The elevated levels of *CRG1* may contribute to the severe filamentation defect of *znf2*Δ mutants during unisexual reproduction. *CRG2* expression in pheromone response mutants was similar to wild type (* indicates P<0.05 and ** indicates P<0.005 compared to the WT). The error bars represent the standard deviations from the mean for the three biological replicates.

4.3.5 Znf3 Governs Sexual Reproduction Through an Independent Pathway

Znf3 is required for hyphal growth during bisexual and unisexual reproduction, and we have shown that it plays an important role in pheromone expression. Although it is not a transcriptional target of the MAPK pathway, it may act downstream and contribute to or enhance the pheromone-induced signal. To investigate the possible role of Znf3 in the pheromone signaling cascade, we engineered an overexpression allele with *ZNF3* under the control of the constitutively active *GPD1* gene promoter. Wild type, a *mat2*Δ mutant, and a *znf3*Δ mutant were transformed with this overexpression allele using biolistic transformation. Based on RT-PCR results, expression of *ZNF3* was increased ~5-fold in the otherwise wild type P_{GPD1}-*ZNF3* background. Hyphal development was assessed on V8 medium by light microscopy. Hyphal growth in XL280α P_{GPD1}-*ZNF3* was similar but slightly more robust compared to wild type (Figure 23). Because a wild type *ZNF3* complementation construct was not available, we transformed the *znf3*Δ mutant with the P_{GPD1}-*ZNF3* allele and found that this overexpression allele restored unisexual reproduction (Figure 23). Hyphal growth was slightly more condensed in the complementation strain due to the ~5 fold increased *ZNF3* expression, and it was moderately enhanced compared to the WT, possibly due to the expression from an exogenous locus.

Mat2 is a major component of the MAPK pathway, and overexpression of a downstream target should bypass its requirement for mating and stimulate hyphal production. However, overexpression of *ZNF3* failed to restore hyphal development in the afilamentous *mat2*Δ mutant, which indicates an independent function for Znf3 in unisexual reproduction (Figure 23). These observations provide further evidence that Znf3 does not act downstream of the pheromone signaling cascade.

Expression profiling showed that Znf3 moderately regulates the expression of *MAT2* in *C. neoformans*, indicating a mode of control on the major regulator of sexual reproduction. Transcriptional control of mating and morphogenesis in the closely related species *U. maydis* involves additional transcription factors upstream of Prf1, the HMG target of the conserved MAPK pathway (Brefort, Muller et al. 2005, Klosterman, Perlin et al. 2007). Constitutive expression of *PRF1* complements the severe defect caused by deletion of these factors. To determine if Znf3 functions upstream of Mat2 we used a *MAT2* allele under the control of the constitutively active *GPD1* promoter (Lin, Jackson et al. 2010). The overexpression *MAT2* allele was introduced into *znf3*Δ mutants via biolistic transformation and hyphal growth was assessed by light microscopy. Overexpression of *MAT2* in the *znf3*Δ background failed to induce the dimorphic switch from yeast to hyphae development (Figure 23). These results provide evidence that Znf3 and Mat2 may act in independent, parallel pathways.

Transcription of *MAT2* is tightly regulated by the presence of pheromone, and during mating a 12-fold increase in expression was observed (Figure 20). Decreased expression of *MAT2* is possibly an indirect effect of the low pheromone levels observed in the *znf3*Δ mutant. The pathway that governs Znf3 and stimulates its control over pheromone expression warrants additional analysis.

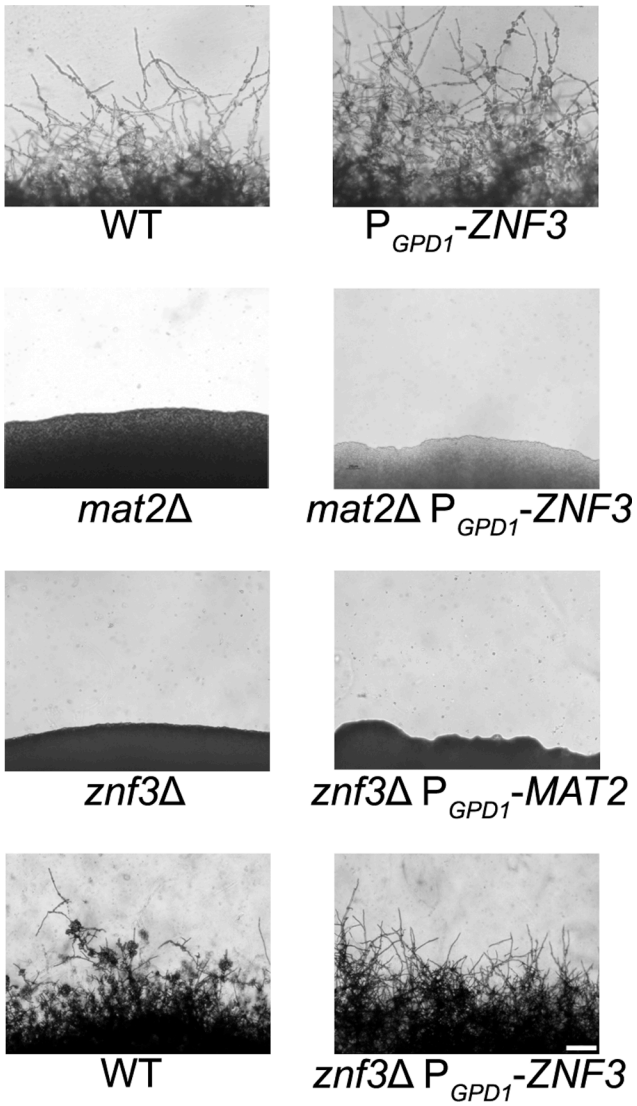

Figure 23. Znf3 is not a transcription target of the MAPK signaling cascade. Wild type XL280α, *mat2*Δ, and *znf3*Δ mutants were transformed with the P_{GPD1}-*ZNF3* transgene, and a *znf3*Δ mutant was transformed with the P_{GPD1}-*MAT2* transgene. The cells were incubated on V8 medium for 14 days in the dark. The *ZNF3* overexpression allele moderately increased hyphal development in the wild type and restored unisexual reproduction in the *znf3*Δ mutant; however, it failed to suppress the sterile phenotype of *mat2*Δ mutants. Similarly, the *MAT2* overexpression allele failed to restore hyphal development of the *znf3*Δ mutant. The scale bar represents 100 μm.

4.3.6 Znf3 Regulates the Expression of Retrotransposons During Sexual Development

A lack of any obvious link between Znf3 and the pheromone-signaling cascade prompted us to analyze the genome-wide transcriptional profile of the *znf3*Δ mutant. We performed a comparative transcriptome analysis between XL280α and the *znf3*Δ and *mat2*Δ mutants during bisexual and unisexual reproduction. In the first level of analysis, we considered genes that were regulated similarly in the *znf3*Δ and *mat2*Δ mutants. As expected, the majority of the genes that were downregulated in the mutants were involved in the pheromone signaling cascade during unisexual reproduction. The expression of the pheromone and pheromone receptor genes was significantly decreased in both *znf3*Δ and *mat2*Δ mutants compared to the WT. However, the whole genome transcriptional profile of the *znf3*Δ mutant was different. A similar phenotype was observed during bisexual reproduction. This result validates our previous findings and supports the hypothesis that Znf3 acts in an independent, parallel pathway.

To determine the role of Znf3 during unisexual reproduction and obtain further mechanistic insights, we extended our genome-wide expression analysis to genes that are upregulated specifically in the *znf3*Δ mutant. More than 500 independent tags yielded more than a two-fold increase in the *znf3*Δ mutant during unisexual reproduction (data not shown). We aligned the highly enriched

tags to the *C. neoformans* JEC21α genome database and found that the majority encoded putative transposases, hypothetical endonucleases, and RNA-dependent DNA polymerases (Table 7). Surprisingly, we also found a significant increase in the expression of the T1 and T3 DNA transposons (Table 7). Previous studies have shown that transposable elements are highly expressed during bisexual and unisexual reproduction; however, the RNAi pathway inhibits transposon activity via Sex-Induced Silencing (SIS) and protects the genome against transposition and mutations (Janbon, Maeng et al. 2010, Wang, Hsueh et al. 2010, Wang, Darwiche et al. 2013). Deletion of *RDP1*, a component of the RNAi pathway (the RNA-dependent RNA polymerase), induces the expression of retrotransposons during sexual development (Janbon, Maeng et al. 2010, Wang, Hsueh et al. 2010). The previously identified expression profile of the *rdp1*Δ mutant exhibits a similar increase in transposable elements and RNA-dependent DNA polymerases as the *znf3*Δ mutant (Table 7). This type of regulation was not observed in the *mat2*Δ mutant, indicating a unique role for Znf3 in transposon silencing. Taking these results together, we conclude that Znf3 is required for transposon silencing and pheromone expression during sexual development, and these interesting findings will provide the foundation for further analysis in future investigations.

Table 7. Transposon-related genes are upregulated during *znf3*Δ mutant unisexual reproduction.

Gene Locus	*znf3*Δ/WT	Annotation
1712.seq.017	69.72	Transposable element T1
1671.seq.034	8.963	Hypothetical protein. Previously found to be upregulated in RNAi-mutant strains
1704.seq.045	8.76	Hypothetical protein. Previously found to be upregulated in RNAi-mutant strains
184.m05079	7.794	DDE Endonuclease, transposase domain
1661.seq.033	7.293	Hypothetical protein. Previously found to be upregulated in RNAi-mutant strains
1744.seq.140	7.231	Integrase, DDE superfamily endonuclease
177.m03075	7.188	DDE Endonuclease, transposase domain
183.m01854	6.929	Hypothetical protein. Previously found to be upregulated in RNAi-mutant strains
181.m08309	6.089	Transposable element T3
179.m00071	5.57	Transposable element T3
180.m00376	5.089	Transposable element T3
184.m04347	4.86	Transposable element T3
164.m02163	4.322	Transposable element T3
184.m05148	3.646	Transposable element T3
1642.seq.046	3.496	Transposable element T3
163.m06563	3.284	Transposable element T3
1631.seq.008	3.044	Transposable element T3
1663.seq.046	2.57	Transposable element T1
1681.seq.010	2.457	Transposable element T1
1682.seq.124	2.19	Transposable element T3
1742.seq.060	2.162	RNA-dependent DNA polymerase, present in transposable elements
1621.seq.158	2.102	Transposable element T3
163.m06565	2.096	Hypothetical transposase (Transposase family tnp2)
1751.seq.002	2.078	RNA-dependent DNA polymerase, present in transposable elements
1701.seq.190	2.018	Hypothetical protein, ATP-dependent DNA helicase domain

4.3.7 Spo11 and Ubc5 are Required for Sporulation

Pheromone production and sensing initiate sexual development by inducing cell fusion and hyphal development. At the termini of the hyphae, a bulb-like structure known as the basidium forms where meiosis and sporulation occur. Previous studies in model organisms have shown that the endonuclease

Spo11 and members of the ubiquitin complex govern meiosis and sporulation. In *S. cerevisiae* homozygous *spo11*/*spo11* mutants exhibit defects in meiosis and sporulation, while Ubc5 has been implicated in sporulation (Seufert and Jentsch 1990, Enyenihi and Saunders 2003, Jin, Dobry et al. 2008). To establish the roles of Spo11 and Ubc5 in sporulation or meiosis in *C. neoformans*, both genes were deleted in XL280α via biolistic transformation and homologous recombination and two independent mutants were isolated for each. Unisexually reproducing cultures were incubated on filamentation-inducing media in the dark at room temperature for 10 days or longer. Hyphal development of the *spo11*Δ mutant was similar to wild type XL280α with hyphae covering the entire periphery of the colony (Figure 24A). Filamentation of the *ubc5*Δ mutants was also similar to *spo11*Δ and XL280α, albeit slower and slightly reduced. Deletion of either the *SPO11* or *UBC5* gene blocked sporulation during unisexual reproduction. In wild type XL280α, the majority of the basidia formed at the termini of the hyphae and were decorated with four long chains of basidiospores (Figure 24A). In the *spo11*Δ and *ubc5*Δ mutants, the basidia were either “bald” and completely lacked spores or had at most one or two spores and occasionally one very short chain of spores (Figure 24B). Complementation of *spo11*Δ and *ubc5*Δ mutants with *SPO11* and *UBC5* genes under the control of their native promoter and terminator, respectively, restored wild type sporulation.

Bisexual reproduction results in significantly longer basidiospore chains in a shorter incubation time compared to unisexual reproduction. We deleted the *SPO11* and *UBC5* genes in the congenic mating partners JEC21α and JEC20**a** to assess their role in unilateral and bilateral crosses. In wild type matings (JEC21α x JEC20**a** and XL280α x JEC20**a**), the basidia formed four long spore chains on filamentation-inducing media after 7 days incubation in the dark at room temperature (Figure 25A). In unilateral crosses *spo11*Δ and *ubc5*Δ mutants were able to form four spore chains, but they were significantly shorter and in some cases, the basidia had only two or three short chains or even as few as only two or three spores. In bilateral *spo11*Δ x *spo11*Δ or *ubc5*Δ x *ubc5*Δ crosses, both mutants exhibited a severe sporulation defect. Most of the basidia were bald or were decorated with only one or two spores on the hyphae of the entire periphery (Figure 25B). Upon prolonged incubation (~3 weeks), hyphal development increased with longer and more dense hyphae; however, the basidia failed to yield more than at most two or three spores (Figure 25). This indicates that Spo11 and Ubc5 are critical for sporulation. A similar phenotype has been observed in the absence of the meiotic-specific recombinase Dmc1 in *C. neoformans* (Lin, Hull et al. 2005). Deletion of *DMC1* results in basidia with a severe sporulation defect during bisexual and unisexual reproduction. In *S. cerevisiae*, Dmc1 is responsible for the repair of DNA double-strand breaks and homologous pairing during meiotic recombination (Bishop, Park et al. 1992).

Considering these results together, and based on the fact that *SPO11* is highly conserved, we hypothesize that its requirement for sporulation is attributable to roles in meiotic recombination occurring during both bisexual and unisexual reproduction.

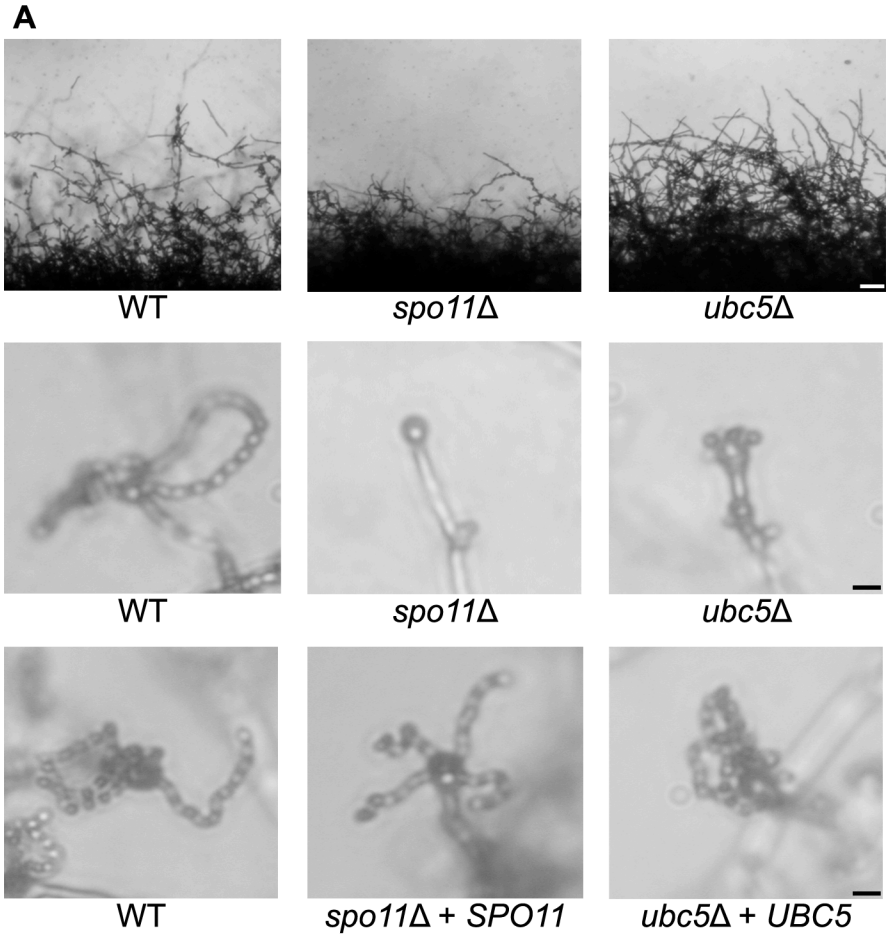
A
WT
spo11Δ
ubc5Δ
WT
spo11Δ
ubc5Δ
WT
spo11Δ + SPO11
ubc5Δ + UBC5
B
WT
spo11Δ
ubc5Δ

Figure 24. Spo11 and Ubc5 are required to complete sporulation during unisexual reproduction. Wild type XL280α and *spo11*Δ and *ubc5*Δ mutants were incubated on V8 medium in the dark at room temperature for 14 days. (**A**) Hyphal development was evaluated by light microscopy. The edges of the colony produced abundant hyphae in WT, *spo11*Δ, and *ubc5*Δ mutants (upper row). In XL280α, basidia were decorated with four spore chains, whereas in *spo11*Δ and *ubc5*Δ mutants, spore production was severely impaired and naked basidia or at most one or two short spore chains were observed. The scale bars represent 100 μm for the upper row and 10 μm for the middle rows. (**B**) Scanning electron microscopic analysis of sporulation defects during unisexual reproduction. The scale bars represent 5 μm.

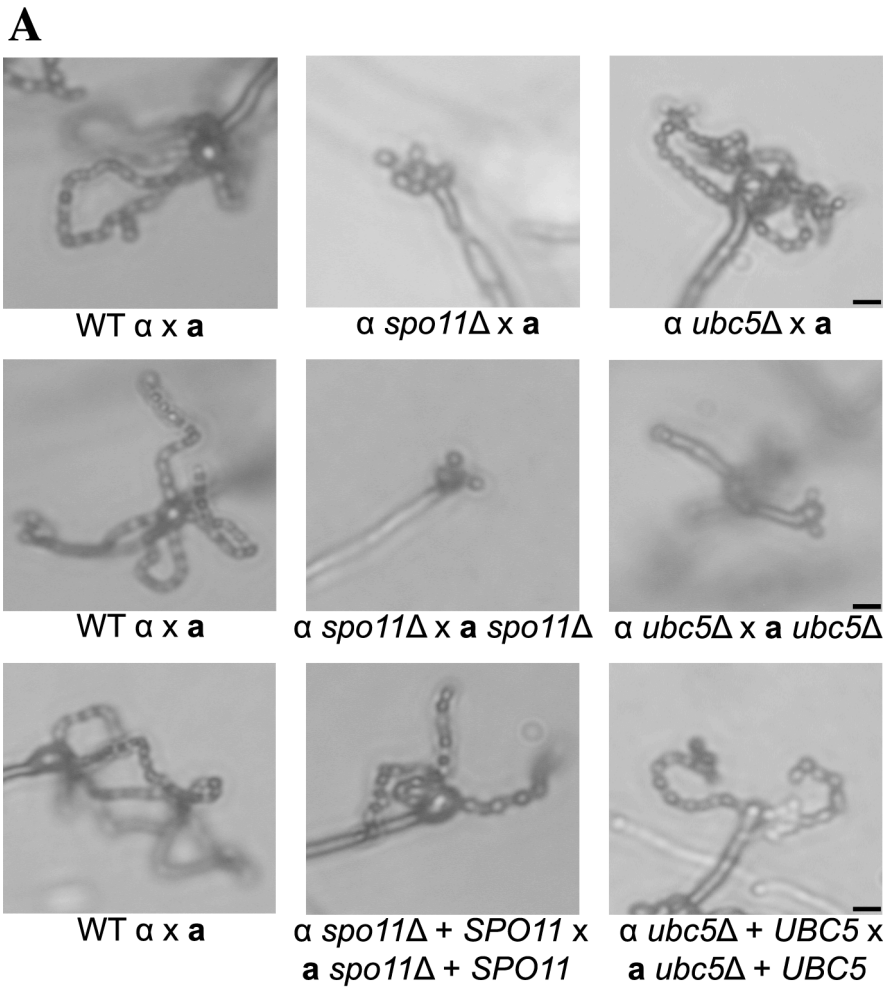
A
WT α x **a**
α *spo11*Δ x **a**
α *ubc5*Δ x **a**
WT α x **a**
α *spo11*Δ x **a** *spo11*Δ
α *ubc5*Δ x **a** *ubc5*Δ
WT α x **a**
α *spo11*Δ + *SPO11* x **a** *spo11*Δ + *SPO11*
α *ubc5*Δ + *UBC5* x **a** *ubc5*Δ + *UBC5*
B
WT α x **a**
α *spo11*Δ x **a** *spo11*
α *ubc5*Δ x **a** *ubc5*Δ

Figure 25. Spo11 and Ubc5 are necessary for sporulation during bisexual reproduction. Sporulation was assessed in wild type (XL280α x JEC20**a**), unilateral (α *spo11*Δ x JEC20**a**, α *ubc5*Δ x JEC20**a**), and bilateral (α *spo11*Δ x **a** *spo11*Δ, α *ubc5*Δ x **a** *ubc5*Δ) mating assays on V8 medium at room temperature in the dark for 7 days. (**A**) Spore production was evaluated by light microscopy. In WT crosses basidia produce abundant spores organized in four chains. In unilateral mutant matings spore production was similar to WT although modestly diminished. Bilateral mutants exhibited a severe defect in sporulation with none, one, or two spores. The scale bar represents 10 μm. (**B**) Scanning electron microscopic analysis of sporulation defects during bisexual reproduction. The scale bar represents 5 μm.

4.3.8 Spo11 is Required for Meiosis

An essential step prior to meiosis and sporulation is karyogamy. Karyogamy is characterized by two important steps: nuclear congression and nuclear fusion (Rose 1996). A series of genes are known to govern these steps in *S. cerevisiae*. In *C. neoformans*, how karyogamy is controlled remains largely unknown. A recent study identified a karyogamy gene, *KAR7* that regulates nuclear fusion during bisexual and unisexual development (Lee and Heitman 2012). Deletion of *KAR7* blocks nuclear fusion and severely impairs sporulation, similar to *spo11*Δ and *ubc5*Δ. To determine possible roles of Spo11 and Ubc5 in karyogamy, bisexual and unisexual reproduction patches of wild type and mutant partners were incubated for 10 days on V8 medium in the dark. The sexual reproduction cultures were fixed in 4% paraformaldehyde and nuclear positioning was visualized with Hoechst staining by fluorescence microscopy. Nuclear fusion in *spo11*Δ and *ubc5*Δ was normal in both hyphae and basidia and similar to wild

type (Figure 26), suggesting that the *spo11*Δ and *ubc5*Δ sporulation phenotype is unrelated to nuclear fusion and that it is caused by defects in a step subsequent to karyogamy.

During meiosis, recombination plays a crucial role in promoting pairing of homologous chromosomes in yeast and mammals. Meiotic recombination is initiated by the formation of DNA double strand breaks (DSBs) induced by Spo11. Spo11 is highly conserved in eukaryotic species and mutations can lead to sterility or offspring with an abnormal chromosome number. Fertility in mice is abolished in the absence of Spo11 (Romanienko and Camerini-Otero 2000); in *S. cerevisiae*, the survival rate of *spo11*Δ meiotic progeny is extremely low with high levels of aneuploidy (Klapholz, Waddell et al. 1985, Cao, Alani et al. 1990). To determine the survival rates in *C. neoformans*, unisexual reproduction cultures of wild type XL280α and *spo11*Δ and *ubc5*Δ mutants were incubated on filamentation-inducing V8 medium in the dark at room temperature for 10 days. Using a microscope with a microdissection needle, we dissected spores from four different mating unisexual development assays for each strain. The results are summarized in Table 8. For wild type XL280α, 30 spores were dissected from each assay. The germination rate of dissected spores ranged from 40% to 70%, as previously observed. Due to sporulation defects, *spo11*Δ and *ubc5*Δ generated only one or two spores per basidium, and thus the number of

dissected spores was lower than wild type. However, the germination frequency of dissected spores for both *spo11*Δ and *ubc5*Δ was significantly lower than the wild type and ranged from 0% to 9%. Extremely low viability of the unisexual progeny is usually attributed to chromosomal abnormalities, which is indicative of abnormal meiosis. Thus the low germination frequency of *spo11*Δ and *ubc5*Δ could be due to high levels of aneuploidy in the spores.

Based on sequence similarity, high homology, and the low germination rate of *spo11*Δ progeny, we reasoned that Spo11 may be required to catalyze DNA DSBs during meiosis in *C. neoformans*. Ionizing radiation has been found to suppress the meiotic defects of *spo11*Δ mutants and partially restore the wild type phenotype in *S. cerevisiae* and *C. cinerea* (Thorne and Byers 1993, Celerin, Merino et al. 2000). To determine the role of Spo11 in DSBs during unisexual reproduction, cultures of XL280α, *ubc5*Δ, and *spo11*Δ were spotted on V8 medium to induce unisexual reproduction, incubated in the dark for 7 days, irradiated using X-rays at different doses (0, 1, 3, 5, 10, and 20 krad), and incubated for two additional days. Following irradiation, the *spo11*Δ mutant exhibited higher sporulation efficiency and a higher germination rate than the non-irradiated *spo11*Δ culture (Table 9). A similar result was observed during *spo11*Δ x *spo11*Δ bisexual reproduction. Unlike the non-irradiated cultures of the *spo11*Δ bilateral cross (α *spo11*Δ x **a** *spo11*Δ), which produced very few spores,

irradiated *spo11*Δ basidia had significantly more spores with considerably enhanced viability (Table 9). Sporulation during both sexual cycles of WT and *ubc5*Δ was not significantly affected by irradiation, although viability was slightly lower, possibly due to higher rates of mutation (Table 9). XL280α, JEC21α, *ubc5*Δ, and *spo11*Δ mutants did not exhibit a growth defect in response to X-irradiation, and vegetative survival was similar between the WT and the mutants.

Taking these results together, we can conclude that 1) Spo11 is required for meiosis, likely by inducing DNA DSBs that promote recombination and homologous pairing, and 2) Ubc5 plays an important role in sporulation that warrants further investigation. That Spo11 operates during unisexual reproduction provides further definitive evidence that this is a meiotic process.

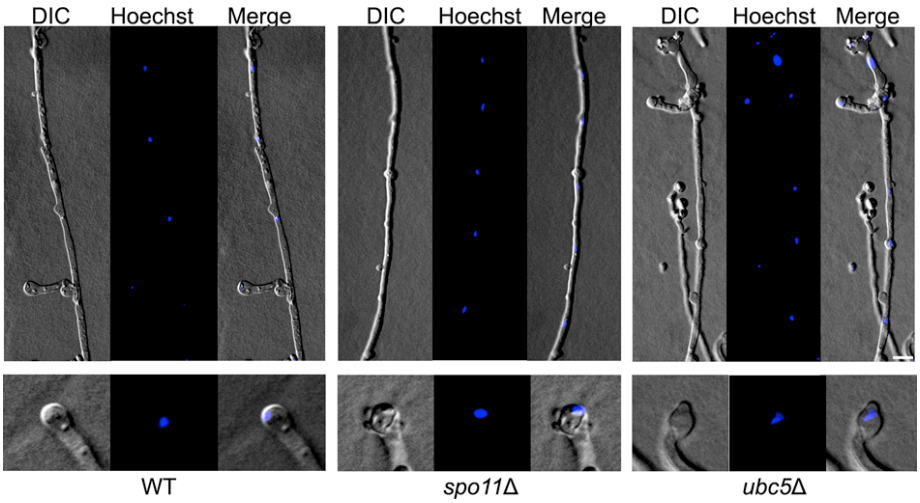

Figure 26. Localization of nuclei during unisexual reproduction. Wild type, *spo11*Δ, and *ubc5*Δ mutants were incubated on MS medium in the dark at room temperature for 10 days. Small patches of agar were excised and stained with Hoechst dye. Nuclear positioning was visualized with fluorescent microscopy. In wild type unisexual reproduction hyphae are monokaryotic with distinct nuclei in each hyphal compartment. In *spo11*Δ and *ubc5*Δ mutants, the unisexual hyphae are similar to wild type. The *kar7*Δ karyogamy mutant impairs hyphal growth by preventing early nuclear diploidization, and also leads to a sporulation defect by blocking late nuclear diploidization, leading to paired unfused nuclei in the basidium (Lee and Heitman 2012). The *spo11*Δ, and *ubc5*Δ mutants have only one nucleus in the basidium similar to the wild type and no hyphal growth impairment, consistent with no observed defects in karyogamy. The scale bar represents 10 μm.

Table 8. Viability of wild type, *spo11*Δ, and *ubc5*Δ unisexual reproduction progeny.

Wild-type		*spo11*Δ		*ubc5*Δ	
# spores dissected	# spores germinated (%)	# spores dissected	# spores germinated (%)	# spores dissected	# spores germinated (%)
30	21 (70%)	22	2 (9%)	24	2 (8%)
30	12 (40%)	18	0 (0%)	17	1 (6%)
30	19 (63%)	25	1 (5%)	21	1 (6%)
30	16 (53%)	16	0 (0%)	16	0 (0%)

Table 9. X-irradiation-induced DSBs partially rescue the spore survival defect of *spo11*Δ mutants during bisexual and unisexual reproduction.

X-ray dose (kRad)	Viable cells/ml[a]	Unisexual reproduction progeny viability			Bisexual reproduction progeny viability			Total progeny
		XL280α (%)	*spo11*Δ (%)	*ubc5*Δ (%)	JEC21α x JEC20**a** (%)	α *spo11*Δ x *spo11*Δ **a** (%)	α *ubc5*Δ x *ubc5*Δ **a** (%)	
0	5.3×10^8	23 (76%)	1 (3%)	2 (6%)	25 (83%)	2 (6%)	4 (13%)	30
1	5.4×10^8	20 (66%)	0 (0%)	1 (3%)	28 (93%)	3 (10%)	3 (10%)	30
3	5.1×10^8	21 (70%)	0 (0%)	3 (10%)	26 (86%)	0 (0%)	4 (13%)	30
5	4.8×10^8	22 (73%)	2 (6%)	2 (6%)	24 (80%)	1 (3%)	5 (16%)	30
10	4.4×10^8	18 (60%)	4 (13%)	0 (0%)	22 (73%)	5 (16%)	2 (6%)	30
20	3.1×10^8	16 (53%)	7 (23%)	2 (6%)	20 (66%)	8 (26%)	3 (10%)	30

Cultures were incubated on V8 medium for six days for unisexual reproduction and four days for bisexual reproduction. Plates were irradiated at the designated dose and incubated in the dark for two days to allow spore production. A total of 30 spores were isolated from each culture.

[a]: Viable CFU determined from vegetative growth on solid media independently for XL280α, *spo11*Δ, *ubc5*Δ, and JEC21α. The viable CFU for each strain at the same dose was similar with minor differences. Here we present the viability of XL280α as reference.

4.4 Discussion

We employed a classical genetic approach to identify genes that orchestrate unisexual reproduction in *C. neoformans*. The screen identified a number of genes that may be directly or indirectly implicated in the dimorphic switch during mating. Importantly, we successfully isolated five previously identified regulators, *CRG1*, *STE7*, *MAT2*, *ZNF2*, and *BWC2*, validating this approach. Our findings provide evidence to implicate *ZNF3*, *SPO11*, and *UBC5* in the control of hyphal development, meiosis, or sporulation during sexual differentiation. The severe defect in filamentation of the *znf3*Δ mutant provides evidence that Znf3 is a regulator of hyphal development during unisexual reproduction. The *znf3*Δ mutant phenotype is similar to that of *ste7*Δ and *mat2*Δ mutants and of other components of the pheromone pathway. In addition, RT-PCR analysis showed that the expression profiles of these mutants and *znf3*Δ followed a similar pattern during bisexual and unisexual reproduction. Hyphal development during bisexual reproduction in the *znf3*Δ mutant is also affected; however, the defect is less pronounced, and filamentation is mainly delayed rather than abolished. These defects are less severe than the defects observed in *ste7*Δ, *mat2*Δ, or *znf2*Δ α-**a** bilateral mutant sexual reproduction assays.

Regulation of pheromone expression is a key function of the components of the MAPK signaling cascade. Pheromone expression is dramatically

attenuated in *ste7*Δ and *mat2*Δ mutants, as shown here and in previous studies (Lin, Jackson et al. 2010). A striking finding was the inhibition of *MAT2* and pheromone expression in the *znf3*Δ mutant. Interestingly, we found that *MAT2* transcription increases during mating (Figure 20), and *znf3*Δ and *ste7*Δ mutations have a similar impact on the transcriptional control of *MAT2* and *MF*α*1* during bisexual reproduction (Figure 21B), indicating that they may be in the same or related pathways. Epistasis analysis suggests Znf3 does not function upstream or downstream of Mat2. The lower expression of *MAT2* could be attributable to the absence of pheromone in the *ste7*Δ and *znf3*Δ mutants. Pheromones activate the pathway that leads to expression of targets, including *MAT2*, whose transcription is regulated by itself, an unknown factor, or both. Based on these findings, we hypothesize that Znf3 imposes a mode of regulation on Mat2 via direct or indirect control of the pheromone through an independent signaling cascade that remains to be defined (Figure 27).

We found that *ZNF3* transcription levels are similar during vegetative and hyphal growth, and *ZNF3* may require activation through phosphorylation by the MAPK signaling cascade or via a different pathway. A recent study by Kruzel *et al*. showed that Mat2 is the pheromone response transcription factor, with a consensus binding motif present as the pheromone response element (PRE) in key mating genes (Kruzel, Giles et al. 2012). The defined PRE sequence lies

upstream of multiple genes (i.e. *MFα1*, *MFα2*, *MFα3*, *STE3α*, *STE12α*, *SXI1α*, and *RAM1*) and is recognized specifically by Mat2 (Kruzel, Giles et al. 2012). However, extensive study of the MAPK signaling cascade in *S. cerevisiae* revealed that the promoter regions of several PRE-containing genes bear additional *cis*-regulatory elements that are recognized by different transcription factors or other elements, conferring additional levels of control (Hwang-Shum, Hagen et al. 1991, Laloux, Jacobs et al. 1994, Madhani and Fink 1997). Different environmental cues may govern these additional transcription factors, likely through pheromone-independent signaling cascades. It is possible that similar networks may contribute to PRE activation in *C. neoformans*. Znf3 may regulate the pheromone genes through another cis-regulatory element induced by a different environmental cue or an independent pathway that confers developmental specificity (Figure 27).

The identification and characterization of the targets of this novel factor will be essential to elucidate its molecular functions during mating. Surprisingly, deletion of *ZNF3* increased the expression of transposons during unisexual reproduction. Combined with the fact that a similar transcriptional profile is observed in RNAi mutant strains, this leads to the conclusion that Znf3 may play a role in sex-induced silencing (SIS) and could be required to defend the genome against transposon mobilization. It is of interest that this protein appears to play a dualistic role during sex. It acts as an activator of pheromone expression and,

simultaneously, as an inhibitor of transposon transcription (Figure 26). A possible explanation is that Znf3 plays a pivotal role in transposon silencing and is a molecular link between SIS and sexual development. Future studies will focus on the mechanism of transposon silencing by Znf3 and explore the links with sexual development.

Sexual reproduction has several stages that are each precisely regulated. Meiosis and sporulation are the ultimate steps. Our screen revealed two genes implicated in meiosis and/or sporulation. The first, *UBC5*, has a homolog in *S. cerevisiae* that is involved in ubiquitin-targeted degradation (Seufert and Jentsch 1990). The second, *SPO11*, is considered a hallmark meiotic gene (Seufert and Jentsch 1990, Schurko and Logsdon 2008). We found that deletion of either gene in *C. neoformans* results in barren basidia or basidia with only one or two spores with a very low germination rate. Deletion of *DMC1*, a previously identified meiosis-specific factor, also results in a severe sporulation defect, similar to the *spo11*Δ mutant (Lin, Hull et al. 2005). We found that X-irradiation-induced DSBs partially restored the WT phenotype and enhanced the germination rate of the *spo11*Δ progeny. Along with the observation that Spo11 shares homology with the *S. cerevisiae* ortholog, we suggest that *Cryptococcus* Spo11 is required for initiating meiosis by catalyzing DSBs and inducing meiotic homologous recombination during bisexual and unisexual development.

Deletion of *UBC5* shares a similar phenotype with the *spo11*Δ mutant, namely a severe sporulation defect and largely inviable meiotic progeny. This result is consistent with presumptive roles in meiosis or sporulation. In addition, *Cryptococcus* Ubc5 exhibits significant homology and identity throughout the fungal kingdom, possibly reflecting a conserved role. The *S. cerevisiae* Ubc5 homolog has been implicated in sporulation; however, the precise role(s) remains unknown. Ubiquitin-conjugating enzymes are associated with structurally similar but distinct recognition subunits that direct these enzymes to proteins that are targeted for degradation. Ubc5 is associated with the proteasome in *S. cerevisiae*, along with multiple E2 enzymes, and there are likely to be multiple physiological substrates, only some of which are involved in sporulation. Based on the highly conserved ubiquitin-conjugating enzyme E2 catalytic domain in *Cryptococcus*, we hypothesize that the role of Ubc5 involves degradation of multiple as yet unknown targets, and depletion of some of these targets is required for meiotic entry or sporulation.

Hallmarks of sexually reproductive species are the presence of recombinant progeny in the population and a group of highly conserved meiotic genes termed the “meiotic toolkit” in their genomes (Schurko and Logsdon 2008). These genes represent the best markers for the capacity for a complete sexual cycle in a fungal species. Meiosis toolkit genes are present in *C. neoformans* and both our study and others have shown that two of these, *SPO11* and *DMC1*, are

required for meiosis and sporulation during bisexual and unisexual reproduction (Lin, Hull et al. 2005). However the majority of meiotic gene candidates remain uncharacterized. *S. cerevisiae* represents an extensively studied meiotic system. Hop1 secures the synapses between homologous chromosome by binding DNA at sites where DSB will be induced by the Spo11 endonuclease (Keeney, Giroux et al. 1997, Wan, de los Santos et al. 2004). Dmc1 is required for DNA DSB repair and catalyzes strand invasion and the formation of Holiday junctions that are stabilized by the Mnd1/Hop2 complex (Shinohara, Gasior et al. 1997, Henry, Camahort et al. 2006). Finally, Msh4 forms a dimer with Msh5 and facilitates crossing over, while Rec8 mediates cohesion between sister chromatids (Buonomo, Clyne et al. 2000, Novak, Ross-Macdonald et al. 2001). Although the sequence of meiotic events is highly conserved in sexual species, the system exhibits exceptional plasticity in the fungal kingdom. For example, no true meiosis has been observed in *C. albicans*, which has a parasexual cycle, where random, concerted, chromosome loss occurs following mating, despite the presence of many meiosis-specific genes (Sherwood and Bennett 2009). On the other hand, sporulation in *C. lusitaniae* is relatively efficient and involves Spo11-induced meiotic recombination, although it is missing multiple meiotic genes (Reedy, Floyd et al. 2009). Moreover, in *U. maydis*, a basidiomycete, sexual development is efficient; however, it lacks key regulators of meiosis (Dmc1, Hop1, Hop2, and Mnd1) and has incorporated novel factors like homologs of *H.*

sapiens BRCA2 and *DSS1* (Holloman, Schirawski et al. 2008). In C*. neoformans*, we have found that Spo11 is required for meiosis, evidently for the induction of DSBs; however, taking into account the mechanistic and evolutionary plasticity of meiotic events in fungal species, the survey of the genome for the repertoire of meiotic-specific factors alone may well miss elements that require genetic approaches such as those applied here to unveil. Future research should focus on the genetic and evolutionary analysis of these and other unidentified genes to explore a possible conserved mechanism or a diverse rewiring network that controls meiosis and sporulation during *C. neoformans* unisexual reproduction.

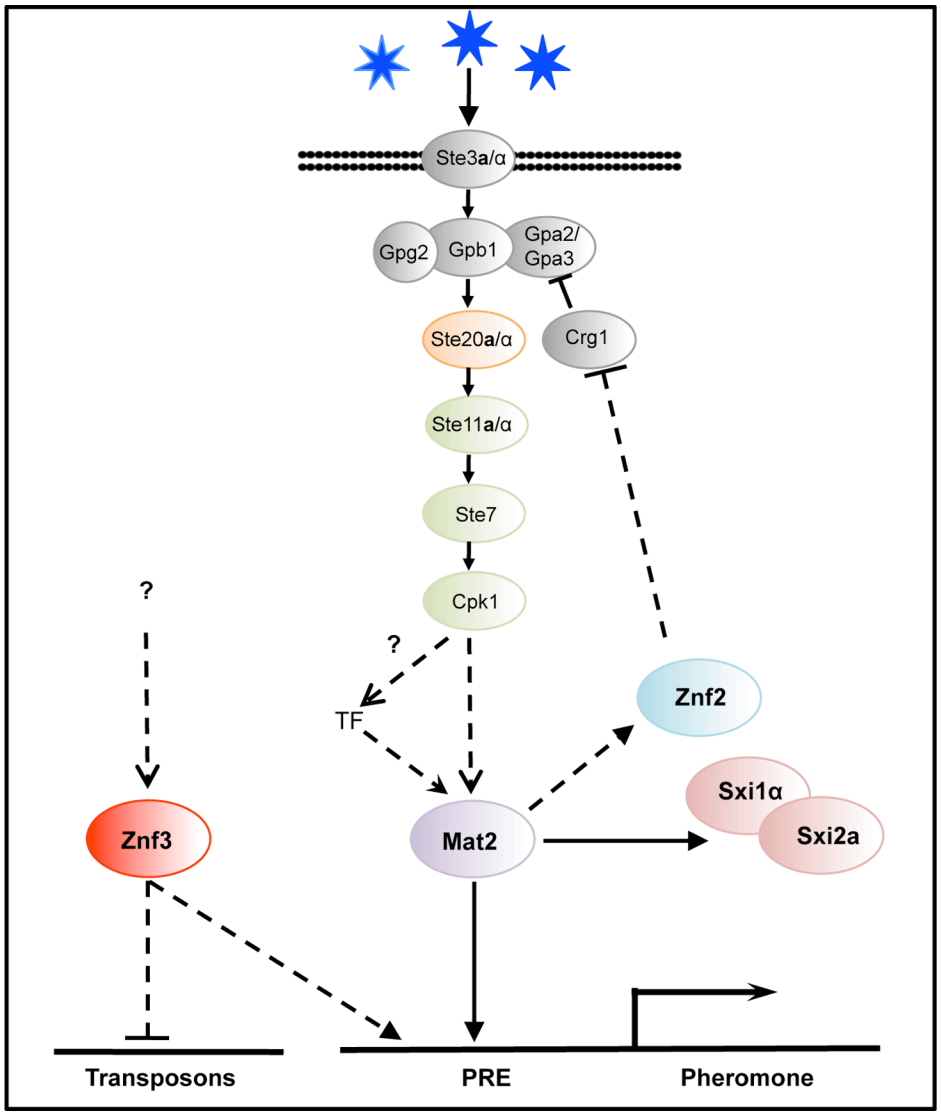

Figure 27. Znf3 regulates pheromone expressions activating the pheromone signaling cascade and promotes transposon silencing. Mat2 is the transcription factor target of the pheromone signaling cascade that binds to the pheromone response element (PRE) in the promoter of the pheromone gene. Znf3 is required for induced levels of the pheromone and transposon silencing. Znf3 may bind additional *cis*-regulatory elements to inhibit transposon mobilization during sexual development or function by binding to RNA targets.

Chapter 5. RNAi Loss in *C. gattii* Reveals Novel Regulators of Silencing in *C. neoformans*

5.1 Introduction

RNA interference (RNAi) is a highly conserved mechanism among eukaryotes that facilitates homology-dependent gene silencing. This transcriptional regulation strategy was initially observed in *Caenorhabditis elegans* where exogenously introduced double-stranded RNA (dsRNA) triggers silencing of the gene complementary to the sequence of dsRNA (Fire, Xu et al. 1998). Since its discovery in *C. elegans*, numerous species of plants, animals, fungi, and protozoans have been found to employ similar strategies to either protect their genome against foreign DNA or to orchestrate gene expression and regulate diverse cellular, developmental, and physiological processes (Kim, Han et al. 2009, Moazed 2009, Lye, Owens et al. 2010, Chang, Zhang et al. 2012).

Homology-dependent gene silencing (HDGS) is induced by the presence of multiple copies of a gene or a sequence. Repetitive sequences are usually found in mobile genetic elements and previous studies found an association between RNAi and transposable elements, which are ubiquitous in eukaryotic organisms. Transposon activation and movement impairs genome stability and increases the mutational burden of the host. Therefore eukaryotes employ different strategies to inhibit and limit their expansion. *Arabidopsis thaliana*, *Drosophila melanogaster*, *Saccharomyces castellii*, *Neurospora crassa*, and *C.*

elegans are a few species that utilize RNAi strategies to control and inhibit transposon expression (Napoli, Lemieux et al. 1990, Volpe, Kidner et al. 2002, Calo, Billmyre et al. 2013, Feretzaki and Heitman 2013, Nicolas, Torres-Martinez et al. 2013).

A well-characterized RNAi strategy in fungi is quelling in *Neurospora crassa*. Quelling is a transgene-induced gene silencing phenomena that post-transcriptionally inactivates duplicated sequences in the genome during vegetative growth (Romano and Macino 1992). Meiotic silencing by unpaired DNA (MSUD) is an alternative RNAi mechanism that silences unpaired DNA during the sexual cycle in *Neurospora crassa* (Aramayo and Metzenberg 1996). The paradigmatic studies of RNAi in *Neurospora crassa* revealed that both mechanisms require the highly conserved components of the RNAi pathway, including the RNA-dependent RNA polymerase (RdRp), Argonaute, and Dicer-like proteins (Aramayo and Metzenberg 1996, Fire, Xu et al. 1998, Kim, Han et al. 2009, Ghildiyal, Xu et al. 2010). During silencing an RdRp generates dsRNA from aberrant single-stranded RNAs (asRNAs) transcribed from highly repetitive regions of the genome. The dsRNA is processed into double-stranded small interfering RNAs (siRNAs) of 21-28 nt by an RNAse III-like Dicer. The siRNAs are loaded onto the RNA-induced silencing complex (RISC), a nuclease complex containing the Argonaute proteins that either have intrinsic nuclease activity or an additional nuclease participates. Argonaute removes the passenger strand of

siRNA and the single-strand siRNA-RISC targets complementary mRNA for degradation. These components are highly conserved in the fungal kingdom and their presence in the genome usually is indicative of an ancestral RNAi pathway. Interestingly, there are species that although they are missing key components of the pathway, they have functional RNAi mechanisms that employ non-canonical proteins to silence their targets (Nicolas, Torres-Martinez et al. 2013). On the other hand, in some cases RNAi components are found to have RNAi-independent functions, such as cell cycle progression, indicating that their role may be diverse inside the cell (Noma, Sugiyama et al. 2004). Therefore the pathway exhibits considerable plasticity and although RNAi is conserved, different species may employ canonical and non-canonical components to induce short RNAs (sRNAs) and regulate silencing.

Previous studies found the human fungal pathogen *Cryptococcus neoformans* employs an RNAi-related pathway to inhibit transposon expression. *C. neoformans* causes severe infections of the central nervous system in immunocompromised individuals. It has a bipolar mating system and it grows as a budding yeast in the environment. Under nutrient limiting conditions opposite mating type cells secrete pheromones that induce a dimorphic transition to hyphal development (Kwon-Chung 1976). The hyphae produce basidia where meiosis and sporulation occur to produce four chains of basidiospores, the recombinant progeny. *C. neoformans* can also undergo unisexual reproduction

where cells of one mating type either fuse or undergo endoreplication, switch to hyphal growth, and produce recombinant haploid meiotic progeny (Lin, Hull et al. 2005, Feretzaki and Heitman 2013). In previous studies, Wang et al. showed that the insertion of a tandem multicopy transgene triggered a homology-dependent gene silencing mechanism during sexual development named sex-induced silencing (SIS) (Wang, Hsueh et al. 2010). They also found that silencing of the transgene also occurs during vegetative growth, named mitotic-induced silencing (MIS), but at relatively low frequency (~3%) in mitotic compared to meiotic progeny (>50%). Further analysis showed that SIS and MIS require the presence of the RNAi components Rdp1 (RNA-depended RNA polymerase), Ago1 (Argonaute), and Dcr1/2 (dicer-like proteins) (Wang, Hsueh et al. 2010). SIS and MIS function to inhibit transposon movement and thus serve as a genome defense mechanism during meiosis and mitosis. The initial observation of transposon silencing during sexual development was made in the highly virulent *C. neoformans* var. *grubii* lineage (serotype A). Later studies found that transgene-related SIS also occurs in the *C. neoformans* var. *neoformans* lineage (serotype D) and the RNAi components are required for transposon silencing during bisexual and unisexual development (Wang, Darwiche et al. 2013).

The RNAi pathway is highly conserved in the *Cryptococcus* lineages (serotypes A and D) and the sibling species *C. gattii*, which usually infects healthy individuals. *C. gattii* isolates are divided into four major genotypes: VGI,

VGII, VGIII, and VGIV. Whole genome sequencing revealed that the VGII strain R265 is missing both of the Argonaute genes and the *RDP1* and *DCR1* genes are both pseudogenes [B. Billmyre and J. Heitman, unpublished results (Wang, Hsueh et al. 2010, D'Souza, Kronstad et al. 2011)]. R265 is a representative isolate of the major genotype responsible for the ongoing outbreak on Vancouver Island and for its expansion into the Pacific Northwest of the United States (Kidd, Hagen et al. 2004, Byrnes, Bildfell et al. 2009, Byrnes, Li et al. 2010). This strain is highly virulent and loss of RNAi may be associated with higher pathogenicity in the host. Previous studies found that R265 may be the progeny of two unknown closely related parents generated through unisexual reproduction (Fraser, Subaran et al. 2003, Fraser, Giles et al. 2005). It is possible that the two VGII parents were missing a functional RNAi mechanism during unisexual reproduction and transposon activation generated robust genetic variation in the progeny that resulted in hypervirulent strains.

The loss of RNAi components in the VGII genotype can be used as a tool to identify novel elements of the pathway. We surveyed the genomes of the R265 (*C. gattii* VGII), WM276 (*C. gattii* VGI), and H99 (serotype A) strains and we found 14 genes missing from R265, including the canonical components of the RNAi pathway (Blake Billmyre, unpublished data). One of these, *ZNF3*, was previously identified as a regulator of hyphal development during unisexual and bisexual reproduction (Feretzaki and Heitman 2013). Deletion of the gene inhibits

hyphal development and pheromone transcription, while retrotransposons are highly expressed during mating in serotype A. In this study we found that Znf3 has a novel zinc finger motif, C2H2_JAZ, which usually binds dsRNAs or DNA/RNA hybrids. In addition, we found that Znf3 is required for transgene-induced silencing during mating (SIS) and vegetative growth (MIS). Microarray expression analysis showed that Znf3 is required for transposon suppression during sexual development in serotype A and shares a similar genome-wide expression profile with Rdp1. Surprisingly, Znf3, which has two nuclear localization signals (NLS), localizes in the P-bodies during mating and vegetative growth, similar to Ago1 and Dcr1/2. Processing bodies are distinct foci in the cells where mRNA decay and RNAi mechanisms occur. Our results suggest that Znf3 participates directly in transgene and transposon silencing and plays a major role in the RNAi pathway. Further studies will establish the functions of Znf3 in the pathway and may reveal a novel mode of control of RNAi in *C. neoformans*.

5.2 Materials and Methods

5.2.1 Strains and Media

The strains and plasmids used in this study are listed in Table 10. The strains were maintained in glycerol stocks at –80^{o}C and grown on rich YPD media at 30^{o}C (Yeast extract Peptone Dextrose). Strains with selectable markers were grown on YPD containing nourseothricin (NAT) and G418 (NEO). Uracil auxotrophic isolates were grown on SD medium lacking uracil and tested on synthetic medium containing 5-FOA (1 gr/l). Mating assays were performed on 5% V8 juice agar medium (pH=5 for serotype A or pH=7 for serotype D) or on MS (Murashige and Skoog) medium minus sucrose (Sigma-Aldrich). The mating cultures were incubated in the dark at room temperature for 1 week.

Table 10. Strains and plasmids used in Chapter 5.

Strain	Genotype	Source/Reference
Serotype A		
H99α	*MAT*α	(Perfect, Ketabchi et al. 1993)
YL99**a**	*MAT***a**	(Semighini, Averette et al. 2011)
JF289**a**	*MAT***a** *sxi2***a**Δ::*NAT ura5 SXI2***a**::URA5*	(Hsueh, Fraser et al. 2008)
YPH348	*MAT***a** *sxi2***a**Δ::*NAT ura5 SXI2***a**::URA5 rdp1*Δ*::NEO*	(Wang, Hsueh et al. 2010)
YPH351	*MAT*α *rdp1*Δ*::NEO*	(Wang, Hsueh et al. 2010)
YPH738	*MAT***a** *sxi2***a**Δ::*NAT ura5 SXI2***a**::URA5 ago1*Δ*::NEO*	(Wang, Hsueh et al. 2010)
YSB299	*MAT*α *ago1*Δ*::NEO*	(Wang, Hsueh et al. 2010)
MF62	*MAT***a** *znf3*Δ*::NEO*	This study
MF65	*MAT*α *znf3*Δ*::NEO*	This study
MF188	*MAT***a** *sxi2***a**Δ::*NAT ura5 SXI2***a**::URA5 znf3*Δ*::NEO*	This study
MF140	*MAT*α P_{GPD1}*-mCherry*::*ZNF3::NEO*	This study
MF153	*MAT*α P_{GPD1}*-mCherry*::*ZNF3::NEO*	This study
MF156	*MAT*α P_{GPD1}*-mCherry*::*ZNF3::NEO GFP::DCP1::NAT*	This study
MF162	*MAT*α P_{GPD1}*-mCherry*::*ZNF3::NEO GFP::NOP1::NAT*	This study
Serotype D		
XL280	*MAT*α	(Lin, Huang et al. 2006)
XW73	*MAT*α *ura5 SXI2***a**::*URA5*	(Wang, Darwiche et al. 2013)
MF119	*MAT*α *ura5 SXI2***a**::*URA5 znf3*Δ*::NEO*	This study
MF121	*MAT*α *ura5 znf3*Δ*::NEO*	(Feretzaki and Heitman 2013)
Plasmids		
pXW11	*DCP1 GFP NAT* Amp^R	(Wang, Hsueh et al. 2010)
pSL04	*NOP1 GFP NAT* Amp^R	(Lee and Heitman 2012)
pMF81	P_{GPD1}*-mCherry*::*ZNF3::NEO*	This study

5.2.2 Genetic Crosses and Spore Dissection

To visualize and isolate spores, strains of interest were co-cultured on V8 for 2 weeks at room temperature in the dark. Basidiospores from the edges of the colonies were randomly isolated using a microdissection microscope equipped

with a 25-μm microneedle (Cora Styles Needles 'N Blocks, Dissection Needle Kit) as previously described (Hsueh, Idnurm et al. 2006). Following germination the colonies were tested on YPD, YPD + NAT or NEO, SD-ura, and 5-FOA and genomic DNA was isolated using a CTAB protocol as previously described (Pitkin, Panaccione et al. 1996). The presence of the *SXI2***a**-*URA5* transgene in the progeny was confirmed by PCR using the primer pair JOHE16835/JOHE16836.

5.2.3 Gene Disruption

The gene of interest was disrupted using a standard overlap PCR approach described previously (Feretzaki and Heitman 2013). Briefly, the 5' and 3' flanking region of *ZNF3* was amplified from H99α genomic DNA, while the selectable markers *NAT* and *NEO* were amplified from pAI3 and pJAF1, respectively. The flanking sequences and the selectable markers generated the full-length deletion cassette in an overlap PCR reaction. The deletion cassettes were introduced into H99α and JF289**a** genome by biolistic transformation (Davidson, Cruz et al. 2000). Gene replacement via homologous recombination was confirmed with PCR and Southern hybridization. The primers used to generate the deletion mutants are listed in Table 11.

Table 11. Oligonucleotides used in this study.

Primer	Sequence (5' to 3')	Comment
M13F	GTAAAACGACGGCCAG	universal oligo
M13R	CAGGAAACAGCTATGAC	universal oligo
JOHE16835	TTGGGTCAACTCTAATAAGGT	*SXI2***a**-*URA5* transgene screening
JOHE16836	TCTATGGCGAACGTGCTCATT	*SXI2***a**-*URA5* transgene screening
JOHE20738	CTGATTTCGCCTTCTTCCTTGT	*ZNF3* disruption (D)
JOHE20745	AGCATCTAGGACTAAAAGTCAGC	*ZNF3* disruption (D)
JOHE20800	CTGGCCGTCGTTTTACGGGGTTAGTAGCTGGCTGTTT	*ZNF3* disruption (D)
JOHE20801	GTCATAGCTGTTTCCTGGTGGGGACAGCAATTCATATAAG	*ZNF3* disruption (D)
JOHE20739	AGCTGCATTTGATGGATGGAAC	*znf3* screening (D)
JOHE20740	TGAGCTTCCTATCTTACGTCTC	*znf3* screening (D)
JOHE20741	TTGCTAGAAGTCAAGTCGTCCT	*znf3* screening (D)
JOHE20742	AAGACGTCGACTTTGAGCTTCCT	*znf3* screening (D)
JOHE20743	CTCACTGCTGAAGGGTAGATCTTA	*znf3* screening (D)
JOHE20744	AGGAGTTCAAGCTTCAATGGTG	*znf3* screening (D)
JOHE21985	TCTGAGTTTGGCGTGTCTGTCACT	*znf3* screening (A)
JOHE21986	TCTTCATAAGTGGCAGCGTGGACT	*znf3* screening (A)
JOHE24058	AAACAGAAGCAGCGTGATAAGGCGG	*ZNF3* deletion (A)
JOHE24059	CTGGCCGTCGTTTTACTAGTAGCTGGCTGTTTCTAAAGATG	*ZNF3* deletion (A)
JOHE24060	GTCATAGCTGTTTCCTGGGGGCAACAATCCATATAGCA	*ZNF3* deletion (A)
JOHE24061	GAGAGAGTAGTAGTCGGGTTGGGTGGC	*ZNF3* deletion (A)
JOHE38286	ACGACCAAGCATCCAACCTAG	Znf3-mCherry (A)
JOHE38287	CTCGCCCTTGCTCACCATCCAGCCACCAGTGTCTCC	Znf3-mCherry (A)
JOHE38288	GGAGACACTGGTGGCTGG ATGGTGAGCAAGGGCGAG	Znf3-mCherry (A)
JOHE38318	CTCCTCCTATCTTTTTTACCAAGCTTGGTACCGAGCTC	Znf3-mCherry (A)
JOHE38319	GAGCTCGGTACCAAGCTTGGTAAAAAAGATAGGAGGAG	Znf3-mCherry (A)
JOHE38727	GGAGTTCATGCGCTTCAAGGTG	Znf3-mCherry (A)
JOHE38728	TTGTAGATGAACTCGCCGTCCTG	Znf3-mCherry (A)
JOHE38790	ATTGTATCTAGATATGCTCACAGCCTTCTTCGGCTA	Znf3-mCherry (A)
JOHE38791	GCGTTAATTAAGAGAGAGTAGTAGTCGGGTTGGGT	Znf3-mCherry (A)
JOHE38792	GGCTCTTCTTTGACAGGAGTTTCG	Znf3-mCherry (A)

5.2.4 Protein Localization

To determine Znf3 cellular localization, we fused the mCherry protein to the N-terminus of Znf3 under the control of the constitutively active promoter of *GPD1* expressed from a plasmid. The genomic sequence of *ZNF3* was amplified from H99α genomic DNA using the primer pairs JOHE37890/JOHE37891 and

cloned into the plasmid pLKB49 (Kozubowski, Aboobakar et al. 2011) digested with XbaI and PacI. Plasmid pMF81 was introduced into the H99α and JF289**a** strains by biolistic transformation and the transformants were screened by PCR and fluorescence microscopy. Stable transformants of *mCherry*::*ZNF3* were also transformed with pXW11 (*DCP1::GFP*) and pSL04 (*NOP1::GFP*) to visualize the P-bodies and the nucleus, respectively.

To visualize mCherry-Znf3 along with Dcp1-GFP and Nop1-GFP the strains of interest were grown on YPD to determine localization during vegetative growth or mixed with the opposite mating type strain on V8 medium for 24 hrs to visualize the proteins during mating. The cells were observed with a Zeiss Axio Imager widefield fluorescence microscope and analyzed using MetaMorph Premier at the Light Microscopy Core Facility at Duke University.

5.2.5 Microarray and Data Analysis

For vegetative growth the cells were grown in 5 ml liquid YPD overnight at 30^{o}C. The following day the cells were harvested, washed, frozen in liquid nitrogen, lyophilized, and kept at -80^{o}C until use. To isolate RNA from mating assays, the desired α and **a** strains were grown in YPD liquid, washed with sterile water, mixed in equal amounts in eppendorf tubes, and a 1 ml suspension was spotted on V8 juice agar pH=5 and incubated in the dark at room temperature for 24 hrs. The next day the mating cultures were harvested, washed with sterile

water, frozen, lyophilized, and stored at -80^{o}C. Total RNA was extracted using the RiboPure^{TM}-Yeast Kit (Ambion) following the manufacturer's instructions (Life Technologies #AM1926). Denaturing agarose gel electrophoresis and NanoDrop were used to assess quality and concentration of the RNA samples. The RNA was amplified using the Ambion® MessageAmp™ Premier RNA Amplification kit following the manufacturer's instructions. cDNA was synthesized using AffinityScript reverse transcriptase (Stratagene), Cy3/Cy5 labeled, and hybridized to a *C. neoformans* microarray slide (*Cryptococcus* Community Microarray Consortium Washington University, St. Louis, MO). Labeling and hybridization were conducted in the DNA Microarray Core Facility at Duke University. The slides were washed, scanned with a GenePix 4000B scanner (Axon Instruments), and processed with GenePix Pro (version 4.0). All microarrays were conducted in triplicate. GeneSpring software was used for statistical analysis employing Lowess normalization, reliable gene filtering, ANOVA analysis (significance $p<0.05$), and Microsoft Excel.

5.3 Results

5.3.1 Znf3 in Closely Related Species

In previous studies we employed an *Agrobacterium tumefaciens* mediated transformation approach to generate 6,100 insertional mutants (Feretzaki and Heitman 2013). A genetic screen identified a mutant with severe defects in hyphal development during bisexual and unisexual reproduction. The mutant had an insertion in the coding region of a gene named *ZNF3* (Feretzaki and Heitman 2013). Deletion of the gene blocks hyphal development and impairs pheromone expression during mating. However, it does not play a direct role in the pheromone-signaling cascade. Surprisingly, microarray expression analysis revealed that deletion of Znf3 increased transposon and transposon-related gene expression during bisexual reproduction (Feretzaki and Heitman 2013). Our results indicate that Znf3 mediates transposon repression and it may play a role in sex-induced silencing (SIS).

ZNF3 lies on chromosome 10 in serotype D and is an exceptionally large gene of ~5,100 bp. The encoded protein of 1,515 aa contains three zinc finger domains, two NLS signals predicted nuclear localization signals (NLS), and a conserved coiled coil region, which is usually involved in protein-protein interactions. In addition, we found that Znf3 also has a putative ribonuclease conserved domain indicating that it may be involved in cleavage of RNA. The C2H2 motif of the zinc finger domains is highly conserved among proteins

associated with DNA binding and it is extremely common in both fungal and mammalian transcription factors. Interestingly, the first two zinc finger domains of Znf3 are surprisingly far apart, ~48 aa, while the last two are only 5 aa apart, which is the usual sequence size of the linker connecting the C2H2 zinc finger motifs in proteins (Iuchi 2001). Bioinformatics analysis of the protein sequence of Znf3 revealed that the first zinc finger belongs to a recently discovered group of nucleotide binding motifs called zf-C2H2_JAZ (Yang, May et al. 1999), while the other two belong to the canonical C2H2 DNA binding motif. The C2H2_JAZ zinc finger proteins are widespread in archea and eukaryotes and preferentially bind double-stranded RNA (dsRNA) or RNA/DNA hybrids rather than DNA alone. The C2H2_JAZ zinc finger motifs are encountered multiple times along a protein and they are connected with flexible but unusually long linkers (28–38 nt) (Yang, May et al. 1999). They were initially identified in embryonic mouse cell lines to regulate growth and G1 cell cycle arrest (Yang, May et al. 1999, Iuchi 2001, Yang, Wu et al. 2011). Further studies, revealed that p53 mediates the expression of C2H2_JAZ zinc finger proteins that bind dsRNA with great affinity, including siRNAs and miRNAs, and promote cell growth in tissue culture (Mendez Vidal, Prahl et al. 2006). Moreover, C2H2_JAZ binding to dsRNA is required for accurate cellular localization of the protein to the nucleus, and particularly to the nucleolus. Based on these findings we hypothesize that Znf3 may bind dsRNA or DNA/RNA hybrids instead of dsDNA.

To determine the functions of Znf3 in *C. neoformans* we employed homology-based approaches (standard nucleotide and protein blast analysis) to identify possible homologs in different species that would possibly have a known or conserved role in a pathway. We found that Znf3 was unique among the *Cryptococcus* lineages and it was missing even among the ancestral outgroup of *Cryptococcus* species including *Tremella mesenterica*, *Cryptococcus heveanensis*, and *Cryptococcus amylolentus*. Even more surprising was the absence of a *ZNF3* functional copy from R265, the major *C. gattii* VGII strain that is causing the Vancouver Island outbreak (Figure 28A). Protein and nucleotide sequence alignments between *Cryptococcus* lineages and species showed that, although *ZNF3* is conserved among serotype A and D and *C. gattii* genotypes VGI, VGIII, and VGIV, there was a deletion of ~4,300 bp in all VGII strains tested (Figure 28B). The remaining ~800 bp region does not contain any functional domains and likely is not expressed. Although most of the *ZNF3* domain is missing from R265, the genomic configuration of the region is highly conserved, including the identity and orientation of the neighboring genes. Previous studies found that the key RNAi components are either missing (Ago1 and Ago2) or they are represented by non-functional pseudogenes (Dcr1 and Rdp1) in R265, indicating that the VGII lineage of *C. gattii* may not have a functional RNAi pathway (Wang, Hsueh et al. 2010). The partial deletion of *ZNF3* in VGII strains

and the presence of a novel RNA-biding motif in the protein suggest that Znf3 may represent a novel component of the RNAi pathway.

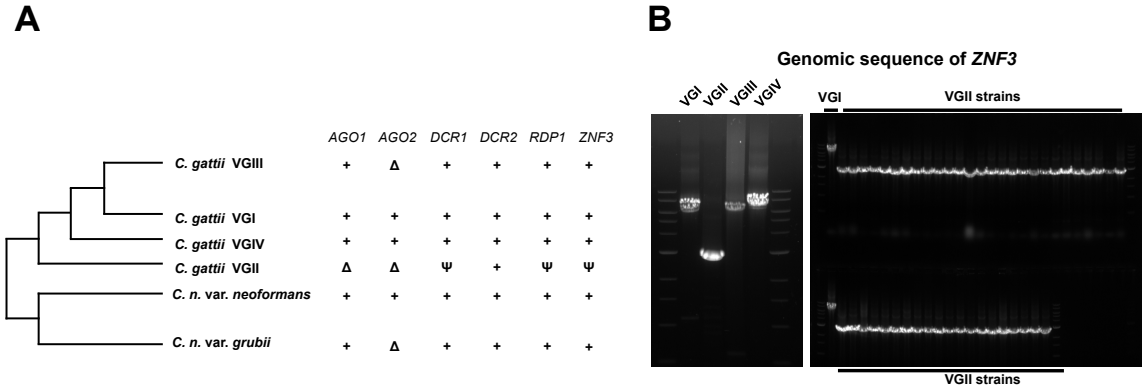

Figure 28. RNAi loss in *C. gattii* VGII strains. (**A**) A whole genome survey of *C. neoformans* var. *neoformans* var. *grubii* and *C. gattii* VGI, VGII, VGIII, and VGIV revealed that *ZNF3* Is highly conserved in *Cryptococcus* species except in *C. gattii* VGII strain R265 where it is present as a pseudogene missing ~80% of its sequence, including all of the predicted regulatory domains. (**B**) PCR screening of environmental and clinical isolates showed that the *ZNF3* deletion is present in all of the VGII strains tested.

5.3.2 Znf3 is Required for Mitotic- and Sex-Induced Silencing (MIS and SIS)

In previous studies, Wang et al. found that a tandem multicopy insertion of a *SXI2***a**-*URA5* transgene triggered silencing of the *URA5* gene during bisexual reproduction in the serotype A lineage (Wang, Hsueh et al. 2010). When F1 progeny were isolated from a cross between WT *MAT*α *URA5* (H99α) and *MAT***a** *SXI2***a**-*URA5* (JF289), 25% were found to be uracil-auxotrophic despite the fact

that all of them had intact copies of the *URA5* allele. Further analysis revealed that 50% of the progeny that inherited the *SXI2***a**-*URA5* transgene were uracil auxotrophic. Recent studies showed that the transgene induced silencing mechanism is activated efficiently during bisexual and unisexual reproduction (SIS) and also during vegetative growth (MIS), although less efficiently (Wang, Wang et al. 2012, Wang, Darwiche et al. 2013). The components of the RNAi pathway regulate SIS and MIS to defend the genome against transposons and foreign DNA.

Deletion of RNA-dependent RNA-polymerase Rdp1 abolished transgene induced silencing during SIS and MIS in both serotype A and D. To investigate the role of Znf3 in silencing during sexual reproduction, we generated *znf3*Δ mutants in the serotype A H99α background and in JF289**a** bearing the *SXI2***a**-*URA5* transgene. To determine the silencing efficiency of *znf3*Δ we performed unilateral (one parent is mutant) and bilateral (both parents are mutants) crosses on V8 medium. Although deletion of Znf3 severely impaired mating in serotype D (Feretzaki and Heitman 2013), hyphal development during bisexual reproduction was similar to WT in serotype A *znf3*Δ mutants, albeit slightly delayed. Among 50 progeny analyzed from *znf3*Δ unilateral matings, 29 inherited the transgene and only 1 (3.4%) isolate was ura^- indicating significantly reduced silencing efficiency compared to WT (51%) (Table 12). When *ZNF3* was deleted in both parents

none of the progeny that inherited the transgene was ura$^-$. The silencing efficiency of *znf3*Δ was compared to *rdp1*Δ and *ago1*Δ mutants during unilateral and bilateral crosses. SIS efficiency was not affected in *ago1*Δ mutant unilateral crosses; however, deletion of the gene in both parents abolished silencing efficiency during bilateral mating. On the other hand, *rdp1*Δ unilateral and bilateral matings generated 24 and 28 progeny, respectively that inherited the transgene and none of them was ura$^-$ (Table 12). These results indicate that Znf3 is required for silencing during mating and deletion of the gene causes a severe silencing defect, similar to *rdp1*Δ.

The sex-induced silencing phenomenon has also been observed in serotype D strains during unisexual and bisexual reproduction (Wang, Darwiche et al. 2013). The hyperfilamentous serotype D strain XL280α, which undergoes robust filamentation during unisexual reproduction, was transformed with 11 copies of the *SXI2***a**-*URA5* transgene. Previous studies showed that the transgenes successfully triggered silencing of the *URA5* gene during unisexual and bisexual reproduction, and vegetative growth (Wang, Darwiche et al. 2013). The components of the RNAi pathway are also required for SIS during unisexual and bisexual reproduction and play a major role during MIS in both serotype A and D. Znf3 is required for hyphal development during mating in serotype D, and therefore we were not able to test its role in silencing during unisexual

reproduction. However, deletion of *ZNF3* in the XL280α *SXI2***a**-*URA5* strain (XW73) severely impaired the efficiency of silencing during vegetative growth (Table 12). The level of transgene-induced mitotic silencing was also decreased in *rdp1*Δ and *ago1*Δ mutants. Similar results were observed in both serotype A and D. Thus, although we were not able to determine the role of Znf3 in silencing during unisexual reproduction, we found that it mediates mitotically induced silencing during vegetative growth in both serotypes, similar to known RNAi components. In conclusion, we found that Znf3 is required for silencing during SIS and MIS and deletion of the gene generates a phenotype similar to *rdp1*Δ, which is the major regulator of an RNAi pathway that initiates the formation of dsRNAs to induce silencing. These results suggest that Znf3 is a novel regulator of the RNAi pathway that may bind dsRNA, either to stabilize the message or recruit other components of the RNAi pathway to the site of silencing (P-bodies).

Table 12. Znf3 is required for SIS and MIS.

Sex-induced silencing progeny							
	a × α	**a** × α *znf3*Δ	**a** *znf3*Δ × α *znf3*Δ	**a** × α *rdp1*Δ	**a** *rdp1*Δ × α *rdp1*Δ	**a** × α *ago1*Δ	**a** *ago1*Δ × α *ago1*Δ
Total progeny	25	29	27	24	28	28	24
Ura^+ progeny	10	28	27	23	28	20	24
ura^- progeny	15	1	0	1	0	8	0
Silencing efficiency	60%	3.4%	0%	4.1%	0%	28%	0%

Mitotic-induced silencing progeny				
	a	**a** *znf3*Δ	**a** *rdp1*Δ	**a** *ago1*Δ
Silencing frequency	$\sim 5 \times 10^{-4}$	$< 2 \times 10^{-8}$	$< 2 \times 10^{-8}$	$< 2 \times 10^{-8}$

All the progeny indicated contained the *SXI2***a**::*URA5* transgene.

5.3.3 Znf3 is Required for Transposon Suppression

In a previous study we found that deletion of Znf3 in serotype D activates transposon expression (Feretzaki and Heitman 2013) and here we showed that it is required for SIS and MIS. Recent studies showed that transposable element expression increases during the sexual cycle and the components of the RNAi pathway maintain genome integrity through an efficient transposon silencing mechanism (Wang, Hsueh et al. 2010). Deletion of *RDP1* results in centromeric and telomeric retrotransposon overexpression during sexual development in serotype A. To investigate the role of Znf3 in transposon silencing in serotype A we performed a comparative transcriptome analysis of *znf3*Δ and *rdp1*Δ mutants during sexual development and vegetative growth. Bilateral matings of *znf3*Δ and *rdp1*Δ mutants were incubated on V8 for 24 hrs, along with the WT. RNA was

isolated from the mating cultures, transcribed to cDNA, and hybridized to a *C. neoformans* microarray.

A genome-wide expression analysis revealed that the majority of genes were upregulated in the *znf3*Δ mutant during sexual development indicating that Znf3 has a repressive role during sexual development. The few downregulated genes were involved in hypoxia, oxidation, ion channels, sugar transport, and possibly sporulation. During *znf3*Δ sexual development more than 80 independent microarray tags exhibited a twofold increase in expression compared with the WT. Further analysis revealed that the majority of these tags correspond to sequences from hypothetical proteins or they aligned to intergenic regions of the *C. neoformans* H99 genome. Alignment to the transposon database showed that almost all of the intergenic probes that were upregulated in *znf3*Δ mutants correspond to retrotransposon sequences found in multiple sites in the genome (Table 13). We found that these retrotransposons have long terminal repeats (LTR) and reside in the centromeric and telomeric regions of the chromosomes. In addition, most of the upregulated hypothetical proteins in *znf3*Δ x *znf3*Δ crosses were found to be RNA and DNA helicases, RNA-dependent DNA polymerases, and other transposon-related proteins (Table 13). During vegetative growth fewer genes were upregulated in *znf3*Δ mutants; however, the genes that exhibited differential expression were also involved in transposon

expression or activation. As was observed previously, the elements Tcn1, Tcn2, and Tcn3 were overexpressed in *znf3*Δ × *znf3*Δ crosses, while their expression was diminished during *znf3*Δ vegetative growth but remained significantly higher than the WT.

The retrotransposons located in centromeric regions of the chromosomes were also highly induced in *rdp1*Δ × *rdp1*Δ crosses and during *rdp1*Δ vegetative growth. The similar mode of control on transposon expression prompted us to compare the genome-wide transcriptional profiles of *rdp1*Δ and *znf3*Δ mutants during sexual development. As expected, the whole genome expression profiles between the two mutants were highly similar (Figure 29). A closer examination revealed that the genes with a 5-fold to 15-fold increase in expression were the same in *rdp1*Δ and *znf3*Δ mutants during both conditions. In conclusion, we found that Znf3 regulates transposon expression during sexual development and vegetative growth in serotype A. As previously observed, we provided further evidence to forge the link between the RNAi components and transposon repression through a genome-wide expression analysis of *rdp1*Δ and *znf3*Δ mutants during sexual development. The highly correlated expression profile of upregulated genes suggests that Znf3 and Rdp1 have similar functions and may mediate retrotransposon silencing through the same RNAi pathway.

Table 13. Transposon overexpressed in *rdp1*Δ and *znf3*Δ mutants during sexual development.

ID tag	*rdp1*Δ × *rdp1*Δ/ a × α	*znf3*Δ × *znf3*Δ/ a × α	Comment
CNAG_01966	15.7	11.44	Tcn1
CNAG_06805	15.59	7.67	Hypothetical methyltransferase
CNAG_05266	14.21	9.174	Putative acetate transporter
CNAG_02244	13.96	8.932	Transposable element
CNAG_00948	13.32	10.7	Transposable element
1772.seq.161	12.19	8.264	Tcn1
1621.seq.152	11.05	6.577	Transposable element
CNAG_01967	10.31	6.721	Transposable element
180.m00139	10.16	6.888	Tcn2
1662.seq.118	9.321	5.597	Tcn1
1761.seq.055	9.213	5.415	Transposable element
CNAG_04421	8.795	6.132	Transposable element
CNAG_04426	8.702	7.056	Tcn1
CNAG_00946	7.735	4.692	Transposable element
1743.seq.172	7.713	5.209	Tcn1
CNAG_00958	7.663	4.896	Tcn1
1751.seq.040	7.351	6.056	Tcn1
CNAG_07042	7.31	4.952	RNA helicase
CNAG_00947	7.201	3.313	Tcn1
1672.seq.136	7.106	4.017	RNA-dependent DNA-polymerase
CNAG_06478	6.761	5.612	Transposable element
1621.seq.150	6.524	4.093	Tcn1
CNAG_06701	5.857	3.679	Transposable element
CNAG_00951	5.713	3.278	Tcn3
1641.seq.049	5.37	5.077	Tcn1
CNAG_02518	5.29	4.821	Transposable element
CNAG_02391	4.891	4.073	Transposable element
CNAG_02390	4.851	4.088	Transposable element
CNAG_02253	4.791	3.477	Tcn1
CNAG_06700	4.477	3.327	Transposable element
CNAG_02560	3.926	3.693	Transposable element
CNAG_02042	3.673	2.976	Transposable element
CNAG_06757	3.493	3.068	RNA helicase
CNAG_06863	3.419	2.911	Putative endonuclease
1742.seq.057	3.266	1.859	RNA-dependent DNA-polymerase
CNAG_01383	3.256	2.763	DNA helicase
CNAG_05212	3.231	2.664	Retrotransposon nucleoside protein
1702.seq.183	3.134	2.191	Tcn1

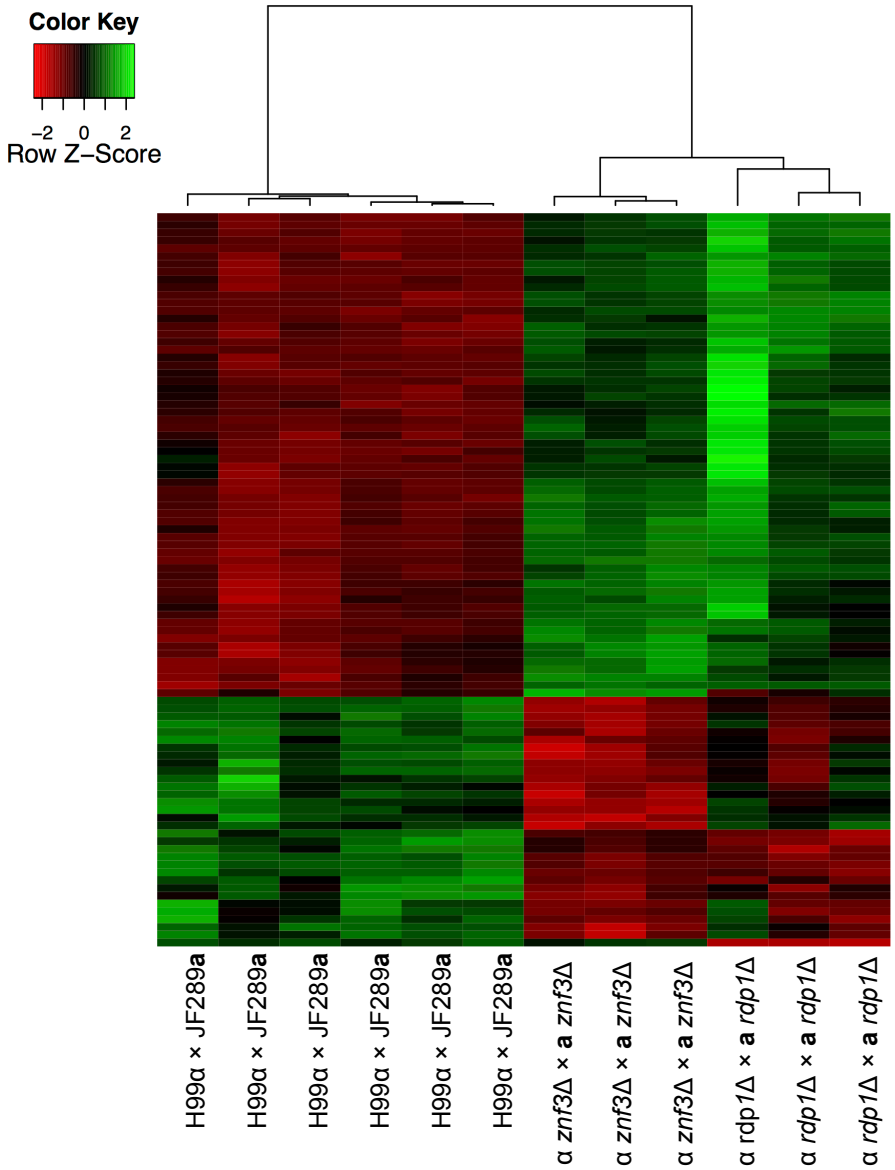

Figure 29. Genome-wide expression profile of *znf3*Δ mutant is similar to *rdp1*Δ. WT, *znf3*Δ, and *rdp1*Δ bilateral mutant cultures were incubated for 24 hrs following RNA isolation. Microarray data was obtained from three independent experiments and each column represents each experiment. The genes filtered by statistical significance ($p<0.05$) are represented by each row. Hierarchally clustered is presented in the heatmap as z-score normalized $\log_2$ expression

values. Green indicates an increase in expression while red represents a decrease.

5.3.4 Znf3 is Sexually Induced

In previous studies we found that, although it regulates sexual development, *ZNF3* expression remains stable during vegetative growth and mating in serotype D (Feretzaki and Heitman 2013). In addition, we know that the expression of the RNAi component mRNAs is also similar between mitotic growth and mating; however, their protein abundance was significantly higher during sexual development indicating that the RNAi components are translationally induced or stabilized by the sexual cycle (Wang, Hsueh et al. 2010). Based on this evidence we hypothesized that *ZNF3* expression would also remain the same between the two conditions in serotype A. RNA was isolated during mitotic growth and mating from WT and *znf3*Δ mutants and the abundance of the transcript was analyzed using quantitative RT-PCR. Unlike serotype D, we found that *ZNF3* expression in serotype A was significantly higher during mating compared to WT (Figure 30A). This was a surprising result given that the expression of the highly conserved allele of *ZNF3* in serotype D remains the same and similar to WT during both conditions. Moreover, Znf3 has a similar role with the RNAi components in SIS and MIS whose expression remains stable. This indicates that Znf3 expression has a unique mode of regulation. Considering that Znf3 is required for MIS and SIS and has a similar function with Rdp1 it may

be involved in the translational regulation of RNAi components, and the severe phenotype of *znf3*Δ mutants may be attributable to the absence of these factors. It is unlikely that Znf3 regulates the transcription of the RNAi components based on microarray expression analysis. Further investigation will elucidate the function of Znf3 on the RNAi components.

We investigated the expression of Znf3 in the absence of the RNAi components during sexual development. Deletion of *RDP1* and *DCR1/2* did not affect the *ZNF3* transcript levels during sexual development, indicating that the RNAi components do not regulate the expression of this gene (Figure 30B). The expression of Znf3 was modestly but significantly increased in the *ago1*Δ mutants, which is the catalytic subunit of the RISC complex. The higher expression of Znf3 may represent a novel response to partially restore the mutant phenotype of *ago1*Δ mutants through a redundant role. Alternatively, Ago1 may be responsible for the silencing of unknown factors that control the transcription of *ZNF3* during sexual development.

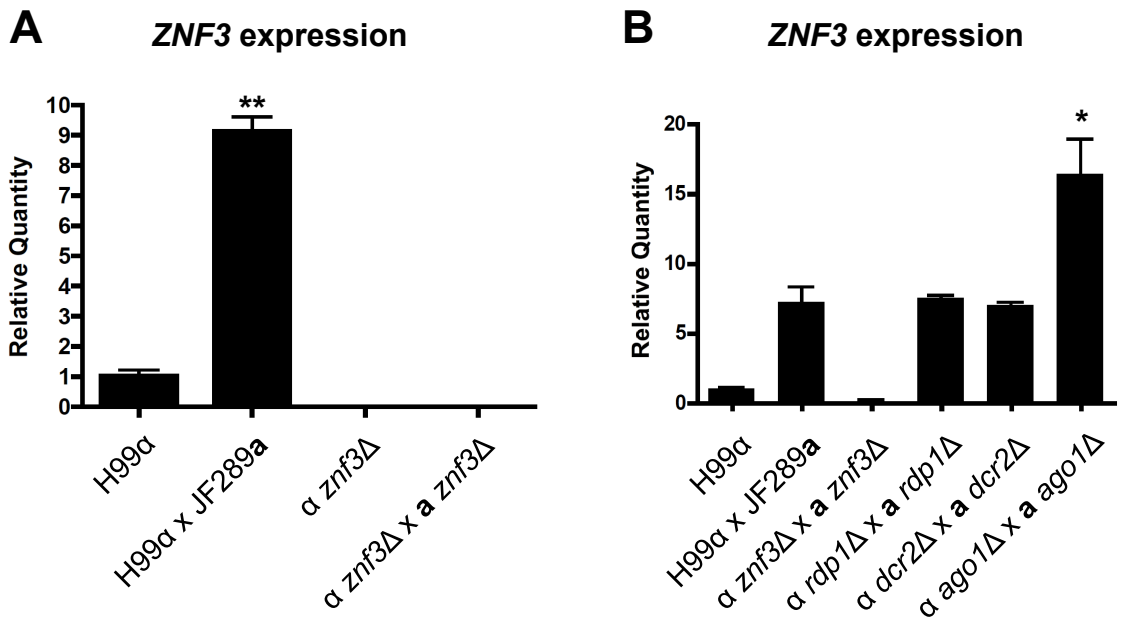

Figure 30. Znf3 is transcriptionally induced during sexual development. Cells were incubated for 24 hrs in on V8 for sexual development and on YPD for vegetative growth. RNA from the strains indicated was isolated and the expression of *ZNF3* was measured by quantitative RT-PCR. (**A)** *ZNF3* transcripts are significantly higher during sexual reproduction compared with vegetative growth. (**B)** *ZNF3* expression remains similar to WT in RNAi depleted strains. The error bars represent the standard deviation from the mean of three biological replicates (* indicates $P<0.05$ and ** indicates $P<0.005$ compared to the WT).

5.3.5 Znf3 Localizes in P-bodies

RNAi silencing is a multifunctional pathway and different steps occur at different sites in the cell. The presence of tandemly repeated genes or retrotransposons in the genome induces the transcription of aberrant ssRNA in the nucleus through an unknown mechanism. Rdp1 generates dsRNA from the mRNA of these sequences and initiates the RNAi mechanism. The dsRNA

travels to P-bodies where mRNA decay and RNA silencing occurs. Dcr1/2 and Ago1, which localize to P-bodies, generate siRNAs that target the gene with complementary sequences for degradation (Wang, Hsueh et al. 2010). These findings suggest that additional components of the pathway will localize either in the nucleus or in P-bodies.

Znf3 has two NLS signals indicating that this protein may also be localized in the nucleus. In addition, the zinc finger motifs of Znf3 are usually found in dsRNA binding proteins localized in the nucleolus. Therefore, we hypothesized that Znf3 localizes in the nucleus and possibly stabilizes or binds the dsRNA signal generated by Rdp1. To investigate the localization of Znf3 the N terminus of the protein was fused to the mCherry protein and expressed from a plasmid. The H99α and JF289**a** strains were transformed with the Znf3-mCherry plasmid and the fluorescence signal was evaluated by light microscopy. Surprisingly, we observed multiple bright foci in the cells indicating that the protein was present in more than one cellular compartment during sexual development (Figure 31). It is possible that Znf3 functions in both the nucleus and in P-bodies during RNAi silencing. To determine cellular localization we utilized two established components, one for the P-bodies and the other for the nucleus. Dcp1, found in the P-bodies, is responsible for decapping mRNAs during exonucleolytic degradation, while Nop1 is a component of the small subunit processome (a ribosome assembly intermediate) complex of the nucleolus and it is usually used

to monitor nuclear/nucleolar localization (Wang, Hsueh et al. 2010, Lee and Heitman 2012). Dcp1 and Nop1 fused with GFP in plasmids were introduced into strains expressing the Znf3-mCherry protein and localization was observed during vegetative growth and sexual development. We found that Znf3 localizes only in the P-bodies during both conditions (Figure 31). These results suggest that Znf3 participates directly in the silencing mechanism and it may represent a novel regulator of the RNAi pathway.

However, the presence of two NLS and the absence of any nuclear export signals suggest that the protein may localize in the nucleus and possibly in the nucleolus. We mentioned earlier that the zf-C2H2_JAZ motif requires RNA binding for proper cellular localization. The zinc finger domains of Znf3 lie ~300 aa from the N terminus of the protein where the mCherry tag has been fused. Thus, it is possible that the mCherry tag affects the conformation of the protein and inhibits nuclear localization. In addition, the expression of *ZNF3*::*mCherry* is under the control of the constitutively active *GPD1* promoter. It is possible that expression levels of *ZNF3* are so high that the nuclear import capabilities of the cells are saturated. Ongoing experiments focus on the construction of a Znf3 copy tagged with mCherry in the C terminus of the protein and under the control of the endogenous promoter. This strain will be transformed with Dcp1-GFP and Nop1-GFP and we will verify cellular colocalization of Znf3-mCherry during vegetative growth and sexual development.

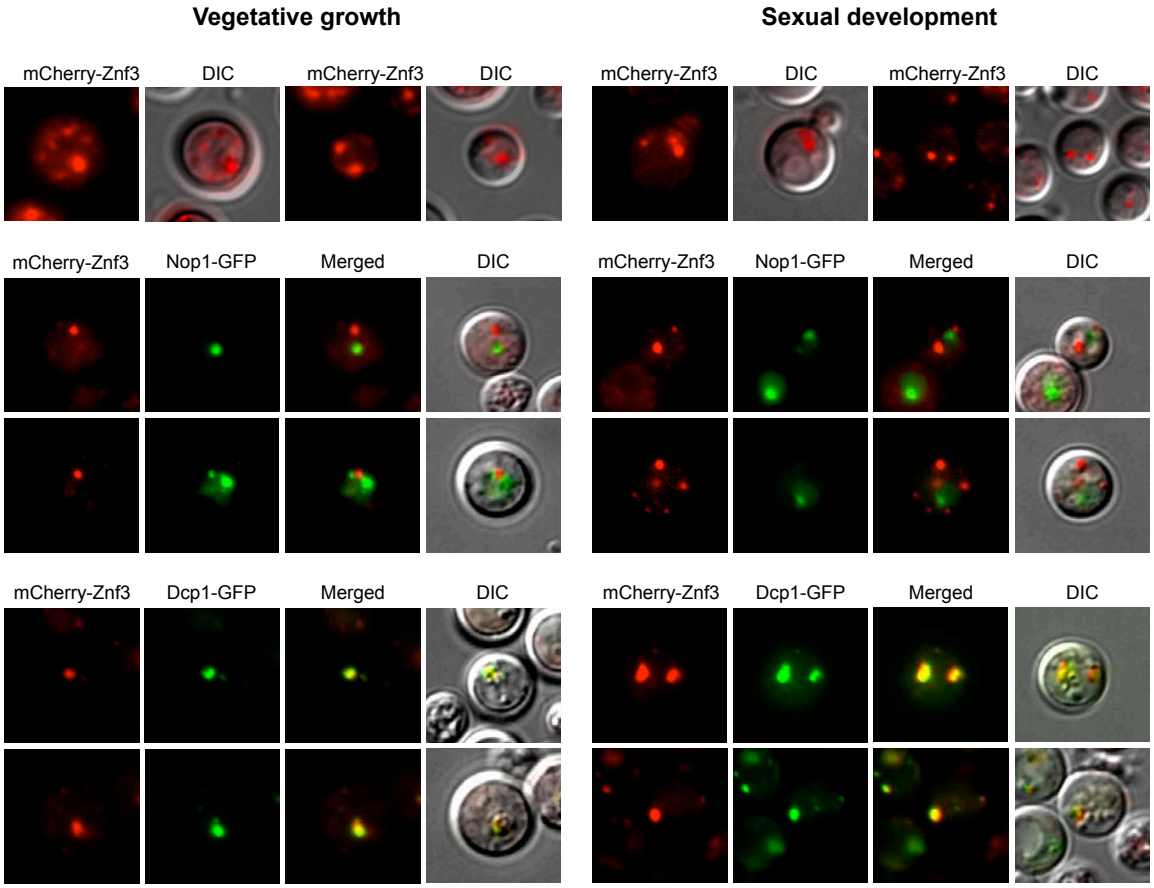

Figure 31. Znf3 localizes to the P-bodies during vegetative growth and sexual development. Strains expressing a Znf3 N-terminal mCherry fusion were transformed with a GFP-tagged *DCP1* (P-body localization marker) and *NOP1* (nuclear localization marker) alleles. The strains were observed by confocal microscopy during vegetative growth and under mating conditions. Colocalization of Znf3 with the P-body marker Dcp1 during mating and vegetative growth further supports the hypothesis that Znf3 is a novel component of the RNAi pathway.

5.4 Discussion

In this study we found that a novel zinc finger protein is required for silencing of the *SXI2***a**-*URA5* transgene during sexual development and vegetative growth. Znf3 contains a recently identified zinc finger motif zf-C2H2_JAZ, which is known to bind dsRNA and localize in the nucleus of the cell. Deletion of the gene confers a severe silencing defect, similar to the major regulator of the RNAi pathway Rdp1. Moreover, we found that *rdp1*Δ and *znf3*Δ mutants have very similar expression profiles during mating that involve overexpression of retrotransposons and other transposon-related genes. Unlike RNAi components, whose expression remains stable during mitotic growth and mating, *ZNF3* is transcriptionally induced by the sexual cycle. Surprisingly, we found that although Znf3 has two NLS tags, it localizes in the P-bodies, along with Dcr1/2 and Ago1, and participates in RNAi pathways.

RNA silencing is a highly conserved mechanism of transcriptional regulation. Since its discovery in *C. elegans* it has been identified in numerous species throughout the eukaryotic kingdom (Fire, Xu et al. 1998, Verdel, Jia et al. 2004, Kim, Han et al. 2009). An RNAi-related phenomenon was initially identified in plants and fungi, and later multiple species have been found to undergo RNA silencing mechanisms. The most well studied RNAi pathway is quelling in *Neurospora crassa*, and since its discovery several fungi, such as *Mucor circinelloides* and *Schizosaccharomyzes pombe*, have been found to employ

similar RNAi mechanisms (Romano and Macino 1992, Volpe, Kidner et al. 2002, Nicolas, Torres-Martinez et al. 2003). However, RNAi has been independently lost in some species, such as *Saccharomyces cerevisiae* and *Ustilago maydis*, which are missing all of the components of the RNAi pathway (Drinnenberg, Fink et al. 2011, Nicolas, Torres-Martinez et al. 2013). Nevertheless, the closely related species of *S. castellii* and *C. albicans* retain some of the RNAi components and substitute for the absence of others by employing noncanonical factors to produce dsRNA and shRNAs that map to transposable elements (Drinnenberg, Weinberg et al. 2009). These results indicate that the RNAi pathway is an ancestral mechanism that protects the genome against foreign DNA. The loss of the pathway in some species may represent the result of a selective pressure that confers benefits upon loss of the pathway under certain circumstances.

The RNAi pathway in *C. neoformans* is responsible for transposon silencing during vegetative growth and sexual development (Wang, Hsueh et al. 2010, Wang, Wang et al. 2012, Wang, Darwiche et al. 2013). Although the pathway is conserved among *Cryptococcus* species, it is missing in the *C. gattii* VGII R265 strain, which is the major strain causing the *C. gattii* outbreak on Vancouver Island. The loss of RNA silencing is possibly associated with higher virulence in this strain, but serotype A or D strains missing RNAi elements are not altered in virulence in the host (Wang, Hsueh et al. 2010) and thus the VGII

loss of RNAi may have had a long-term impact on virulence trajectory. We found that Znf3, which is required for RNA silencing, is also missing in VGII strains. This further supports the hypothesis that loss of RNAi may be beneficial under certain conditions. The loss of canonical RNAi components in R265/VGII can be used as a tool to identify novel factors of the RNAi pathway. A whole genome survey between R265 and WM276 (VGI) will reveal possible regulators of the pathway that may participate in SIS and MIS in *Cryptococcus*.

We showed here that Znf3 is directly involved in transgene induced silencing during mitotic growth and sexual reproduction. Deletion of the gene severely impaired silencing efficiency, even in unilateral crosses where only one parent was mutant. This phenotype was similar to the *rdp1*Δ mutant, which completely inhibited silencing during unisexual mating and impacted silencing efficiency in unilateral bisexual crosses. Given that Rdp1 is a major regulator of silencing, and that it is responsible for the initial steps generating dsRNAs, we conclude that Znf3 also plays an important role in the pathway, possibly further downstream. Although the RNAi components Dcr1/2 and Ago1 are required for SIS, their deletion only lowers the silencing efficiency indicating that their role may be redundant or largely complemented during unilateral crosses. Therefore, it is possible that Znf3 interacts with these proteins and may participate in the formation of the RISC complex. Because Znf3 is an exceptionally large protein (~1515 aa) and has a novel dsRNA-binding motif, it may act as a scaffold that

brings the components of the RNAi pathway in complex with the dsRNA substrate to generate shRNAs and trigger silencing of the complementary genes. Localization of Znf3 in P-bodies, where Dcr1/2 a nd Ago1 process the dsRNAs, may further support this hypothesis.

Alternatively, Znf3, whose expression is sexually induced, may be involved in translational regulation of the RNAi components. It was previously hypothesized that a transcriptionally induced gene during sexual development may produce a product that binds to the 5' or 3' untranslated region of the other RNAi genes and induces the translation of the proteins specifically during sexual reproduction (Wang, Hsueh et al. 2010). Thus, Znf3 may participate in the translational control of RNAi components as an RNA operon and the severe phenotypes of the *znf3*Δ mutant may be a combinatorial effect of the absence of RNAi proteins, including Rdp1.

The silencing deficiency of unilateral crosses of *rdp1*Δ and *znf3*Δ mutants suggests that the presence of the protein in only one of the parents is not sufficient to evoke the silencing mechanism. It has been previously suggested that aberrant single-stranded transgenic transcripts initiate transgene-induced silencing, where an RNA-dependent RNA polymerase converts the ssRNAs to dsRNAs (Cogoni, Irelan et al. 1996, Lee, Aalto et al. 2010). However, the presence of transgenic DNA alone is not sufficient to evoke silencing. Previous studies revealed that overexpression of the transgene or dsRNAs significantly

increased the silencing efficiency in plants (Llave, Kasschau et al. 2002). In addition, the copy number of the transgene is correlated with the silencing efficiency of tandemly repeated loci in *C. neoformans* and *N. crassa* (Romano and Macino 1992, Wang, Hsueh et al. 2010). These results indicate that silencing may be triggered by exceeding a given threshold of transgenic mRNAs and subsequently dsRNAs. Recent studies showed that Qde-1 (an RNA-dependent RNA-polymerase) triggers and maintains the silencing pathway in *N. crassa* through a dosage-dependent mechanism that depends upon the concentration of both transgenic ssRNA and dsRNA (Cogoni and Macino 1999). Based on these findings, we hypothesize that Rdp1 is responsible for generating high concentrations of dsRNAs that exceed a given threshold and elicit a silencing response. Thus, deletion of *RDP1* in one of the parents during sexual development significantly impacts the abundance of the protein and subsequently the level of dsRNAs such that they fail to induce the silencing mechanism in the dikaryon or diploid nucleus. The phenotype of *znf3*Δ mutants also suggests that a similar dosage effect inhibits silencing in unilateral crosses. Like Rdp1, Znf3 may play a major regulatory role that requires higher levels of the protein to trigger silencing.

Previous studies found that the RNAi components that are involved in sex-induced silencing are responsible for retrotransposon silencing during sexual development (Janbon, Maeng et al. 2010, Wang, Hsueh et al. 2010). We found

that deletion of *ZNF3* results in higher transposition rates during sexual reproduction and vegetative growth. Similar to the *rdp1*Δ mutant, transcription of telomeric and centromeric transposable elements and transposon-related proteins was significantly higher in *znf3*Δ mutants compared to WT. Moreover, we found that the *znf3*Δ mutant expression profile was very similar to that of *rdp1*Δ mutants. These results further support the hypothesis that Znf3 has a similar and major role in transposon silencing.

Sex-induced silencing is an efficient mechanism that protects the genome against mobile elements. Previous studies showed that ~5% of the *Cryptococcus* genome consists of transposons that cluster together in blocks and reside in both telomeric and centromeric regions on the chromosomes (Loftus, Fung et al. 2005). Transposon activation and movement may drive genome instability and phenotypic variation. Wang et al. found that transposons are transcriptionally induced specifically during sexual development, but they are silenced post-transcriptionally by the RNAi pathway (Wang, Hsueh et al. 2010). These results suggest that the transposons are possibly derepressed during mating, which could increase the mutational burden of the progeny unless counteracted by the SIS RNAi pathway. During unisexual reproduction this mechanism could generate *de novo* genotypic and phenotypic variation in clonal populations and enable rapid adaptation to new environments. Thus, loss of the RNAi components may confer a beneficial advantage in a clonal population.

Chapter 6. Conclusions and future directions

From an evolutionary perspective, sexual development drives genetic recombination throughout eukaryotic organisms and serves to purge deleterious mutations from the genome. Typical sexual cycles involve mate recognition, cell-cell fusion generating a zygote, recombination through meiosis, and generation of a divergent repertoire of progeny. Although the process is universal different species have developed distinct mating strategies to safeguard sexual development and subsequently retain genetic diversity within the population. However, sex also comes with costs. Locating a potential mating partner requires time and energy. In addition, sexual reproduction may disrupt well-adapted genomic combinations that are favorable to the respective environment. Interestingly, species that have long been thought to be asexual, in part due to the absence of an opposite mating compatible partner, were recently found to undergo sexual development between cells of the same-mating type. Unisexual reproduction eliminates some costs associated with sex by allowing sexual development between mother-daughter cells and maintaining genomic configurations that have already successfully run the gauntlet of Darwinian selection.

We now appreciate that eukaryotic microbial pathogens, including fungi and parasites, are not clonal and asexual, but rather have extant sexual cycles that are cryptic, parasexual, or even unisexual. Two of the three most common

systemic human fungal pathogens (*Candida* and *Cryptococcus*) have retained extant sexual and parasexual cycles involving both bisexual and unisexual reproduction, which may provide a broader range of adaptive evolutionary strategies. Similar paradigms have now emerged for several eukaryotic parasites, suggesting this may be a general mode of adaptation for microbial pathogens enabling them to preserve well-adapted genotypes. Given that sex is ubiquitous throughout the eukaryotic tree of life and yet we are confronted with a panoply of diverse mechanisms via which mating type (or sex) is specified and mating partners (or gametes) are distinguished and recognized, one possibility is that unisexual reproduction was the original ancestral form of sexual reproduction to which mating types and sexes were added later. If this sex before sexes model holds, the finding that extant unisexual reproduction occurs in both fungal and parasitic pathogens may reflect a return to a more ancestral mode of reproduction rather than the emergence of an entirely new process promoting genetic change and exchange.

Our studies have focused on unisexual reproduction of *Cryptococcus neoformans*. We identified a unique ability of unisexual reproduction to induce genotypic and phenotypic diversity *de novo*, including aneuploidy that can confer antifungal drug resistance. We investigated the implications of unisexual reproduction in virulence and identified a hyperfilamentous strain that causes severe pulmonary and nervous system infections, similar to highly virulent strains

of *C. gattii*. In addition, we identified novel regulators of unisexual and bisexual reproduction that orchestrate hyphal development and sporulation. Further studies revealed that one of them, Znf3, is required for a recently identified phenomenon involving gene silencing by RNAi. Znf3 and components of the RNAi pathway mediate both sex- and mitotic-induced silencing of transposable elements during sexual development and vegetative growth, respectively.

6.1 Unisexual and Heterosexual Meiotic Reproduction Generate Aneuploidy and Phenotypic Diversity de novo in the Yeast Cryptococcus neoformans

In chapter 2 we report that unisexual reproduction between genetically identical cells (mother-daughter) generates genotypic and phenotypic diversity *de novo*. The hyperfilamentous strain XL280α undergoes robust hyphal development during unisexual reproduction and generates abundant recombinant progeny. Genomic analysis of XL280α revealed that it shares 81% genetic identity with the parental strain JEC21α, and this allows molecular analysis of XL280α unisexual reproduction progeny using the genetic tools developed for the established congenic pair JEC21α/JEC20**a**. We isolated 90 progeny through micromanipulation and subjected them to a series of phenotypic assays, including growth in the presence of antifungal drugs, including fluconazole, and growth at high temperature, hallmark virulence attributes. We

found that 6 isolates (~6.6%) had a significantly different phenotype compared to the WT parent. Extensive genetic analysis revealed that one isolate was diploid, while a second one had a SNP in the gene encoding a conserved heat shock protein that is responsible for the temperature sensitive phenotype. Surprisingly, based on CGH and NGS we found that the four remaining isolates were aneuploid and we provided evidence that the mutant phenotype is attributable to the aneuploid chromosome of each strain. We developed a facile multiplex PCR-based method that allowed rapid and accurate detection of aneuploid chromosomes. Using multiplex PCR we screened all 90 progeny and we did not detect any additional aneuploids in the progeny of XL280 or in an equivalent set of 96 mitotic asexual progeny.

We further demonstrated that the aneuploid strains remained largely stable inside the host and were two as virulent as the WT parent in the animal model. In addition, we showed that three aneuploid strains had a competitive fitness advantage in the presence of fluconazole compared with the WT *in vitro*. Aneuploidy is also generated during bisexual reproduction of congenic and genetically distinct strains. Our results suggest that unisexual reproduction, which reduces or eliminates costs associated with sex, not only maintains well-adapted genomic configurations, but it also introduces limited genetic diversity in a clonal population that can confer an evolutionary advantage in selective niches and may facilitate rapid adaptation to novel environments (Ni, Feretzaki et al. 2013).

Our studies implicate unisexual reproduction as a hypermutagenic process, which introduces *de novo* genetic diversity in clonal population that appears to be beneficial during infection and may be responsible for the generation of hypervirulent “superbugs” in the environment.

Further studies should focus on the mechanisms via which unisexual reproduction generates diversity. One hypothesis suggests that the transient diploid state during unisexual reproduction may act as a capacitor for evolution. This enables the rise of recessive mutations that individually may be deleterious for the cells and thus they are counterselected in the population; however, the sheltered diploid state may allow the accumulation of multiple mutations that may be beneficial in combination when released into the haploid state. In a recent study Schoustra et al. generated homozygous diploid strains of *Aspergillus nidulans* and compared their fitness with the haploid parents following 3,000 mitotic generations (Schoustra, Debets et al. 2007). They found that the diploid strains, which had become haploids during the experiment through the parasexual cycle, exhibited higher fitness compared to the WT haploids due to the accumulation of recessive mutations in the diploid state that exhibit inverse epistasis in the haploid state. Therefore we propose isolating diploid *C. neoformans* cells generated by unisexual reproduction and allowing them to replicate for multiple generations on rich media along with the original WT haploid parent. Following meiosis and sporulation the progeny of diploid and

haploid parents will be subjected to extensive phenotypic analysis in order to determine and compare the rate of phenotypic and genotypic diversity. Similar to *Aspergillus*, unisexual reproduction may allow the beneficial combination of otherwise deleterious haploid mutations to arise in the population and thereby facilitate more rapid evolution.

6.2 Cryptococcus neoformans Hyperfilamentous Strain is Hypervirulent in a Murine Model of Cryptococcal Meningoencephalitis

As discussed earlier, unisexual reproduction facilitates the production of spores that are thought to be the infectious propagules of *C. neoformans*. However, isolates of the lineage that undergoes unisexual reproduction have been often associated with lower virulence in animal models. In chapter 3 we report the discovery of a hyperfilamentous strain that undergoes robust filamentation and is hypervirulent in the animal model. XL280α is the F1 progeny of two well-established serotype D strains that exhibit low pathogenicity in an animal model. Phenotypic analysis of the major virulence factors showed that, besides hyphal development, melanin and capsule production and growth at high temperature were similar between XL280α and JEC21α. However, we found that mice infected intranasally with XL280α developed severe pulmonary and neurological symptoms associated with cryptococcal meningitis and the animals

succumbed to the disease within 35 days post infection. On the other hand, JEC21α caused mild symptoms associated with pulmonary infections and the animals were able to successfully overcome the disease and survive throughout the course of the experiment (~125 days). In addition, we found that XL280α caused a persistent infection in the lung and the central nervous system at 2 and 4 weeks post infection, while JEC21α, although it was detectable in both organs, was considerably less prevalent 4 weeks post infection. Although XL280α undergoes robust filamentation during unisexual reproduction, we did not detect any hyphae formation *in vivo*. However, we observed that XL280α cells were elongated, oblong, and resembled "football" like structures, while JEC21α cells were smaller and rounder. Strikingly, we found that XL280α elicits a less-protective Th2-type immune response, which is usually associated with the hypervirulent strains of *C. gattii*. Histological analysis of pulmonary tissues of XL280 infected animals revealed neutrophil infiltration and goblet cell metaplasia at the site of infection, features that usually accompany Th2 immunity. While JEC21α was readily phagocytosed by alveolar macrophages, XL280α cells were resistant to phagocytosis and occupied airway and alveolar spaces. Our studies offer new insights into the roles of unisexual reproduction and reveal the virulence potential of serotype D strains.

One central question worth further investigation is the apparent resistance of XL280α to phagocytosis by macrophages. During infection *C. neoformans* serotype A and D cells are readily phagocytosed *in vivo* and *in vitro*. Previous studies show that macrophage cell lines are able to engulf more than one *Cryptococcus* cell and successfully eliminate them. However, the presence of giant/titan cells during cryptococcal infections inhibits macrophage phagocytosis and contributes to the virulence composite of a given strain (Okagaki, Strain et al. 2010, Zaragoza, Garcia-Rodas et al. 2010). Therefore, the elongated morphology of XL280α may contribute to phagocytosis resistance during infection. In addition, in many cases alterations in cell surface composition may affect interactions with cells of the immune system. Thus, we propose to conduct phagocytosis assays to determine the phagocytic index of XL280α and JEC21α *in vitro*. In addition, to further support the hypothesis that XL280α induces a Th2 type immunity a quantitative analysis of cellular infiltration in the lung should be performed. Bronchoalveolar lavage of mice infected with XL280α and JEC21α, following FACS, could quantitatively determining the type and percentage of leukocytes at the site of the infection and may predict the outcome of disease.

These studies provide a technological advantage to dissect the potential virulence of mating- and hyphae-associated genes in serotype D and possibly identify a link between morphogenesis and virulence. A possible study of interest

could be to explore the pathogenesis of XL280α-derived hyperfilamentous and hypofilamentous strains compared with WT. In previous studies we generated an *Agrobacterium tumefaciens* insertional mutant library and identified ~250 stable mutants with distinct hyphal defects. We propose to test the virulence of these strains and compare them with against XL280α and JEC21α and possibly identify novel regulators of pathogenicity that are also involved in morphogenesis.

6.3 Genetic Circuits that Govern Bisexual and Unisexual Reproduction in Cryptococcus neoformans

The pheromone-signaling cascade orchestrates the response to pheromone and regulates unisexual and bisexual reproduction. Although the pathway is highly conserved in the fungal kingdom, the targets of the pathway are largely unknown. In chapter 4 we employed an *Agrobacterium tumefaciens* mediated transformation approach to mutagenize the hyperfilamentous strain and identify novel regulators of hyphal development during unisexual reproduction.

The *Agrobacterium tumefaciens* insertional mutagenesis yielded ~6,000 mutants that were screened by microscopy for a hyphal defect. We found 250 stable mutants that were categorized based on their phenotype: no hyphae, hyperfilamentous, or a sporulation defect. In addition to elements known to be

involved in sexual development (Crg1, Ste7, Mat2, and Znf2), three key regulators of sexual development were identified by our screen: Znf3, Spo11, and Ubc5. Spo11 and Ubc5 promote sporulation during both bisexual and unisexual reproduction. We found that Spo11 is a highly conserved component of meiosis that initiates meiotic recombination by inducing double strand breaks (DSBs) and triggers strand invasion. We showed that exogenously induced DSBs via X-irradiation partially suppressed the sporulation defect of *spo11*Δ mutant during unisexual and bisexual reproduction.

Phenotypic analysis of sexual development showed that Znf3 is required for hyphal development during unisexual reproduction and also plays a central role during bisexual reproduction. Znf3 promotes cell fusion and pheromone production through a pathway parallel to and independent of the pheromone-signaling cascade. Surprisingly, Znf3 participates in transposon silencing during unisexual reproduction and may serve as a link between RNAi silencing and sexual development. Our studies illustrate the power of unbiased genetic screens to reveal both novel and conserved circuits that operate sexual reproduction (Feretzaki and Heitman 2013).

As discussed in chapter 4 the meiotic toolkit genes are hallmarks of meiosis in sexually reproducing species. Our survey of the *C. neoformans* genome revealed that most of the key meiotic regulators are conserved and previous studies, and ours, showed that Spo11 and Dmc1 are involved in

meiosis and sporulation (Lin, Hull et al. 2005). However, meiotic species exhibit considerable plasticity in the components involved in meiosis, although the sequence of meiotic events is highly conserved in fungal species. In *C. albicans* for example, where the meiosis toolkit genes are present, the species engages in a parasexual cycle rather than a meiotic sexual one (Bennett and Johnson 2003). On the other hand, sporulation and meiosis in *C. lusitaniae* are highly efficient in the absence of key regulators of this process (Reedy, Floyd et al. 2009). In addition *Ustilago maydi*s employs novel factors, homologs of *H. sapiens BRCA2* and *DSS1* to complete the meiotic cycle (Holloman, Schirawski et al. 2008). These findings indicate that meiosis is conserved; however, novel regulators are implicated in different species, and thus homology-based approaches may miss elements involved in the *C. neoformans* meiotic cycle. We propose to explore the function of other conserved meiotic regulators in *C. neoformans* through gene deletion and phenotypic analysis of mutants. In addition, an *A. tumefaciens* insertional mutagenesis screen focused on sporulation defective mutants would unveil novel factors of the pathway and offer further mechanistic insights into meiosis and sporulation.

Znf3 is a highly unique regulator as it is required for hyphal development and pheromone expression during sexual development. However, its function is distinct from the pheromone signaling cascade. The identification and characterization of its targets will elucidate its functions during mating. One

unexpected feature of Znf3 is its role in transposon expression during mating. Znf3 is required for transposon silencing, indicating that this protein is implicated in genome defense and RNA interference. It is possible that Znf3 is a missing link between sexual development and transposon silencing. Thus, we propose that its roles during silencing and possible functions in the RNAi pathways should be further investigated. In addition, we will analyze the functions of Znf3 in sexual development in serotype A and determine if it has a conserved role in sex- and mitotic-induced silencing. Znf3 is a large protein (~170 kDa) with a coiled coil region that is typically involved in protein-protein interactions. We propose to fuse Znf3 with a protein tag and perform immunoprecipitations to isolate protein complexes during mating. Any proteins that interact with Znf3 will be identified by mass spectrometry. This approach will identify possible Znf3 regulators, co-factors and potential downstream targets. We will investigate their functions during mating and transposon silencing, using established genetic and biochemical approaches. These experiments will identify the pathways that Znf3 regulates and further elucidate its functions during hyphal development and transposon silencing during unisexual and bisexual reproduction.

6.4 RNAi Loss in C. gattii Reveals Novel Regulators of Silencing in C. neoformans

Genome instability and mutations provoked by transposon movement are counteracted by novel defense mechanisms in organisms as diverse as fungi, plants, and mammals. In the human fungal pathogen *C. neoformans* we have previously characterized an RNAi silencing pathway that defends the genome against mobile elements and artificially introduced repeats of homologous DNA. Repetitive transgenes and transposons are silenced by an RNAi-dependent pathway during sexual development (sex-induced silencing, SIS) and during vegetative mitotic growth (MIS). RNAi silencing pathways are conserved in the *Cryptococcus* pathogenic species complex and are mediated by core RNAi components, including an RNA-dependent RNA polymerase (Rdp1), Argonaute (Ago1 and Ago2), and Dicer (Dcr1 and Dcr2).

Surprisingly, all of the canonical known RNAi components are missing from all *C. gattii* VGII strains, the molecular type responsible for the North American Pacific Northwest outbreak. To identify novel components of the RNAi pathway, in chapter 5 we surveyed the genome of the *C. gattii* R265 isolate for missing genes (in collaboration with Blake Billmyre). One of the most interesting is *ZNF3*. In previous studies we found that Znf3, a protein with three zinc finger domains, is required for bisexual and unisexual reproduction in *C. neoformans* var. *neoformans*. One of the zinc finger motifs, C2H2-JAZ, belongs to a recently

identified family of zinc finger domains that is known to bind dsRNA or DNA/RNA hybrids. Surprisingly, in *C. neoformans* var. *grubii ZNF3* is not essential for sexual development. However, it is required for mitotic- and sex-induced silencing via RNAi. SIS is less efficient in *znf3*Δ unilateral matings and is abolished in *znf3*Δ x *znf3*Δ bilateral matings, similar to the phenotypes of *rdp1*Δ mutants. Znf3 is also required for transgene-induced mitotic silencing; *znf3*Δ and *rdp1*Δ mutations abrogate silencing of repetitive transgenes during vegetative growth. Znf3 tagged with mCherry is localized in the cytoplasm in bright, distinct foci. Co-localization of Znf3 with the P-body marker Dcp1-GFP further supports the hypothesis that Znf3 is a novel element of the RNAi pathway. Therefore, we propose that Znf3 operates to defend the genome during sexual development and vegetative growth.

In addition to the identical silencing phenotype, *znf3*Δ and *rdp1*Δ mutants share a very similar genome-wide expression profile during sexual development. However, the transcriptional regulation patterns of *ZNF3* and *RDP1* are strikingly distinct. The expression of *RDP1* (and of the other RNAi components) remains constant during vegetative growth and mating, while *ZNF3* transcription is sexually induced. Previous studies hypothesized that a co-regulation mechanism orchestrates the translation of the RNAi components' transcripts. We propose that Znf3 may bind at the 5' or 3' untranslated region of mRNAs and

translationally co-regulate the RNAi components during mating. We will delete *ZNF3* in strains where the RNAi components have been fused with the mCherry tag. mCherry fused proteins will be isolated in the presence and absence of Znf3 during vegetative growth and sexual development and we will conduct immunoprecipitation, western blotting, and also examine protein levels by fluorescence microscopy of the mCherry derivatives. Reduction of Rdp1-mCherry or Ago1-mCherry in the *znf3*Δ mutant during sexual development will demonstrate possible translational regulation of the RNAi components by Znf3.

In our current model, the RNAi pathway is initiated in the nucleus with Rdp1 generating abundant dsRNAs from repetitive sequences, which travel to P-bodies where they are cleaved by Dcr1/2 and loaded onto RISC where Ago1 removes the passenger strand and triggers silencing of targets with a complementary sequence. The factors that recognize the repetitive sequences in the genome and the proteins interacting with Dcr1/2 and Ago1 are largely unknown. Given that Znf3 is an exceptionally large protein that localizes in the P-bodies and encompasses a dsRNA binding motif and a protein-protein interaction domain, we hypothesize that Znf3 may act as a scaffold that facilitates interactions between Dcr1/2 and Ago1 with the dsRNA target. We will fuse Znf3 with GFP and conduct co-immunoprecipitation with Dcr1/2-mCherry and Ago1-mCherry during mating. We will also perform mass spectrometry analysis to identify any additional unknown factors that interact with Znf3 during silencing. To

identify the RNA targets of Znf3 we will conduct an RNA-binding protein immunoprecipitation followed by microarray analysis (RIP-Chip or PAR-CLIP). These experiments will elucidate the function of Znf3 in silencing and directly implicate this novel regulator in the RNAi pathway of *C. neoformans*.

References

Akopyants, N. S., N. Kimblin, N. Secundino, et al. (2009). "Demonstration of genetic exchange during cyclical development of *Leishmania* in the sand fly vector." Science **324**(5924): 265-268.

Alby, K. and R. J. Bennett (2011). "Interspecies pheromone signaling promotes biofilm formation and same-sex mating in *Candida albicans*." Proc Natl Acad Sci U S A **108**(6): 2510-2515.

Alby, K., D. Schaefer and R. J. Bennett (2009). "Homothallic and heterothallic mating in the opportunistic pathogen *Candida albicans*." Nature **460**(7257): 890-893.

Alonso, J. M., A. N. Stepanova, T. J. Leisse, et al. (2003). "Genome-wide insertional mutagenesis of *Arabidopsis thaliana*." Science **301**(5633): 653-657.

Alspaugh, J. A., J. R. Perfect and J. Heitman (1997). "*Cryptococcus neoformans* mating and virulence are regulated by the G-protein alpha subunit GPA1 and cAMP." Genes Dev **11**(23): 3206-3217.

Alvarez, M. and A. Casadevall (2006). "Phagosome extrusion and host-cell survival after *Cryptococcus neoformans* phagocytosis by macrophages." Curr Biol **16**(21): 2161-2165.

Anandi, V., P. G. Babu and T. J. John (1991). "Infection due to *Cryptococcus neoformans* of unusual morphology in a patient with AIDS." Mycoses **34**: 377-379.

Aramayo, R. and R. L. Metzenberg (1996). "Meiotic transvection in fungi." Cell **86**(1): 103-113.

Argueso, J. L., J. Westmoreland, P. A. Mieczkowski, et al. (2008). "Double-strand breaks associated with repetitive DNA can reshape the genome." Proc Natl Acad Sci U S A **105**(33): 11845-11850.

Arnaise, S., D. Zickler and N. L. Glass (1993). "Heterologous expression of mating-type genes in filamentous fungi." Proc Natl Acad Sci U S A **90**(14): 6616-6620.

Bahn, Y. S., G. M. Cox, J. R. Perfect, et al. (2005). "Carbonic anhydrase and CO2 sensing during *Cryptococcus neoformans* growth, differentiation, and virulence." Curr Biol **15**(22): 2013-2020.

Barchiesi, F., M. Cogliati, M. C. Esposto, et al. (2005). "Comparative analysis of pathogenicity of *Cryptococcus neoformans* serotypes A, D and AD in murine cryptococcosis." J Infect **51**(1): 10-16.

Bartlett, K. H., P. Y. Cheng, C. Duncan, et al. (2012). "A decade of experience: *Cryptococcus gattii* in British Columbia." Mycopathologia **173**(5-6): 311-319.

Bartlett, K. H., S. E. Kidd and J. W. Kronstad (2008). "The emergence of *Cryptococcus gattii* in British Columbia and the Pacific Northwest." Curr Infect Dis Rep **10**(1): 58-65.

Beenhouwer, D. O., S. Shapiro, M. Feldmesser, et al. (2001). "Both Th1 and Th2 cytokines affect the ability of monoclonal antibodies to protect mice against *Cryptococcus neoformans*." Infect Immun **69**(10): 6445-6455.

Benjamini, Y. and Y. Hockberg (1995). "Controlling the false discovery rate: a practical and powerful approach to multiple testing." Journal of the Royal Statistical Society Series **57**(1): 289-300.

Bennett, R. J. and A. D. Johnson (2003). "Completion of a parasexual cycle in *Candida albicans* by induced chromosome loss in tetraploid strains." EMBO J **22**(10): 2505-2515.

Bennett, R. J. and A. D. Johnson (2006). "The role of nutrient regulation and the Gpa2 protein in the mating pheromone response of *C. albicans*." Mol Microbiol **62**(1): 100-119.

Bentley, D. R. (2006). "Whole-genome re-sequencing." Curr Opin Genet Dev **16**(6): 545-552.

Bishop, D. K., D. Park, L. Xu, et al. (1992). "*DMC1*: a meiosis-specific yeast homolog of *E. coli recA* required for recombination, synaptonemal complex formation, and cell cycle progression." Cell **69**(3): 439-456.

Botts, M. R., S. S. Giles, M. A. Gates, et al. (2009). "Isolation and characterization of *Cryptococcus neoformans* spores reveal a critical role for capsule biosynthesis genes in spore biogenesis." Eukaryot Cell **8**: 595-605.

Brefort, T., P. Muller and R. Kahmann (2005). "The high-mobility-group domain transcription factor Rop1 is a direct regulator of *PRF1* in *Ustilago maydis*." Eukaryot Cell **4**(2): 379-391.

Bui, T., X. Lin, R. Malik, et al. (2008). "Isolates of *Cryptococcus neoformans* from infected animals reveal genetic exchange in unisexual, alpha mating type populations." Eukaryot. Cell **7**(10): 1771-1780.

Buonomo, S. B., R. K. Clyne, J. Fuchs, et al. (2000). "Disjunction of homologous chromosomes in meiosis I depends on proteolytic cleavage of the meiotic cohesin Rec8 by separin." Cell **103**(3): 387-398.

Burkholder, A. C. and L. H. Hartwell (1985). "The yeast alpha-factor receptor: structural properties deduced from the sequence of the *STE2* gene." Nucleic Acids Res **13**(23): 8463-8475.

Byrnes, E. J., 3rd, R. J. Bildfell, S. A. Frank, et al. (2009). "Molecular evidence that the range of the Vancouver Island outbreak of *Cryptococcus gattii* infection has expanded into the Pacific Northwest in the United States." J Infect Dis **199**(7): 1081-1086.

Byrnes, E. J., 3rd, W. Li, Y. Lewit, et al. (2010). "Emergence and pathogenicity of highly virulent *Cryptococcus gattii* genotypes in the northwest United States." PLoS Pathog **6**(4): e1000850.

Byrnes, E. J., 3rd, W. Li, Y. Lewit, et al. (2009). "First reported case of *Cryptococcus gattii* in the Southeastern USA: implications for travel-associated acquisition of an emerging pathogen." PLoS One **4**(6): e5851.

Calo, S., R. B. Billmyre and J. Heitman (2013). "Generators of phenotypic diversity in the evolution of pathogenic microorganisms." PLoS Pathog **9**(3): e1003181.

Campbell, L. T., B. J. Currie, M. Krockenberger, et al. (2005). "Clonality and recombination in genetically differentiated subgroups of *Cryptococcus gattii*." Eukaryot. Cell **4**(8): 1403-1409.

Cao, L., E. Alani and N. Kleckner (1990). "A pathway for generation and processing of double-strand breaks during meiotic recombination in *S. cerevisiae*." Cell **61**(6): 1089-1101.

Celerin, M., S. T. Merino, J. E. Stone, et al. (2000). "Multiple roles of Spo11 in meiotic chromosome behavior." EMBO J **19**(11): 2739-2750.

Cetin, B. and D. W. Cleveland (2010). "How to survive aneuploidy." Cell **143**(1): 27-29.

Chang, S. S., Z. Zhang and Y. Liu (2012). "RNA interference pathways in fungi: mechanisms and functions." Annu Rev Microbiol **66**: 305-323.

Chang, Y. C. and K. J. Kwon-Chung (1994). "Complementation of a capsule-deficient mutation of *Cryptococcus neoformans* restores its virulence." Mol. Cell. Biol. **14**: 4912-4919.

Chang, Y. C., L. A. Penoyer and K. J. Kwon-Chung (2001). "The second *STE12* homologue of *Cryptococcus neoformans* is MATa-specific and plays an important role in virulence." Proc Natl Acad Sci U S A **98**(6): 3258-3263.

Chang, Y. C., B. L. Wickes and K. J. Kwon-Chung (1995). "Further analysis of the *CAP59* locus of *Cryptococcus neoformans*: structure defined by forced expression and description of a new ribosomal protein-encoding gene." Gene **167**: 179-183.

Chang, Y. C., B. L. Wickes, G. F. Miller, et al. (2000). "*Cryptococcus neoformans STE12*α regulates virulence but is not essential for mating." J. Exp. Med. **191**: 871-882.

Charlier, C., F. Chretien, M. Baudrimont, et al. (2005). "Capsule structure changes associated with *Cryptococcus neoformans* crossing of the blood-brain barrier." Am J Pathol **166**(2): 421-432.

Charlier, C., K. Nielsen, S. Daou, et al. (2009). "Evidence of a role for monocytes in dissemination and brain invasion by *Cryptococcus neoformans*." Infect Immun **77**(1): 120-127.

Chen, G. H., D. A. McNamara, Y. Hernandez, et al. (2008). "Inheritance of immune polarization patterns is linked to resistance versus susceptibility to *Cryptococcus neoformans* in a mouse model." Infect Immun **76**(6): 2379-2391.

Chen, S., T. Sorrell, G. Nimmo, et al. (2000). "Epidemiology and host- and variety-dependent characteristics of infection due to *Cryptococcus neoformans* in Australia and New Zealand." Clin Infect Dis **31**(2): 499-508.

Cheng, P. Y., A. Sham and J. W. Kronstad (2009). "*Cryptococcus gattii* isolates from the British Columbia cryptococcosis outbreak induce less protective inflammation in a murine model of infection than *Cryptococcus neoformans*." Infect Immun **77**(10): 4284-4294.

Chowdhary, A., S. S. Hiremath, S. Sun, et al. (2011). "Genetic differentiation, recombination and clonal expansion in environmental populations of *Cryptococcus gattii* in India." Environ Microbiol **13**(7): 1875-1888.

Chun, C. D. and H. D. Madhani (2010). "Ctr2 links copper homeostasis to polysaccharide capsule formation and phagocytosis inhibition in the human fungal pathogen *Cryptococcus neoformans*." PLoS One **5**(9): e12503.

Clarke, D. L., G. L. Woodlee, C. M. McClelland, et al. (2001). "The *Cryptococcus neoformans STE11*alpha gene is similar to other fungal mitogen-activated protein kinase kinase kinase (MAPKKK) genes but is mating type specific." Mol Microbiol **40**(1): 200-213.

Cogoni, C., J. T. Irelan, M. Schumacher, et al. (1996). "Transgene silencing of the al-1 gene in vegetative cells of *Neurospora* is mediated by a cytoplasmic effector and does not depend on DNA-DNA interactions or DNA methylation." EMBO J **15**(12): 3153-3163.

Cogoni, C. and G. Macino (1999). "Gene silencing in *Neurospora crassa* requires a protein homologous to RNA-dependent RNA polymerase." Nature **399**: 166-169.

Cooper, M. A., R. D. Adam, M. Worobey, et al. (2007). "Population genetics provides evidence for recombination in *Giardia*." Curr Biol **17**(22): 1984-1988.

Crabtree, J. N., L. H. Okagaki, D. L. Wiesner, et al. (2012). "Titan cell production enhances the virulence of *Cryptococcus neoformans*." Infect Immun **80**(11): 3776-3785.

D'Souza, C. A., J. W. Kronstad, G. Taylor, et al. (2011). "Genome variation in *Cryptococcus gattii*, an emerging pathogen of immunocompetent hosts." mBio **2**(1): e00342-00310.

Dalle, F., B. Wachtler, C. L'Ollivier, et al. (2010). "Cellular interactions of *Candida albicans* with human oral epithelial cells and enterocytes." Cell Microbiol **12**(2): 248-271.

Davidson, R. C., J. R. Blankenship, P. R. Kraus, et al. (2002). "A PCR-based strategy to generate integrative targeting alleles with large regions of homology." Microbiology **148**: 2607-2615.

Davidson, R. C., M. C. Cruz, R. A. L. Sia, et al. (2000). "Gene disruption by biolistic transformation in serotype D strains of *Cryptococcus neoformans*." Fung. Genet. Biol. **29**: 38-48.

Davidson, R. C., C. B. Nichols, G. M. Cox, et al. (2003). "A MAP kinase cascade composed of cell type specific and non-specific elements controls mating and differentiation of the fungal pathogen *Cryptococcus neoformans*." Mol Microbiol **49**(2): 469-485.

Day, J. N., T. T. Chau, M. Wolbers, et al. (2013). "Combination antifungal therapy for cryptococcal meningitis." N Engl J Med **368**(14): 1291-1302.

Dohlman, H. G. and J. W. Thorner (2001). "Regulation of G protein-initiated signal transduction in yeast: Paradigms and principles." Annual Review of Biochemistry **70**: 703-754.

Dong, Z. M. and J. W. Murphy (1995). "Effects of the two varieties of *Cryptococcus neoformans* cells and culture filtrate antigens on neutrophil locomotion." Infect. Immun. **63**: 2632-2644.

Drinnenberg, I. A., G. R. Fink and D. P. Bartel (2011). "Compatibility with killer explains the rise of RNAi-deficient fungi." Science **333**(6049): 1592.

Drinnenberg, I. A., D. E. Weinberg, K. T. Xie, et al. (2009). "RNAi in budding yeast." Science **326**(5952): 544-550.

Elion, E. A. (2000). "Pheromone response, mating and cell biology." Curr Opin Microbiol **3**(6): 573-581.

Enyenihi, A. H. and W. S. Saunders (2003). "Large-scale functional genomic analysis of sporulation and meiosis in *Saccharomyces cerevisiae*." Genetics **163**(1): 47-54.

Feretzaki, M. and J. Heitman (2013). "Genetic circuits that govern bisexual and unisexual reproduction in *Cryptococcus neoformans*." PLoS Genet **9**(8): e1003688.

Feretzaki, M. and J. Heitman (2013). "Genetic circuits that govern bisexual and unisexual reproduction in *Cryptococcus neoformans*." PLoS Genet **In press to be published online August 15, 2013.**

Feretzaki, M. and J. Heitman (2013). "Unisexual reproduction drives evolution of eukaryotic microbial pathogens." PLoS Pathog **9**(10): e1003674.

Fire, A., S. Xu, M. K. Montgomery, et al. (1998). "Potent and specific genetic interference by double-stranded RNA in *Caenorhabditis elegans*." Nature **391**(6669): 806-811.

Forche, A., K. Alby, D. Schaefer, et al. (2008). "The parasexual cycle in *Candida albicans* provides an alternative pathway to meiosis for the formation of recombinant strains." PLoS Biol **6**(5): e110.

Fraser, J. A., S. S. Giles, E. C. Wenink, et al. (2005). "Same-sex mating and the origin of the Vancouver Island *Cryptococcus gattii* outbreak." Nature **437**(7063): 1360-1364.

Fraser, J. A., J. C. Huang, R. Pukkila-Worley, et al. (2005). "Chromosomal translocation and segmental duplication in *Cryptococcus neoformans*." Eukaryot. Cell **4**(2): 401-406.

Fraser, J. A., R. L. Subaran, C. B. Nichols, et al. (2003). "Recapitulation of the sexual cycle of the primary fungal pathogen *Cryptococcus neoformans* variety *gattii*: implications for an outbreak on Vancouver Island." Eukaryot. Cell ***2***: 1036-1045.

Freed, E. R., R. J. Duma, H. J. Shadomy, et al. (1971). "Meningoencephalitis due to hyphae-forming *Cryptococcus neoformans*." Am. J. Clin. Path. **55**: 30-33.

Fromtling, R. A., R. Blackstock, N. K. Hall, et al. (1979). "Immunization of mice with an avirulent pseudohyphal form of *Cryptococcus neoformans*." Mycopathologia **68**(3): 179-181.

Fromtling, R. A., R. Blackstock, N. K. Hall, et al. (1979). "Kinetics of lymphocyte transformation in mice immunized with viable avirulent forms of *Cryptococcus neoformans*." Infect Immun **24**(2): 449-453.

Fu, J., C. Mares, A. Lizcano, et al. (2011). "Insertional mutagenesis combined with an inducible filamentation phenotype reveals a conserved *STE50* homologue in *Cryptococcus neoformans* that is required for monokaryotic fruiting and sexual reproduction." Mol Microbiol **79**(4): 990-1007.

Galanis, E., L. Macdougall, S. Kidd, et al. (2010). "Epidemiology of *Cryptococcus gattii*, British Columbia, Canada, 1999-2007." Emerg Infect Dis **16**(2): 251-257.

Garcia-Hermoso, D., F. Dromer and G. Janbon (2004). "*Cryptococcus neoformans* capsule structure evolution in vitro and during murine infection." Infect Immun **72**(6): 3359-3365.

Garcia-Hermoso, D., G. Janbon and F. Dromer (1999). "Epidemiological evidence for dormant *Cryptococcus neoformans* infection." J Clin Microbiol **37**(10): 3204-3209.

Gaunt, M. W., M. Yeo, I. A. Frame, et al. (2003). "Mechanism of genetic exchange in American trypanosomes." Nature **421**(6926): 936-939.

Gazzoni, A. F., M. Oliveira Fde, E. F. Salles, et al. (2010). "Unusual morphologies of *Cryptococcus* spp. in tissue specimens: report of 10 cases." Rev Inst Med Trop Sao Paulo **52**(3): 145-149.

Gentleman, R. C., V. J. Carey, D. M. Bates, et al. (2004). "Bioconductor: open software development for computational biology and bioinformatics." Genome Biol **5**(10): R80.

Ghildiyal, M., J. Xu, H. Seitz, et al. (2010). "Sorting of *Drosophila* small silencing RNAs partitions microRNA strands into the RNA interference pathway." RNA **16**(1): 43-56.

Giles, S. S., T. R. Dagenais, M. R. Botts, et al. (2009). "Elucidating the pathogenesis of spores from the human fungal pathogen *Cryptococcus neoformans*." Infect Immun **77**(8): 3491-3500.

Glass, N. L., V. S. J., C. Staben, et al. (1988). "DNAs of the two mating-type alleles of *Neurospora crassa* are highly dissimilar." Science **241**(4865): 570-573.

Glass, N. L. and M. L. Smith (1994). "Structure and function of a mating-type gene from the homothallic species *Neurospora africana*." Mol Gen Genet **244**(4): 401-409.

Goldman, D. L., H. Khine, J. Abadi, et al. (2001). "Serologic evidence for *Cryptococcus neoformans* infection in early childhood." Pediatrics **107**(5): E66.

Gomez, B. L. and J. D. Nosanchuk (2003). "Melanin and fungi." Curr Opin Infect Dis **16**(2): 91-96.

Gordon, D. J., B. Resio and D. Pellman (2012). "Causes and consequences of aneuploidy in cancer." Nat Rev Genet **13**(3): 189-203.

Guillot, L., S. F. Carroll, R. Homer, et al. (2008). "Enhanced innate immune responsiveness to pulmonary *Cryptococcus neoformans* infection is associated with resistance to progressive infection." Infect Immun **76**(10): 4745-4756.

Hardison, S. E., S. Ravi, K. L. Wozniak, et al. (2010). "Pulmonary infection with an interferon-gamma-producing *Cryptococcus neoformans* strain results in classical macrophage activation and protection." Am J Pathol **176**(2): 774-785.

Hartwell, L. H. (1980). "Mutants of *Saccharomyces cerevisiae* unresponsive to cell division control by polypeptide mating hormone." J. Cell Biol. **85**: 811-822.

Heitman, J. (2010). "Evolution of eukaryotic microbial pathogens via covert sexual reproduction." Cell Host Microbe **8**(1): 86-99.

Heitman, J., B. Allen, J. A. Alspaugh, et al. (1999). "On the origins of the congenic *MAT*alpha and *MAT***a** strains of the pathogenic yeast *Cryptococcus neoformans*." Fungal Genet. Biol. **28**: 1-5.

Heitman, J., T. R. Kozel, K. J. Kwon-Chung, et al. (2011). *Cryptococcus*: from human pathogen to model yeast, ASM Press.

Henry, J. M., R. Camahort, D. A. Rice, et al. (2006). "Mnd1/Hop2 facilitates Dmc1-dependent interhomolog crossover formation in meiosis of budding yeast." Mol Cell Biol **26**(8): 2913-2923.

Herskowitz, I. (1989). "A regulatory hierarchy for cell specialization in yeast." Nature **342**(6251): 749-757.

Hickman, M. A., G. Zeng, A. Forche, et al. (2013). "The 'obligate diploid' *Candida albicans* forms mating-competent haploids." Nature **494**(7435): 55-59.

Hiremath, S. S., A. Chowdhary, T. Kowshik, et al. (2008). "Long-distance dispersal and recombination in environmental populations of *Cryptococcus neoformans* var. *grubii* from India." Microbiology **154**(Pt 5): 1513-1524.

Hoang, L. M., J. A. Maguire, P. Doyle, et al. (2004). "*Cryptococcus neoformans* infections at Vancouver Hospital and Health Sciences Centre (1997-2002): epidemiology, microbiology and histopathology." J Med Microbiol **53**(Pt 9): 935-940.

Hodgkin, J. (2005). "Karyotype, ploidy, and gene dosage." WormBook: 1-9.

Holloman, W. K., J. Schirawski and R. Holliday (2008). "The homologous recombination system of *Ustilago maydis*." Fungal Genet Biol **45 Suppl 1**: S31-39.

Hsueh, Y. P., A. Idnurm and J. Heitman (2006). "Recombination hotspots flank the *Cryptococcus* mating-type locus: implications for the evolution of a fungal sex chromosome." PLoS Genet **2**(11): e184.

Hsueh, Y. P., X. Lin, K. J. Kwon-Chung, et al. (2011). Sexual reproduction of *Cryptococcus*. *Cryptococcus*: from human pathogen to model yeast. J. Heitman, T. R. Kozel, K. J. Kwon-Chung, J. R. Perfect and A. Casadevall. Washington, DC, ASM Press**:** pp. 81-96.

Hu, G., I. Liu, A. Sham, et al. (2008). "Comparative hybridization reveals extensive genome variation in the AIDS-associated pathogen *Cryptococcus neoformans*." Genome Biol **9**(2): R41.

Hu, G., J. Wang, J. Choi, et al. (2011). "Variation in chromosome copy number influences the virulence of *Cryptococcus neoformans* and occurs in isolates from AIDS patients." BMC Genomics **12**: 526.

Huffnagle, G. B., M. B. Boyd, N. E. Street, et al. (1998). "IL-5 is required for eosinophil recruitment, crystal deposition, and mononuclear cell recruitment during a pulmonary *Cryptococcus neoformans* infection in genetically susceptible mice (C57BL/6)." J Immunol **160**(5): 2393-2400.

Huffnagle, G. B. and M. F. Lipscomb (1998). "Cells and cytokines in pulmonary cryptococcosis." Res Immunol **149**(4-5): 387-396; discussion 512-384.

Hull, C. M., M. J. Boily and J. Heitman (2005). "Sex-specific homeodomain proteins Sxi1α and Sxi2**a** coordinately regulate sexual development in *Cryptococcus neoformans*." Eukaryot Cell **4**(3): 526-535.

Hull, C. M., R. C. Davidson and J. Heitman (2002). "Cell identity and sexual development in *Cryptococcus neoformans* are controlled by the mating-type-specific homeodomain protein Sxi1α." Genes Dev. **16**(23): 3046-3060.

Hull, C. M. and J. Heitman (2002). "Genetics of *Cryptococcus neoformans*." Annu Rev Genet **36**: 557-615.

Hull, C. M., R. M. Raisner and A. D. Johnson (2000). "Evidence for mating of the "asexual" yeast *Candida albicans* in a mammalian host." Science **289**(5477): 307-310.

Hwang-Shum, J. J., D. C. Hagen, E. E. Jarvis, et al. (1991). "Relative contributions of *MCM1* and *STE12* to transcriptional activation of a- and alpha-specific genes from *Saccharomyces cerevisiae*." Mol Gen Genet **227**(2): 197-204.

Idnurm, A. (2010). "A tetrad analysis of the basidiomycete fungus *Cryptococcus neoformans*." Genetics **185**(1): 153-163.

Idnurm, A., Y. S. Bahn, K. Nielsen, et al. (2005). "Deciphering the model pathogenic fungus *Cryptococcus neoformans*." Nat Rev Microbiol **3**(10): 753-764.

Idnurm, A. and J. Heitman (2005). "Light controls growth and development via a conserved pathway in the fungal kingdom." PLoS Biol **3**(4): e95.

Idnurm, A., J. L. Reedy, J. C. Nussbaum, et al. (2004). "*Cryptococcus neoformans* virulence gene discovery through insertional mutagenesis." Eukaryot. Cell **3**(2): 420-429.

Imwidthaya, P. and N. Poungvarin (2000). "Cryptococcosis in AIDS." Postgrad Med J **76**(892): 85-88.

Inbar, E., N. S. Akopyants, M. Charmoy, et al. (2013). "The mating competence of geographically diverse *Leishmania major* strains in their natural and unnatural sand fly vectors." PLoS Genet **9**(7): e1003672.

Iuchi, S. (2001). "Three classes of C2H2 zinc finger proteins." Cell Mol Life Sci **58**(4): 625-635.

Jain, A. V., Y. Zhang, W. B. Fields, et al. (2009). "Th2 but not Th1 immune bias results in altered lung functions in a murine model of pulmonary *Cryptococcus neoformans* infection." Infect Immun **77**(12): 5389-5399.

Janbon, G., S. Maeng, D. H. Yang, et al. (2010). "Characterizing the role of RNA silencing components in *Cryptococcus neoformans*." Fungal Genet Biol **47**(12): 1070-1080.

Jin, R., C. J. Dobry, P. J. McCown, et al. (2008). "Large-scale analysis of yeast filamentous growth by systematic gene disruption and overexpression." Mol Biol Cell **19**(1): 284-296.

Kavanaugh, L. A., J. A. Fraser and F. S. Dietrich (2006). "Recent evolution of the human pathogen *Cryptococcus neoformans* by intervarietal transfer of a 14-gene fragment." Mol Biol Evol **23**(10): 1879-1890.

Keeney, S., C. N. Giroux and N. Kleckner (1997). "Meiosis-specific DNA double-strand breaks are catalyzed by Spo11, a member of a widely conserved protein family." Cell **88**(3): 375-384.

Keller, S. M., M. A. Viviani, M. C. Esposto, et al. (2003). "Molecular and genetic characterization of a serotype A *MAT***a** *Cryptococcus neoformans* isolate." Microbiology **149**(Pt 1): 131-142.

Kidd, S. E., P. J. Bach, A. O. Hingston, et al. (2007). "*Cryptococcus gattii* dispersal mechanisms, British Columbia, Canada." Emerg Infect Dis **13**(1): 51-57.

Kidd, S. E., Y. Chow, S. Mak, et al. (2007). "Characterization of environmental sources of the human and animal pathogen *Cryptococcus gattii* in British Columbia, Canada, and the Pacific Northwest of the United States." Appl Environ Microbiol **73**(5): 1433-1443.

Kidd, S. E., F. Hagen, R. L. Tscharke, et al. (2004). "A rare genotype of *Cryptococcus gattii* caused the cryptococcosis outbreak on Vancouver Island (British Columbia, Canada)." Proc Natl Acad Sci U S A **101**(49): 17258-17263.

Kim, V. N., J. Han and M. C. Siomi (2009). "Biogenesis of small RNAs in animals." Nat Rev Mol Cell Biol **10**(2): 126-139.

Klapholz, S., C. S. Waddell and R. E. Esposito (1985). "The role of the *SPO11* gene in meiotic recombination in yeast." Genetics **110**(2): 187-216.

Klein, B. S. and B. Tebbets (2007). "Dimorphism and virulence in fungi." Curr Opin Microbiol **10**(4): 314-319.

Klosterman, S. J., M. H. Perlin, M. Garcia-Pedrajas, et al. (2007). "Genetics of morphogenesis and pathogenic development of *Ustilago maydis*." Adv Genet **57**: 1-47.

Ko, Y. J., Y. M. Yu, G. B. Kim, et al. (2009). "Remodeling of global transcription patterns of *Cryptococcus neoformans* genes mediated by the stress-activated HOG signaling pathways." Eukaryot Cell **8**(8): 1197-1217.

Koguchi, Y. and K. Kawakami (2002). "Cryptococcal infection and Th1-Th2 cytokine balance." Int Rev Immunol **21**(4-5): 423-438.

Kozel, T. R. (1995). "Virulence factors of *Cryptococcus neoformans*." Trends Microbiol. **3**: 295-299.

Kozel, T. R. and E. C. Gotschlich (1982). "The capsule of *Cryptococcus neoformans* passively inhibits phagocytosis of the yeast by macrophages." J. Immunol. **129**: 1675-1680.

Kozubowski, L., E. F. Aboobakar, M. E. Cardenas, et al. (2011). "Calcineurin colocalizes with P-bodies and stress granules during thermal stress in *Cryptococcus neoformans*." Eukaryot Cell **10**(11): 1396-1402.

Kraus, P. R., M. J. Boily, S. S. Giles, et al. (2004). "Identification of *Cryptococcus neoformans* temperature-regulated genes with a genomic-DNA microarray." Eukaryot. Cell **3**(5): 1249-1260.

Kronstad, J. W. and S. A. Leong (1989). "Isolation of two alleles of the b locus of *Ustilago maydis*." Proc Natl Acad Sci U S A **86**(3): 978-982.

Kruzel, E. K., S. S. Giles and C. M. Hull (2012). "Analysis of *Cryptococcus neoformans* sexual development reveals rewiring of the pheromone-response network by a change in transcription factor identity." Genetics **191**(2): 435-449.

Kwon-Chung, K. J. (1975). "A new genus, *Filobasidiella*, the perfect state of *Cryptococcus neoformans*." Mycologia **67**: 1197-1200.

Kwon-Chung, K. J. (1976). "Morphogenesis of *Filobasidiella neoformans*, the sexual state of *Cryptococcus neoformans*." Mycologia **68**(4): 821-833.

Kwon-Chung, K. J. (1976). "A new species of *Filobasidiella*, the sexual state of *Cryptococcus neoformans* B and C serotypes." Mycologia **68**(4): 943-946.

Kwon-Chung, K. J. and J. E. Bennett (1978). "Distribution of α and **a** mating types of *Cryptococcus neoformans* among natural and clinical isolates." Am. J. Epidemiol. **108**: 337-340.

Kwon-Chung, K. J. and J. E. Bennett (1984). "Epidemiologic differences between the two varieties of *Cryptococcus neoformans*." Am J Epidemiol **120**(1): 123-130.

Kwon-Chung, K. J. and Y. C. Chang (2012). "Aneuploidy and drug resistance in pathogenic fungi." PLoS Pathog **8**(11): e1003022.

Kwon-Chung, K. J., J. C. Edman and B. L. Wickes (1992). "Genetic association of mating types and virulence in *Cryptococcus neoformans*." Infect. Immun. **60**(2): 602-605.

Laloux, I., E. Jacobs and E. Dubois (1994). "Involvement of SRE element of Ty1 transposon in TEC1-dependent transcriptional activation." Nucleic Acids Res. **22**: 999-1005.

Lang, G. I., A. W. Murray and D. Botstein (2009). "The cost of gene expression underlies a fitness trade-off in yeast." Proc Natl Acad Sci U S A **106**(14): 5755-5760.

Lee, H. C., A. P. Aalto, Q. Yang, et al. (2010). "The DNA/RNA-dependent RNA polymerase QDE-1 generates aberrant RNA and dsRNA for RNAi in a process requiring replication protein A and a DNA helicase." PLoS Biol **8**(10).

Lee, S. C., N. Corradi, S. Doan, et al. (2010). "Evolution of the sex-related locus and genomic features shared in microsporidia and fungi." PLoS One **5**(5): e10539.

Lee, S. C. and J. Heitman (2012). "Function of *Cryptococcus neoformans KAR7* (*SEC66*) in karyogamy during unisexual and opposite-sex mating." Eukaryot Cell **11**(6): 783-794.

Lee, S. C., S. Phadke, S. Sun, et al. (2012). "Pseudohyphal growth of *Cryptococcus neoformans* is a reversible dimorphic transition in response to ammonium that requires Amt1 and Amt2 ammonium permeases." Eukaryot Cell **11**(11): 1391-1398.

Lengeler, K. B., G. M. Cox and J. Heitman (2001). "Serotype AD strains of *Cryptococcus neoformans* are diploid or aneuploid and are heterozygous at the mating-type locus." Infect Immun **69**(1): 115-122.

Lengeler, K. B., D. S. Fox, J. A. Fraser, et al. (2002). "Mating-type locus of *Cryptococcus neoformans*: a step in the evolution of sex chromosomes." Eukaryot Cell **1**(5): 704-718.

Lengeler, K. B., P. Wang, G. M. Cox, et al. (2000). "Identification of the *MAT***a** mating-type locus of *Cryptococcus neoformans* reveals a serotype A *MAT***a** strain thought to have been extinct." Proc. Natl. Acad. Sci. USA **97**(26): 14555-14460.

Leprohon, P., D. Legare, F. Raymond, et al. (2009). "Gene expression modulation is associated with gene amplification, supernumerary chromosomes and chromosome loss in antimony-resistant *Leishmania infantum*." Nucleic Acids Res **37**(5): 1387-1399.

Levitz, S. M. and C. A. Specht (2006). "The molecular basis for the immunogenicity of *Cryptococcus neoformans* mannoproteins." FEMS Yeast Res **6**(4): 513-524.

Li, H. and R. Durbin (2009). "Fast and accurate short read alignment with Burrows-Wheeler transform." Bioinformatics **25**(14): 1754-1760.

Lin, X. (2009). "*Cryptococcus neoformans*: morphogenesis, infection, and evolution." Infect Genet Evol **9**(4): 401-416.

Lin, X. and J. Heitman (2006). "The biology of the *Cryptococcus neoformans* species complex." Annu Rev Microbiol **60**: 69-105.

Lin, X. and J. Heitman (2007). Mechanisms of homothallism in fungi--transitions between heterothallism and homothallism. Sex in Fungi: molecular determination and evolutionary implications. J. Heitman, J. W. Kronstad, J. W. Taylor and L. A. Casselton. Washington, DC, ASM Press**:** pp. 35-58.

Lin, X., J. Huang, T. Mitchell, et al. (2006). "Virulence attributes and hyphal growth of *C. neoformans* are quantitative traits and the *MAT*α allele enhances filamentation." PLoS Genet **2**(11): e187.

Lin, X., C. M. Hull and J. Heitman (2005). "Sexual reproduction between partners of the same mating type in *Cryptococcus neoformans*." Nature **434**(7036): 1017-1021.

Lin, X., J. C. Jackson, M. Feretzaki, et al. (2010). "Transcription factors Mat2 and Znf2 operate cellular circuits orchestrating opposite- and same-sex mating in *Cryptococcus neoformans*." PLoS Genet **6**(5): e1000953.

Lin, X., A. P. Litvintseva, K. Nielsen, et al. (2007). "αADα hybrids of *Cryptococcus neoformans*: evidence of same-sex mating in nature and hybrid fitness." PLoS Genet **3**(10): 1975-1990.

Lin, X., K. Nielsen, S. Patel, et al. (2008). "Impact of mating type, serotype, and ploidy on the virulence of *Cryptococcus neoformans*." Infect Immun **76**(7): 2923-2938.

Lin, X., S. Patel, A. P. Litvintseva, et al. (2009). "Diploids in the *Cryptococcus neoformans* serotype A population homozygous for the alpha mating type originate via unisexual mating." PLoS Pathog **5**(1): e1000283.

Lindsley, D. L., L. Sandler, B. S. Baker, et al. (1972). "Segmental aneuploidy and the genetic gross structure of the *Drosophila* genome." Genetics **71**(1): 157-184.

Litvintseva, A. P., L. Kestenbaum, R. Vilgalys, et al. (2005). "Comparative analysis of environmental and clinical populations of *Cryptococcus neoformans*." J Clin Microbiol **43**(2): 556-564.

Litvintseva, A. P., X. Lin, I. Templeton, et al. (2007). "Many globally isolated AD hybrid strains of *Cryptococcus neoformans* originated in Africa." PLoS Pathog **3**(8): *e114*.

Litvintseva, A. P., R. E. Marra, K. Nielsen, et al. (2003). "Evidence of sexual recombination among *Cryptococcus neoformans* serotype A isolates in sub-Saharan Africa." Eukaryot. Cell **2**(6): 1162-1168.

Litvintseva, A. P., R. Thakur, R. Vilgalys, et al. (2006). "Multilocus sequence typing reveals three genetic subpopulations of *Cryptococcus neoformans* var. *grubii* (serotype A), including a unique population in Botswana." Genetics **172**(4): 2223-2238.

Liu, H. P., C. A. Styles and G. R. Fink (1993). "Elements of the yeast pheromone response pathway required for filamentous growth of diploids." Science **262**(5140): 1741-1744.

Llave, C., K. D. Kasschau, M. A. Rector, et al. (2002). "Endogenous and silencing-associated small RNAs in plants." Plant Cell **14**(7): 1605-1619.

Lo, H. J., J. R. Kohler, B. DiDomenico, et al. (1997). "Nonfilamentous *C. albicans* mutants are avirulent." Cell **90**(5): 939-949.

Loftus, B. J., E. Fung, P. Roncaglia, et al. (2005). "The genome of the basidiomycetous yeast and human pathogen *Cryptococcus neoformans*." Science **307**(5713): 1321-1324.

Lorenz, M. C., J. A. Bender and G. R. Fink (2004). "Transcriptional response of *Candida albicans* upon internalization by macrophages." Eukaryot. Cell **3**(5): 1076-1087.

Lu, Y. K., K. H. Sun and W. C. Shen (2005). "Blue light negatively regulates the sexual filamentation via the Cwc1 and Cwc2 proteins in *Cryptococcus neoformans*." Mol Microbiol **56**(2): 480-491.

Lurie, H. I. and H. J. Shadomy (1971). "Morphological variations of a hypha-forming strain of *Cryptococcus neoformans* (Coward strain) in tissues of mice." Sabouraudia **9**: 10-14.

Lye, L. F., K. Owens, H. Shi, et al. (2010). "Retention and loss of RNA interference pathways in trypanosomatid protozoans." PLoS Pathog **6**(10): e1001161.

Ma, H., J. E. Croudace, D. A. Lammas, et al. (2006). "Expulsion of live pathogenic yeast by macrophages." Curr Biol **16**(21): 2156-2160.

Ma, H., F. Hagen, D. J. Stekel, et al. (2009). "The fatal fungal outbreak on Vancouver Island is characterized by enhanced intracellular parasitism driven by mitochondrial regulation." Proc Natl Acad Sci U S A **106**(31): 12980-12985.

Ma, H. and R. C. May (2009). "Virulence in *Cryptococcus* species." Adv Appl Microbiol **67**: 131-190.

Madhani, H. D. and G. R. Fink (1997). "Combinatorial control required for the specificity of yeast MAPK signaling." Science **275**: 1314-1317.

Madhani, H. D. and G. R. Fink (1998). "The control of filamentous differentiation and virulence in fungi." Trends Cell Biol. **8**: 348-353.

Magditch, D. A., T. B. Liu, C. Xue, et al. (2012). "DNA mutations mediate microevolution between host-adapted forms of the pathogenic fungus *Cryptococcus neoformans*." PLoS Pathog **8**(10): e1002936.

Magee, B. B. and P. T. Magee (2000). "Induction of mating in *Candida albicans* by construction of *MTL***a** and MTLα strains." Science **289**(5477): 310-313.

Mahoney, D. P., L. H. Huang and M. P. Backus (1976). "New homothallic *Neurosporas* from tropical soils." Mycologia **61**(2): 264-272.

Mannaert, A., T. Downing, H. Imamura, et al. (2012). "Adaptive mechanisms in pathogens: universal aneuploidy in *Leishmania*." Trends Parasitol **28**(9): 370-376.

Maresca, B. and G. S. Kobayashi (2000). "Dimorphism in *Histoplasma capsulatum* and *Blastomyces dermatitidis*." Contrib Microbiol **5**: 201-216.

Marra, R. E., J. C. Huang, E. Fung, et al. (2004). "A genetic linkage map of *Cryptococcus neoformans* variety *neoformans* serotype D (*Filobasidiella neoformans*)." Genetics **167**(2): 619-631.

McClelland, C. M., Y. C. Chang, A. Varma, et al. (2004). "Uniqueness of the mating system in *Cryptococcus neoformans*." Trends Microbiol. **12**(5): 208-212.

McCullagh, E., A. Seshan, H. El-Samad, et al. (2010). "Coordinate control of gene expression noise and interchromosomal interactions in a MAP kinase pathway." Nat Cell Biol **12**(10): 954-962.

Mendez Vidal, C., M. Prahl and K. G. Wiman (2006). "The p53-induced Wig-1 protein binds double-stranded RNAs with structural characteristics of siRNAs and miRNAs." FEBS Lett **580**(18): 4401-4408.

Moazed, D. (2009). "Small RNAs in transcriptional gene silencing and genome defence." Nature **457**(7228): 413-420.

Moyrand, F., Y. C. Chang, U. Himmelreich, et al. (2004). "Cas3p belongs to a seven-member family of capsule structure designer proteins." Eukaryot Cell **3**(6): 1513-1524.

Napoli, C., C. Lemieux and R. Jorgensen (1990). "Introduction of a chimeric chalcone synthase gene into petunia results in reversible co-suppression of homologous genes in trans." Plant Cell **2**(4): 279-289.

Neilson, J. B., M. H. Ivey and G. S. Bulmer (1978). "*Cryptococcus neoformans*: Pseudohyphal forms surviving culture with *Acanthamoeba polyphaga*." Infect. Immun. **20**: 262-266.

Nemecek, J. C., M. Wuthrich and B. S. Klein (2006). "Global control of dimorphism and virulence in fungi." Science **312**(5773): 583-588.

Ngamskulrungroj, P., Y. Chang, E. Sionov, et al. (2012). "The primary target organ of *Cryptococcus gattii* is different from that of *Cryptococcus neoformans* in a murine model." mBio **3**(3): e00103-00112.

Nguyen, V. Q. and A. Sil (2008). "Temperature-induced switch to the pathogenic yeast form of *Histoplasma capsulatum* requires Ryp1, a conserved transcriptional regulator." Proc Natl Acad Sci U S A **105**(12): 4880-4885.

Ni, M., M. Feretzaki, W. Li, et al. (2013). "Unisexual and heterosexual meiotic reproduction generate aneuploidy and phenotypic diversity *de novo* in the yeast *Cryptococcus neoformans*." PLoS Biol **11**(9): e1001653.

Ni, M., M. Feretzaki, S. Sun, et al. (2011). "Sex in fungi." Annu Rev Genet **45**: 405-430.

Nichols, C. B., J. A. Fraser and J. Heitman (2004). "PAK kinases Ste20 and Pak1 govern cell polarity at different stages of mating in *Cryptococcus neoformans*." Mol Biol Cell **15**(10): 4476-4489.

Nicolas, F. E., S. Torres-Martinez and R. M. Ruiz-Vazquez (2003). "Two classes of small antisense RNAs in fungal RNA silencing triggered by non-integrative transgenes." EMBO J **22**(15): 3983-3991.

Nicolas, F. E., S. Torres-Martinez and R. M. Ruiz-Vazquez (2013). "Loss and retention of RNA interference in fungi and parasites." PLoS Pathog **9**(1): e1003089.

Nielsen, K., G. M. Cox, P. Wang, et al. (2003). "Sexual cycle of *Cryptococcus neoformans* var. *grubii* and virulence of congenic **a** and α isolates." Infect Immun **71**(9): 4831-4841.

Nielsen, K., A. L. De Obaldia and J. Heitman (2007). "*Cryptococcus neoformans* mates on pigeon guano: implications for the realized ecological niche and globalization." Eukaryot. Cell **6**(6): 949-959.

Nielsen, K., R. E. Marra, F. Hagen, et al. (2005). "Interaction between genetic background and the mating-type locus in *Cryptococcus neoformans* virulence potential." Genetics **171**(3): 975-983.

Noma, K., T. Sugiyama, H. Cam, et al. (2004). "RITS acts in cis to promote RNA interference-mediated transcriptional and post-transcriptional silencing." Nat Genet **36**(11): 1174-1180.

Novak, J. E., P. B. Ross-Macdonald and G. S. Roeder (2001). "The budding yeast Msh4 protein functions in chromosome synapsis and the regulation of crossover distribution." Genetics **158**(3): 1013-1025.

Noverr, M. C., G. M. Cox, J. R. Perfect, et al. (2003). "Role of *PLB1* in pulmonary inflammation and cryptococcal eicosanoid production." Infect Immun **71**(3): 1538-1547.

Nygren, K., R. Strandberg, A. Wallberg, et al. (2011). "A comprehensive phylogeny of *Neurospora* reveals a link between reproductive mode and molecular evolution in fungi." Mol Phylogenet Evol **59**(3): 649-663.

O'Meara, T. R., C. Hay, M. S. Price, et al. (2010). "*Cryptococcus neoformans* histone acetyltransferase Gcn5 regulates fungal adaptation to the host." Eukaryot Cell **9**(8): 1193-1202.

Odds, F. C., M. E. Bougnoux, D. J. Shaw, et al. (2007). "Molecular phylogenetics of *Candida albicans*." Eukaryot Cell **6**(6): 1041-1052.

Okagaki, L. H., A. K. Strain, J. N. Nielsen, et al. (2010). "Cryptococcal cell morphology affects host cell interactions and pathogenicity." PLoS Pathog **6**(6): e1000953.

Otto, S. P. and T. Lenormand (2002). "Resolving the paradox of sex and recombination." Nat Rev Genet **3**(4): 252-261.

Park, B. J., K. A. Wannemuehler, B. J. Marston, et al. (2009). "Estimation of the current global burden of cryptococcal meningitis among persons living with HIV/AIDS." AIDS **23**(4): 525-530.

Patau, K., D. W. Smith, E. Therman, et al. (1960). "Multiple congenital anomaly caused by an extra autosome." Lancet **1**(7128): 790-793.

Patterson, D. (2009). "Molecular genetic analysis of Down syndrome." Hum Genet **126**(1): 195-214.

Pavelka, N., G. Rancati, J. Zhu, et al. (2010). "Aneuploidy confers quantitative proteome changes and phenotypic variation in budding yeast." Nature **468**(7321): 321-325.

Phadke, S. S., M. Feretzaki and J. Heitman (2013). "Unisexual reproduction enhances fungal competitiveness by promoting habitat exploration via hyphal growth and sporulation." Eukaryot Cell **12**(8): 1155-1159.

Pitkin, J. W., D. G. Panaccione and J. D. Walton (1996). "A putative cyclic peptide efflux pump encoded by the *TOXA* gene of the plant-pathogenic fungus *Cochliobolus carbonum*." Microbiology **142**: 1557-1565.

Pontecorvo, G. and E. Kafer (1958). "Genetic analysis based on mitotic recombination." Adv Genet **9**: 71-104.

Poxleitner, M. K., M. L. Carpenter, J. J. Mancuso, et al. (2008). "Evidence for karyogamy and exchange of genetic material in the binucleate intestinal parasite *Giardia intestinalis*." Science **319**(5869): 1530-1533.

Ramesh, M. A., S. B. Malik and J. M. Logsdon, Jr. (2005). "A phylogenomic inventory of meiotic genes; evidence for sex in *Giardia* and an early eukaryotic origin of meiosis." Curr Biol **15**(2): 185-191.

Rancati, G., N. Pavelka, B. Fleharty, et al. (2008). "Aneuploidy underlies rapid adaptive evolution of yeast cells deprived of a conserved cytokinesis motor." Cell **135**(5): 879-893.

Reedy, J. L., A. M. Floyd and J. Heitman (2009). "Mechanistic plasticity of sexual reproduction and meiosis in the *Candida* pathogenic species complex." Curr Biol **19**(11): 891-899.

Reese, A. J. and T. L. Doering (2003). "Cell wall alpha-1,3-glucan is required to anchor the *Cryptococcus neoformans* capsule." Mol Microbiol **50**(4): 1401-1409.

Ren, P., D. J. Springer, M. J. Behr, et al. (2006). "Transcription factor STE12alpha has distinct roles in morphogenesis, virulence, and ecological fitness of the primary pathogenic yeast *Cryptococcus gattii*." Eukaryot. Cell **5**(7): 1065-1080.

Roberts, R. L. and G. R. Fink (1994). "Elements of a single MAP kinase cascade in *Saccharomyces cerevisiae* mediate two developmental programs in the same cell type: mating and invasive growth." Genes & Dev. **8**: 2974-2985.

Rojas, R., L. Valderrama, M. Valderrama, et al. (2006). "Resistance to antimony and treatment failure in human *Leishmania* (Viannia) infection." J Infect Dis **193**(10): 1375-1383.

Romanienko, P. J. and R. D. Camerini-Otero (2000). "The mouse *Spo11* gene is required for meiotic chromosome synapsis." Mol Cell **6**(5): 975-987.

Romano, N. and G. Macino (1992). "Quelling: transient inactivation of gene expression in *Neurospora crassa* by transformation with homologous sequences." Mol. Microbiol. **6**: 3343-3353.

Rosas, A. L. and A. Casadevall (1997). "Melanization affects susceptibility of *Cryptococcus neoformans* to heat and cold." FEMS Microbiol. Ltrs. **153**: 265-272.

Rose, M. D. (1996). "Nuclear fusion in the yeast *Saccharomyces cerevisiae*." Annu Rev Cell Dev Biol **12**: 663-695.

Rougeron, V., A. L. Banuls, B. Carme, et al. (2011). "Reproductive strategies and population structure in *Leishmania*: substantial amount of sex in *Leishmania Viannia guyanensis*." Mol Ecol **20**(15): 3116-3127.

Rupp, S., E. Summers, H. J. Lo, et al. (1999). "MAP kinase and cAMP filamentation signaling pathways converge on the unusually large promoter of the yeast *FLO11* gene." EMBO Journal **18**(5): 1257-1269.

Saag, M. S., R. J. Graybill, R. A. Larsen, et al. (2000). "Practice guidelines for the management of cryptococcal disease. Infectious Diseases Society of America." Clin Infect Dis **30**(4): 710-718.

Saul, N., M. Krockenberger and D. Carter (2008). "Evidence of recombination in mixed-mating-type and alpha-only populations of *Cryptococcus gattii* sourced from single eucalyptus tree hollows." Eukaryot. Cell **7**(4): 727-734.

Schein, J. E., K. L. Tangen, R. Chiu, et al. (2002). "Physical maps for genome analysis of serotype A and D strains of the fungal pathogen *Cryptococcus neoformans*." Genome Res **12**(9): 1445-1453.

Schoustra, S. E., A. J. Debets, M. Slakhorst, et al. (2007). "Mitotic recombination accelerates adaptation in the fungus *Aspergillus nidulans*." PLoS Genet **3**(4): e68.

Schurko, A. M. and J. M. Logsdon, Jr. (2008). "Using a meiosis detection toolkit to investigate ancient asexual "scandals" and the evolution of sex." BioEssays **30**(6): 579-589.

Selman, M., B. Sak, M. Kvac, et al. (2013). "Extremely reduced levels of heterozygosity in the vertebrate pathogen *Encephalitozoon cuniculi*." Eukaryot Cell **12**(4): 496-502.

Selmecki, A., A. Forche and J. Berman (2006). "Aneuploidy and isochromosome formation in drug-resistant *Candida albicans*." Science **313**(5785): 367-370.

Selmecki, A. M., K. Dulmage, L. E. Cowen, et al. (2009). "Acquisition of aneuploidy provides increased fitness during the evolution of antifungal drug resistance." PLoS Genet **5**(10): e1000705.

Seufert, W. and S. Jentsch (1990). "Ubiquitin-conjugating enzymes *UBC4* and *UBC5* mediate selective degradation of short-lived and abnormal proteins." EMBO J **9**(2): 543-550.

Shadomy, H. J. and H. I. Lurie (1971). "Histopathological observations in experimental cryptococcosis caused by a hypha-producing strain of *Cryptococcus neoformans* (Coward strain) in mice." Sabouraudia **9**: 6-9.

Shadomy, H. J. and J. P. Utz (1966). "Preliminary studies on a hypha-forming mutant of *Cryptococcus neoformans*." Mycologica **58**: 383-390.

Shao, X., A. Mednick, M. Alvarez, et al. (2005). "An innate immune system cell is a major determinant of species-related susceptibility differences to fungal pneumonia." J Immunol **175**(5): 3244-3251.

Sheltzer, J. M., H. M. Blank, S. J. Pfau, et al. (2011). "Aneuploidy drives genomic instability in yeast." Science **333**(6045): 1026-1030.

Shen, G., Y. L. Wang, A. Whittington, et al. (2008). "The RGS protein Crg2 regulates pheromone and cyclic AMP signaling in *Cryptococcus neoformans*." Eukaryot Cell **7**(9): 1540-1548.

Sherwood, R. K. and R. J. Bennett (2009). "Fungal meiosis and parasexual reproduction--lessons from pathogenic yeast." Curr Opin Microbiol **12**(6): 599-607.

Shibuya, K., A. Hirata, J. Omuta, et al. (2005). "Granuloma and cryptococcosis." J Infect Chemother **11**(3): 115-122.

Shinohara, A., S. Gasior, T. Ogawa, et al. (1997). "*Saccharomyces cerevisiae recA* homologues *RAD51* and *DMC1* have both distinct and overlapping roles in meiotic recombination." Genes Cells **2**(10): 615-629.

Sia, R. A., K. B. Lengeler and J. Heitman (2000). "Diploid strains of the pathogenic basidiomycete *Cryptococcus neoformans* are thermally dimorphic." Fungal Genet. Biol. **29**: 153-163.

Sionov, E., H. Lee, Y. C. Chang, et al. (2010). "*Cryptococcus neoformans* overcomes stress of azole drugs by formation of disomy in specific multiple chromosomes." PLoS Pathog **6**(4): e1000848.

Sirinavin, S., U. Intusoma and S. Tuntirungsee (2004). "Mother-to-child transmission of *Cryptococcus neoformans*." Pediatr Infect Dis J **23**(3): 278-279.

Smyth, G. K. (2005). Limma: limear models for microarray data. Bioinformatics and Computational Biology Solutions Using R and Bioconductor. V. C. R. Gentleman, S. Dudoit, R. Irizarry, W. Huber Springer**:** pp. 397-420.

Springer, D. J., D. Saini, E. J. Byrnes, et al. (2013). "Development of an aerosol model of *Cryptococcus* reveals humidity as an important factor affecting the viability of *Cryptococcus* during aerosolization." PLoS One **8**(7): e69804.

Sterkers, Y., L. Lachaud, N. Bourgeois, et al. (2012). "Novel insights into genome plasticity in Eukaryotes: mosaic aneuploidy in *Leishmania*." Mol Microbiol **86**(1): 15-23.

Sudbery, P. E. (2011). "Growth of *Candida albicans* hyphae." Nat Rev Microbiol **9**(10): 737-748.

Sun, S. and J. Xu (2009). "Chromosomal rearrangements between serotype A and D strains in *Cryptococcus neoformans*." PLoS One **4**(5): e5524.

Syme, R. M., J. C. Spurrell, E. K. Amankwah, et al. (2002). "Primary dendritic cells phagocytose *Cryptococcus neoformans* via mannose receptors and Fcgamma receptor II for presentation to T lymphocytes." Infect Immun **70**(11): 5972-5981.

Tanaka, R., H. Taguchi, K. Takeo, et al. (1996). "Determination of ploidy in *Cryptococcus neoformans* by flow cytometry." J Med Vet Mycol **34**(5): 299-301.

Thorne, L. W. and B. Byers (1993). "Stage-specific effects of X-irradiation on yeast meiosis." Genetics **134**(1): 29-42.

Tibayrenc, M. and F. J. Ayala (2012). "Reproductive clonality of pathogens: a perspective on pathogenic viruses, bacteria, fungi, and parasitic protozoa." Proc Natl Acad Sci U S A **109**(48): E3305-3313.

Todd, R. L. and W. W. Herrmann (1936). "The life cycle of the organism causing yeast meningitis." J. Bacteriol. **32**: 89-101.

Torres, E. M., N. Dephoure, A. Panneerselvam, et al. (2010). "Identification of aneuploidy-tolerating mutations." Cell **143**(1): 71-83.

Torres, E. M., T. Sokolsky, C. M. Tucker, et al. (2007). "Effects of aneuploidy on cellular physiology and cell division in haploid yeast." Science **317**(5840): 916-924.

Tscharke, R. L., M. Lazera, Y. C. Chang, et al. (2003). "Haploid fruiting in *Cryptococcus neoformans* is not mating type α-specific." Fungal Genet Biol **39**(3): 230-237.

Tucker, S. C. and A. Casadevall (2002). "Replication of *Cryptococcus neoformans* in macrophages is accompanied by phagosomal permeabilization and accumulation of vesicles containing polysaccharide in the cytoplasm." Proc Natl Acad Sci U S A **99**(5): 3165-3170.

Ubeda, J. M., D. Legare, F. Raymond, et al. (2008). "Modulation of gene expression in drug resistant *Leishmania* is associated with gene amplification, gene deletion and chromosome aneuploidy." Genome Biol **9**(7): R115.

Uhrigshardt, H., A. Singh, G. Kovtunovych, et al. (2010). "Characterization of the human HSC20, an unusual DnaJ type III protein, involved in iron-sulfur cluster biogenesis." Hum Mol Genet **19**(19): 3816-3834.

van der Horst, C. M., M. S. Saag, G. A. Cloud, et al. (1997). "Treatment of *Cryptococcal meningitis* associated with the acquired immunodeficiency syndrome. National Institute of Allergy and Infectious Diseases Mycoses Study Group and AIDS Clinical Trials Group." N. Engl. J. Med. **337**(1): 15-21.

Vecchiarelli, A., D. Pietrella, P. Lupo, et al. (2003). "The polysaccharide capsule of *Cryptococcus neoformans* interferes with human dendritic cell maturation and activation." J Leukoc Biol **74**(3): 370-378.

Velagapudi, R., Y. P. Hsueh, S. Geunes-Boyer, et al. (2009). "Spores as infectious propagules of *Cryptococcus neoformans*." Infect Immun **77**(10): 4345-4355.

Verdel, A., S. Jia, S. Gerber, et al. (2004). "RNAi-mediated targeting of heterochromatin by the RITS complex." Science **303**(5658): 672-676.

Viviani, M. A., R. Nikolova, M. C. Esposto, et al. (2003). "First European case of serotype A *MAT***a** *Cryptococcus neoformans* infection." Emerg Infect Dis **9**(9): 1179-1180.

Volpe, T. A., C. Kidner, I. M. Hall, et al. (2002). "Regulation of heterochromatic silencing and histone H3 lysine-9 methylation by RNAi." Science **297**(5588): 1833-1837.

Walton, F. J., A. Idnurm and J. Heitman (2005). "Novel gene functions required for melanization of the human pathogen *Cryptococcus neoformans*." Mol Microbiol **57**(5): 1381-1396.

Wan, L., T. de los Santos, C. Zhang, et al. (2004). "Mek1 kinase activity functions downstream of *RED1* in the regulation of meiotic double strand break repair in budding yeast." Mol Biol Cell **15**(1): 11-23.

Wang, L., B. Zhai and X. Lin (2012). "The link between morphotype transition and virulence in *Cryptococcus neoformans*." PLoS Pathog **8**(6): e1002765.

Wang, P., J. Cutler, J. King, et al. (2004). "Mutation of the regulator of G protein signaling Crg1 increases virulence in *Cryptococcus neoformans*." Eukaryot. Cell **3**(4): 1028-1035.

Wang, P., C. B. Nichols, K. B. Lengeler, et al. (2002). "Mating-type-specific and nonspecific PAK kinases play shared and divergent roles in *Cryptococcus neoformans*." Eukaryot. Cell **1**(2): 257-272.

Wang, X., S. Darwiche and J. Heitman (2013). "Sex-induced silencing operates during opposite-sex and unisexual reproduction in *Cryptococcus neoformans*." Genetics **193**(4): 1163-1174.

Wang, X., Y. P. Hsueh, W. Li, et al. (2010). "Sex-induced silencing defends the genome of *Cryptococcus neoformans* via RNAi." Genes Dev **24**(22): 2566-2582.

Wang, X., P. Wang, S. Sun, et al. (2012). "Transgene induced co-suppression during vegetative growth in *Cryptococcus neoformans*." PLoS Genet **8**(8): e1002885.

Wang, Y., P. Aisen and A. Cadadevall (1995). "*Cryptococcus neoformans* melanin and virulence: mechanism of action." Infect. Immun. **63**: 3131-3136.

Wang, Y. and A. Casadevall (1994). "Decreased susceptibility of melanized *Cryptococcus neoformans* to UV light." Appl. Environ. Microbiol. **60**: 3864-3866.

Wang, Y. and A. Casadevall (1994). "Susceptibility of melanized and nonmelanized *Cryptococcus neoformans* to nitrogen- and oxygen-derived oxidants." Infect. Immun. **62**: 3004-3007.

Weaver, B. A. and D. W. Cleveland (2006). "Does aneuploidy cause cancer?" Curr Opin Cell Biol **18**(6): 658-667.

Webster, R. H. and A. Sil (2008). "Conserved factors Ryp2 and Ryp3 control cell morphology and infectious spore formation in the fungal pathogen *Histoplasma capsulatum*." Proc Natl Acad Sci U S A **105**(38): 14573-14578.

Wendte, J. M., M. A. Miller, D. M. Lambourn, et al. (2010). "Self-mating in the definitive host potentiates clonal outbreaks of the apicomplexan parasites *Sarcocystis neurona* and *Toxoplasma gondii*." PLoS Genet **6**(12): e1001261.

Whiteway, M., L. Hougan, D. Dignard, et al. (1989). "The *STE4* and *STE18* genes of yeast encode potential β and γ subunits of the mating factor receptor-coupled G protein." Cell **56**: 467-477.

Wickes, B. L., U. Edman and J. C. Edman (1997). "The *Cryptococcus neoformans STE12*α gene: a putative *Saccharomyces cerevisiae STE12* homologue that is mating type specific." Mol. Microbiol. **26**: 951-960.

Wickes, B. L., M. E. Mayorga, U. Edman, et al. (1996). "Dimorphism and haploid fruiting in *Cryptococcus neoformans*: association with the α-mating type." Proc. Natl. Acad. Sci. USA **93**(14): 7327-7331.

Williams, B. R., V. R. Prabhu, K. E. Hunter, et al. (2008). "Aneuploidy affects proliferation and spontaneous immortalization in mammalian cells." Science **322**(5902): 703-709.

Williams, K. L., F. L. Wormley, Jr., S. Geunes-Boyer, et al. (2011). Pulmonary innate and adaptive defenses against *Cryptococcus*. *Cryptococcus*: from human pathogen to model yeast. J. Heitman, T. R. Kozel, K. J. Kwon-Chung, J. R. Perfect and A. Casadevall. Washington, DC, ASM Press**:** pp. 451-464.

Williamson, J. D., J. F. Silverman, C. T. Mallak, et al. (1996). "Atypical cytomorphologic appearance of *Cryptococcus neoformans*." Acta Cytologica **40**: 363-370.

Wright, L., W. Bubb, J. Davidson, et al. (2002). "Metabolites released by *Cryptococcus neoformans* var. *neoformans* and var. *gattii* differentially affect human neutrophil function." Microbes Infect **4**(14): 1427-1438.

Xu, J., R. Vilgalys and T. G. Mitchell (2000). "Multiple gene genealogies reveal recent dispersion and hybridization in the human pathogenic fungus *Cryptococcus neoformans*." Mol Ecol **9**(10): 1471-1481.

Xue, C., Y. S. Bahn, G. M. Cox, et al. (2006). "G protein-coupled receptor Gpr4 senses amino acids and activates the cAMP-PKA pathway in *Cryptococcus neoformans*." Mol Biol Cell **17**(2): 667-679.

Xue, C., Y. Tada, X. Dong, et al. (2007). "The human fungal pathogen *Cryptococcus* can complete its sexual cycle during a pathogenic association with plants." Cell Host Microbe **1**(4): 263-273.

Yang, M., W. S. May and T. Ito (1999). "JAZ requires the double-stranded RNA-binding zinc finger motifs for nuclear localization." J Biol Chem **274**(39): 27399-27406.

Yang, M., S. Wu, J. Jia, et al. (2011). "JAZ mediates G1 cell cycle arrest by interacting with and inhibiting E2F1." Cell Cycle **10**(14): 2390-2399.

Yona, A. H., Y. S. Manor, R. H. Herbst, et al. (2012). "Chromosomal duplication is a transient evolutionary solution to stress." Proc Natl Acad Sci U S A **109**(51): 21010-21015.

Zaragoza, O., R. Garcia-Rodas, J. D. Nosanchuk, et al. (2010). "Fungal cell gigantism during mammalian infection." PLoS Pathog **6**(6): e1000945.

Zerbino, D. R. and E. Birney (2008). "Velvet: algorithms for *de novo* short read assembly using de Bruijn graphs." Genome Res **18**(5): 821-829.

Zhai, B., P. Zhu, D. Foyle, et al. (2013). "Congenic strains of the filamentous form of *Cryptococcus neoformans* for studies of fungal morphogenesis and virulence." Infect Immun **81**(7): 2626-2637.

Zhu, W. and S. G. Filler (2010). "Interactions of *Candida albicans* with epithelial cells." Cell Microbiol **12**(3): 273-282.

Zimmer, B. L., H. O. Hempel and N. L. Goodman (1983). "Pathogenicity of the hyphae of *Filobasidiella neoformans*." Mycopathologia **81**(2): 107-110.

Biography

Marianna Feretzaki

Education

Bachelor of Science June 2005
Department of Biology, University of Crete, Crete, Greece

Research Experience

Graduate student September 2007 – present
University Program in Genetics and Genomics, Duke University, Durham, NC, USA

Project Intern September 2005 – May 2007
Department of Human Genetics, Baylor College of Medicine, Houston, TX, USA

Undergraduate research assistance September 2003 – May 2005
Laboratory of Human Genetics, Department of Biology, University of Crete, Crete, Greece

Summer exchange student May 2003 – September 2003
Department of Hematopathology, MD Anderson Cancer Center, Houston, TX, USA

Activities and Awards

2013: Recipient of Eukaryotic Cell Young Investigator Award for poster presentation at the 27th Fungal Genetics Conference, Asilomar, Pacific Grove, CA, USA

2013: Genetic Society of America travel award to attend to attend the 27th Fungal Genetics Conference, Asilomar, Pacific Grove, CA, USA

2012: Recipient of Duke Mycology Meritorious Research Travel Award to attend Gordon Research Conference on Cellular and Molecular Fungal Biology, Plymouth, NH, USA

2011: Recipient of a Graduate Student conference travel from Duke University Graduate School to attend the 26th Fungal Genetics Conference, Asilomar, Pacific Grove, CA, USA

2011: Gerondelis Foundation scholarship

2010: Recipient of a Graduate Student conference travel from Duke University Graduate School to attend the 1st International Conference on Model Hosts, Crete, Greece

2010: Recipient of Duke Mycology Meritorious Research Travel Award to attend Molecular Mycology Course" Woods Hole, Massachusetts USA

2010: Recipient of Woods Hole scholarship Excellence award for *in vivo* research for "Molecular Mycology Course" Woods Hole, Massachusetts USA

2008: Junior investigator travel award for the 7th International Conference on Cryptococcus and Cryptococcosis, Nagasaki, Japan

2008 – present: Member of the Genetic Society of America

2008 – present: Member of the American Society for Microbiology

2008 – present: Member of the American Society for Microbiology, North Carolina Regional Branch

Grants/Proposals

2010: "Role of hyphal development in virulence in *Cryptococcus neoformans*" **Principal Investigator**. Agency: CFAR grant (NIH-funded Center For AIDS Research at Duke University, 2P30 AI64518-07). (2011-2013)

Presentations

Feretzaki M, Wang X., Billmyre, B., Heitman, J., Poster presentation, The 27th Fungal Genetics Conference at Asilomar, California, March 12 – 17, 2013

Feretzaki M, Heitman, J., Poster presentation, Gordon Research Conference: Cellular and Molecular Fungal Biology, Holderness, New Hampshire. June 17-22, 2012

Feretzaki M, Min N., Hardison SH., Floyd FL. Jr., Heitman, J., Poster presentation, The 8th International Conference on Cryptococcus and Cryptococcosis, Charleston, South Carolina, USA. May 1-5, 2011

Feretzaki M, Heitman, J., Oral presentation. The 8th International Conference on Cryptococcus and Cryptococcosis, Charleston, South Carolina, USA. May 1-5, 2011. Invited speaker

Feretzaki M, Min N., Hardison SH., Floyd FL. Jr., Heitman, J., Oral presentation, The 26th Fungal Genetics Conference at Asilomar, California, March 15 – 20, 2011. Invited speaker

Feretzaki M, Heitman, J., Poster presentation, The 26th Fungal Genetics Conference at Asilomar, California, March 15 – 20, 2011

Feretzaki M, Heitman, J., Poster presentation, The 25th Fungal Genetics Conference at Asilomar, California, March 17 – 22, 2009

Feretzaki M, Heitman, J., Poster presentation, The 2008 NC ASM regional branch meeting Greensboro, North Carolina, October 10, 2008

Feretzaki M, Heitman, J., Poster presentation, The 7th International Conference on Cryptococcus and Cryptococcosis, Nagasaki, Japan, September 11 – 14, 2008

Feretzaki M, Rassidakis G, Grammatikakis I, Lin Q, Lai R, Medeiros L.J, Amin HM. Poster Presentation. *Cold Spring Harbor Laboratory Cancer Genetics & Tumor Suppressor Genes Meeting*, Cold Spring Harbor, NY, August 18-22, 2004

H.M. Amin, R. Lai, Q. Lin, **M. Feretzaki**, I. Grammatikakis, L.J. Medeiros, G.Z. Rassidakis. Poster Presentation. *93rd United States and Canadian Academy of Pathology Annual Meeting, Vancouver, BC, Canada, March 6-12, 2004.* (abstract #1001 published in *Laboratory Investigation 84 (1): p238A,* and in *Modern Pathology 17 (1): p238A, January 2004*).

M.P. Oyarzo, L.J. Medeiros, **M. Feretzaki**, H.M. Amin, G.Z. Rassidakis. Poster presentation. 93rd United States and Canadian Academy of Pathology Annual Meeting, Vancouver, BC, Canada, March 6-12, 2004. (abstract #1111 published in Laboratory Investigation 84 (1): p264A, and in Modern Pathology 17 (1): p264A, January 2004)

Publications

Feretzaki M, Billmyre RB, Wang X, Heitman J. RNAi loss in *C. gattii* reveals novel regulators of silencing in *C. neoformans*. **In preparation**.

Roach KC, **Feretzaki M**, Heitman J. Foraging for mates through unisexual reproduction. **In preparation**.

Roach KC, **Feretzaki M**, Sun S, Heitman J. Unisexual Reproduction. **Submitted** to *Advances in Genetics*.

Feretzaki M, Hardison SE, Wormley FL Jr, Heitman, J. *Cryptococcus neoformans* hyperfilamentous strain is hypervirulent in a murine model of cryptococcal meningoencephalitis. **Submitted** to *Infection and Immunity.*

Billmyre RB, Calo S, **Feretzaki M**, Wang X, Heitman J. RNAi function, diversity, and loss in the fungal kingdom. *Chromosome Res.* 2013 Oct 31. [Epub ahead of print].

Feretzaki M, Heitman J. Unisexual reproduction drives evolution of eukaryotic microbial pathogens. *PLoS Pathog*. 2013 9(10): e1003674.

Ni M*****, **Feretzaki M***, Li W, Floyd-Averette A, Mieczkowski P, Dietrich FS, Heitman J. Unisexual and heterosexual meiotic reproduction

generate aneuploidy and phenotypic diversity *de novo* in the yeast *Cryptococcus neoformans. PLoS Biol*. 2013 Sep;11(9):e1001653. (***** Denotes equal contribution) –Featured in Live Science, Duke Today, and highlighted in Nature Reviews Microbiology.

Feretzaki M, Heitman J. Genetic circuits that govern opposite- and same-sex mating in *Cryptococcus neoformans*. *PLoS Genet*. 2013 Aug;9(8):e1003688 -Featured on F1000.

Phadke SS*****, **Feretzaki M***, Heitman J. Unisexual reproduction enhances fungal competitiveness by promoting habitat exploration via hyphal growth and sporulation. Eukaryot Cell. 2013 Aug;12(8):1155-9. (***** Denotes equal contribution).

Wang X, Li W, Sun S, Kozubowski L, Lee SC, **Feretzaki M**, Heitman J. Know Your Enemy: How to Build and Vanquish a Global Fungal Scourge. *Mycopathologia*. 2012 Jun;173(5-6):295-301.

Ni M, **Feretzaki M**, Sun S, Wang X, Heitman J. Sex in Fungi. *Annu Rev Genet*. 2011;45:405-30.

Lin X, Jackson J., **Feretzaki M**, Xue C, Heitman J. Transcription factors Mat2 and Znf2 operate circuits orchestrating opposite and same-sex mating in *Cryptococcus neoformans*. *PLoS Genetics*, 2010 May 13;6(5):e1000953.

Oyarzo MP, Medeiros LJ, Atwell C, **Feretzaki M**, Wang S, Drakos E, Amin HM, Rassidakis GZ. C-FLIP Confers resistance to Fas-mediated apoptosis in anaplastic large cell lymphoma. *Blood*. 2006 Mar 15;107(6):2544-7.

Rassidakis GZ, **Feretzaki M,** Atwell C, Grammatikakis I, Lin Q, Lai R, Claret FX, Medeiros LJ, Amin HM. Inhibition of Akt increases p27Kip1 levels and induces cell cycle arrest in anaplastic large cell lymphoma. *Blood*. 2005 Jan 15;105(2):827-9.

Amin HM, Medeiros LJ, Ma Y, **Feretzaki M,** Das P, Leventaki V, Rassidakis GZ, O'Connor SL, McDonnell TJ, Lai R. Inhibition of JAK3 induces apoptosis and decreases anaplastic lymphoma kinase activity in anaplastic large cell lymphoma. *Oncogene*. 2003 Aug 21;22(35):5399-407.